THE UNIVERSITY
of EDINBURGH

The role of activin receptors in driving central nervous system regeneration of myelin

Alessandra Dillenburg

Doctor of Philosophy
The University of Edinburgh
2018

Abstract

Myelin damage in central nervous system white matter disorders such as multiple sclerosis (MS) leads to axonal dysfunction/degeneration and clinical disability. Regeneration of myelin (termed remyelination) can occur and requires oligodendrocyte progenitor cells (OPCs) to differentiate into mature oligodendrocytes, which are then able to make contact with axons and ensheath them. However, this process fails in progressive MS. The lack of approved therapies aimed at promoting remyelination highlight the need to identify mechanisms driving this regenerative process to develop novel therapeutic strategies.

Previous work in the lab identified the TGF-β superfamily member activin-A as being increased during remyelination *in vivo* and sufficient in stimulating activin receptor-driven OPC differentiation into mature oligodendrocytes *in vitro*. Here, these studies were followed up by undertaking a comprehensive assessment of the role of activin receptors and their ligands during remyelination. Using an *ex vivo* brain explant model of demyelination, the stimulation of activin receptors using activin-A was sufficient to enhance remyelination. Blocking activin receptors using an endogenous inhibitor (Inhibin) hindered remyelination, demonstrating the requirement of activin receptor signalling for this process. Surprisingly, blocking the binding of endogenous activin-A to activin receptors using follistatin did not impact remyelination, suggesting that other activin receptor ligands are involved in driving remyelination. As activin receptors may bind other ligands in the TGF-β superfamily, the expression and function of alternative ligands was investigated, and each was found to be important for remyelination (albeit with distinct timing/effects). Both activin receptors and their ligands were expressed on microglia/macrophages in mouse and human disease tissue. Finally, analysis of activin receptor expression on oligodendrocytes in human tissue revealed potential functional differences between receptor subtypes.

Together, these results demonstrate previously undefined roles of a subset of TGF-β superfamily members in regulating remyelination, and have implications for the development of novel approaches to enhancing remyelination in disease.

Lay Summary

Multiple sclerosis (MS) is an autoimmune disease whereby the myelin sheath, or the coating around nerve fibres, is destroyed. The brain is capable of regenerating myelin (termed remyelination); however, with disease progression, this process fails, leading to increasing clinical disability. There are no approved drug therapies to promote remyelination. To address this challenge, we sought to discover new ways through which remyelination could be promoted in MS to identify a novel therapeutic target.

Previous work from our lab points towards an important role for a naturally produced molecule called activin-A. This thesis explored the role of its binding partners, activin receptors, in regulating the cellular responses required for remyelination. In an animal model, when the activin receptors were 'turned on' using activin-A, there was an increase in remyelination. Conversely, when receptors were switched off, the regeneration of myelin was impaired. Interestingly, results showed that the main molecule which turns receptors on (activin-A) was not needed for remyelination to take place. Next, it was important to identify other molecules that affect the activity of activin receptors in the context of myelin repair. In this thesis, three other molecules related to activin-A were identified that are important for remyelination. In the absence of these naturally occurring molecules, remyelination is impaired, suggesting that there are many compounds that may affect this repair process. Finally, results showed that there are two main cell types in the brain where activin receptors are active: myelin-making cells (oligodendrocytes), and immune cells (microglia/macrophages).

Taken together, the work in this thesis characterizes the location and function of activin receptors and their many ligands as a novel therapeutic target for myelin regeneration.

Declaration of Original Work

I am the sole author of this thesis, and the work within it is entirely my own unless otherwise indicated. This work has not been submitted for any other degree or professional qualification. The included publication on which I am shared first author contains work from this thesis, and this work is clearly highlighted within each chapter.

Alessandra Dillenburg

Acknowledgements

I'd like to thank my funding body, the Commonwealth Scholarship Commission, without which I would not have had the opportunity to continue my work in the UK.

Thank You

First and foremost, I'd like to thank my supervisors, Veronica Miron and Anna Williams. These two incredible women were not only my go-to science wizards, they also doubled as my role models and mentors. I simply could not have done this work without their support and advice. A special thanks to Veronica for being an amazing advisor: you helped me become an independent scientist, supported my ideas, spent an inordinate amount of time discussing my future career and goals (even when they became non-academic), allowed me space to pursue my writing and outreach activities, and gave us all a day off on the one day of summer in Scotland. Thank you!!!

I also owe a huge thanks to my lab group - Amy Lloyd, Claire Davies, Frances Evans, Graeme Ireland, Irene Molina, and Rebecca Holloway (and all the BSc/MSc students: Becky, Makis, Neil, Sophie, and Sharan). Each one of you contributed massively at one point or another to helping my project along, be it with experimental advice, teaching me protocols, or listening to me vent about antibodies that just wouldn't work or surgery days that would never end. It has been amazing to work alongside you, and I feel lucky to have had such a great group of friends at work. A big thanks to my summer student, Dawid Kargul, for working so hard during those two months and doing (arguably the most boring and time-consuming) part of my work with no complaints!

I'm also very grateful to have been part of the outstanding team of scientists here at the Edinburgh MS Centre. Interacting with several groups (notably the Williams and ffrench-Constant labs) was both exciting and humbling all at once. The knowledge and support that members of these lab groups provided was invaluable to my work. Further, being part of the Centre for Reproductive Health (despite this not really being the focus of my work) was important to my project. The Pollard, Greaves, and Qian labs are excellent people to share a lab/office space (and the yearly Christmas drink) with, and were always very helpful around the lab.

There are several people that I'd like to thank for sharing their time and expertise with me. Daniel Soong was instrumental to setting up some of my imaging and quantifications, and I'm very grateful for his help and

advice. Pam Brown was an enormous help during a time of extreme qPCR-related stress, and solved a seemingly insurmountable problem within minutes. The CALM facility (Charlotte Buckley, Trudi Gillespie, Rachel Verdon, and Rolly Wiegand) spent hours with me over several months (including on a weekend!) helping me set up automated imaging. The Flow facility (Shonna Johnston, Will Ramsay, and Mari Pattison) were a huge help in the final stretch of my PhD when I just needed one extra experiment (using a technique I had never done before) - thank you for spending time teaching me about Flow! Last but certainly not least, an enormous thanks to Steve Mitchell for processing my (many) samples in such an efficient manner, for his help and advice on protocols, and for being such a joy to chat to during some of the most stressful times of my PhD.

Lastly, I owe an indescribable amount of thank-you's to my family and friends. To my parents (all 3 of you!): thank you for providing me with everything I could possibly need, even when I didn't ask for it. Mom, you've always been my biggest cheerleader and your (oft-misplaced and blind) belief in me has powered me through some of the toughest times during this PhD. Dad, your weird jokes have been a source of comic relief (and also thanks for the unconditional love). Glenn, thank you for being an incredible step-dad, thinking of me as one of your own children, and for caring for my mom while her daughter is in a far away land. To my sister (mana, manona, 'the person I admire most'): I honestly cannot put my thanks into words, but I'll try. You know how much you have helped me along the way, in every aspect of my life, not only during my PhD but extending back to the last 26 years. I would not be here without you. To my extended family in Brazil, my grandparents and numerous aunts/uncles/cousins: muito obrigada por tudo - o amor que eu recebi dessa família não tem igual.

My friends, both near and far, have been the most amazing support network during the last 4 years. To my friends in Canada, many of whom came to visit me (and let me sleep on their couches when I came to visit) - you were a constant reminder that good friends are not bothered by how many thousands of miles are between them. To my friends here in Edinburgh: it's thanks to all of you incredible people that my experience

here was so enjoyable. Exploring the pentlands, going for pints/drams, cycling around the city, going on trips together, playing board games, or just snuggling in Chewbacca onesies made weekends off so much better. So, to all of you who I consider my chosen family: thank you.

Finally, I owe indefinite thanks to the two best boys in my life. First, to my partner Billy: I can't imagine a better person to go through this doctorate journey with. You made everything better, in all the ways possible. Second, to my (borrowed) dog Marley and his family, Lucie and Tom: being able to hang out with such a lovely, happy furry friend did wonders for my well-being. Thank you for sharing him with me!

Scotland will always have a special place in my heart: the people, the culture, and the mountains make this a wonderful place to live. I'm eternally grateful to have had the chance to experience this incredible country during my studies. Thank you everyone!

Contents

List of Tables

List of Figures

1 Chapter 1: Introduction

Multiple sclerosis (MS) is an autoimmune disease where the protective coating around axons (myelin) is degenerated leading to axonal damage and loss. The central nervous system (CNS) is capable of regenerating myelin via a process termed remyelination. For successful remyelination to occur, oligodendrocyte progenitor cells (OPCs) must become activated, proliferate, survive, and differentiate into mature myelinating oligodendrocytes. While there is evidence suggesting remyelination occurs in early stages of MS, this process fails with disease progression and cognitive and motor functions worsen. No currently approved therapies promote remyelination; therefore, there is a pressing need to identify strategies to achieve this.

This chapter will describe myelin generation, injury, and repair, as well as the required oligodendrocyte lineage cell responses for this process. Further, I will review the clinical features and disease pathology of MS. Finally, I will outline current available therapies for MS, discuss remyelination drugs that are in the pipeline, as well as explore activin receptors as a novel therapeutic target for remyelination.

1.1 Myelination

1.1.1 Composition of myelin

Myelin is an important component of both central and peripheral nervous systems. Myelin insulates neurons, provides trophic and metabolic support, and allows for rapid transduction of electrical signals [1, 2]. In the CNS, oligodendrocytes pro-

duce plasma membranes that make contact with and wrap around axons in a spiral shape, resulting in a multi-layered myelin sheath [2]. The dry mass of myelin is mostly composed of lipids (70-85%) and proteins (15-30%). This high lipid to protein ratio is characteristic of myelin. Of the many lipids within myelin (i.e. cholesterol, lecithin, and sphingomyelin), cerebroside (also known as galactosylceramide) is the most typical, with total concentrations being directly proportional to the amount of myelin in the brain [3]. Surprisingly, in a study where the final step in cerebroside biosynthesis was knocked out, resulting in an elimination of this lipid, myelin formation was normal, likely due to a compensatory effect from glucocerebroside, a previously unidentified lipid in myelin. However, aged knockout animals eventually developed hindlimb paralysis and myelin abnormalities in the spinal cord, suggesting that while these lipids may not be required for myelin formation, they play an important role in myelin maintenance [4]. The remaining components of myelin are proteins, including myelin basic protein (MBP), proteolipid protein (PLP), Myelin/oligodendrocyte glycoprotein (MOG), Myelin-associated glycoprotein (MAG), $2', 3'-$cyclic nucleotide $3'-$phosphodiesterase (CNPase), and oligodendrocyte/myelin glycoprotein (OMgp).

1.1.2 Process of myelination

While rodent myelination begins only post-natally, human myelination starts in midgestation (17-22 weeks) and continues well into adulthood, with new myelin being continuously generated in a healthy adult brain [5–8]. Indeed, adult myelin is also constantly remodelled, with recent evidence showing white matter volume

changes after practising a new skill [9, 10] or learning a language [11]. This change in adult myelin could arise from production of new membrane by existing mature oligodendrocytes, or from oligodendrocyte progenitors undergoing a process similar to developmental myelination.

Developmental myelination is a tightly regulated process that begins with highly proliferative OPCs migrating from the subventricular zone into what will become the white matter of the brain [1]. OPCs then begin to differentiate and mature into myelin-making cells, express myelin-associated proteins, and make contact with axons [12]. Important strides made in imaging techniques in recent years have allowed researchers to explore how actively myelinating cells actually form wraps; a question whose answer had been long debated but not fully elucidated. A study from 2011 used live imaging of enhanced green fluorescent protein (EGFP) expressing mice to show that oligodendrocytes extend triangular processes which then coil around the axon as membrane spreads longitudinally [13]. Another study from 2014 used high resolution *in vivo* imaging combined with 3D reconstructions of the optic nerve to show that myelination involves an incorporation of the oligodendrocyte plasma membrane alongside the axon, and this new membrane expands laterally to form paranodal loops [14]. During developmental myelination, cytoplasmic channels enable communication between the outside environment and the inside of the nascent myelin sheath; once myelination is complete, these channels resolve. When PTEN (an Akt/mTOR signalling inhibitor) was deleted in adult mice, these cytoplasmic channels were re-introduced and the thickness of existing myelin sheaths

was increased. While a single factor or mechanism regulating myelination remains unidentified, the authors provide evidence that Akt/mTOR signalling can control these channels, and therefore, could be one of the regulators of myelination.

During development, oligodendrocytes will produce an amount of myelin that is proportional to the diameter of an axon; smaller axons have thinner sheaths, and larger axons have thicker sheaths [1]. Another outstanding question in the field is how an oligodendrocyte determines how much myelin to make for a specific axon. An interesting study in zebrafish revealed that oligodendrocytes can adapt to localized cues from axons—a single oligodendrocyte can produce the correct amount of myelin for both small and large calibre axons at the end of different processes, suggesting that the amount of myelin is locally determined [15]. A likely hypothesis is that there is synergistic cross-talk between axons and oligodendrocytes that regulate the selection of axons to be myelinated and the thickness of the sheath produced; however, the exact signalling pathways involved remain elusive.

1.1.3 Myelin is important for normal neuronal function

Myelin does not simply serve as a static insulating material; rather, axons and oligodendrocytes engage in dynamic bidirectional communication. This interaction is essential for the many functions of myelin, including rapid transduction of electrical impulses along the axon, and trophic and metabolic support [1].

Myelin ensheaths long segments of axons (termed internodes); between these segments are Nodes of Ranvier, or short sections of axons that remain unmyelinated.

The Node of Ranvier formation allows clustering of sodium channels at the node and facilitates saltatory conduction of electrical impulses, increasing conduction speeds 20-100 fold depending on the diameter of the axon [2, 16, 17]. The rapid neuronal signalling facilitated by myelinated axons in the CNS is important for normal motor, sensory, and cognitive functions [2]. Axo-glial interactions involving myelin are also important for axonal survival. Mice lacking PLP, a myelin protein, may only be expected to exhibit a myelin phenotype, but they also show long-term axonal degeneration as well as disrupted axo-plasmic transport [18, 19]. Furthermore, myelinating oligodendrocytes have been implicated in providing trophic and metabolic support to neurons [20–22]. Specifically, there is experimental evidence of trophic exchange of energy metabolites between oligodendrocytes and axons via monocarboxylate transporter 1 (MTC1) [20]. Axons lacking these energy metabolites are more prone to neurodegeneration. Therefore, oligodendrocytes and myelin are essential components of the CNS required for fast neuronal signaling and axonal health.

1.1.4 Diseases associated with myelin abnormalities

The importance of myelin in both the central and peripheral nervous systems is perhaps best exemplified by the many diseases associated with myelin abnormalities. Table 1 includes a list of such diseases [23].

Table 1. Diseases associated with myelin abnormalities.

Category	Disease
Central Nervous System	Multiple Sclerosis
	Acute-disseminated encephalomyelitis
	Acute hemorrhagic leucoencephalitis
	Central pontine myelinolysis
	Progressive multifocal leukoencephalopathy
	Subacute sclerosing panencephalitis
	Small vessel disease
	Binswanger's disease
Peripheral Nervous System	Guillain-Barré syndrome
	Chronic inflammatory demyelinating polyradiculoneuropathy
	Paraproteinemic demyelinating neuropathy
	Charcot-Marie-Tooth disease

1.2 Myelin regeneration requires oligodendrocyte lineage cell responses

In the event myelin is damaged and lost (for example, in demyelinating diseases such as MS), it can be regenerated in a process called remyelination. For adult remyelination to successfully occur, adult oligodendrocyte progenitor cells (aOPCs) must become activated, proliferate, migrate into the lesion, differentiate, and survive such that mature oligodendrocytes are able to contact axons and regenerate the myelin sheath (Figure 1) [24, 25]. The timely execution and coordination of these processes is essential for efficient remyelination, and as such, investigations have been carried out to elucidate the intricacies of oligodendrocyte maturation [26]. Current knowledge regarding factors and mechanisms involved in the phases of this important process is discussed in this section.

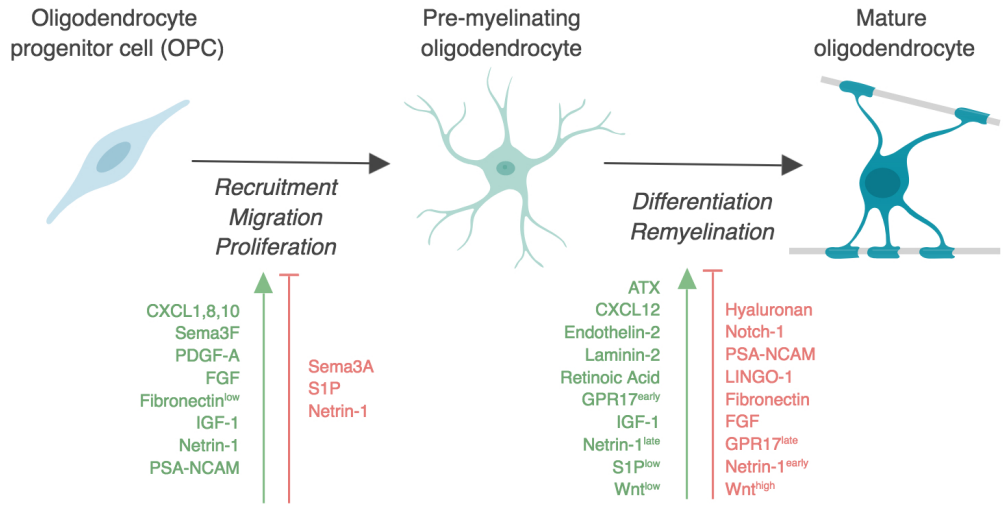

Figure 1. Oligodendrocyte progenitor cell responses required for remyelination and associated factors.

1.2.1 Activation of adult oligodendrocyte progenitor cells

Adult oligodendrocyte progenitor cells, or aOPCs, make up about 6% of cells in the brain, and they work to generate new oligodendrocytes throughout adulthood [27]. Given that these cells derive from developmental OPCs which are still present in adulthood [28], a likely hypothesis is that aOPCs generate new oligodendrocytes that contribute to remyelination after injury. Genetic fate mapping studies have been able to confirm this hypothesis: marker genes expressed by aOPCs (PDGFR-α/NG2) allowed researchers to follow their differentiation fates, providing evidence that new oligodendrocytes are indeed a product of aOPCs [29–31]. Interestingly, a study seeking to identify the developmental origins of aOPCs using dual-coloured reporter mice saw differences between regenerative capacity of aOPCs derived from dorsal and ventral origins, where the former had increased recruitment and differentiation [32]. This suggests that lesions may have different repair success rates depending

on where the recruited aOPCs derive from. Neural stem cell populations in the subventricular zone have also been shown to contribute to new oligodendrocytes in nearby areas of injury [33–35]; however, aOPCs are the major contributors to new oligodendrocytes after injury.

The first step in this process is the activation of aOPCs, where a number of injury-induced morphological and gene expression changes occur. An elegant study established the genetic profiles of resting aOPCs in non-injured white matter and activated aOPCs post-demyelination, and compared these to developmental OPCs and mature oligodendrocytes [36]. While resting aOPCs had transcriptomes similar to mature oligodendrocytes, once activated, they resembled developmental OPCs, showing that genes regulating production of new oligodendrocytes are similar in development and adulthood. While the exact mechanisms driving aOPC activation are not yet understood, a working hypothesis postulates that after tissue injury, signalling molecules are released from microglia, astrocytes, and damaged cells, resulting in a distinct set of signals (such as factors discussed in Table 2) that cause aOPCs to activate [26].

1.2.2 Coordination of oligodendrocyte recruitment, differentiation, and myelin formation

Once activated, aOPCs are recruited to injured areas to produce sufficient oligodendrocytes to carry out remyelination. In general, proliferation of progenitors produces a surplus of cells that are later pruned to the amount required; however, there

are some clinical cases where a failure in remyelination has been associated with lack of progenitors [37, 38]. The factors controlling OPC proliferation and migration to lesion sites are many, and the redundancy of these signals speaks to the complexity and importance of these cellular responses. Sources of such factors include microglia and macrophages, activated astrocytes, cells of the vasculature, and cell-intrinsic OPC signals [36, 39, 40]. A selection of important factors and their roles are illustrated in Figure 1 and listed in Table 2, with the notable exception of transforming growth factor (TGF-β) superfamily to be discussed in detail in section 1.5. Following recruitment of aOPCs to lesions, progenitors must exit the cell cycle in a timely manner [41] in order to extend membrane processes around axons and produce a new myelin sheath. While not much detail is known about this transition process, one proposed mechanism involves a high progenitor density triggering differentiation, and conversely, a low cell density inducing progenitor recruitment [42–44].

The final stage required for effective remyelination is compact myelin sheath formation. Regenerated myelin sheaths are shorter and thinner than developmental myelin [26], suggesting that some of the axo-glial signalling regulating these properties are absent or not required for remyelination. This difference in length and thickness of myelin can be quantified using the g ratio, or the ratio of axonal circumference to the circumference of the axon plus myelin. As such, the gold standard for identifying areas of remyelination is to calculate the g ratio by electron microscopy. An alternative method is to use fluorescent microscopy, which can show colocalization of axonal and myelin immunolabeling, or be used to visualize internodes using para-

nodal protein and sodium channel immunolabeling [45]. Since the length of myelin is shorter in remyelination, it is expected that there will be a greater number of internodes in areas where remyelination has occurred [46]. We can use this method to compare between areas of demyelination, where sodium channels will appear more spread along the axon due to a lack of myelin, and areas of remyelination, where sodium channels are distributed normally but more frequently along the axon. It is unclear why this physical difference between myelinated and remyelinated sheaths exists; however, one proposed hypothesis is that the interactions between myelinating cells and growing axons during myelination differ from those between myelinating cells and mature axons during remyelination, due to changes in dynamic stress experienced by these cell types, as well as differences in signalling pathways [47]. The thinner myelin sheath produced by remyelination is an important consideration in determining whether a full functionality is restored to axons. Conduction velocity is greater in axons with thicker myelin sheaths; computational studies predict that while some conduction is restored in remyelinated axons, it would not fully return to normal [48]. Further studies are required to determine the full and long-term effects of remyelination on the function of neuronal circuits. However, it is clear that the intricately choreographed mechanism of remyelination—from activation of adult oligodendrocyte progenitors to mature myelin-producing cells—is an important post-injury repair process resulting in the regeneration of a functionally relevant compact myelin sheath.

Table 2. Factors regulating oligodendrocyte lineage cell responses

Factor	Roles	References
Positive regulators		
Autotaxin (ATX)	Promotes differentiation Regulates process outgrowth and branching Reduced expression in MS post-mortem brains	[49–54]
CXCLs	CXCL1,8,10 promote recruitment/migration via CXCR1-3 CXCL1,8,10 expressed on reactive astrocytes in MS lesions CXCL1 overexpression results in milder EAE CXCL12 promotes differentiation via CXCR4 Inhibition of CXCL12 reduces remyelination	[55–59]
Endothelin-2	Enhances differentiation Promotes myelination and remyelination Receptor expressed by oligodendrocytes and in MS lesions	[59–61]
IGF-1	Required for differentiation and myelin production Induces development and proliferation via MAPK and Akt Deletion reduces number of myelinating cells Promotes survival in demyelinating conditions	[54, 62–69]
Laminin-2	Promotes myelin production via integrin receptors Regulates survival and proliferation Increased expression during remyelination	[54, 70–77]
PDGF-A	Promotes proliferation and survival Enhances recruitment and migration PDGFα receptor expressed on OPCs	[54, 59, 78–80]
Retinoic Acid	Boosts differentiation/remyelination via RXRγ receptor Differentiation block in RXRγ KO mice rescued by agonist	[59, 81]
Sema3F	Chemoattractant during development and post-injury Promotes recruitment and migration to injury site	[37, 59, 82–84]
Negative regulators		
Hyaluronan	Blocks differentiation Accumulates in inflammatory lesions after spinal cord injury Increased production by astrocytes in demyelinating lesions	[54, 59, 85–87]
LINGO-1	Negatively regulates differentiation and remyelination KO mice increased remyelination in EAE Blocking antibody treatment promoted differentiation Clinical trial results discussed in 1.4.2	[59, 88–90]
Notch-1	Notch-1/Jagged signalling inhibits differentiation KO results in accelerated differentiation/myelination	[59, 91–93]
Sema3A	Chemorepellent during development and post-injury Reduces OPC recruitment and remyelination Expressed in MS lesions lacking OPCs/remyelination	[37, 59, 83]

(continued on next page)

Table 2, continued

Factor	Roles	References
Pleiotropic effectors		
Fibronectin	Upregulated during demyelination Promotes migration and proliferation at low concentration Inhibitory role for differentiation and remyelination	[54, 94–97]
FGF	Promotes proliferation Inhibits differentiation Effect dependent on ligand-receptor complex/cell type	[54, 98–102]
GPR17	Early activation promotes differentiation Late activation inhibits maturation and myelination Upregulated in demyelinating lesions Expressed mainly by newly formed oligodendrocytes	[54, 103–108]
Netrin-1	Early chemoattractant for OPC migration in optic nerve Chemorepellent regulating OPC dispersal in spinal cord Early expression impairs remyelination Late expression enhances branching of processes Expression in MS associated with low migration	[82, 109–115]
PSA-NCAM	Low expresson coincides with differentiation/myelination Downregulation crucial for myelin maintenance Required for OPC chemotaxis/recruitment	[54, 116–122]
S1P/ Fingolimod	Low concentrations promote differentiation High concentrations inhibit differentiation Associated with cytoprotective effects Both null and positive effects on remyelination	[54, 123–129]
Wnt/ β-catenin	Delays maturation High signalling inhibits differentiation and remyelination Low signalling promotes differentiation and remyelination Effects may depend on developmental stage	[54, 59, 130–134]

1.2.3 Animal models of myelin injury and repair

There are no experimental animal models that fully recapitulate the complex pathology of demyelinating diseases such as Multiple Sclerosis. Rather, different models serve to mimic isolated aspects of the disease [26]. Focal lesioning models, where a demyelinating toxin is introduced to a brain region and repair occurs

along a standardised time course, may be used to study the process of remyelination independent of T-cell driven inflammatory response. Immune-mediated myelin damage models, where acute demyelinating lesions can develop into chronic ones, offer mechanistic insight into some potential aspects of MS immunopathogenesis. Neither of these can truly mimic MS, however, as they do not reflect the characteristics of disease progression, including a mix of acute and chronic inflammatory lesions, remyelination success and/or failure, and axonal degeneration. Models, such as the ones described below, can still be valuable to study specific disease features within the complex web of MS pathology (discussed further in the next section).

Focal lesioning models. Commonly, one of two toxins is used to induce demyelinating lesions in white matter tracts of the CNS: ethidium bromide or lysolecithin. These toxins differ mechanistically: ethidium bromide induces nucleated cell death by intercalating DNA, thereby affecting oligodendrocytes and OPCs but sparing axons, and lysolecithin acts as a detergent and strips away myelin membranes [135]. Both are excellent tools to study the process of remyelination, with clear temporal distinction between myelin injury and spontaneous repair [136–138]. Some important factors to consider when using *in vivo* stereotaxic injection models are issues with traumatic injury induced by toxin injection, blood-brain barrier breakdown, and potential axonal damage [139–141]. Lysolecithin-induced demyelination can also be employed to study remyelination in *ex vivo* organotypic brain slices, which recapitulate *in vivo* cytoarchitecture and provide an excellent environment for pharmacological manipulation [142, 143].

Cuprizone model. Another method by which investigators can induce lesions is by oral administration of cuprizone (bis-cyclo-hexanone oxaldihydrazone), a copper-chelating toxin. Copper chelation has been implicated in dysregulating energy production of oligodendrocytes via impairment of copper-dependent mitochondrial function [144]. Cuprizone administration results in oligdendrocyte cell death, vacuolization of myelin membranes, and demyelination [145]. Demyelination and remyelination are not temporally distinct in this model: OPC proliferation and recruitment begins during demyelination, and robust spontaneous myelin repair is seen as early as 4 days post cuprizone withdrawal [145, 146].

Immune-mediated myelin damage models. The most widely used model for studying the T-cell driven inflammatory mechanisms of MS is Experimental Autoimmune Encephalomyelitis, or EAE. This model comes in many forms, where experimental animals (commonly mice, but other animals such as marmosets have been used [147]) are immunized against a myelin antigen (usually MOG, but also PLP and MBP) leading to inflammation-induced demyelination. While remyelination occurs in this model, it is difficult to study due to the stochastic nature of the timing and location of lesions [148]. Another interesting model is Theiler's murine encephalomyelitis virus (TMEV), where a picornavirus infection in the CNS results in oligodendrocyte death, axonal damage, and demyelination [148, 149]. Limited remyelination occurs in this model, possibly as a result of dysregulated oligodendrocyte maturation [150]. Like EAE, lesions in TMEV models are randomly distributed temporally and spatially. Nevertheless, these are valuable models for answering mechanistic questions

relating to the immune-mediated damage seen in MS.

1.3 Myelin injury and repair in Multiple Sclerosis

1.3.1 Clinical presentation of Multiple Sclerosis

Multiple Sclerosis exemplifies the critical role of myelin and oligodendrocytes. MS is characterized by multi-centric demyelinating plaques: inflammatory lesions with loss of oligodendrocytes and myelin, glial scarring, and initial preservation of axons followed by irreversible axonal injury with disease progression [151, 152]. Patients with MS typically first experience relapse-remitting MS (RRMS, 80-90%), where their neurological symptoms resolve and relapse repeatedly, followed by secondary progressive MS (SPMS), where the disease progresses steadily, symptoms no longer resolve, and disability accumulates [46, 153]. Some patients (10%) experience primary progressive MS (PPMS), where they have progressively worsening disability with no remissions from the onset of disease [46, 151].

MS is a heterogeneous disease, with unknown causes and a disease course that is largely unpredictable. Natural history studies have postulated that about 10% of patients with an initial presentation of symptoms have a mild form of the disease, and about 70% of those with RRMS develop secondary progression. Predictors of a more severe disease course include frequent relapses in the first two years, male sex, and early motor and cerebellar abnormalities. Female sex and patients with mainly sensory symptoms often have a better prognosis [154–156]. MS disease onset

occurs typically at 20-40 years of age and affects females at approximately a 2:1 ratio compared to males. MS is geographically varied, with the highest prevalence being in northern Europe, southern Australia, and North America [151]. While the cause of MS remains elusive, there is evidence for both environmental and genetic factors playing a role in disease onset [157, 158]. Several studies have shown various lines of evidence for environmental risk factors, including geographical and temporal clustering of cases [159, 160], changes in the frequency of MS in individuals who migrate to and from high prevalence areas [161, 162], and vitamin D deficiency [163]. Genetic risk factors have also been identified, the strongest and most studied of which is the major histocompatability complex (MHC) class II region. However, MHC-associated alleles are not sufficient to cause disease or predict its development, suggesting a complex relationship between genetics and phenotype [151, 158]. Large international genome-wide association studies (GWAS) have recently revealed over 50 non-MHC genetic risk factors (single nucleotide polymorphisms, or SNPs) associated with MS [158]; however, given the heterogeneity of disease course and epidemiology, it is evident that an intricate interaction between genes and environment underlies individual susceptibility to MS.

1.3.2 Demyelination and neurodegeneration in Multiple Sclerosis

In MS, heterogeneity exists not only in clinical course, but also between lesions—even within the same patient. This may point to different pathological processes including autoimmune responses, primary oligodendrocyte dysfunction, and viral

infection [164]. Alternatively, differences between lesions may also reflect different stages of repair. As mentioned previously, the cause of MS is unknown; however, there are two major competing theories. The first is the 'outside-in' auto-antigen hypothesis, which postulates that there is a primary auto-reactive T cell driven process whereby these cells cross the blood-brain barrier, and with the help of B cells and macrophages, target and destroy myelin [151, 165, 166]. There are several lines of evidence supporting this model. As mentioned above, there is an association of the disease with MHC genes, which is part of the antigen-presenting machinery T cells can use to target myelin [167]. T cells derived from MS patients show higher reactivity to myelin antigens MBP, PLP, MAG, and MOG compared to healthy participants [168, 169]. Additionally, the EAE mouse model of autoimmune myelin damage can be induced by adoptive transfer of anti-MBP and anti-MOG_{35-55} reactive T cells [170, 171]. Demyelination may also be triggered by monocyte infiltration into the CNS. Evidence from EAE studies suggests that while tissue resident microglia are not required for EAE induction/progression, infiltrating macrophages are [172–175]. Indeed, depletion of monocytes results in inhibition of disease initiation and progression in EAE mice [176], suggesting auto-reactive T cells are not the only immune cells driving myelin destruction.

The second 'inside-out' theory of MS argues that there is a primary oligodendrocyte degeneration and this leads to a secondary autoimmune and inflammatory response [165, 166]. There is evidence supporting this theory both in human and rodent studies. Specifically, human studies have revealed evidence for oligodendro-

cyte death preceding significant T and B cell infiltration. Using tissue from patients with rapidly deteriorating MS, the authors noted new brainstem lesions featuring high oligodendrocyte death accompanied by activated microglia, but lacking infiltrating lymphocytes or myelin phagocytes [177, 178]. Interestingly, when one study combined *in vivo* induction of oligodendrocyte death with favourable conditions for autoimmunity (removal of regulatory T cells, presence of myelin-reactive T cells) in rodents, the authors found no subsequent CNS inflammation, suggesting oligodendrocyte death may not induce anti-CNS immunity, even with immune activation [179]. Conversely, another recent study used genetic ablation of oligodendrocytes in a mouse model (*Plp1-CreER^T;ROSA26-eGFP-DTA*) and saw recovery from an initial demyelinating event followed by late-onset demyelination and axon loss coinciding with infiltration of myelin-specific T cells, suggesting oligodendrocyte death can, in fact, trigger CNS autoimmunity [180]. While these studies seem contradictory, it is important to note that the former study used a direct administration of diphtheria toxin leading to a severe neurodegeneration and early death, precluding any possible findings of a late-onset disease in this model. The authors of the latter study note that it may be important to give the autoimmune response time to develop, rendering long-term animal survival post induction of oligodendrocyte ablation an important caveat to studying triggers for CNS autoimmunity.

Neuronal degeneration could also play an important role in demyelination [166, 181]. There is indisputable evidence for neurodegeneration in MS: axonal transection and loss can be seen in post-mortem MS brains [152], there is progressive atrophy

in brains of MS patients [12], and reduced expression of neuronal marker N-acetyl aspartic acid (NAA) [182]. Importantly, in active lesions undergoing inflammatory demyelination, amyloid precursor protein (APP) can be detected, suggesting disruption of fast axonal transport and axonal transection [183]. The prevalence of transected axons is correlated with inflammation [152, 183], suggesting the inflammatory microenvironment is implicated in neurodegeneration. Other factors may be responsible for this effect, however. Glutamate-induced excitotoxicity can induce neurodegeneration [184, 185], and evidence from MS tissue shows elevated glutamate levels in acute lesions and normal-appearing white matter [186]. Another potential contributor to neuronal degeneration in MS is intrinsic axonal dysfunction. Indeed, gene expression studies in postmortem MS brains show evidence for mitochondrial dysfunction in axons causing neurodegeneration [187, 188]. Together, these theories purport the culprit behind the destruction of myelin to be the autoimmune response, oligodendrocyte death, or neuronal injury. Given the heterogeneity of lesions within patients, as well as differences between individuals with MS, it is possible that these theories do not preclude one another: one or all of these proposed mechanisms could be responsible for demyelination in MS.

Regardless of the responsible demyelinating mechanism, the prevailing idea is that permanent disability in late stage SPMS and PPMS patients is due to irreversible axonal damage as a result of loss of metabolic support offered by oligodendrocytes (Figure 2) [22, 189]. While axonal damage and loss is also ample in early acute lesions, neuronal plasticity may account for the lack of disability accumulation in early

stages of RRMS. A few studies used functional magnetic resonance imaging (fMRI) to show activation of new cortical regions that could be part of this compensation mechanism [190–193]. Once CNS plasticity is no longer able to counterbalance the extensive neuronal loss, RRMS transitions to SPMS and brain atrophy worsens without development of new inflammatory lesions, suggesting alternative mechanisms are at play [166, 194]. The elusiveness of the underlying causes of MS render its prevention a difficult task. While there are now several effective drugs to counteract the inflammatory response and reduce relapses in patients, these drugs are not effective in progressive MS (with the exception of one promising new drug, ocrelizumab, discussed further below). One idea is to hinder disease progression by developing therapies targeted at reducing neurodegeneration. Since myelin is important to neuronal health, harnessing the innate remyelination capabilities of the CNS may be a way to achieve this goal.

1.3.3 Myelin regeneration in Multiple Sclerosis

Remyelination, distinct from developmental myelination, is a process that occurs after injury. Both experimental and clinical evidence exist showing that remyelination can occur spontaneously post demyelination (see Figure 2). First, the experimental evidence from toxin-induced demyelination in animal models (most commonly using cuprizone or lysolecithin), both *in vivo* and *ex vivo*, suggests that while this effect diminishes with age, axons generally do not remain demyelinated and robust remyelination is achieved [26, 195, 196]. Further, there is evidence from post-

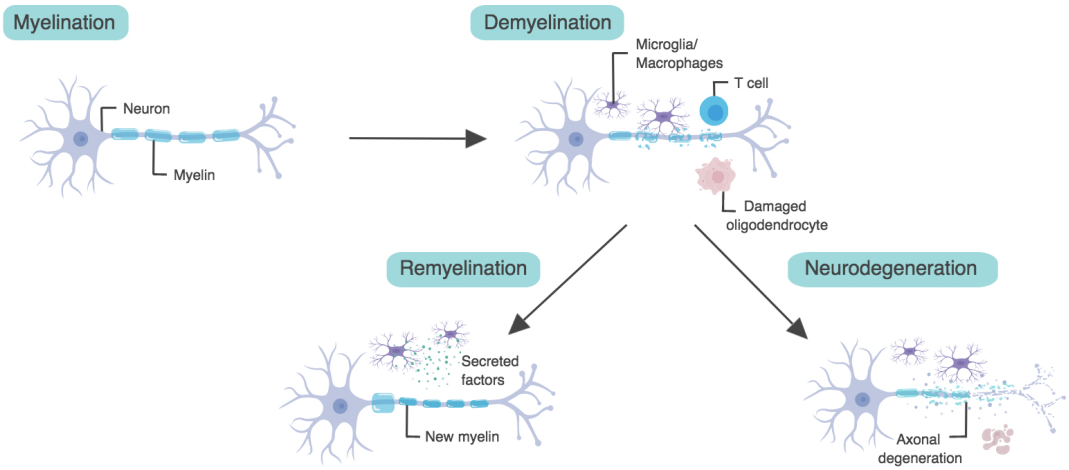

Figure 2. Myelination, demyelination, and subsequent responses.

mortem human tissue for demyelination and remyelination co-existing in MS lesions [197–200]. Importantly, one study examined MS lesions by electron microscopy and found thinner and shorter internodes, which is indicative of reformed myelin [197].

Given the important role of myelin in the CNS, it is not surprising that restoring myelin after a demyelinating injury is an important process. Remyelination is neuroprotective; it restores axonal health both functionally and metabolically [26]. Evidence from human postmortem tissue indicates that neurodegeneration is more prevalent in acute and chronic lesions compared to remyelinated lesions [201, 202]. Further, several convincing studies using different techniques in animals have shown the neuroprotective effects of remyelination [203–205]. One study used a cuprizone demyelination model combined with irradiation to prevent endogenous remyelination. After transplanting progenitor cells leading to restoration of remyelination capacity

and therefore remyelination, they saw a decrease in axonal injury [203]. A second study genetically eliminated adult oligodendrocytes, leading to axonal injury which was not resolved by blocking the axon-damaging effects of the adaptive immune system [204]. Finally, in an EAE model, enhancing oligodendrocyte differentiation (and thus remyelination) led to an increase in axonal preservation [205].

Evidence for the functionally restorative role of remyelination is well-established in animal models [206, 207]. Remyelination was shown to restore rapid conduction in the spinal cord and brainstem of rodents as measured by electrophysiology [206]. Further, a study done in cats with a demyelinating condition showed that endogenous remyelination of intact axons reverses clinical deficits seen during demyelination [207]. Taken together, the evidence suggests that remyelination is an important endogenous post-injury repair process.

1.3.4 Failure of remyelination in Multiple Sclerosis

As MS advances, remyelination often fails and neuronal loss occurs leading to the progressive degeneration seen in PPMS and SPMS, an idea supported by both experimental and clinical reports (see Figure 2) [46, 166, 195, 208]. In a marmoset model of EAE, axonal spheroids and amyloid precursor protein (APP) were observed in areas of inflammation and demyelination [147]. APP-positive axonal spheroids are early markers of axonal injury and deficiencies in axonal transport, which can eventually result in neuronal loss [196, 209–211]. Further, in post-mortem tissue collected from MS patients, axonal spheroids containing APP are present in areas

of demyelination and inflammation [183, 212, 213]. Remyelination is believed to be critical for dampening disease progression and reducing severe long-term disability; as such, it is important to understand why this process fails. A reduction or failure of OPC recruitment, maturation, and ensheathment could be due to generic factors such as ageing [214–217], or due to disease-specific factors, such as the post-injury microenvironment and inflammation [26, 218]. While remyelination can fail due to arrested development of oligodendrocytes at any stage, the current evidence points towards a key failure in OPC differentiation and maturation in MS, as 70% of lesions contain OPCs but lack mature oligodendrocytes, compared to 30% of lesions lacking OPCs, indicating insufficient recruitment [37, 80, 208, 217, 219–222].

In general, ageing is associated with decreased efficiency of regenerative processes; it therefore follows that regeneration of myelin also slows down with age [223–225]. Cohort studies support the hypothesis that the transition from RRMS to SPMS is likely associated with an age-related decline in remyelination efficiency combined with consequent progressive neurodegeneration. Specifically, MS patients of certain age groups tend to have a similar level of disability, regardless of heterogeneity in initial disease patterns and age of onset [214]. Further, both imaging and pathology studies show evidence for age-related decline in remyelination efficiency [215, 216]. The relationship between ageing and remyelination failure could be due to ageing-driven intrinsic changes in oligodendrocytes. For example, one study found that young brains are efficient in epigenetic control of gene expression, enabling the recruitment of histone deacetylases (HDAC) to promoter regions of genes important for

oligodendrocyte differentiation. Old brains, however, lack this efficiency in HDAC recruitment, leading to poor control of gene expression required for remyelination [226].

Another reason for a failure in oligodendrocyte maturation could be the post-injury microenvironment. Indeed, there is evidence from both human and animal studies showing inhibitory factors are present in demyelinated lesions (hyaluronan [85, 86], PSA-NCAM [117, 227]). Lesions may also lack signals that promote differentiation (IGF-1, TGF-β [47]) — see Table 2 for a list of selected extracellular factors that influence remyelination. These factors are part of an environment that is not conducive to OPC maturation, and thus affect the efficiency of remyelination [195]. Additionally, evidence from post-mortem MS brains show that in some chronic lesions, pre-myelinating oligodendrocytes are present and associate with demyelinated axons but do not myelinate, possibly due to a a dysregulation of growth factors, inhibitory signals, or a changing molecular composition of axonal signals preventing myelin wrapping [228].

Remyelination efficiency may also be affected by the immune response to demyelination [26]. One function of post-injury inflammation is to prepare the damaged tissue for repair, and while the inflammatory response in MS has typically been seen as detrimental [229, 230], it is clear that some immune cells in MS (microglia and macrophages) have a complex role, with both beneficial and detrimental aspects. Investigations in toxin-induced demyelination (models where the immune response is a product of demyelination, not vice-versa) showed that depleting macrophages

can impair remyelination [231], suggesting an important interaction between the immune response and regeneration potential. An abundance of myelin debris is produced post-injury, which has been shown to be detrimental to OPC differentiation and subsequent remyelination [232–235]. Both resident microglia and recruited macrophages are responsible for clearing this debris, and their efficiency in performing this task impacts the efficiency of repair processes [26]. However, these immune cells may have different functions depending on their activation state or phenotype. It has been shown that pro-inflammatory microglia are important during the early recruitment stage of remyelination, while pro-repair microglia are required during oligodendrocyte differentiation. A timely transition from pro-inflammatory to pro-repair microglia is critical for effective remyelination; therefore, one possible factor influencing a failure in remyelination is the persistence of pro-inflammatory immune cells [142]. Indeed, MS post-mortem tissue studies have shown that a high number of pro-inflammatory microglia/macrophages is associated with chronic inactive lesions, where remyelination is poor [142, 236]. Further, in the EAE mouse model, an imbalance in microglia/macrophage activation towards pro-inflammatory phenotypes is associated with a more severe disease course [237]. Both human and experimental evidence suggests a persistence in pro-inflammatory immune cells can result in poor outcomes in demyelinating lesions. Together, these data suggest that both ageing and lesion microenvironment may affect remyelination, particularly in the final stages of maturation where oligodendrocytes fail to make myelin that subsequently wraps in a compact manner around axons.

1.4 Therapeutic targets for Multiple Sclerosis

1.4.1 Immunomodulatory therapies

As previously mentioned, MS is a complex and heterogenous disease; accordingly, individual patient outcomes from the various available drugs vary, rendering the selection of treatment a complex process. There are several disease-modifying therapies (DMTs) currently approved for RRMS to reduce the rate of relapses. Each have different mechanisms of action and considerations (i.e. efficacy, side effects, delivery route/frequency) that are taken into account by the physician and the patient [238]. Therapies discussed in this section are summarized in Table 3.

The first generation DMTs (which new therapies are often compared to in clinical trials) are Interferon-beta and Glatiramer acetate. These were common first-line treatment options for individuals with RRMS, as they have good safety profiles and clinical efficacy. Interferon-beta is thought to work by lowering levels of blood-brain barrier disruption and regulating immune cell function, while Glatiramer acetate likely modulates function of regulatory T cells [239]. Since the first Interferon-beta drug was approved in 1993, a plethora of other more effective treatments have become available, including orally administered DMTs (Fingolimod, Teriflunomide, Dimethyl fumarate, Cladribine), and infusions (Natulizumab, Alemtuzumab, and Ocrelizumab) [238, 240–242]. Depending on the severity of side effects, relevant contra-indications, and recent MS activity, these may be recommended as first- or second-line therapies for RRMS. Patient factors, such as drug preference/tolerability

and adherence to dose regimen, are also considered when prescribing medications [238].

Generally, physicians utilize a sequential DMT monotherapy strategy for RRMS patients. After an appropriate DMT is selected, a patient will undergo surveillance for a period of time to monitor clinical and radiological disease activity, as well as drug tolerability, adherence, and safety [238]. Ideally, the patient would experience remission with no significant side effects, in which case the therapy would continue with occasional reassessment. However, if disease continues to be active (albeit slowly in some cases), patients will eventually relapse—likely due to the partial efficacy of DMTs. At this time, the clinician is faced with a difficult decision that often lacks concrete evidence-based support: has the drug failed, and is it time to revise the treatment plan? As there is little research comparing specific DMTs, or on the effects of using different DMTs sequentially, the clinical decision on which DMT to prescribe next can be tough. Most DMTs, while effective in reducing relapse rate, do not slow disease progression, and are not a cure. In a recent phase 3 trial, however, Ocrelizumab showed promising results in slowing disability progression of primary progressive MS patients compared to placebo controls. The authors found that Ocrelizumab treatment lowered the risk of disability progression by 25%; further, MRI scans revealed a decrease in total brain lesion volume in patients treated with Ocrelizumab compared to an increase in patients treated with placebo [242]. While this B cell-depleting drug may be a promising avenue, it only focusses on inflammatory aspects of the disease. None of these drugs target the underlying neu-

rodegeneration and long-term demyelination. Developing drugs that target these processes represents the greatest unmet need in multiple sclerosis therapeutics.

1.4.2 Clinical trials for remyelination therapies

A novel therapeutic approach that has been under investigation by several groups is to target the underlying axonal degeneration by identifying pro-remyelination therapies. Indeed, some pro-remyelination therapies for MS have undergone or are currently in clinical trials stage (e.g. anti-LINGO-1 antibody, bexarotene, clemastine) [81, 88, 243]. LINGO-1 is a negative regulator of oligodendrocyte differentiation and remyelination, and in an EAE mouse model, administration of an anti-LINGO-1 antibody resulted in improved remyelination [88]. Unfortunately, anti-LINGO-1 antibody (developed under the name Opicinumab) recently failed to meet its primary endpoints in a Phase II clinical trial. There are several possible reasons for this failed trial, including the use of an inappropriate patient population, the timing of drug delivery, a short follow-up period, and questions regarding the antibody's efficacy in crossing the blood brain barrier. The complex results of this trial are still being analysed, and at the very least will provide clues to improve clinical trial design for remyelination outcomes [240, 244, 245]. More recently, clemastine fumarate, an over-the-counter antihistamine with off-target, pro-remyelination anti-muscarinic effects, has been tested in a small clinical trial. Two independent screens identified clemastine as a compound with positive effects on oligodendrocyte differentiation and myelination [243, 246]. Preclinical work validated these findings,

showing that clemastine treatment reduced clinical severity, improved myelin area, and exerted neuroprotective effects in an EAE mouse model [205]. Interestingly, there was no change the number of infiltrating immune cells, suggesting this effect was not immune-mediated. Using knockout experiments, the authors identified Chrm1 as the muscarinic receptor target of clemastine. Deletion of this receptor resulted in enhanced differentiation and accelerated remyelination in a focal lesion model [205]. When clemastine was tested in human cells, it was found to induce OPC differentation and myelination [247]. These encouraging preclinical results led to a randomised, controlled, double-blind crossover phase II clinical trial in 50 RRMS patients with chronic demyelinating optic neuropathy. This is the first study to show the efficacy of a pro-regenerative drug in the context of a chronic demyelinating disease; however, there was only a small increase in optic nerve conduction velocity and no clinical change in vision. These measures are commonly used to assess myelin damage and remyelination, and are discussed further below. Nevertheless, these results are promising and suggest that myelin repair is possible even after long-term damage [247].

Two other interesting targets for myelin repair being developed include GSK239512 and MD1003 (high-dose biotin). Histamine H3 receptors expressed by neurons and OPCs have been shown to play a role in OPC differentiation [243], and pre-clinical studies showed that H3 antagonist/inverse agonist GSK239512 stimulates OPC differentiation *in vitro* and promotes remyelination in a cuprizone mouse model. When it was trialled in RRMS patients as an add-on therapy in conjuction with Interferon-

beta or Glatiramer acetate, there was no visible impact in conventional MRI or clinical assessments. However, an MRI marker of myelination called magnetisation transfer ratio (MTR) showed a small positive effect of the drug compared to placebo at 48 weeks [248]. It is possible that a longer follow-up study or the participation of patients with more severe disease activity could yield interesting results for this drug. Finally, high-dose biotin may boost myelin repair by stimulating fatty acid synthesis, and may enhance neuroprotection via increased energy production in neurons [249, 250]. High-dose biotin (MD1003) was tested in a small randomised, double-blind, placebo-controlled trial in patients with progressive MS after a pilot study showing promising results [249, 251]. The new trial found that a significantly higher proportion (13%) of patients in the biotin treatment arm showed disability improvement at 9 and 12 months compared to the placebo arm. These results have led to a larger study currently underway, and suggest that biotin treatment may help a subset of progressive MS patients [251].

While these recent developments with pro-remyelinating drugs is encouraging, given the heterogeneity of lesions both within and across patients [164], it is likely that personalized medicine will play a role in future treatments of MS and different combinations of disease-modifying therapies and pro-remyelinating and/or neuroprotective targets may be important for effective treatment of individuals.

Table 3. Therapies for Multiple Sclerosis

Phase	Therapy	Mechanism of Action
Approved	Interferon-beta	Lowers levels of blood-brain barrier disruption Regulates immune cell function
	Glatiramer acetate	Modulates function of T cells
	Fingolimod	Reduces exit of T and B cells from Lymph nodes
	Teriflunomide	Lowers inflammation Reduces T cell infiltration
	Dimethyl Fumerate	Reduces inflammation
	Cladribine	Lowers T and B cell infiltration
	Natulizumab	Reduces T cell infiltration
	Alemtuzumab	Reduces T and B cell infiltration
	Ocrelizumab	Depletes B cells
Clinical trials	Clemastine fumerate	Anti-histamine with pro-regenerative effects Induces OPC differentiation and myelination
	GSK239512	Histamine H3 receptor agonist Stimulates OPC differentiation/remyelination
	MD1003	High-dose biotin May improve myelin production/repair

1.4.3 Identifying targets for remyelination therapy

Although some progress has been made, there are still no approved remyelination therapies, hence a global effort spanning academia and industry is focused on identifying regenerative therapy targets for multiple sclerosis. In order to do this, researchers are taking a candidate approach and studying specific signals regulating oligodendrocye responses required for remyelination, or using unbiased high-throughput screens allowing large libraries of small molecules or already approved drugs to be tested for effects on oligodendrocyte responses [26, 252]. While it is en-

couraging that these strategies have yielded several factors (some of which are listed in Table 2) shown to promote oligodendrocyte responses *in vitro*, and even in animal models, translating these preclinical findings to clinically relevant applications is a challenge. With the latter strategy, drugs being tested are already approved, thus easing their progression into clinical trials. The clemastine trial mentioned above is a good example of a drug identified in one such screen quickly being moved into relevant human testing [247]. In the former strategy, preclinical studies of candidate targets are hampered by the lack of a single appropriate disease model. Without an experimental animal model that recapitulates the intricate interactions between inflammation, regeneration, and neurodegeneration, promising preclinical targets can often flounder in clinical trials [26].

As targeting remyelination is a recent development on the clinical stage, there are a few aspects of trial design and outcome measurements that must be optimized. Major hurdles include a lack of ability to accurately measure remyelination in patients receiving therapy, as well as concerns about lesion heterogeneity and the consequences on effect size. Currently, the preferred way to measure myelin damage and repair in humans is through visually evoked potentials (VEP). This measure was used in both the clemastine and anti-LINGO-1 trials described above, and is often used as a diagnostic tool, even in patients without visual symptoms [253]. Since myelinated axons fire up to 100 times faster than unmyelinated axons, researchers can measure delays in firing responses to visual stimuli as an output of myelin damage in the anterior visual pathway [253–255]. Clearly, this is not an ideal measure of

remyelination, as it is indirect and focused only on one neuronal tract. To address this, two promising approaches are currently being developed: MRI-based magnetization transfer ratio (MTR, mentioned above) [256–258], as well as PET-based radiolabelled myelin-incorporating compounds [259, 260]. Additionally, identifying types of lesions within and across patients is important to administer the appropriate therapy. If a pro-differentiation drug is given to a patient with mostly lesions that lack progenitor cells, it will likely fail (and vice-versa). As different patients given a single treatment may have impairments at different stages of oligodendrocyte maturation, a drug that is effective for some yet fails in a subset of the group could contribute to an overall small effect size and a 'failed' trial. Advances in imaging techniques that would allow patient group stratification based on lesion type would greatly improve trial design and outcomes [26]. While strategies to improve these aspects of clinical trials are underway, it is important to continue the preclinical search for targets that may fulfil the unmet need of a regenerative therapy for MS.

One candidate approach for developing remyelination targets is identifying factors secreted by immune cells that could be contributing to inhibitory or permissive lesion microenvironments. As mentioned in section 1.3.4, CNS-resident microglia and peripherally-derived macrophages may exhibit anti-inflammatory, pro-regenerative properties, depending on their phenotype [46, 142, 235, 261, 262]. Early work from our lab showed that microglia and macrophages undergo a switch in phenotype during remyelination—from pro-inflammatory to anti-inflammatory—and that this shift drives OPC differentiation. The switch to anti-inflammatory factors is critical for

OPC differentiation, and a dysregulation in efficacy or timing in this switch could underlie the loss of remyelination potential in MS patients [142]. These findings suggest that identifying anti-inflammatory macrophage-derived factors and their downstream targets could be important for promoting remyelination.

1.5 Activin receptors and their ligands

1.5.1 Activin-A, the primary ligand for activin receptors, is an anti-inflammatory macrophage-derived factor

Previous work by Miron and colleagues identified activin-A as an anti-inflammatory macrophage-derived factor having a role in remyelination: i) its expression increases during remyelination *in vivo*, ii) it promotes OPC differentiation in primary cultures, and iii) blocking its action in microglia-conditioned media led to a reduction in mature oligodendrocytes in *ex vivo* brain slice cultures [142, 263]. In addition to promoting differentiation in primary OPC cultures, unpublished work from our lab suggests that activin-A can also promote OPC proliferation and survival at different concentrations. Further, activin-A is present in the cerebrospinal fluid of human MS patients at a slightly increased concentration, indicating its possible relevance in the neurodegenerative disease [264, 265].

Activin-A is a growth factor in the TGF-β superfamily; it is a homodimer composed of two β_A subunits linked by a single disulfide bond. Two other functional activins exist: activin-B (two β_B subunits) and activin-AB (a heterodimer of β_A and

β_B subunits) [266]. These activins are structurally similar but functionally different, as *in vitro* assays have demonstrated distinct potency and cellular outcomes [267]. Additionally, when transgenic mice with a β_A knockout were modified to substitute β_B into the β_A locus, some effects of β_A knockout were rescued—albeit not fully, suggesting that the β_B subunit could not completely compensate for the functions of β_A [268]. Activin-A is the best characterized member of the activins, and while it was originally identified as a reproductive factor, it has since been shown to be involved in inflammation and repair in many systems [265, 269]. Specifically, activin-A is expressed during inflammation and modulates the immune response via cytokine release and production of nitric oxide [266].

In the CNS, activins and other TGF-β ligands are widely expressed and required at many stages of development [270]; importantly, they have been shown to be relevant during myelination and oligodendrocyte development (discussed further below) [271, 272]. Activin-A has also been shown to be neuroprotective following oxygen-glucose deprivation to a neuronal cell line *in vitro* [273], as well as essential for neurogenesis following excitotoxic-induced neurodegeneration *in vivo* [274]. Further, activin-A promotes astrocyte differentiation from CNS progenitors *in vitro* [275], as well as supports neuronal differentiation of cortical neuronal progenitor cells [276]. In the healthy brain, activin signaling is involved in synaptic plasticity, cognition, and behaviour (summarized in [277]). Impaired activin signaling has been associated with a variety of neurodegenerative diseases (summarized in [278]). Specifically, mouse models of Huntington's and Parkinson's disease (excitotoxic quinolinic acid

model and 6-hydroxydopamine model, respectively) treated with activin-A exhibited neuroprotective effects [279, 280]. The mechanism underlying this neuroprotective effect was found to be an important synergistic interaction between brain-derived neurotrophic factor (BDNF) and activin-A. In essence, activity-dependent BDNF signalling leads to increased production of activin-A via synaptic NMDA receptors, which then negatively regulate extrasynaptic NMDA receptors. As neuronal health is in part dictated by the balance between synaptic NMDA signalling (pro-survival) and extrasynaptic NMDA signalling (pro-death), a disturbance in the interplay between BDNF and activin-A could lead to the neuronal pathogensis seen in these disorders [278, 281].

Clearly, activin-A is an important growth factor during development and repair in the CNS, and further study of its binding partners and downstream effects is key to understanding its potential use in therapeutics.

1.5.2 Activin receptor expression and mechanism

Activin-A binds with high affinity to serine-threonine kinase type II activin receptors Acvr2a and Acvr2b. Once bound, this leads to the transphosphorylation and activation of the type I co-receptor Acvr1b, which results in downstream signalling [270] involving pathways previously associated with driving OPC proliferation, differentiation, survival and myelination (including the canonical Smad2/3, and non-canonical PI3K, p38, MAPK, ERK1/2, and Rac/Cdc42 pathways—see Figure 3) [272, 282–286]. Activin receptors are extensively expressed in the CNS and are

important during development and injury. Specifically, activin receptors have been shown to be expressed on axons during embryonic development and following excitotoxic injury in adult rodents, both *in vitro* and *in vivo* [274, 276]. Further, there is *in vivo* experimental evidence showing that activin receptors 2a, 2b, and 1b are expressed on OPCs and microglia/macrophages in remyelinating lesions [142], and microarray data suggest that this expression is upregulated during remyelination [81]. Taken together, this evidence indicates a potential role for activin receptors in white matter neurodegenerative diseases.

Like many of the receptors of the TGF-β superfamily, activin receptor activity is tightly regulated both by inhibitory ligands such as inhibin and follistatin, as well as auto-inhibitory feedback mechanisms (inhibitory Smads, Smad6 and Smad7, see Figure 4) [286, 287]. Inhibin is a heterodimer made up of two subunits (α and β_A) and directly competes with activin-A to bind the receptors and block downstream signalling [288]. Follistatin works by sequestering the activin-A ligand and preventing its binding to the activin receptors [287]. Therefore, blocking the activity of activin receptors using these two different inhibitors can elucidate the role of the primary ligand versus the role of the receptors.

Activin receptor subtypes have different binding affinities for ligands. Acvr2b shows a higher affinity for activin-A compared to Acvr2a [304]; however, Activin receptors can also bind other ligands in the TGF-β superfamily including myostatin, bone morphogenic proteins (BMPs), growth and differentiation factors (GDFs), and nodal (Table 4) [305]. Binding affinity of activin receptors for their many ligands

Table 4. Ligands with affinity for activin receptors

Ligand	**Role in CNS**	**Antagonists**	**Mouse CNS Expression**				
			A	N	O	M	E
Activin-A	Inflammation & repair Neurogenesis Neuroprotection Astrocyte differentiation Neuronal differentiation Synaptic plasticity Oligodendrocyte responses Myelination [142, 273–277]	Inhibin Follistatin	✓	✓	✓	✓	
Activin-B	Oligodendrocyte responses Myelination [272]	Follistatin	✓	✓	✓		✓
Nodal	Neural tube patterning Forebrain maintenance Stem cell maintenance [289]	Lefty-1					✓
GDF-1	Forebrain development Developmental differentiation [290]	Lefty-1		✓			
GDF-5	Neuroprotective Maintenance & development of dopaminergic neurons [291, 292]	Grem2		✓			
GDF-8/ Myostatin	Associated with olfactory system [293]	GASP-1 GASP-2		✓			
GDF-11	Neurogenesis Spinal cord patterning [294–296]	GASP-1	✓	✓	✓		
BMP-2	Cortical development Neuronal differentiation Astrocyte differentiation Inhibitor of oligodendrocyte differentiation [297]	Chordin Noggin		✓	✓	✓	✓
BMP-6	Reduces ischemic brain injury Implicated in defective neurogenesis [298, 299]	Sclerostin		✓	✓		
BMP-7	Neuroprotective in stroke models Eye development [300, 301]	Noggin	✓	✓	✓		
BMP-15	None known	None known	✓		✓		✓

All data in *Mouse CNS Expression* column reflects levels in P7 developing mouse brain and was obtained from Barres RNASeq database [302] and from the literature [303]. A=Astroyctes, N=Neurons, O=Oligodendrocyte lineage cells, M=microglia, E=Endothelial cells.

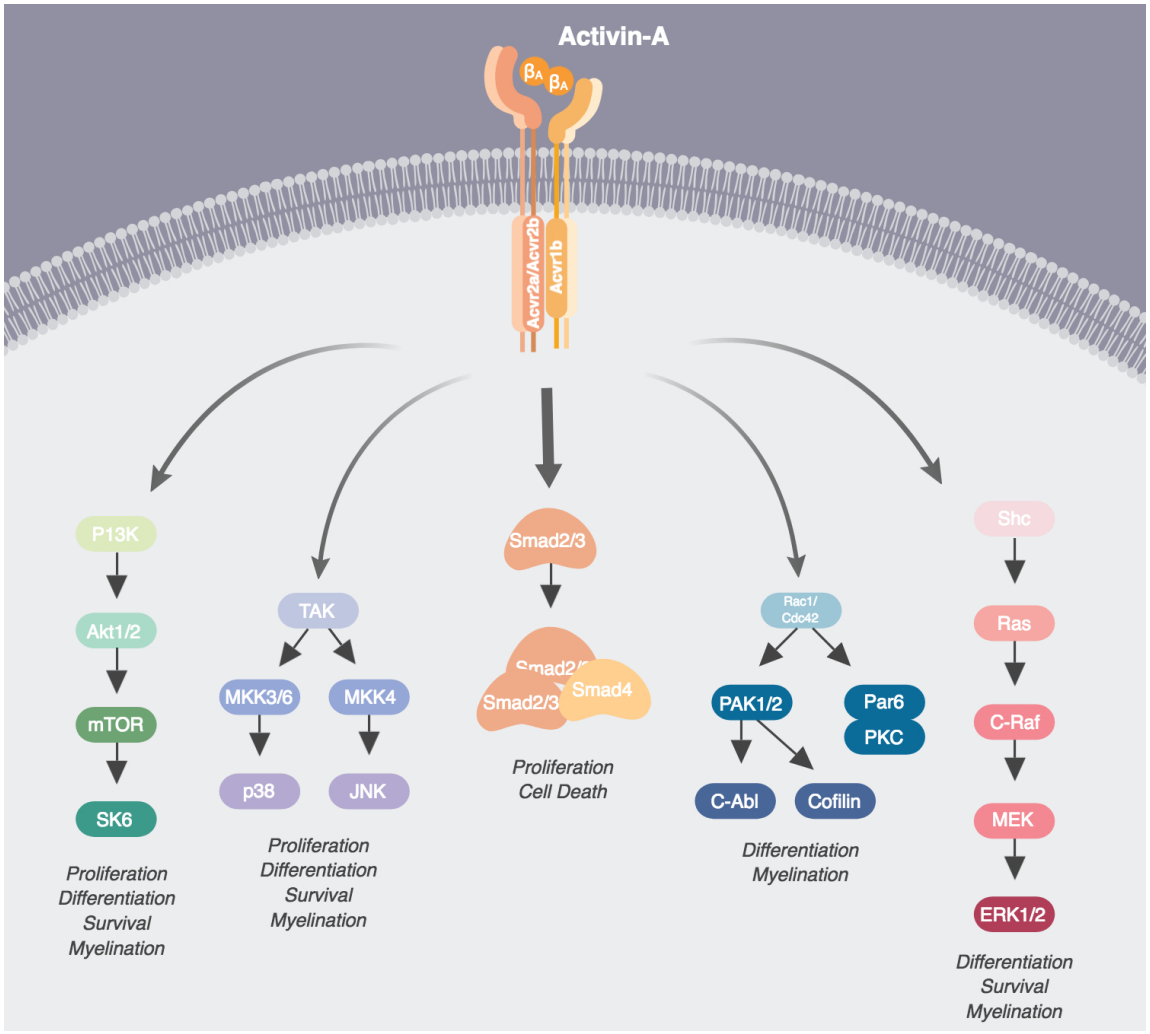

Figure 3. Activin receptors drive signalling implicated in remyelination.

is not the only factor dictating downstream cellular responses. Several factors, including availability and concentration of ligand, microenvironment, and endogenous modulators of signalling are involved in the determining the many possible outcomes of activin receptor activation.

1.5.3 Determinants of TGF-β/activin receptor activation and outcome

The TGF-β superfamily is an enormously complex group of proteins, receptors, co-receptors, and downstream effectors. Considering the family contains over 30 ligands—spanning transforming growth factors (TGFs), bone morphogenic proteins (BMPs), and growth and differentiation factors (GDFs), among others—as well as 5 type II receptors and 7 type I receptors, there are an overwhelming number of interaction possibilities [286, 306, 307]. Since their discovery nearly 40 years ago, researchers have been working to dissect the many functions and roles of TGF-β family members, which include cell proliferation, differentiation, and morphogenesis, as well as tissue homeostasis and regeneration. Some of these roles seem paradoxical; indeed, many different and sometimes opposing effects have been reported for the same TGF-β ligand [307]. The signalling mechanisms of TGF–β superfamily receptor activation have been largely elucidated, and are relatively straight-forward: a subset of oligomeric receptor-ligand complexes activate Smad1/5/8 phosphorylation (generally BMPs), and another subset activate Smad2/3 (generally activins, GDFs, and TGF-βs). These Smads, termed receptor-activated Smads (R-Smads), form a trimeric complex with a common Smad (Smad4) and translocate to the nucleus, exerting downstream effects by regulating gene expression. As mentioned above, Smad6/7 are auto-inhibitory Smads that disrupt these trimeric complexes and polyubiquitinate Smad proteins and type I receptors for subsequent degradation (Figure 4) [286, 307]. However, within this relatively simple mechanistic framework,

the outcome can be one of many discrete cellular responses. Clearly, cellular context is an important determinant of the response to TGF-β superfamily signalling.

Contextual features influencing TGF-β signalling include factors regulating signal transduction, gene transcription, and epigenetic status. In terms of signal transduction, there are several extracellular variables that determine the degree of receptor stimulation, including: level of ligand expression, ligand-trapping proteins (such as follistatin [287], GASP-1, Sclerostin, and Noggin [308]), antagonistic ligands (such as inhibin [288]), available receptor subtypes, and presence of accessory receptors (such as betaglycan, which can present inhibin ligand to activin receptors [309]). Transcription factors can also modulate TGF-β signalling, as availability of protein binding partners determines which genes are targeted and how their expression is affected. Finally, the epigenetic status of the cell, such as DNA methylation status and histone modifications, will control which genes are amenable to expression changes. For example, when a cell is differentiating, genes involved in differentiation will be 'open', allowing transcriptional machinery downstream of TGF-β signalling to engage [307]. If this cell receives an aberrant input to activate proliferation genes, the epigenetic landscape may hinder expression of those target genes. Taken together, these contextual cues confer a level of specificity to the pleiotropic effects triggered by members of this protein superfamily.

Several studies have been carried out to elucidate the many contextual possibilities dictating the overall effect of activin receptor signalling on the cell [269, 277, 278, 288, 310, 311]. Table 4 lists all known ligands with binding affinity for activin

receptors 2a and 2b, their CNS-specific roles, cell-type specific expression during development, as well as known modulators of signalling. Given the level of complexity of both intracellular and extracellular factors affecting signal transduction within this superfamily, we must be careful not to generalize findings from the effects of a ligand in one specific set of circumstances. It is important to clearly define the conditions under which a TGF-β ligand is studied, and to understand that the same ligand could have different—even opposing—effects under different conditions.

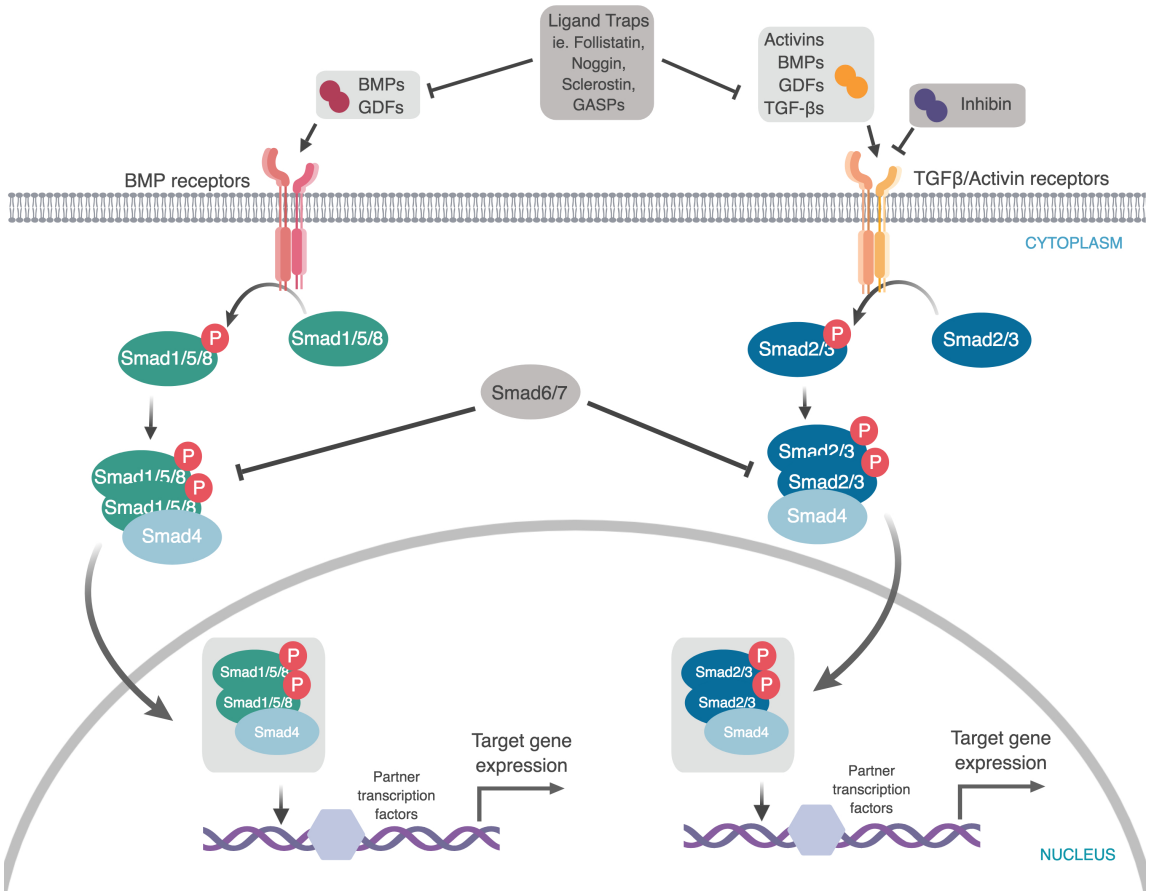

Figure 4. Agonists and antagonists of canonical TGF-β superfamily signalling.

1.5.4 TGF-β superfamily in myelination and myelin disorders

In the CNS, some TGF-β ligand/receptor complexes have been shown to regulate oligodendrocyte lineage cells and myelination [270, 312, 313]; specifically, recent papers show that TGF-β and activins are important for developmental myelination and oligodendrocyte maturation [271, 272].

TGF-β signalling in oligodendrocyte development

One study [272] sought to determine the role of TGF-β and activins in oligodendrocyte development and myelination. To address this, the authors first investigated the expression of TGF-β ligands, receptors, and their canonical downstream effectors in the developing mouse spinal cord by immunohistochemistry, and found that in early embryonic development (E12.5), TGF-β1 ligand and both TGF-β receptor 2 (TGFβRII) and Acvr2b were present on Olig2$^+$ oligodendrocytes in the periventricular zone, accompanied by phosphorylated Smad3 (pSmad3, the active form of Smad3 signalling). No activin-B or activin-A was detected at this time. By late embryonic development (E14.5) and up to postnatal day 5 (P5), oligodendrocyte-specific pSmad3 expression overlapped with both TGF-β1 and activin-B ligand, as well as their respective receptors. This progressive overlap in Smad3 and ligand expression suggests that TGF-β1 mediates Smad3 signalling in early oligodendrocyte development, and late development is mediated by both TGF-β1 and activin-B. Indeed, these differences in expression are reflected in distinct signalling profiles induced by the two ligands in oligodendrocyte cultures (both Oli-Neu cell lines and

primary OPCs). Importantly, these signalling profiles also correlated with distinct functional outcomes. Specifically, when primary OPC cultures were treated with TGF-β1 alone, the authors observed a decrease in apoptosis (by caspase-3 staining), an increase in BrdU$^+$Olig2$^+$ proliferating cells, as well as an increase in total number of Olig2$^+$ oligodendrocytes. When cultures were treated with activin-B alone, an increase in number of mature MBP$^+$ oligodendrocytes was observed. When both treatments were administered together, there was a combinatorial effect, including a strong reduction in apoptosis, a higher number of total Olig2$^+$ cells, and an increase in both proliferating and mature oligodendrocytes. Further, in oligodendrocyte/neuron co-cultures, while activin-B treatment alone was sufficient to enhance myelin formation, co-treatment with TGF-β resulted in an additive effect. Finally, in activin-B (*Inhbb*$^{-/-}$) knock-out mice, a transient impairment in embryonic oligodendrocyte development was detected; however, by P5 there were no differences in myelination. In *Smad3*$^{-/-}$ knock-out mice, a more severe phenotype was observed, with delays in myelination persisting until P28. Together, these results provide a potential model for TGF-β superfamily ligands contributing to oligodendrocyte development in the spinal cord via Smad3 signalling [272].

The results of this study are supported by previous literature highlighting the importance of TGF-β in oligodendrocyte development and myelination [270, 312, 313]. Interestingly, the the authors mentioned in their discussion that activin-A treatment provided similar results to activin-B in their oligodendrocyte cell cultures, which is divergent from two previous studies implicating activin-A and TGF-β1 in

oligodendrocyte apoptosis [314, 315]. The reason behind this mismatch is unclear; however, both of these studies focussed on cell culture assays, and given the pleitropic and context-dependent effects of this superfamily, caution must be taken when interpreting these results. An additional point to consider is the differences between the activin-B and Smad3 knock-out animals [272]. It is possible that the activin-B ligand knock-out had less severe effects due to compensatory effects from activin-A, compared to the Smad3 knock-out which ablates signalling of both activins. Given their results from treatment of oligodendrocyte cultures were similar across activins (this data was not shown but mentioned in the discussion), it would have been interesting to know whether activin-A is expressed post-natally in the developing spinal cord, and to test whether a compensatory mechanism is responsible for the observed differences between activin-B and Smad knock-out. Finally, while the authors provide good evidence for roles of different ligands in the TGF-β superfamily during myelination, they do not directly manipulate the receptors, and thus do not address the question of which receptor (TGF-β or activin) mediated the observed effects.

TGF-β signalling in oligodendrocyte differentiation

Interestingly, another study also found that TGF-β signalling was important for oligodendrocyte development and myelination, but due to its effects on differentiation, not proliferation [271]. Despite the differences in proposed mechanisms between this study and the one discussed above—which could be due to distinct myelination programs across brain regions [1] or embryonic vs post-natal differences—both studies confirm an important role for TGF-β in developmental myelination. Consistent

with this study, there is much evidence for the anti-proliferation, pro-differentiation role of TGF-β in many systems [316–320]. The authors elegantly demonstrated the role of TGFβRII in promoting oligodendrocyte differentiation and myelination in subcortical white matter via loss-of-function and gain-of-function experiments both *in vivo* and *in vitro* [271]. Using PCR and Western blot techniques, the authors first characterized the expression of TGF-β ligands, receptors, and downstream Smads during subcortical white matter development in mice (between P8-P60), and found that the expression profiles of these factors coincided with the transition of oligodendrocytes from progenitors to pre-myelinating cells. Next, the authors administered TGF-β1 ligand to both OPCs *in vitro* and systemically to P5 mice, and observed accelerated differentiation and myelination, along with higher levels of myelin proteins MBP, CNP, and MOG. This effect was blocked when TGF-β1 treatment was administered with a TGFβRII antagonist, suggesting this receptor mediates the effects seen with TGF-β1. Further, when this receptor was genetically deleted in OPCs using two different inducible Cre drivers (PDGFα-Cre and NG2-Cre), the authors noted a decease in number of mature oligodendrocytes, an increase in OPCs, and a decrease in mature myelin markers MBP, CNP, and MOG. Additional experiments found that this effect was due to a regulation in cell cycle exit by TGF-β signalling—specifically, Smad2/3 activation by TGF-β leads to nuclear localization via Smad4; this complex then cooperates with transcription factors FoxO1 and Sp1 to modulate transcription of anti-mitotic target genes (*c-myc* and *p21*) involved in regulating cell cycle exit and differentiation. Importantly, the authors found that this effect

was cell-autonomous: when TGF-β1 was administered to mice lacking TGF-βRII in OPCs, there was no effect on oligodendrocyte differentiation or myelination, despite the presence of these receptors on other cell types (microglia and astrocytes). All together, this data suggests an important role for the TGF-β pathway in oligodendrocyte responses and developmental myelination. As such, it has been speculated that disruption of these pathways could be involved in myelin and neurodegenerative disorders of the CNS.

Negative myelination effects of some TGF-β ligands

Consistent with this, members of the TGF-β superfamily have been implicated in myelin destruction and repair. Interestingly, BMP4 has been shown to have an inhibitory effect on oligodendroglial differentiation in a cuprizone model of demyelination [321]. Specifically, the authors found that an increase in BMP signalling (identified by pSmad1/5/8$^+$ staining) following cuprizone-induced demyelination *in vivo* was blocked by administration of Noggin, a BMP4 antagonist, and this resulted in an increase in density of mature oligodendrocytes and improved remyelination. Conversely, exogenous BMP4 administration resulted in higher pSmad1/5/8 signalling, and an increase in BrdU$^+$ proliferating oligodendrocytes during demyelination followed by a decrease in oligodendrocyte density during recovery. While the authors observed increased numbers of astrocytes during recovery in BMP4 treated animals, they found that these cells did not originate from the BrdU$^+$ proliferating oligodendrocytes. Rather, their results suggest that BMP4 treatment promoted oligodendrocyte apoptosis via caspase-3 during recovery. This evidence suggests that

while BMP-driven Smad1/5/8 signalling seems to promote proliferation of OPCs, its downregulation during myelin injury could be beneficial for oligodendrocyte differentiation and myelination.

Additionally, a recent investigation into the effects of the coagulation factor fibrinogen on oligodendrocyte progenitors and remyelination found that *in vitro*, fibrinogen inhibits oligodendrocyte maturation and myelination via activation of Smad1/5/8-mediated BMP signalling in OPCs [322]. These effects were reversed using a BMP type I receptor (Acvr1) inhibitor, but not a BMP ligand inhibitor, suggesting that fibrinogen exerts its effects in a BMP-ligand independent manner. The authors also found that *in vivo*, fibrinogen depletion resulted in a decrease of Smad1/5/8 accumulation in the nucleus and enhanced remyelination [322]. These results are in line with previous research suggesting the inhibitory role of BMPs in myelination and remyelination [323–326].

Addressing the pleiotropic effects of TGF-β signalling

Taken together, the results of these studies provide evidence for divergent effects of members of the TGF-β superfamily on oligdendrocyte lineage cells, myelination, and remyelination. Specifically, the evidence to date suggests opposing effects on OPC proliferation and differentiation for Smad1/5/8-mediated signalling versus Smad2/3-mediated signalling. However, as mentioned above, the ultimate cellular response resulting from activation of either pathway is complicated by the many regulatory mechanisms both upstream and downstream of Smad signalling. Starting with the ligand-receptor interaction, there are several factors in the extracellular

environment that determine whether a ligand will bind a particular receptor, including availability of the ligand, concentration of the ligand compared to antagonists, and concentration of competing ligands. Once a specific ligand has bound a type II receptor, the downstream signalling events are mediated by a type I receptor, which may activate either canonical (Smads) or non-canonical (see Figures 3 and 4) pathways, eliciting a number of potential responses. As mentioned above, Smad-mediated pathways are controlled by inhibitory Smads (Smad6/7), which can negatively regulate signalling post ligand-binding. Taking into account the many roles identified for TGF-βs, it is not surprising that these pathways are finely tuned—in fact, the pleiotropic and context-dependent effects of this superfamily are likely a result of this feature.

Therefore, given the diverse potential effects of TGF-β-mediated signalling, it is crucial to understand the function and mechanism of these various protein/receptor interactions and their downstream effectors in context. In terms of elucidating how this superfamily influences myelination and remyelination, it is important not to make assumptions or generalizations based on any individual model, receptor, or ligand. While the previous literature has focused on a handful of ligands (activin-B, BMP4, TGF-β1) and receptors (TGFβRII, BMPRII, Acvr1, Acvr1c), the role of activin-A and its receptors (Acvr2a, Acvr2b, and Acvr1b) in myelination and remyelination remains unexplored.

Our lab, including my own work, was the first to identify activin receptors 2a and 2b as important regulators of oligodendrocyte lineage cell responses in health

and disease across the lifespan [327]. Parts of this thesis have been published in our paper (see Appendix), and results will be discussed in relevant chapters.

1.6 Aims of Thesis

Given the evidence suggesting activin-A and activin receptors could have a regenerative role in the CNS, and specifically in the regeneration of myelin, my PhD project sought to determine whether activin receptor modulation could be a therapeutic target for regeneration in demyelinating diseases.

Hypothesis: Activin receptors are required to drive remyelination, and ligands binding these receptors can be used to enhance remyelination.

Aims:

1. Assess the requirement of activin receptors during remyelination

2. Identify alternative activin receptor ligands and elucidate their involvement in remyelination

3. Determine the mechanism of action of activin receptors in remyelination

2 Chapter 2: Materials and Methods

2.1 Animals used and ethics statements

CD1 wild-type mice were utilised for organotypic cerebellar slice culture experiments. For *in vivo* lesioning experiments, 8-12 week old male C57Bl/6J mice from Charles River Laboratories were purchased. Transgenic mice used include Smad2/3 reporter mice (pR26-228 AR8-TA-mCherry; henceforth described as AR8-mCherry) purchased from Jackson Laboratories, as well as MacGreen macrophage/microglial reporter mice (B6N.Cg-Tg(Csf1r-EGFP)1Hume/J), which were bred to AR8-mCherry mice and used for live imaging experiments (referred to as AR8-mCherry/MacGreen). All experiments were of moderate severity, and performed under the UK Home Office project licenses issued under the Animals (Scientific Procedures) Act. For *in vivo* experiments, adult male mice were utilized to reduce hormonal effects. When using osmotic pumps to administer compounds, animals were single-housed post surgery in closed-top cages to minimize injury. In experiments where pumps were not used, mice were group-housed, with 4-5 mice in each open-top cage. Mice were randomized before surgery, and blinded post-perfusion. In all experiments a minimum of 3 and a maximum of 6 mice were used per condition.

2.2 Genotyping

Genomic DNA was extracted from ear or tail tissue using the Wizard SV genomic purification system (Promega) according to the manufacturer's instructions.

AR8-mCherry mice were genotyped according to Jackson Laboratories' instructions. Briefly, standard PCR was performed with primers 16938 (ACGTTTCCGACTTGAGTTGC) and 16939 (AATACTCCGAGGCGGATCAC). MacGreens were genotyped using primers primers 79 (ATCATGGCCGACAAGCAGAAGAAC) and 80 (GTACAGCTCGTCCATGCCGAGAGT).

2.3 Animal models of remyelination

Organotypic cerebellar slice cultures. Brains from P0-P3 wildtype CD1, AR8-mCherry, and AR8-mCherry/MacGreen mouse pups were extracted followed by the isolation of hindbrain and cerebellum, and sectioned into 300μm sagittal slices using a McIlwain tissue chopper (as previously described in [142]). Six slices were plated onto Millipore-Millicel-CM mesh insert (Fisher Scientific) placed into 6-well plates with 1 ml slice culture media per well. Each well contained slices from one animal only. Media was changed every 2-3 days, and composed of 50% minimum essential media, 25% heat-inactivated horse serum, 25% Earles balanced salt solution (all from GIBCO), 1% penicillin-streptomycin, 1% glutamax, and 6.5 mg ml^{-1} glucose (all from Sigma). At 21 days *in vitro*, demyelination was induced via lysolecithin (0.5 mg ml^{-1}, Sigma) in media for 18-20 hours. Slices were washed in media for 10 minutes and left for 2 days to recover. Experiments were then either left untreated, or treated with Activin receptor ligands (both inhibitors and stimulators of receptor activity, all treatments listed in Table 5). Treatment was administered with every media change until 7, 10, or 14 days post lysolecithin (dpl). Slices were then fixed

in 4% Paraformaldehyde (PFA) in PBS for 10 minutes.

Table 5. Treatments used in *ex vivo* and *in vivo* experiments.

Treatment	Effect	Control	Concentration	Company	Cat No
Activin	Acvr agonist	4mM HCl	100 ng/ml	R&D	338-AC-010
Inhibin	Acvr antagonist	4mM HCl	100 ng/ml	R&D	8346-IN-010
Follistatin	Activin inhibitor	0.1%BSA in PBS	10 ng/ml	R&D	769-FS-025
α-Activin-A Antibody	Activin inhbitor	Goat IgG	5 μg/ml	R&D	AF338
BMP6	Acvr ligand	4mM HCl	100 ng/ml	Creative BioMart	bmp6-28M
GDF11	Acvr ligand	4mM HCl	100 ng/ml	R&D	1958-GD-010
GDF1	Acvr ligand	PBS	100 ng/ml	MyBioSource	MBS2012351
Sclerostin	BMP6 inhibitor	0.1%BSA in PBS	100 ng/ml	R&D	1589-ST-025
GASP-1	GDF11 inhibitor	0.1%BSA in PBS	100 ng/ml	PeproTech	120-41
Lefty-1	GDF1 inhibitor	0.1%BSA in PBS	100 ng/ml	R&D	994-LF-025

***In vivo* corpus callosum lesion model.** 8-12 week old male C57BL/6J mice were anaesthetised using Isofluorane and given an analgesic (Vetergesic/Rimadyl, mixed at a 2:1 ratio, administered at 0.06ml subcutaneously per mouse). To prevent eye dryness during surgery, animals were given one drop of a lubricating ointment (Lacri-lube, Refresh) per eye. Using a diamond-tipped drill, a marker hole was made in the skull at Bregma and a burr hole made at 1.2mm posterior and 0.5mm laterally to the right. Demyelinating lesions were induced in the corpus callosum of mice by stereotaxic injection of 1% lysolecithin using a Hamilton syringe. Sham lesions

were induced by phosphate-buffered saline (PBS) injection. The Hamilton syringe was loaded on the rig with either compound, and inserted into the burr hole at 1.4mm ventral to the surface of the skull. A total 2μl of compound was injected into the brain at 0.5μl per minute. In experiments where mice were given a treatment post-lesion, implantable osmotic infusion pumps were used (Alzet/Durect). Pumps were inserted subcutaneously in a small pocket created by blunt dissection from an incision between the scapulae. A polyethylene tube connected the micro-osmotic pumps to a brain catheter, which was inserted into the lesion site and glued onto the skull. Mice were then sutured using Mersilk 6-0 (Ethicon). The pumps released 0.11μl of compound per hour for up to 28 days. Treatments administered include Activin-A, Inhibin, GASP-1, Sclerostin, and Lefty-1, with their respective controls and at the same concentrations listed in Table 5. Mice were intracardially perfused at 3, 7, 10, 14, and 21 days post lesion (dpl) with (i) PBS for subsequent lesion dissection and RNA extraction, (ii) 4% paraformaldehyde (PFA, wt/vol, Sigma) for immunohistochemical assays, or (iii) 4% PFA with 2% glutaraldehyde (vol/vol, TAAB Laboratories) in 0.1M phosphate buffer for electron microscopy embedding.

2.4 Immunofluorescent staining and imaging

Organotypic cerebellar slice cultures. Fixed explants were blocked (0.3% TritonX and 5% heat-inactivated horse serum in PBS) for 1 hour at room temperature and primary antibody applied for 2 nights overnight at 4°C. Primary antibodies used are listed in Table 6. Slices were washed twice in PBS-0.1% TritonX before apply-

ing fluorescently conjugated secondary antibodies (AlexaFluor, Life Technologies, 1:500) for 2 hours at room temperature. Following counterstaining with Hoechst for 10 minutes (1:1000), slices were washed 3 times in PBS-0.1% TritonX before being mounted with Fluoromount-G (Southern Biotech) on glass slides and coverslipped, or in 96-well plates with Coverglass base (Thermo). Z-stacks were captured using the Olympus spinning disk confocal microscope (60x and 30x silicone oil objective) and SlideBook software (3i). Images were cropped to 14 slices (0.59 μm/slice) in SlideBook (3i) and exported as TIFFs. TIFF files were blinded and imported into Volocity (Perkin Elmer) as an image sequence. A measurement protocol was used to quantify voxels in each channel as well as overlapping voxels between channels. Remyelination index was calculated by normalizing colocalization values (MBP^+NF^+) to NF^+ voxel counts, and this value for treated slices was further normalized to vehicle controls. All data was compiled and managed in Microsoft Excel, and statistical analyses were performed in GraphPad Prism.

***In vivo* corpus callosum lesions.** Brains from animals intracardially perfused with 4% PFA (wt/vol, Sigma) were post-fixed overnight and cryoprotected in sucrose prior to embedding in OCT (Tissue-Tech) and stored at -80°C. 10 μm tissue cryosections were air dried then blocked (0.3% TritonX and 5% heat-inactivated horse serum in PBS) for 1 hour at room temperature. Primary antibodies were applied overnight at 4°C (listed in Table 6). Sections were washed three times in PBS before applying fluorescently conjugated secondary antibodies (AlexaFluor, Life Technologies,

1:500) for 2 hours at room temperature. Following counterstaining with Hoechst for 10 minutes (1:1000), sections were washed 3 times in PBS before being coverslipped with Fluoromount-G (Southern Biotech). Single plane images were captured using the Olympus spinning disk confocal microscope (60x and 30x silicone oil objective) and SlideBook software (3i). Images were exported as TIFFs.

Human Multiple Sclerosis tissue. Post-mortem tissue from multiple sclerosis patients and non-neurological controls were obtained. Diagnosis of multiple sclerosis was confirmed by neuropathological means. Post-mortem delay (time from death to tissue preservation) was 7-31 hours. Frozen unfixed tissue blocks (2x2x1 cm) were cut at 10 μm and stored at -80 °C by laboratory technicians in the Williams, ffrench-Constant (SCRM) and Miron groups. Multiple sclerosis lesions were classified by neurologist Anna Williams according to the International Classification of Neurological Disease using luxol fast blue staining and $CD68^+$ immunoreactivity. We analyzed 4 control blocks and 10 tissue blocks from 8 multiple sclerosis patients; in total, we analysed 7 active lesions, 10 chronic active lesions, 8 chronic inactive lesions and 23 remyelinated lesions. See Table 7 for further details on human post-mortem tissue. Sections were fixed in 4% PFA for 1 hour at room temperature, washed in TBS, and permeabilized in methanol for 10 minutes at -20°C. Following washes in 0.1% Tween20 (vol/vol) in TBS, sections were microwaved in Vector unmasking solution for 10 minutes on medium power, washed once with TBS/Tween20 and endogenous phosphatase and peroxidase activity blocked for 10 minutes (Bloxall,

Vector). Primary antibody was prepared in 2.5% Normal Horse Serum (Vector) and applied overnight in a humid chamber at 4°C. Primary antibodies used are listed in Table 6. Following three washes in TBS, alkaline phosphatase-conjugated secondary antibody to mouse or rabbit was applied for 30 minutes at room temperature in a humid chamber. Sections were washed in TBS and stains were visualised by Vector Blue substrate kit used as per the manufacturer's instructions. After three further TBS washes, the sections were blocked to quench any remaining phosphatase activity (Bloxall, Vector) and the next primary antibody was applied as above. The second primary antibody was developed using Vector Red substrate kit according to the manufacturer's instructions. Following washes in water, the sections were counter-stained with Hoechst (1:10000) for one minute and coverslipped with Fluoromount-G. Slides were imaged using Zeiss AxioScan SlideScanner. Images were prepared using Zeiss Zen2 software. Lesions were identified using luxol fast blue maps of each tissue (provided by Anna Williams). Fields of 360 μm x 360 μm were counted per lesion and counts were multiplied to determine density of immunopositive cells per mm^2.

Table 6. Primary antibodies used for immunofluorescence.

Antigen	Species	Dilution	Company	Cat No
Myelin Basic Protein (MBP)	Rat	1:250	AbD Serotec	MCA409S
Olig2	Mouse	1:100	Millipore	MABN50
Olig2	Rabbit	1:100	Abcam	AB9610
Neurofilament-H	Mouse	1:1000	EnCor	MCA9B12
β-tubulinIII	Mouse	1:400	Sigma-Aldrich	T8578-200UL
Activin receptor IIA	Rabbit	1:100	Invitrogen	PA5-13886
Activin receptor IIB	Rabbit	1:100	Invitrogen	PA5-13888
Activin receptor IB	Rabbit	1:100	Abnova	PAB18053
CD68 [FA-11]	Rat	1:100	Abcam	AB53444
CD68	Mouse	1:100	Dako	M0814
GFAP	Chicken	1:1000	Covance	Z0334
PU.1 [D-19]	Goat	1:100	Santa Cruz	SC5949
GDF1	Rabbit	1:50	Abcam	AB139721
GDF11	Rabbit	1:100	Biorbyt	ORB101175
BMP6	Rabbit	1:100	Novus	NBP1-19733

Table 7. Postmortem Multiple Sclerosis lesion tissue.

	Classification	Sex	Age	Disease duration (yrs)	Block	Lesions Analyzed			
						Active	Chronic Active (rim)	Chronic Inactive	Remyel-inated
MS Cases	SPMS	M	44	10	1	1	0	2	0
	SPMS	M	40	9	1	1	0	1	3
					2	1	3	2	2
	PPMS	M	37	27	1	0	1	1	5
	SPMS	F	57	27	1	0	0	0	4
	SPMS	F	46	25	1	0	1	1	5
					2	0	2	0	0
	SPMS	F	42	19	1	2	0	0	2
	SPMS	F	49	14	1	2	1	0	0
	SPMS	F	57	19	1	0	2	1	2
TOTAL						**7**	**10**	**8**	**23**
Controls	Carcinoma of the tongue	M	35	-	1	-	-	-	-
	Myelodys-plastic syndrome, RA	M	82	-	1	-	-	-	-
	Cardiac failure	M	64	-	1	-	-	-	-
	Ovarian cancer	F	60	-	1	-	-	-	-

2.5 RNA extraction, reverse transcription, and RT-qPCR

Organotypic cerebellar slice cultures. Slices were washed with PBS, lysed with RLT buffer supplemented with β-mercaptoethanol, scraped, and homogenized with 21 gauge needles. RNA extraction was performed using the Qiagen minikit (with on-column DNase treatment), and reverse transcription performed using the Invitrogen Superscipt First-strand synthesis system for RT-PCR, both according to the manufacturer's instructions. A custom quantitative PCR array plate (Qiagen) was designed to include genes for TGF-β family members that have a binding affinity for Activin receptors. Quantitative PCR was carried out using the ABI7900HT Standard. Ct values were obtained using the second derivative maximum method and ΔCt was calculated by subtracting average value from a housekeeping gene (*Actb*). Expression is represented as $2^{-\Delta Ct}$.

***In vivo* corpus callosum lesions.** Brains were dissected from PBS perfused mice (as described above in 2.2) and using a brain matrix, a 2mm coronal section was cut and placed in cold PBS. The lesion area was dissected and homogenized using a glass dounce (Wheaton) and QIAshredder tubes (Qiagen). RNA extraction was performed using the Qiagen All-Prep kit (with on-column DNase treatment), and reverse transcription performed using the Invitrogen Superscript First-strand synthesis system for RT-PCR, both according to manufacturer's instructions. Custom plates and qPCR methods were identical to the ones listed above.

2.6 Protein extraction and Western blotting

Organotypic cerebellar slices were washed with PBS, scraped and collected in 1mL 4°C PBS, and homogenized with 21 gauge needles. Samples were immediately centrifuged at 13,000 rpm for 7 minutes, supernatant was removed, and pellets were resuspended in RIPA buffer (Sigma-Aldrich) supplemented with protease and phosphotase inhibitors (1:100, Sigma-Aldrich). Samples were kept at -80 °C until total protein concentrations were determined using the Pierce BCA Protein Assay Kit as per manufacturer's instructions (Thermo Scientific). Samples were diluted in Laemmli buffer (Bio-Rad), supplemented with 5% β-mercaptoethanol, heated at 95°C for 2 min, and 10 μg of protein was loaded onto a polyacrylamide gel (4-15%, Bio-Rad). Gel electrophoresis was performed in a Tris-hydorxyethyl piperazineethanesulfonic acid (HEPES)-sodium dodecyl sulfate (SDS) running buffer (Thermo Scientific) at 100V for 45 min. Proteins were transferred onto polyvinylidene difluoride (PVDF) membranes (Thermo Scientific) for 2 h at 10V in 10% Pierce transfer buffer (Thermo Scientific) and 20% methanol diluted in H_2O. Membranes were blocked with 4% bovine serum albumin (BSA) in Tris-buffered saline-0.1% Tween-20 (vol/vol) (TBST, Thermo Scientific) for 1 hour at room temperature on an orbital shaker, and incubated overnight at 4°C with rabbit anti-BMP6 (1:500, Novus Biologicals), rabbit anti-GDF1 (1:1000, Abcam), and rabbit anti-GDF11 (1:1000, Biorbyt). Membranes were washed three times in TBST for 10 minutes, and incubated with horseradish peroxidase (HRP)-conjugated anti-rabbit IgG secondary antibody (Cell Signalling

Technology, 1:2000) for 1 hour at room temperature. Chemiluminescent substrate detection reagent ECL (Thermo Scientific) and digital imaging was performed using the LI-COR Odyssey Fc system. Membranes were re-blotted with antibody to mouse Actin (1:20000, Cell Signalling Technology) and HRP-conjugated anti-mouse IgG secondary antibody (LI-COR, 1:2000) as above for loading control purposes.

2.7 Resin embedding, semi-thin sections, and electron microscopy

Mice were intracardially perfused with 4% PFA (wt/vol) and 2% glutaraldehyde (vol/vol; TAAB Laboratories) in 0.1 M phosphate buffer. Tissue was post-fixed overnight at 4°C and transferred to 1% glutaraldehyde (vol/vol) until embedding. 1 mm tissue sections were processed into araldite resin blocks, followed by microtome cutting of 1 μm sections. Sections were stained with a 1% toluidine blue/ 2% sodium borate solution prior to bright field imaging at 100X magnification using a Zeiss Axio microscope. Ultrathin sections (60 nm) were cut from corpus callosum, stained in uranyl acetate and lead citrate, and grids imaged on a JEOL Transmission Electron Microscope. Axon diameter and myelin thickness were calculated from measured area based on assumption of circularity using Fiji/ImageJ (Fiji.sc), with a minimum of 100 axons per animal analyzed. Standard g ratio analysis of myelin thickness was calculated by determining the ratio of the inner axonal diameter to the total outer diameter of the axon plus myelin. Myelinated axon density was counted blindly in

8.62μm x 8.62μm images of the corpus callosum and scaled up to determine density per mm^2. A minimum of 3 images per animal were analyzed; each experimental condition contained 3-5 animals. Measurements were compiled in Microsoft Excel and organized using RStudio. 'Proportion of myelinated axons' by axon diameter was determined by plotting the proportion of a sample of 100 myelinated axons from each animal that were of a specific diameter, which was fitted with a best-fit polynomial regression curve. To compare treatment and vehicle control curves, a Kolmogorov-Smirnov test was used to test whether cumulative distributions of myelinated axon diameters differed between conditions. To compare proportion of myelinated axons by bin between treatments, data was plotted in Microsoft Excel and a 2-way ANOVA with Bonferroni's multiple comparisons test was carried out. All statistical tests were done using GraphPad Prism 7.

2.8 Flow cytometry

Organotypic slice cultures from AR8-mCherry mice were pooled (3-6 slices per sample) at 0, 2 and 7 days post lesion (dpl) and homogenised with a 2 ml dounce tissue homogeniser. A Percoll (Sigma-Aldrich) gradient was used to isolate cells from myelin debris. Samples were blocked with Fc-block (LEAF-purified anti-mouse CD16/32 (Biolegend, 101321), then incubated with fluorochrome-conjugated antibodies CD11b-AF647 (BioLegend 101218, 1:200) or PDGFRa-PE (BioLegend, 135905, 1:100), MAG-FITC (EMD Millipore, FCMAB337F, 1:100), and O4-APC (R&D, FAB1326A, 1:100) for 30 minutes on ice. Following washes in buffer, samples were

incubated with DAPI and run on the BD LSR Fortessa (6 laser) analyser, and analysed using FACSDiva software (BD). Gating was based on live ($DAPI^-$) $mCherry^+$ cells, followed by gating for singlet cells, and finally forward and side scatter to eliminate cell debris and clusters. Cell populations were then gated for $CD11b^+$ (microglia), $PDGFRa^+$ (oligodendrocyte progenitors), $O4^+$ (immature oligodendrocytes), and MAG^+ (mature myelinating oligodendrocytes).

2.9 Live imaging

An insert with cultured cerebellar slices was adhered by the feet to a single 4 cm petri dish with molten wax and left briefly to dry. Media was first pipetted into the petri dish to diffuse under the mesh then gently pipetted onto the surface of mesh. Z-stacks were acquired as snapshots using a 20X wet-immersion objective on the Olympus spinning disk confocal microscope, incubated at 37°C (high humidity) and 5% CO^2.

2.10 Statistics

All statistical tests were performed using GraphPad Prism 7, and power calculations performed using the free online tool OpenEpi. Statistical tests carried out for each type of experiment will be discussed in turn.

Organotypic slice culture experiments. Slice culture experiments were analyzed by treatment group and by time point. The goal was to compare differences between

treatment and their respective controls at separate times during remyelination. To do this, treatment values for each animal were normalized to the averaged control value (n=3 for controls). Therefore, the control value is a hypothetical value of 1, and changes with treatment are expressed as fold change. In order to determine whether these changes are statistically significant, column statistics were used. Specifically, a one-sample t-test compared to a theoretical mean of 1 (control) was performed. A comparison of this method to a Kruskal-Wallis with Dunn's Multiple comparisons test on the raw data (where none of the data was averaged or normalized) revealed similar results (see Figure 6 in Chapter 3). Since comparison between treatments is better visualized when data is normalized to their respective vehicle controls, and since this method is an accurate representation of the raw data, this was the chosen method of data visualization for all further slice culture experiments. When data was entered into OpenEpi to determine statistical power, all slice culture experiments had at least 80% power. Group sizes for each experiment are between 3-6 animals per treatment per time point and specifically stated in each figure.

***In vivo* lesioning experiments**. *In vivo* experiments were analysed by treatment group in order to compare each treatment to their respective vehicle controls during remyelination. G ratios were analysed, both by individual axon counts (100 axons per animal, 3-5 animals per group) and by animal averages. To compare G ratios, a Mann-Whitney test was used, as data was unpaired and non-parametric. G ratio was also analysed by axon diameter, and here an extra sum of squares F-test was

used, as this test compares the goodness of fit between 2 models. As such, the line of best fit of data points in the treatment group was compared to the control group. Next, to determine whether the number of myelinated axons was different between treatment and controls, two different analyses were carried out. First, myelinated axons were counted per field in 10 images per animal, and the average for each animal was multiplied up to mm^2. A Mann-Whitney test was used, as again data was unpaired and non-parametric. Second, 100 myelinated axons were counted per animal and the axon diameter was measured for each axon. The relative percentages of number of myelinated axons of specific diameters were then plotted. To compare the distribution of axon diameters of treatment to vehicle control, a 4th-order polynomial best-fit curve was plotted, and a Kolmogorov-Smirnov test was carried out. In order to further compare treatment vs control across all axon diameters and within each bin of diameter, a 2-way ANOVA with Bonferroni's multiple comparisons test was carried out. Many of these experiments did not reveal statistically significant results, perhaps because they were underpowered.

Post-mortem human multiple sclerosis tissue analysis. To compare percentage of cells co-expressing markers for activin receptors or receptor ligands across 4 different lesion types and control tissue, a Kruskal-Wallis test was used. This is a non-parametric test comparing 3 or more unmatched groups. Dunn's multiple comparisons test was performed to compare differences in the sum of ranks with the expected difference based on number of groups and their size. Each lesion type

was further compared to control tissue. N numbers for these experiments are stated above, and presented in Table 7.

3 Chapter 3: Activin receptors are required for effective remyelination

3.1 Introduction

As described in detail in Chapter 1, myelin is an important component of the central nervous system, providing insulation for electrical impulse conduction as well as trophic and metabolic support to neurons [1, 2, 18, 22]. In diseases where myelin is damaged and lost (such as multiple sclerosis), axons become vulnerable to degeneration, leading to sensory and motor deficits. Myelin can be regenerated, and requires oligodendrocyte progenitor cells (OPCs) to activate, migrate to the site of injury, proliferate, and differentiate into mature myelin-making cells [24–26]. While this process can be efficient early in MS, it often fails with disease progression [46, 166, 195, 208]. One proposed therapeutic strategy is to improve clinical outcome by targeting the remyelination process. Promoting myelin regeneration would restore support to axons, which may confer protection from neurodegeneration, ultimately slowing or stopping disease progression. However, mechanisms underlying drivers of remyelination and reasons for its failure in MS are not fully understood.

Previous work in our lab identified the TGF-β superfamily member activin-A as being increased during remyelination *in vivo* and sufficient in stimulating activin receptor-driven OPC differentiation *in vitro* [142]. However, it was not clear whether activin receptor-mediated activity could directly influence remyelination.

This chapter focusses on determining whether activin receptor signalling is required for remyelination in focal demyelinating lesion models *ex vivo* and *in vivo*.

3.2 Results

3.2.1 Creating a quantification method for remyelination in slices

The gold standard for quantifying remyelination *in vivo* is using electron microscopy to calculate g ratio (as described in section 1.2.2). As this is technically difficult in *ex vivo* slices (protocol outlined in Figure 5a), an alternative method for quantifying myelin regeneration was required. Using images from immunofluorescently stained slices, a quantification method was developed for calculating area of axons, area of myelin, and the area in which these two stains overlap. A theoretically simple idea was difficult to carry out in practice, as the axonal stain was not robust in myelinated areas, potentially due to antibody penetration issues. It is counter-productive to carry out a more effective tissue permeabilization protocol, as this would disrupt myelin structure. To acquire images of sufficient quality for quantification, staining and image acquisition protocols were optimized. Then, using image analysis software (Volocity, PerkinElmer), parameters were set for determining objects in each stain: axons (neurofilament, NF) and myelin (myelin basic protein, MBP). Filters were set for minimum object size, and a threshold was applied individually to blinded images. A mask was created for voxels in which the two objects co-localize. The total voxel count for these three objects (NF, MBP, and co-localized) was extracted. These numbers were used to calculate the remyelination index: area of co-localization divided by area of axons (Figure 5). This new protocol allowed for an objective quantification of myelin regeneration in slice cultures.

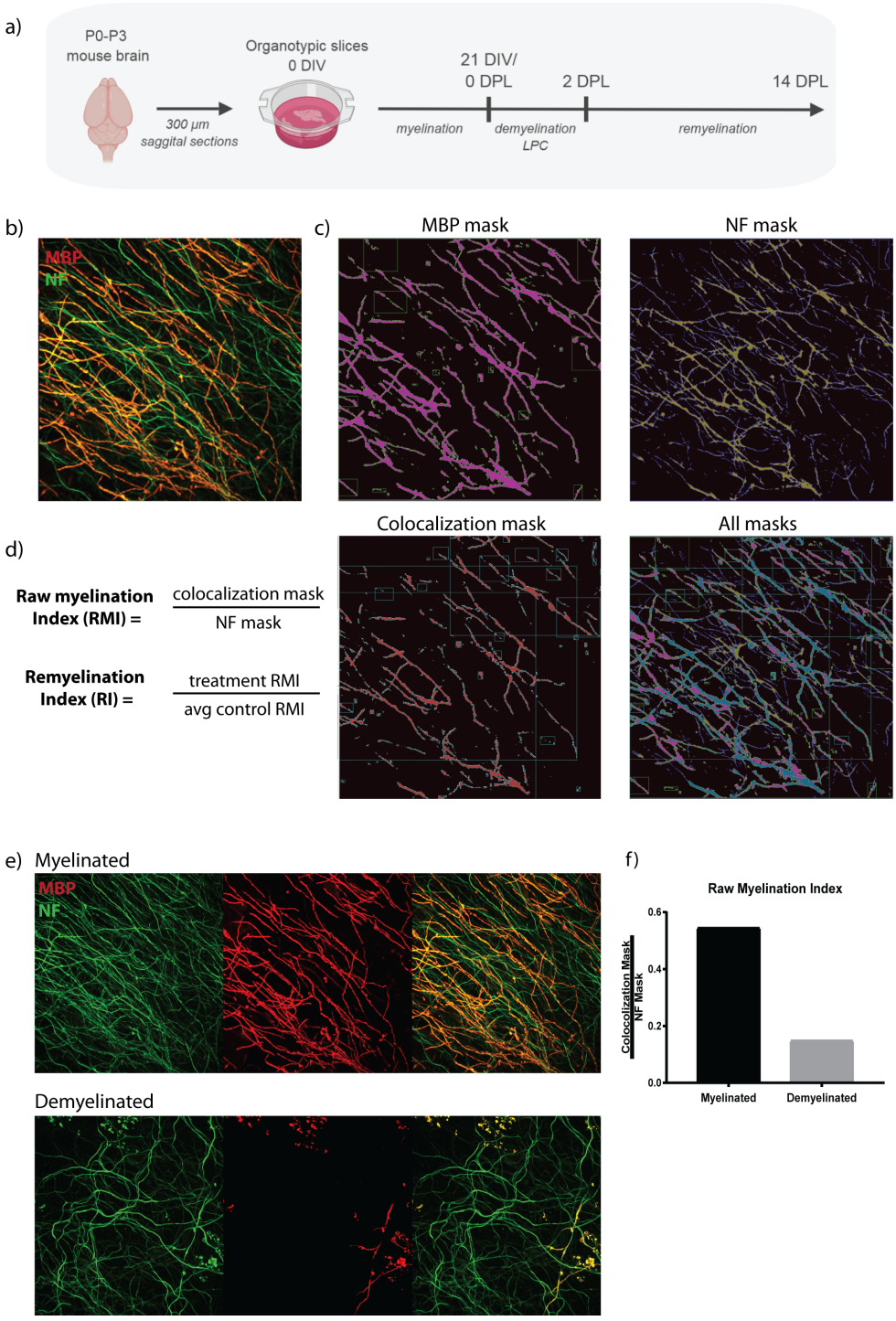

Figure 5. Developing a method for quantifying remyelination *ex vivo*. a) Protocol timeline for organotypic slice cultures. b) Sample image stained with Myelin Basic Protein (MBP, red) and Neurofilament (NF, green). c) Masks of individual stains and colocolization area of (b). All masks shown together in bottom right panel. d) Formula for calculating remyelination index. e) Sample images of myelinated (top) and demyelinated (bottom). f) Raw myelination indices of (e).

3.2.2 Activin receptor stimulation can accelerate remyelination *ex vivo*

To examine whether stimulation of activin receptors affects remyelination, demyelinated *ex vivo* cerebellar slices were treated with activin-A, the primary ligand for activin receptors. Activin-A has the highest binding affinity for activin receptors, and once bound, activates downstream signalling pathways leading to expression of target genes. Slices treated with activin-A significantly increased remyelination at 7 days post lesion compared to vehicle controls (Figure 6b, **P=0.0057). No significant differences were observed in remyelination index at 10 and 14 days post lesion, likely due to remyelination processes occurring efficiently in controls. Thus, this data suggests that stimulating activin receptors using activin-A is sufficient to accelerate remyelination. This result was published in our recent paper [327]. To confirm whether normalized data was representative of raw data, raw data was plotted and analysed (Figure 6d). Raw myelination index of activin-A treated slices was significantly higher than vehicle control at 7dpl, but not at 10dpl or 14dpl. Raw myelination index values for vehicle controls show that as myelin regeneration proceeds with time, slices naturally become increasingly myelinated, and eventually catch up to the accelerated remyelination seen with activin-A treatment. Therefore, normalized data (as shown in Figure 6b) is representative of the raw data, and is suitable for analysis of further slice culture remyelination index data within this thesis.

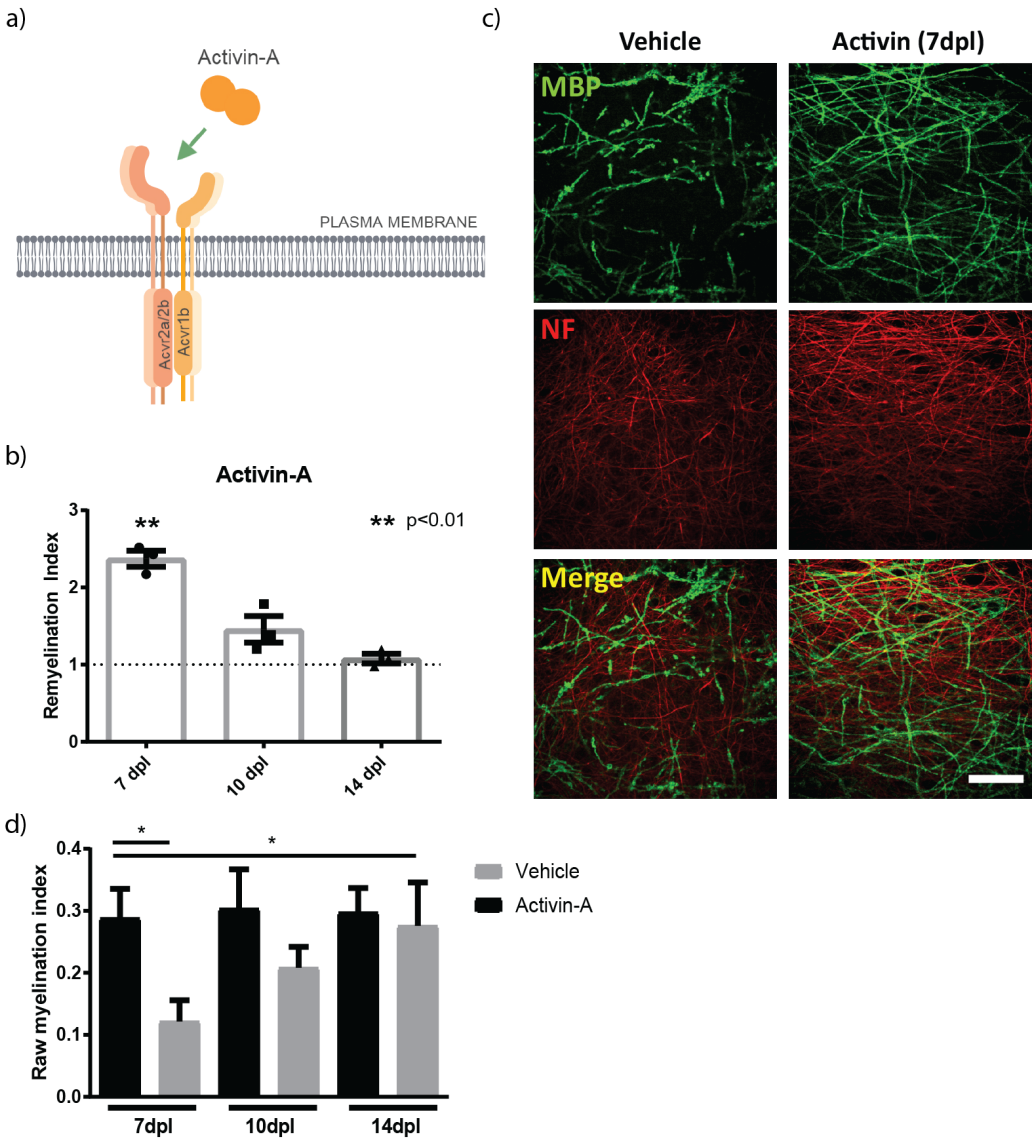

Figure 6. Activin-A accelerates remyelination in *ex vivo* cerebellar slices. a) Activin-A binds with high affinity to activin receptors and activates downstream signalling pathways. b) Mean remyelination index ± s.e.m. in activin-A treated *ex vivo* slices at 7, 10, and 14 days post lysolecithin (dpl) normalized to vehicle control from the respective time point. n=3 animals, one-sample t-test compared to a theoretical mean of 1 (control), **P=0.0057 at 7dpl. c) Representative images of slice cultures at 7dpl treated with vehicle control or activin-A during remyelination, immunostained against myelin basic protein (MBP, green) and axonal neurofilament-H (NF, red). Scale bar, 50 μm. d) Raw myelination index data ± s.e.m. from (c) for activin-A (black bars) and vehicle controls (grey bars) at 7, 10, and 14dpl. Kruskal-Wallis test (*P=0.0181) with Dunn's multiple comparisons (*P=0.0259 at 7dpl).

3.2.3 Activin receptors are required for remyelination *ex vivo*

To determine whether activin receptors are required for remyelination, demyelinated *ex vivo* cerebellar slices were treated with inhibin, an activin receptor inhibitor. Inhibin competitively binds activin receptors, preventing binding of endogenous ligands, and blocking downstream signalling (Figure 7a). Treatment with inhibin significantly reduced remyelination at 7, 10, and 14 days post lesion compared to vehicle controls (Figure 7b), suggesting for the first time that activin receptor signalling is required for remyelination. This result was published in our recent paper [327].

3.2.4 Activin receptor modulation influences remyelination in a calibre-dependent manner *in vivo*

To confirm whether modulating activin receptor activity using activin-A/inhibin affects remyelination in an *in vivo* model, implantable osmotic mini-pumps with attached brain cannula were used to supplement compounds directly to lysolecithin-induced focal lesions in the corpus callosum (CC) of mice (Figure 8a). Lesion areas were processed at 7 days post lesion (dpl) in activin-A treated mice, and at 14dpl in inhibin treated mice. These time points were chosen based on results from the above *ex vivo* experiments. Electron microscopy was then carried out to determine effects on myelin thickness and density of myelinated axons. In activin-A treated mice, there were no significant differences between treatment and control in terms of g ratio (Figure 8b-d) or density of myelinated axons (Figure 8e). However, when the data was stratified by axon diameter, a non-significant trend emerged in number

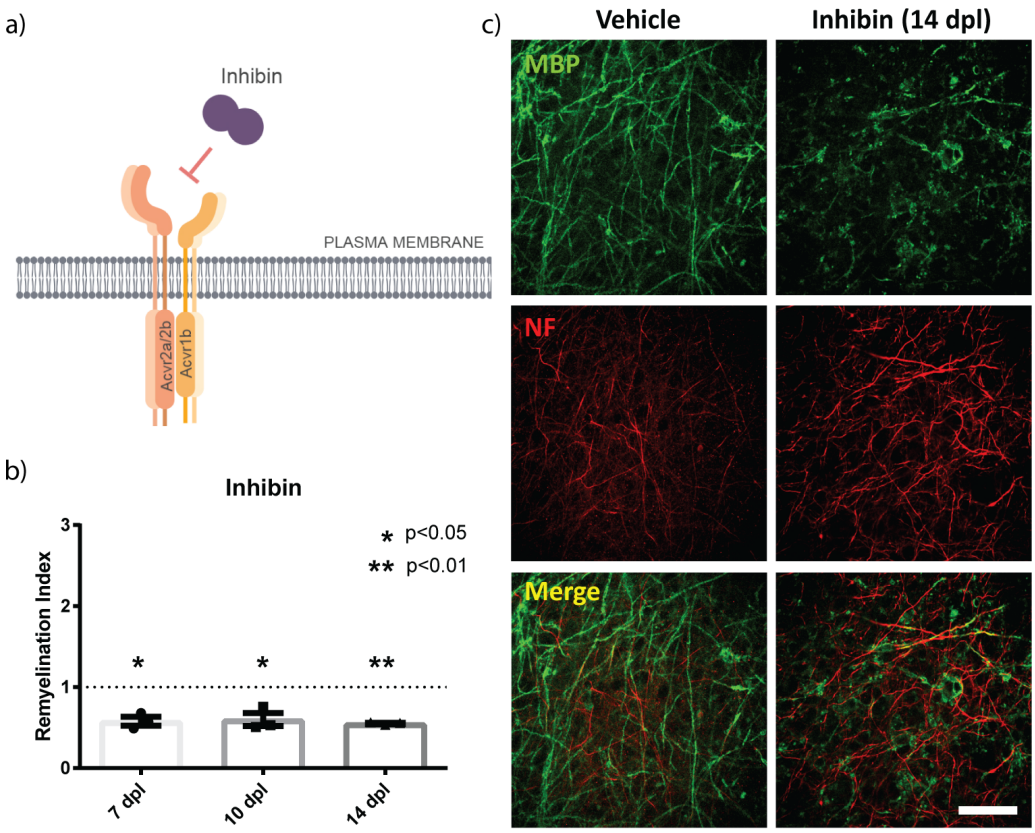

Figure 7. Inhibin blocks remyelination in *ex vivo* cerebellar slices. a) Activin receptor activity is blocked by inhibin, which competes with activin-A for the receptor binding site. b) Mean remyelination index ± s.e.m. in inhibin treated *ex vivo* slices at 7, 10, and 14 days post lysolecithin (dpl) normalized to vehicle control from the respective time point. n=3 animals, one-sample t-test compared to a theoretical mean of 1 (control), *P=0.0165, *0.0374, **0.0004, respectively. c) Representative images of slice cultures at 14dpl treated with vehicle control or inhibin during remyelination, immunostained against myelin basic protein (MBP, green) and axonal neurofilament-H (NF, red). Scale bar, 50 μm.

of myelinated axons: a higher number of myelinated axons were observed in axons smaller than 0.4 μm in diameter (Figure 8f). Representative images are shown in Figure 8g.

In inhibin treated mice, there were no differences in overall g ratio between treatment and control (Figure 9a,b). However, when g ratio was plotted against axon diameter, slopes were significantly different (Figure 9c), suggesting distinct distribution of myelin thickness across axon diameters between inhibin and vehicle treated lesions. While there were no differences between overall density of myelinated axons (Figure 9d), when data was segmented by axon diameter, the cumulative distributions (represented by the curves in Figure 9e) were significantly different between treatments. This data suggests that blocking activin receptors results in a shift in the distribution of diameters of myelinated axons. Representative images are shown in Figure 9f.

Taken together, this *in vivo* data corroborates the effect of activin receptor modulation on remyelination seen in the *ex vivo* model, albeit with an important caveat. Axon diameter appears to be a potential determinant of how activin receptor modulation ultimately affects repair, suggesting there may be distinct mechanisms supporting small versus large calibre axon remyelination.

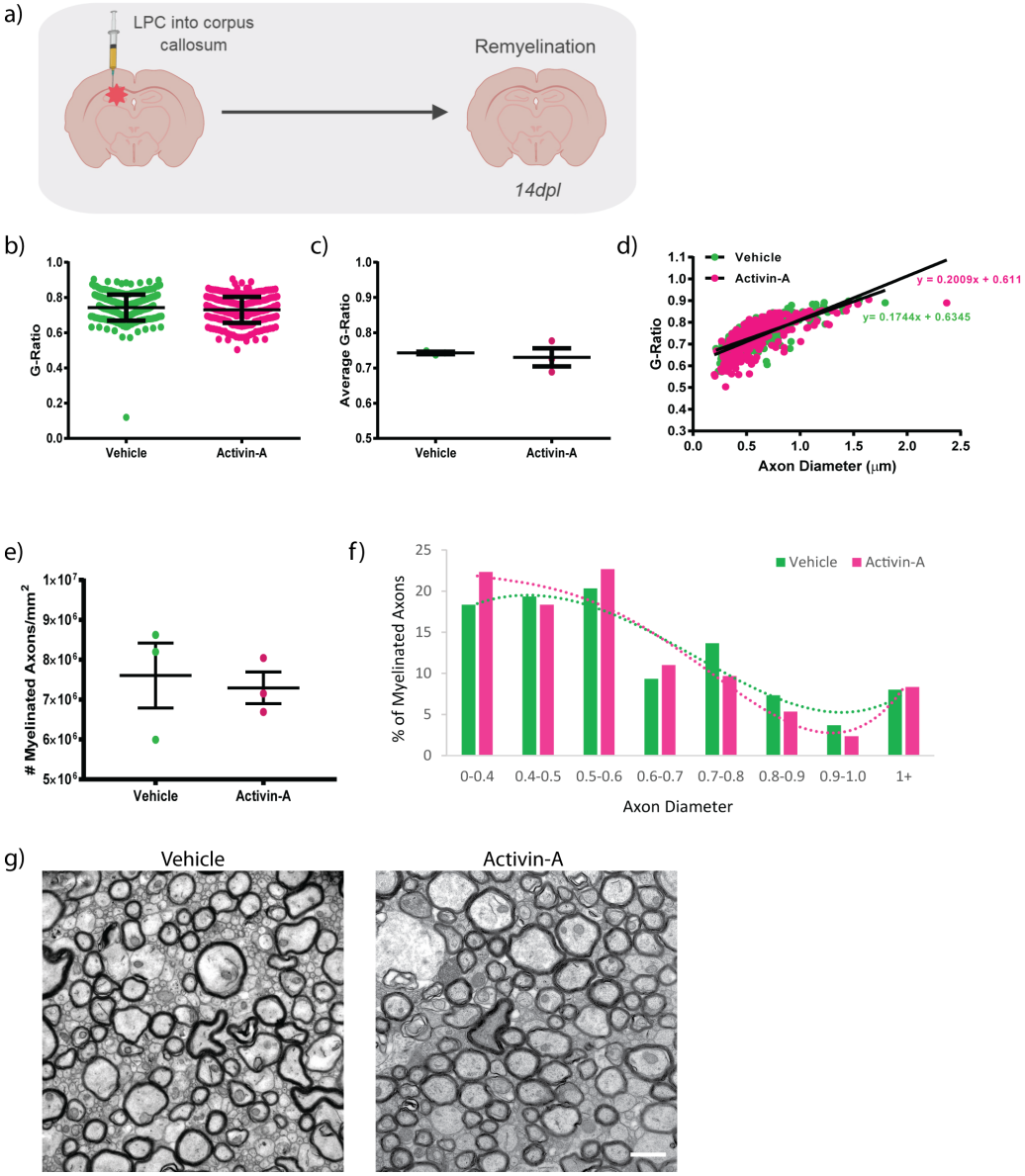

Figure 8. Activin-A treatment in focal lesions *in vivo*. a) Protocol diagram for *in vivo* focal lesions. b) Overall g ratio ±s.d. of activin-A treated animals compared to control, n=100 per animal, 3 animals per condition. Mann-Whitney test, no significant differences. c) G ratio ±s.e.m. of Activin-A treated animals compared to control averaged by animal. Mann-Whitney test, no significant differences. d) Dot plot of g ratio and axon diameter in Activin-A treated (magenta) and vehicle controls (green). Extra sum of squares F-test between slopes, non-significant. e) Mean of total number of myelinated axons ±s.e.m. per mm^2. Mann-Whitney test, non-significant. f) Proportion of myelinated axons by axon diameter, in Activin-treated mice (magenta) and vehicle control (green), overlaid with polynomial best-fit regression curves (Kolmogorov-Smirnov test, non-significant). n=3 mice per condition, 100 axons measured per animal. 2-way ANOVA with Bonferroni's multiple comparisons test, non-significant. g) Representative images of Activin-A and vehicle treated corpus callosum. Scale bar, 1μm.

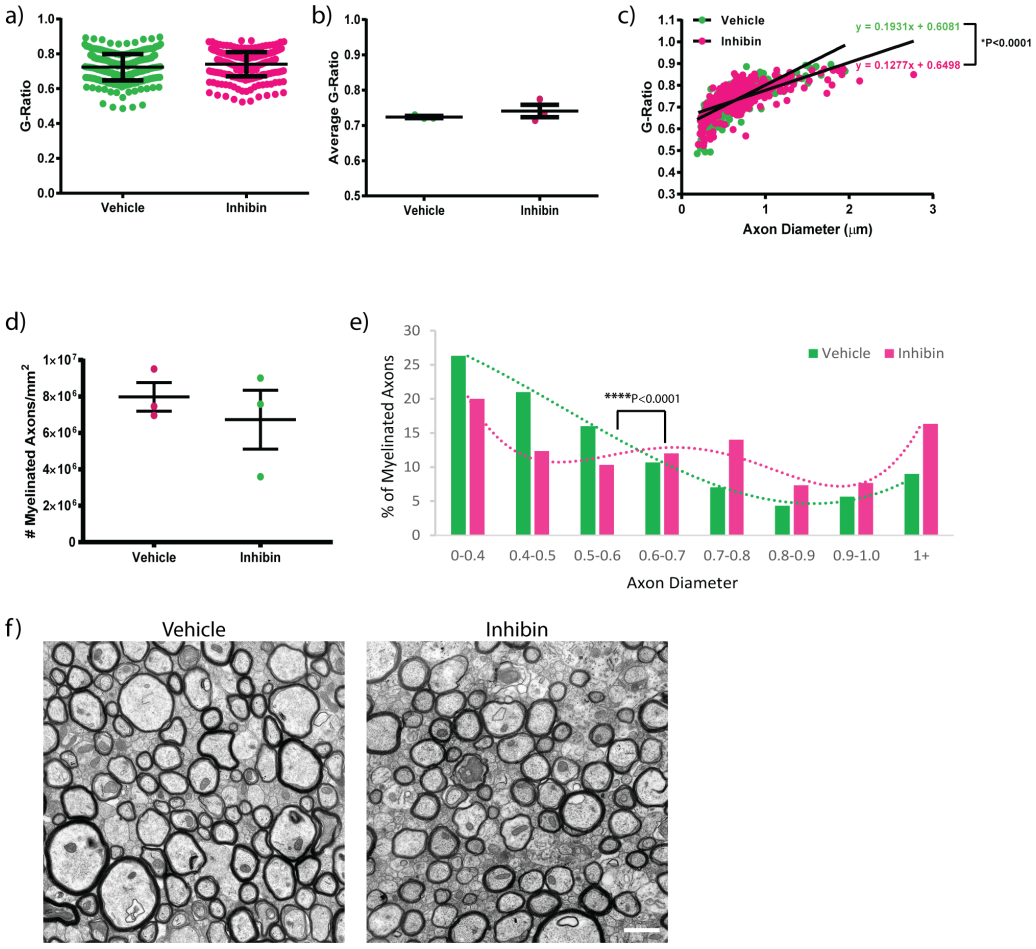

Figure 9. Inhibin treatment in focal lesions *in vivo* results in differences in g ratio across axon diameters a) Overall g ratio ±s.d. of Inhibin-treated animals compared to control, n=100 per animal, 3 animals per condition. Mann-Whitney test, no significant differences. b) Mean of g ratio ±s.e.m. of Inhibin-treated animals compared to control. Mann-Whitney test, non-significant. c) G-ratio versus axon diameter in Inhibin treated (magenta) and vehicle controls (green). Extra sum of squares F-test between slopes, *P<0.0001. d) Mean of total number of myelinated axons ±s.e.m. per mm^2 in Inhibin treated animals and vehicle controls. Mann-Whitney test, non-significant. e) Proportion of myelinated axons by axon diameter, in Inhibin treated mice (magenta) and vehicle control (green), overlaid with polynomial best-fit regression curves (Kolmogorov-Smirnov test, ****P<0.0001). n=3 mice per condition, 100 axons measured per animal. 2-way ANOVA with Bonferroni's multiple comparisons test, non-significant. f) Representative images of Inhibin and vehicle treated corpus callosum. Scale bar, 1μm.

3.2.5 Activin-A ligand is not required for remyelination *ex vivo*

Since activin receptor activity was found to be important during remyelination both *ex vivo* and *in vivo*, the requirement for its primary ligand, activin-A, was subsequently examined. Activin-A activity was blocked in cerebellar slice cultures using follistatin, a protein which sequesters activin-A with very high affinity and prevents it from binding to its receptors. A separate control consisted of treatment with an α-activin-A antibody (Figure 10a). Treatment with these blocking agents did not affect the remyelination index (Figure 10b). Taken together, this data shows that although activin receptors are required for remyelination *ex vivo*, the primary ligand is not, indicating the likely activity of other ligands with binding capacity to these receptors in the absence of activin-A.

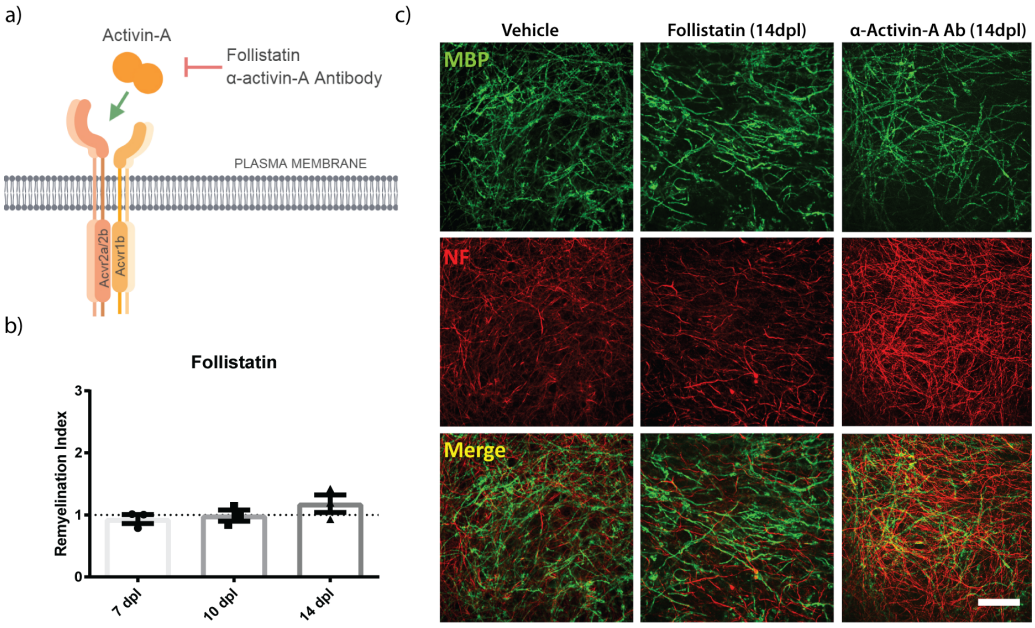

Figure 10. Activin-A is not required for remyelination in *ex vivo* cerebellar slices. a) Activin-A activity is blocked by follistatin, which sequesters activin-A and prevents it from binding to its receptor. b) Mean remyelination index ± s.e.m. in follistatin treated *ex vivo* slices at 7, 10, and 14 days post lysolecithin (dpl) normalized to vehicle control from the respective time point. n=3 animals, one-sample t-test compared to a theoretical mean of 1 (control). No significant differences were observed. c) Representative images of slice cultures at 14dpl treated with vehicle control or follistatin during remyelination, immunostained against myelin basic protein (MBP, green) and axonal neurofilament-H (NF, red). Follistatin results were confirmed using α-activin-A antibody; representative image shown on right. Scale bar, 50 μm.

3.3 Discussion

Activin receptor signalling is sufficient and required for remyelination

In this chapter, I reveal both a sufficiency and requirement for activin receptor signalling during remyelination *ex vivo*. Treatment of cerebellar slice cultures with activin receptor ligand activin-A resulted in an acceleration in remyelination, while blocking activin receptors with inhibin hindered remyelination. This data is in line with our previous work identifying activin-A as a pro-differentiation factor [142], as well as previous literature suggesting a neuroprotective role for activin receptor signalling [273, 274]. These results support the notion that specific ligand/receptor complexes in the TGF-β superfamily must be carefully studied in context, as the data in this chapter contradicts previous studies showing a negative effect of this superfamily on remyelination. Importantly, these previous studies were on distinct receptors (BMP receptor I, Acvr1) and downstream pathways (Smad1/5/8) [321, 322].

The data from Figures 6 and 7 were published in our recent paper alongside developmental data implicating Activin receptors as regulators of the oligodendrocyte lineage across the lifespan. In the paper, we also deleted Activin receptor 1b (the functional signalling receptor associated with Acvr2a/2b) from oligodendrocyte progenitors (PDGFRα-Cre; Acvr1b$^{fl/fl}$) in mice and observed hypomyelination, a decrease in myelin-associated protein expression, and low numbers of differentiating and mature oligodendrocytes. This data, together with the observed phenotype

associated with myelin abnormalities (tremor, hunched posture, stiff tail, juvenile death) are evidence for the important role of Activin receptor signalling in developmental myelination. Clearly, signalling mediated by Acvr2a/Acvr2b/Acvr1b is crucial during both development and regeneration.

Potential mechanism of action of activin receptors

To delve deeper into the underlying mechanism of activin signalling during remyelination, it would have been interesting to determine effects of activin-A/inhibin treatment on oligodendrocyte lineage cells within cerebellar slices. While we have determined that *in vitro*, different concentrations of activin-A treatment drives OPC proliferation, maturation, and survival [142, 263, 327], we only observed effects on oligodendrocyte differentiation in our *in vivo* assays. It is therefore not clear whether one or all of these are driving remyelination *ex vivo*. A direct test for this would have been to look for differences between treatment and controls in populations of oligodendrocyte lineage cells using markers for each stage of maturation by immunohistochemistry. This experiment may have yielded interesting insight on which oligodendrocyte responses are affected by activin receptor stimulation in the slices. Given slice cultures were treated with 100 ng/ml activin-A, I would hypothesize a greater effect on oligodendrocyte survival, as this is the response elicited by this concentration of activin-A on OPC cultures [263]. Further, I would hypothesize that inhibin treatment may affect all potential oligodendrocyte responses, as blocking activin-A's access to receptors would prevent all of its effects. Interestingly, in

our recent paper we also uncovered a role for activin receptors in driving oligodendrocyte membrane compaction during development. Mice lacking Acvr1b in OPCs (PDGFRα-Cre; Acvr1b$^{fl/fl}$) had enlarged inner tongue thickness compared to controls, along with a lack of MBP in MAG^{+} sheaths, a mark of non-compact myelin. Importantly, this compaction effect was not due to differences in membrane growth, but rather membrane actin disassembly, a required step in myelin compaction [327]. To test for compaction effects following activin or inhibin treatment in the slice culture, electron microscopy would have had to be carried out. As mentioned above, this is technically difficult in slices, so compaction effects were analyzed in the *in vivo* focal demyelination model, discussed further below.

Differences between ex vivo and in vivo models

Given the redundancy of signals regulating remyelination (see Table 2), it is perhaps surprising that blocking activin receptors *ex vivo* had such a significant effect. This could be due to the isolated nature of the *ex vivo* culture system, reducing the compensatory potential for expression of alternative receptors driving remyelination. Indeed, the effects of inhibin treatment in the *in vivo* focal demyelination model are less pronounced, perhaps due to other factors contributing to remyelination.

Overall, the *in vivo* results generally supported the *ex vivo* findings (although only a trend was observed in axons under 0.4μm in diameter): treatment with activin-A led to an increase, while inhibin treatment led to a decrease, in the number of myelinated axons. However, the *ex vivo* effects were clearly more robust than *in vivo*, both

in terms of variability and magnitude of effects. These discrepancies could be accounted for by differences between models, such as compensatory potential described above. This lack of potential *ex vivo* could affect the 'adaptability' of lesions during repair, with increased input from other brain regions/periphery *in vivo* leading to more flexibility in the regenerative response. Additionally, the nature of the lesion itself could affect the resources available for orchestrating repair. Specifically, the *ex vivo* model utilizes a global lesioning system: the entire slice is exposed to the demyelinating toxin 21 days after the brain is dissected into 300 μm sections (a fairly severe injury event alone). Conversely, the *in vivo* system is focal, and only a small area of the corpus callosum is demyelinated in an otherwise intact animal, allowing for resources such as immune cells and oligodendrocyte progenitors to migrate from healthy brain regions or the periphery.

Further, there is a shift in the timeline of repair between these two models. Previous research characterizing LPC-induced demyelination and remyelination in *ex vivo* and *in vivo* models suggests that regeneration occurs faster in the former model, with oligodendrocyte differentiation/early remyelination starting around 7dpl, and being complete by 14dpl [45]. *In vivo*, this process is extended, with differentiation and early remyelination starting at 10dpl and completing by 21dpl [142]. As an effect with activin-A treatment was only observed early during remyelination—at 7dpl—in our *ex vivo* model, it is possible that due to a shift in timing of repair, this effect was missed when results were examined at 7dpl *in vivo*.

There is a fundamental difference between these two models in terms of age and

brain region. The *ex vivo* model uses cerebellar brain slices from P0-P2 newborn mice, and these slices are then grown in culture until myelination is complete (P21). These P21 slices are considered 'adult' slices, as they have a fully myelinated cerebellum similar to an adult mouse. However, adult mice used in *in vivo* experiments are 8 weeks old, and the lesioning is done in the corpus callosum, a different white matter tract. As age has been implicated in modulating repair processes [26], it is possible that this could, in part, account for discrepancies between models. Differences in function, structure, and physiology have been reported between neonatal and adult slice cultures [328]. While brains from younger animals are generally preferable in organotypic cultures due to their enhanced viability and regenerative potential [329, 330], adult slices may have rendered more comparable results to our adult *in vivo* lesioning. Indeed, previous research suggests that there are age-related differences in remyelination speed and efficiency [221, 226, 331], as well as microglial cell populations [332, 333]. Further, the models are lesioned in separate white matter tracts (corpus callosum and cerebellum). This could affect the repair process, as each tract contains different neuronal cell types and thus different ranges of axon diameters and properties, as well as some distinct populations of oligodendrocytes [334–336]

Axon diameter as a determinant of activin receptor signalling outcome

Additionally, axon calibre may be important for determining the outcome of activin receptor modulation. In our paper, we found that all effects from our Acvr1b conditional knock-out (PDGFRα-Cre; Acvr1b$^{fl/fl}$) were observed only on small di-

ameter axons. At P16, myelin produced by cKO animals was shifted towards small diameter axons compared to controls. The increase in inner tongue thickness was also only observed in small calibre axons [327]. Taken together, this data suggests that activin receptor-mediated myelination and remyelination effects are dependent on axon calibre, potentially pointing towards differences in activin receptor ligand expression across axon size. Consistent with this hypothesis, one study found that upon experimentally enlarging axon diameter to support myelination, activin-A subunit expression was increased [337]. To my knowledge, this is the first time an axon calibre-dependent remyelination mechanism by a single receptor has been described. This finding complicates future therapeutic potential, as targeting an activin receptor ligand to axons of specific diameters would be a complex pharmacological task. Nevertheless, it is important to first understand the mechanisms underlying myelin regeneration in health and disease to develop appropriate therapeutics.

Alternative activin receptor ligands may also drive remyelination

Finally, blocking activin-A activity in *ex vivo* slice cultures with Follistatin and anti-activin-A antibody did not affect remyelination, suggesting that in the absence of activin-A, other TGF-β ligands may bind activin receptors and drive remyelination. Previous research on the promiscuity of TGF-β superfamily binding partners supports this hypothesis [338–343]. First, it is important to note that while this superfamily contains over 30 ligands, there are only five type II receptors and seven type I receptors. As such, it is clear that one receptor can bind more than one lig-

and, and we cannot assume a one factor - one receptor - one function mechanism. Activin receptors 2a and 2b in particular are among the most promiscuous, binding members of the TGF-β, GDF, and BMP subfamilies [342]. Additionally, knock-out studies of single ligands or receptors within the superfamily vary in their phenotypic severity, suggesting that in the absence of one protein, another within the family can compensate [343].

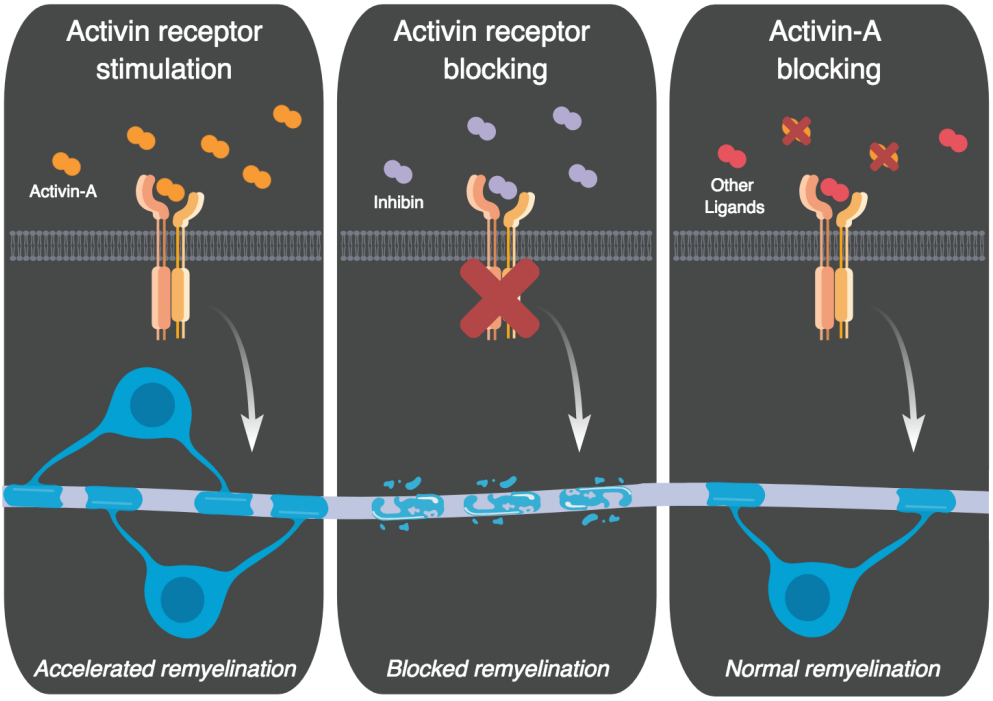

Figure 11. Hypothetical model of how Activin receptors and their ligands influence remyelination. When activin receptors are stimulated with activin-A, remyelination is accelerated. When activin receptors are blocked using Inhibin, remyelination fails. However, if activin-A is blocked, normal remyelination occurs, hinting at the involvement of alternate ligands.

This proposed compensation mechanism by other TGF-β proteins in the absence of activin-A highlights the importance of this regenerative process. Given the previously established requirement of activin receptors during *ex vivo* remyelination, it

follows that other activin receptor ligands must be present in the slice (see Figure 11 for summary). There are several candidate proteins within the TGF-β superfamily with binding affinity for activin receptors, many with functions in development and progenitor cell differentiation (see Table 4). The role of these candidates in remyelination is explored in the following chapter.

4 Chapter 4: Alternative activin receptor ligands influence remyelination

4.1 Introduction

As introduced in Section 1.5, the TGF-β superfamily is a large, complex, and interacting group of agonists, antagonists, and receptors. The ultimate effects of receptor activity depend on ligand availability and concentration, cellular context, concentration of antagonists, and downstream regulatory factors. Importantly, this superfamily is known for a myriad of functions, including cell proliferation, differentiation, and morphogenesis, as well as tissue homeostasis and regeneration [306, 307]. Such a wide variety in cellular responses hints at the complexity of signalling within this superfamily, and rejects the simple idea of one ligand - one receptor - one function.

Activin receptors 2a and 2b comprise two of the five type II receptors, and are among the most promiscuous in terms of ligand binding [342]. Table 4 lists all ligands with binding affinity for activin receptors, their roles in the CNS, their main antagonists, and their cell-specific expression in the developing mouse brain. Of these ligands, only three (activin-A, activin-B, and BMP-2) have been previously implicated in regulating oligodendrocyte responses. Activin-A's involvement in remyelination was primarily studied in our lab and has been covered in the previous chapter. Work on activin-B and BMP-2 as a driver and inhibitor of oligodendrocyte

development (respectively) focussed on developmental myelination. None of the ligands in Table 4 (with the exception of activin-A) have been studied in the context of remyelination. In this chapter, I identified activin receptor ligands expressed during remyelination, and used both gain-of-function and loss-of-function strategies to determine their sufficiency and requirement for myelin regeneration.

4.2 Results

4.2.1 Alternative activin receptor ligands are differentially expressed during remyelination *ex vivo* and *in vivo*

Since work from Chapter 3 suggested that activin receptors are required for remyelination *ex vivo*, but the primary ligand activin-A is not, I next sought to determine which activin receptor binding ligands (see Table 4) are present in both the organotypic slice culture and the *in vivo* focal lesioning models. To investigate which of these ligands are endogenously present in our *ex vivo* model, I used quantitative real-time PCR (qPCR) to establish the relative quantities of ligand mRNA in the slices at important time points (Figure 12a). Figure 12b shows a heat map of ligand mRNA expression at myelination (21 days in vitro, div), demyelination (2 days post lysolecithin, dpl), and remyelination (7 and 14dpl). Interestingly, I found that while some ligands are expressed differentially during myelination, demyelination, and remyelination, others are not expressed at all (Figure 12b). Importantly, while GDF1, GDF11, BMP6, and activin-A (gene name *Inhba*) are highly expressed at myelination, they are re-expressed at different times during remyelination. Specifically, GDF1, GDF11, and BMP6 are upregulated at 14dpl, and activin-A is upregulated earlier at 7dpl, suggesting that these ligands may have distinct functions during endogenous remyelination. Many ligands, such as myostatin, nodal, and GDF5, are not expressed at all, indicative of their lack of involvement in remyelination in this model. As qPCR data only reveals the relative quantities of mRNA, I next per-

formed Western blots using slice culture lysates to determine whether the top hits from the qPCR experiment were expressed at the protein level. Here, I saw that all three top hits (GDF1, GDF11, and BMP6) were indeed expressed at the protein level at 7 and 14dpl (Figure 12c). It was intriguing to note that while the mRNA-level expression changes between these two time points, the protein-level expression is stable. This suggests that there may be post-transcriptional feedback mechanisms regulating protein expression during repair.

Next, I investigated whether ligands expressed in the *ex vivo* slice culture paralleled those expressed during *in vivo* remyelination. To do this, I extracted RNA from lysolecithin-induced focal corpus callosum lesions and ran quantitative real-time PCR to determine relative quantities of mRNA, as above (Figure 13a). Figure 13b shows a heat map of ligand mRNA expression at important time points during remyelination *in vivo*, including when oligodendrocyte differentiation/ensheathment begins (10dpl), is underway (14dpl), and is complete (21dpl). Consistent with the *ex vivo* results, ligands highly expressed during *in vivo* remyelination were GDF1, GDF11, and BMP6. Surprisingly, activin-A was not highly expressed during remyelination. However, previous work from our lab [142] confirmed activin-A protein expression in remyelinating lesions, suggesting post-transcriptional regulation mechanisms are at work. To confirm protein-level expression of alternative ligands, I analyzed GDF1, GDF11, and BMP6 expression in lesions by immunohistochemistry, and found that all three ligands were present within the lesion area (Figure 13c).

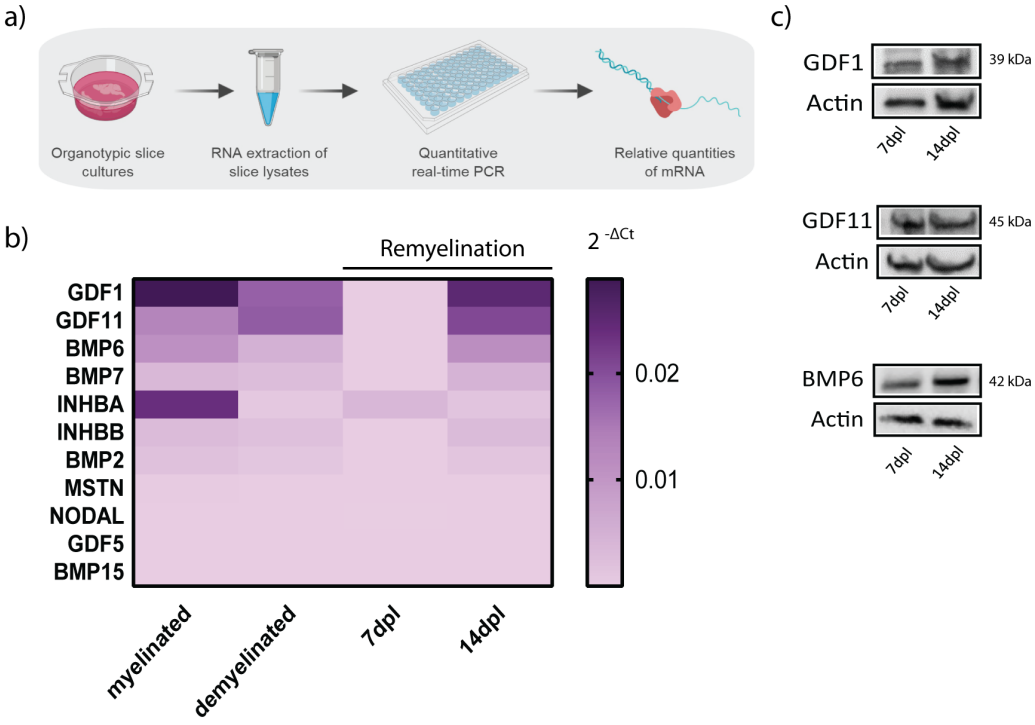

Figure 12. Activin receptor ligand expression during remyelination *ex vivo*. a) Slice culture processing protocol for qPCR analysis. b) Heat map of relative mRNA expression of activin receptor-binding ligands during myelination, demyelination, and remyelination. Scale is shown on left. Darker colours indicate higher $2^{-\Delta Ct}$ values, and thus higher expression. Values shown are an average of 4 separate experiments, with 6 slices (1 well) per lysate. c) Western blot of top 3 hits from (b) to confirm protein-level expression at 7dpl and 14dpl.

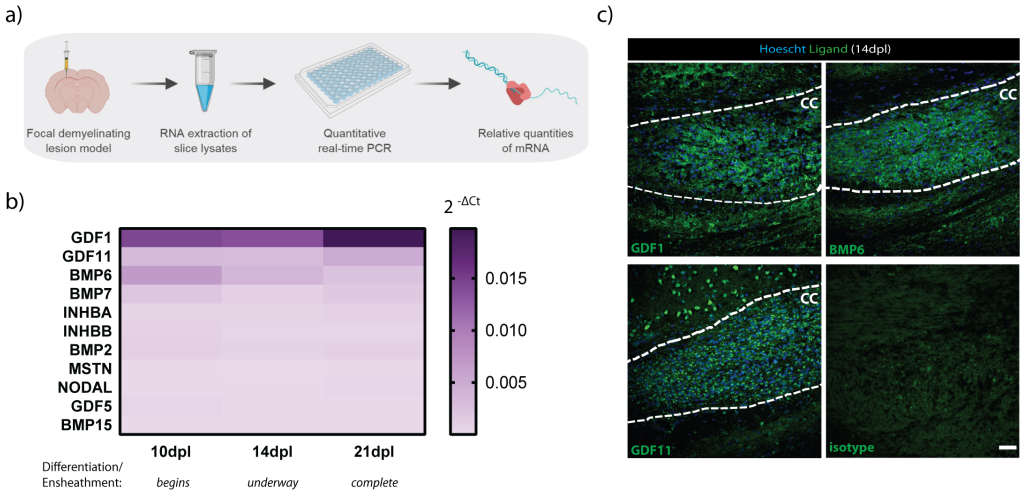

Figure 13. Activin receptor ligand expression during remyelination *in vivo*. a) In vivo lesioning protocol for qPCR analysis. b) Heat map of relative mRNA expression of activin receptor-binding ligands during remyelination. Scale is shown on left. Darker colours indicate higher $2^{-\Delta Ct}$ values, and thus higher expression. Values shown are an average of 3 separate experiments. c) Immunohistochemistry of top 3 hits from (b) to confirm protein-level expression in focal lesions at 14dpl with isotype control (rabbit IgG, green). Dotted lines indicate lesion areas. Scale bar, 50μm.

4.2.2 GDF1 is important during late remyelination *ex vivo*

Since previous work pointed towards a requirement for activin receptors, but not the primary ligand (activin-A) during remyelination, I next sought to determine whether any of the other highly expressed activin-receptor binding ligands identified in Figures 12 and 13 were required for remyelination. The first ligand tested was GDF1. To block GDF1 action in *ex vivo* slices, Lefty-1 was used, a protein which blocks a required co-receptor for GDF1's binding to activin receptors (Figure 14a). While remyelination index was not significantly affected at 7dpl or 14dpl in Lefty-1 treated slices compared to controls, there was a trend decrease in remyelination at 14dpl. This is supported by the representative images in Figure 14b, where there is a clear reduction in myelin basic protein immunostaining. Surprisingly, at 7dpl, there is a slight increase in the remyelination index. Lefty-1 works by inhibiting an EGF-CFC (Embryonic Growth Factor-Cripto/FRL-1/Cryptic) co-receptor, which is required for GDF1 binding to activin receptors; however, this co-receptor also blocks activin-A's access to activin receptors [344, 345]. As such, the slight increase in remyelination at 7dpl with Lefty-1 treatment may be due to a disinhibitory effect on activin-A mediated activin receptor signalling. It is possible that this signalling is only important early (at 7dpl), as a disinhibitory effect is not apparent later at 14dpl.

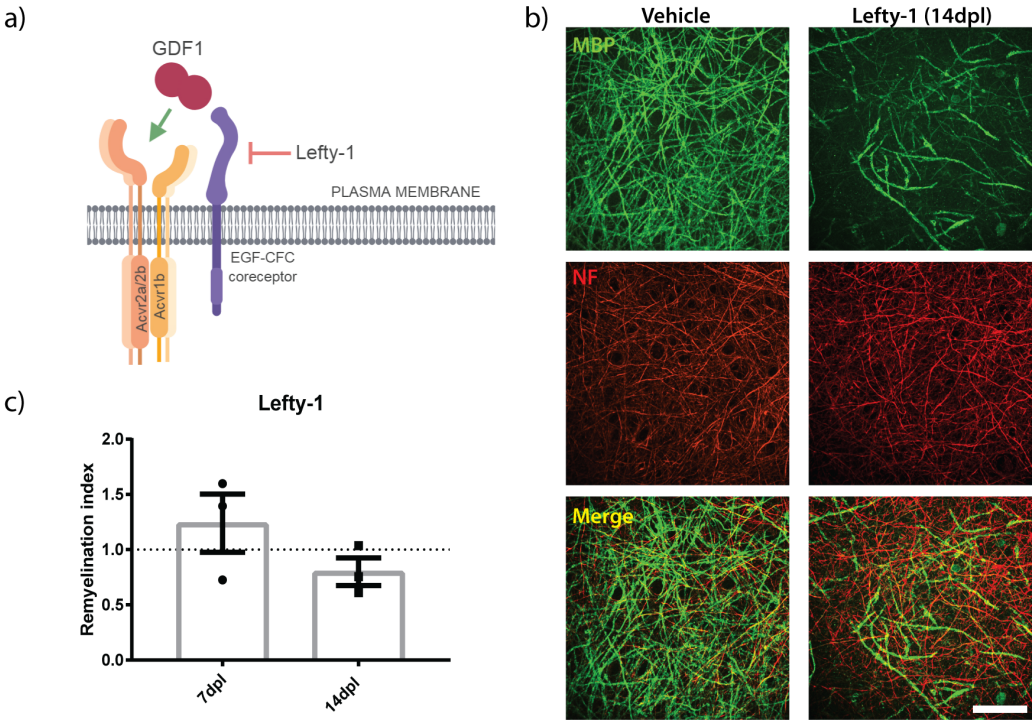

Figure 14. GDF1 inhibition has a slight effect on late remyelination. a) GDF1 is blocked by Lefty-1, which inhibits a required co-receptor (EGF-CFC) and prevents GDF1 from binding Activin receptors. b) Representative images of slice cultures at 14dpl treated with vehicle control or Lefty-1 during remyelination, immunostained against myelin basic protein (MBP, green) and axonal neurofilament-H (NF, red). Scale bar, 50 μm. c) Mean remyelination index ±s.e.m. in Lefty-1 treated *ex vivo* slices at 7 and 14 days post lysolecithin (dpl) normalized to vehicle control from the respective time point. n=3 animals, one-sample t-test compared to a theoretical mean of 1 (control). No significant differences were observed.

Next, to determine whether a combination of activin receptor ligands were required for remyelination, I blocked both activin-A and GDF1 together during remyelination in *ex vivo* slice cultures (Figure 15a). Activin-A was blocked by Follistatin (as in Chapter 3), and GDF1 was blocked by Lefty-1. Interestingly, when both ligands were blocked together, there was a significant reduction in remyelination at 14dpl (Figure 15b,c), suggesting that together, the ligands are important for late remyelination. At 7dpl, remyelination was 'reduced' back to vehicle levels with Follistatin and Lefty-1 treatment compared to Lefty-1 treatment alone (Figure 14c). This is consistent with the disinhibition effect hypothesis stated above: when EGF-CFC co-receptors are blocked by Lefty-1, activin-A has increased access to activin receptors, thereby resulting in increased remyelination. If activin-A is also blocked using follistatin, however, remyelination returns to baseline (Figure 15c).

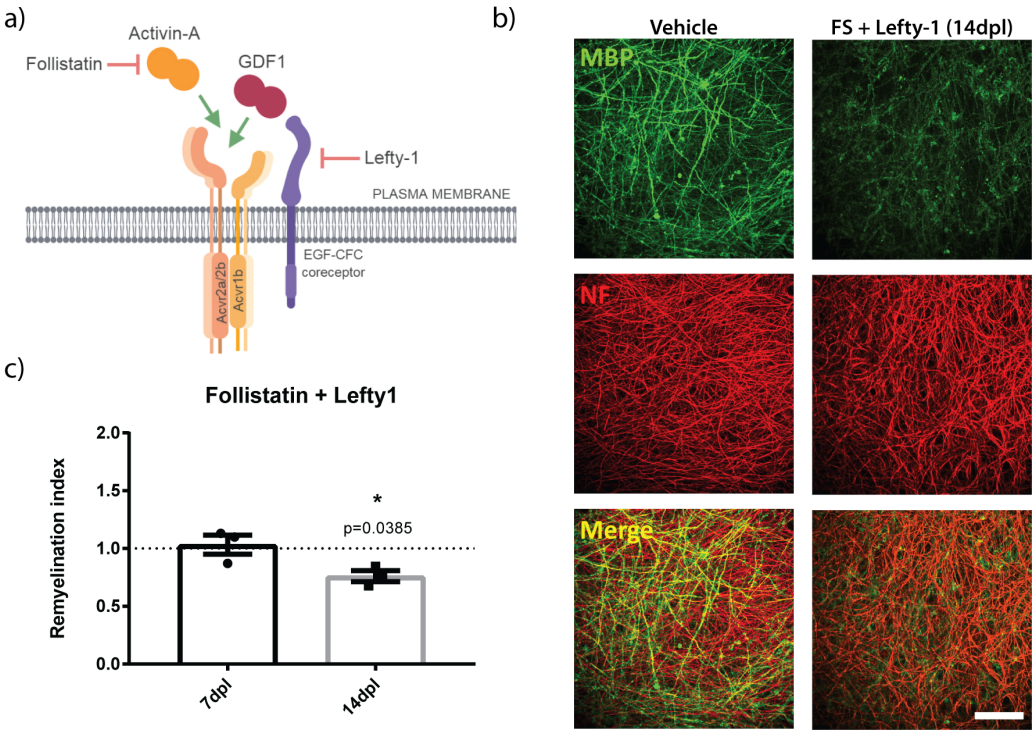

Figure 15. Blocking GDF1 and activin-A together inhibits late remyelination. a) GDF1 and activin-A are blocked by Lefty-1 and Follistatin. b) Representative images of slice cultures at 14dpl treated with vehicle control or Follistatin (FS) + Lefty-1 during remyelination, immunostained against myelin basic protein (MBP, green) and axonal neurofilament-H (NF, red). Scale bar, 50 μm. c) Mean remyelination index ±s.e.m. in Follistatin (FS) + Lefty-1 treated *ex vivo* slices at 7 and 14 days post lysolecithin (dpl) normalized to vehicle control from the respective time point. n=3 animals, one-sample t-test compared to a theoretical mean of 1 (control), *P=0.0385 at 14dpl.

4.2.3 GDF1 inhibition *in vivo* affects g ratio and number of myelinated axons

As blocking GDF1 had a negative effect during late remyelination *ex vivo*, I next wanted to determine whether this was also reflected in an *in vivo* model of remyelination. To do this, implantable osmotic mini-pumps with attached brain cannula were used to supplement Lefty-1 or vehicle control directly to lysolecithin-induced focal lesions in the corpus callosum of mice. Lesion areas were processed at 14dpl based on the above *ex vivo* results. Electron microscopy imaging was then carried out to determine effects on myelin thickness and density of myelinated axons. There were no significant differences in overall or average g ratio (Figure 16a, b); however, when g ratio was plotted against axon diameter, slopes were significantly different (Figure 16c), suggesting differences in myelin thickness by axon diameter between Lefty-1 treatment and controls. Interestingly, the overall number of myelinated axons was significantly higher in Lefty-1 treated animals compared to controls (Figure 16d). When number of myelinated axons was stratified by axon diameter, there were non-significant trends, with Lefty-1 mostly increasing number of myelinated axons below 0.4 μm and between 0.7-0.8 μm in diameter (Figure 16e). Together, this data suggests that blocking GDF1 *in vivo* has calibre-dependent effects on myelin thickness and increases the overall number of myelinated axons.

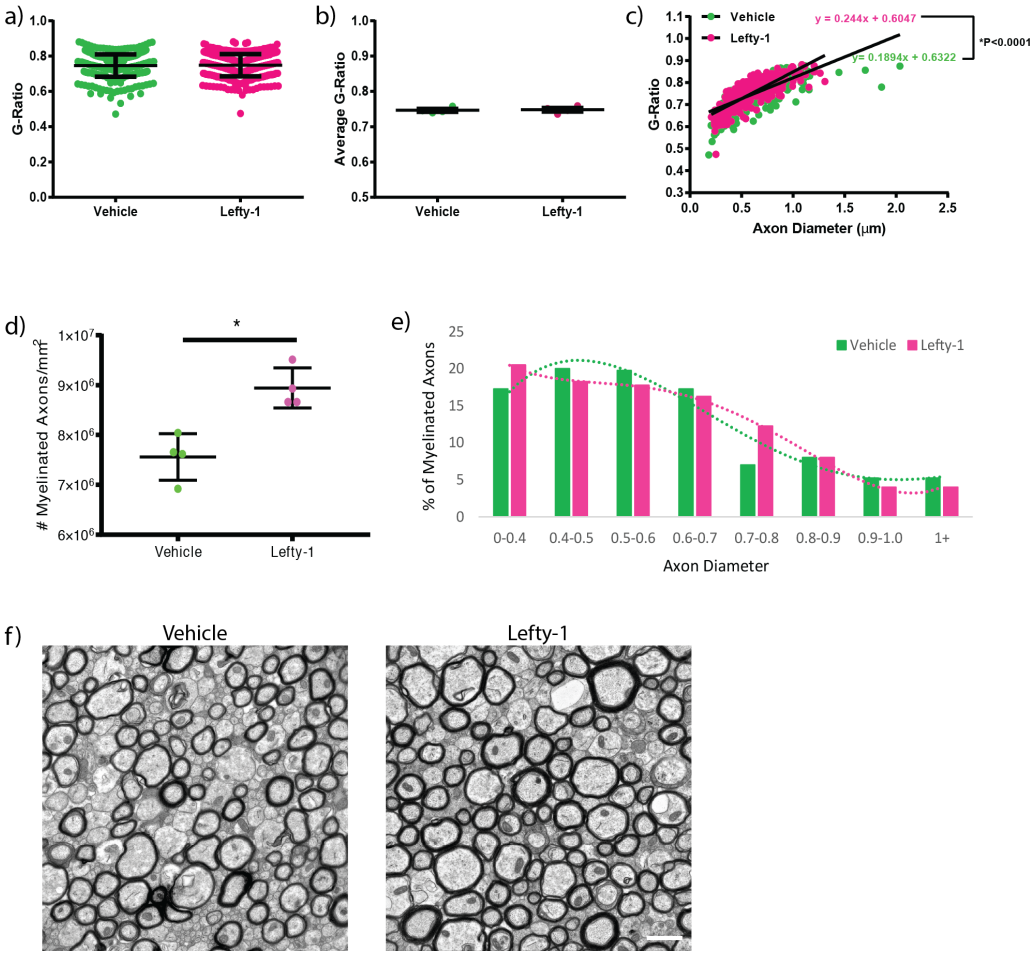

Figure 16. Inhibiting GDF1 in focal lesions *in vivo* affects g ratio and number of myelinated axons. a) Overall g ratio ±s.d. of Lefty-1 treated animals compared to control, n=100 per animal, 4-5 animals per condition. Mann-Whitney test, non-significant. b) Mean of g ratio ±s.e.m. of Lefty-1 treated animals compared to control. Mann-Whitney test, non-significant. c) G ratio versus axon diameter in Lefty-1 treated (magenta) and vehicle controls (green). Extra sum of squares F-test between slopes, *P<0.0001. d) Mean of total number of myelinated axons ±s.e.m. in Lefty-1 treated animals and vehicle controls, Mann-Whitney test, *P=0.0286. e) Proportion of myelinated axons by axon diameter in Lefty-1 treated mice (magenta) and vehicle control (green), overlaid with polynomial best-fit regression curves (Kolmogorov-Smirnov test, non-significant). n=4-5 animals per condition, 100 axons per animal. 2-way ANOVA with Bonferroni's multiple comparisons test, non-significant. f) Representative images of Lefty-1 and vehicle treated corpus callosum. Scale bar, 1μm.

4.2.4 GDF11 is required during early and late remyelination *ex vivo*

The next activin receptor ligand tested for effects on remyelination was GDF11. To block GDF11 activity, GASP-1 was administered to organotypic slice cultures (Figure 17a). GASP-1 works as a ligand trap and prevents GDF11 from binding to receptors. Blocking GDF11 significantly impaired remyelination both at 7dpl and 14dpl (Figure 17c). Representative images (Figure 17b) show reduced myelin basic protein (MBP, green) immunostaining at 7dpl in GASP-1 treated slices compared to control. Here, it is interesting to note the morphology of the MBP stain. Specifically, the MBP looks to be mostly surrounding cell bodies, and not running along axons, pointing to an inhibitory effect on terminal oligodendrocyte differentiation.

To determine whether blocking GDF11 and activin-A together affects remyelination, Follistatin and GASP-1 were administered to *ex vivo* slice cultures (Figure 18a). Remyelination was significantly impaired both at 7dpl and 14dpl (Figure 18b, c). The morphology of the MBP stain here is similar to that of Figure 17b; however, there looks to be overall less myelin, suggesting this potential effect on oligodendrocyte differentiation is consistent.

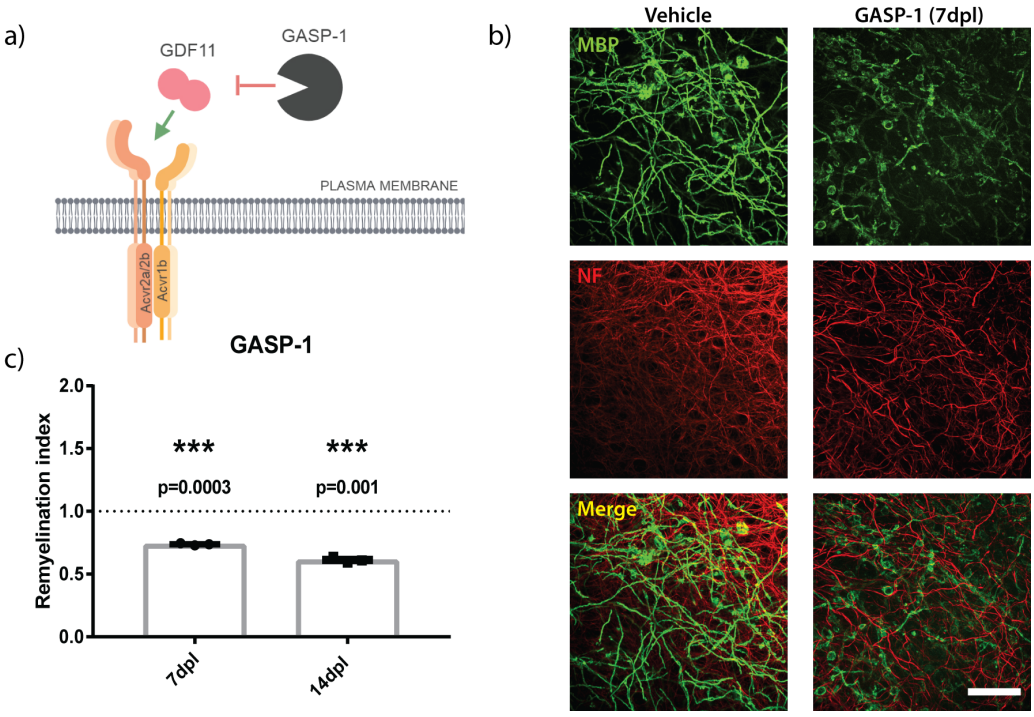

Figure 17. GDF11 inhibition strongly blocks early and late remyelination. a) GDF11 is blocked by GASP-1, which works as a ligand trap and prevents GDF11 from binding its receptors. b) Representative images of slice cultures at 7dpl treated with vehicle control or GASP-1 during remyelination, immunostained against myelin basic protein (MBP, green) and axonal neurofilament-H (NF, red). Scale bar, 50 μm. c) Mean remyelination index ±s.e.m. in GASP-1 treated *ex vivo* slices at 7 and 14 days post lysolecithin (dpl) normalized to vehicle control from the respective time point. n=3 animals, one-sample t-test compared to a theoretical mean of 1 (control), ***P=0.0003 and ***P=0.001 at 7dpl and 14dpl, respectively.

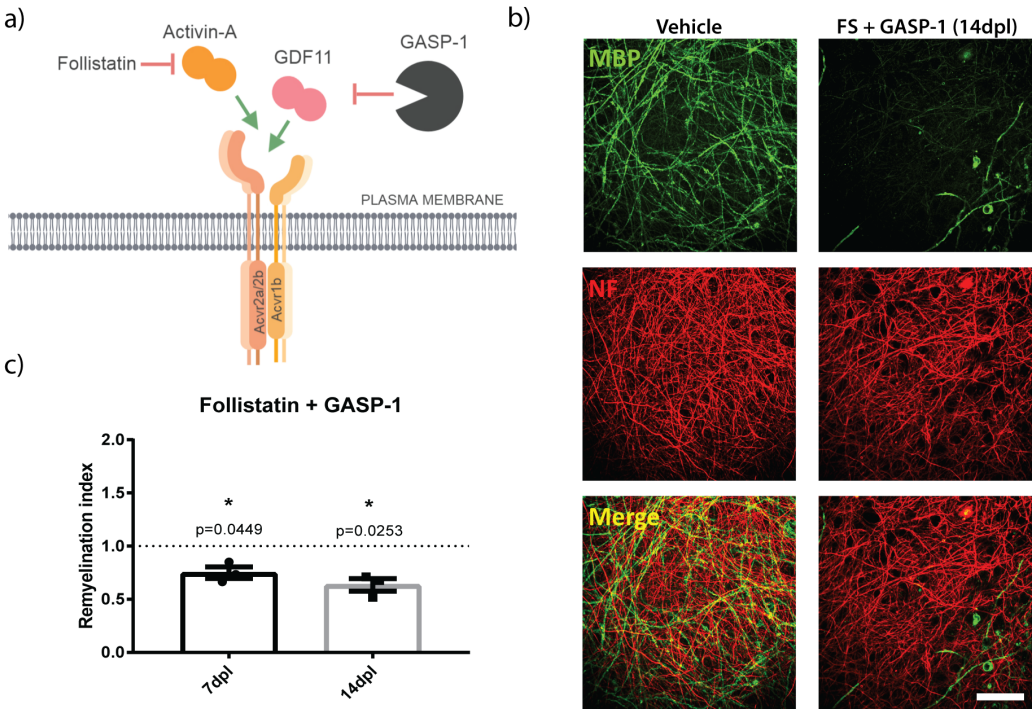

Figure 18. Blocking GDF11 and activin-A together inhibits early and late remyelination. a) GDF11 and activin-A are blocked by GASP-1 and Follistatin. b) Representative images of slice cultures at 14dpl treated with vehicle control or Follistatin (FS) + GASP-1 during remyelination, immunostained against myelin basic protein (MBP, green) and axonal neurofilament-H (NF, red). Scale bar, 50 μm. c) Mean remyelination index ±s.e.m. in Follistatin + GASP-1 treated *ex vivo* slices at 7 and 14 days post lysolecithin (dpl) normalized to vehicle control from the respective time point. n=3 animals, one-sample t-test compared to a theoretical mean of 1 (control), *P=0.0449 and *P=0.0253 at 7dpl and 14dpl, respectively.

4.2.5 Blocking GDF11 *in vivo* affects number of myelinated axons by diameter

To determine whether blocking GDF11 affects remyelination *in vivo*, implantable osmotic mini-pumps with attached brain cannula were used to supplement GASP-1 or vehicle control directly to lysolecithin-induced focal lesions in the corpus callosum of mice. Lesion areas were processed at 14dpl based on the above *ex vivo* results. Electron microscopy was then carried out to determine effects on myelin thickness and density of myelinated axons. There were no differences between GASP-1 treated and vehicle controls in terms of overall or average g ratio (Figure 19a, b). Additionally, when g ratio was plotted by axon diameter, slopes were not significantly different between treatments (Figure 19c). GASP-1 treated animals had a slightly (non-significant) lower number of overall myelinated axons; however, when this data was stratified by axon diameter, there was a significantly higher number of small diameter (<0.4 μm) myelinated axons. Further, the cumulative distribution of myelinated axon diameters (represented by the curves in Figure 19e) were significantly different between treatments. This data suggests that blocking GDF11 in an *in vivo* focal demyelinating model affects the number of myelinated axons in a calibre-dependent manner.

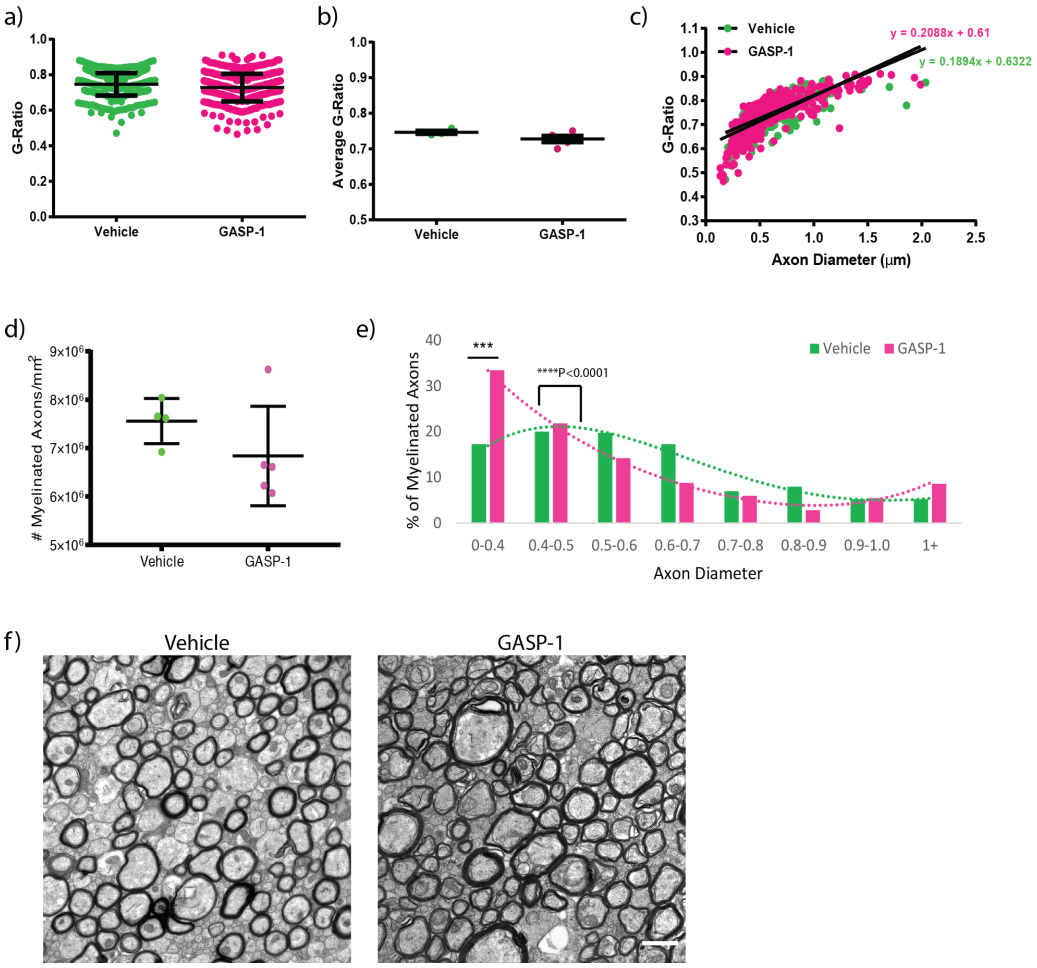

Figure 19. Blocking GDF11 in focal lesions *in vivo* results in differences in number of myelinated axons by diameter. a) Overall g ratio ±s.d. of GASP-1 treated animals compared to control, n=100 per animal, 4-5 animals per condition. Mann-Whitney test, non-significant. b) Mean of g ratio ±s.e.m. of GASP-1 treated animals compared to control. Mann-Whitney test, non-significant. c) G ratio versus axon diameter in GASP-1 treated (magenta) and vehicle controls (green). Extra sum of squares F-test between slopes, non-significant. d) Mean of total number of myelinated axons ±s.e.m. in GASP-1 treated animals and vehicle controls. Mann-Whitney test, non-signifcant. e) Analysis of distribution of number of myelinated axons in relation to axon diameter, in GASP-1 treated mice (magenta) and vehicle control (green), overlaid with polynomial best-fit regression curves (Kolmogorov-Smirnov test, ****P<0.0001). n=4-5 animals per condition, 100 axons measured per animal. 2-way ANOVA with Bonferroni's multiple comparisons test, ***P=0.0004 at 0-0.4 μm diameter. f) Representative images of GASP-1 and vehicle treated corpus callosum. Scale bar, 1μm.

4.2.6 BMP6 is required during late remyelination *ex vivo*

The final activin receptor ligand tested was bone morphogenic protein (BMP) 6. To block BMP6, Sclerostin (SOST), a BMP6-specific ligand trap, was used (Figure 20a). Supplementing SOST to *ex vivo* slice cultures resulted in a significant impairment in remyelination at 14dpl (Figure 20b, c). This data suggests BMP6 is required during late remyelination.

To determine whether blocking a combination of activin receptor ligands affects remyelination, Follistatin and SOST were administered to *ex vivo* remyelinating slice cultures (Figure 21a). Here, blocking BMP6 and activin-A together resulted in a significant reduction in remyelination at both 7dpl and 14dpl (Figure 21b, c). Together, these results implicate an early synergistic effect between BMP6 and activin-A: while alone, neither is required at 7dpl, loss of both impairs remyelination at this time point.

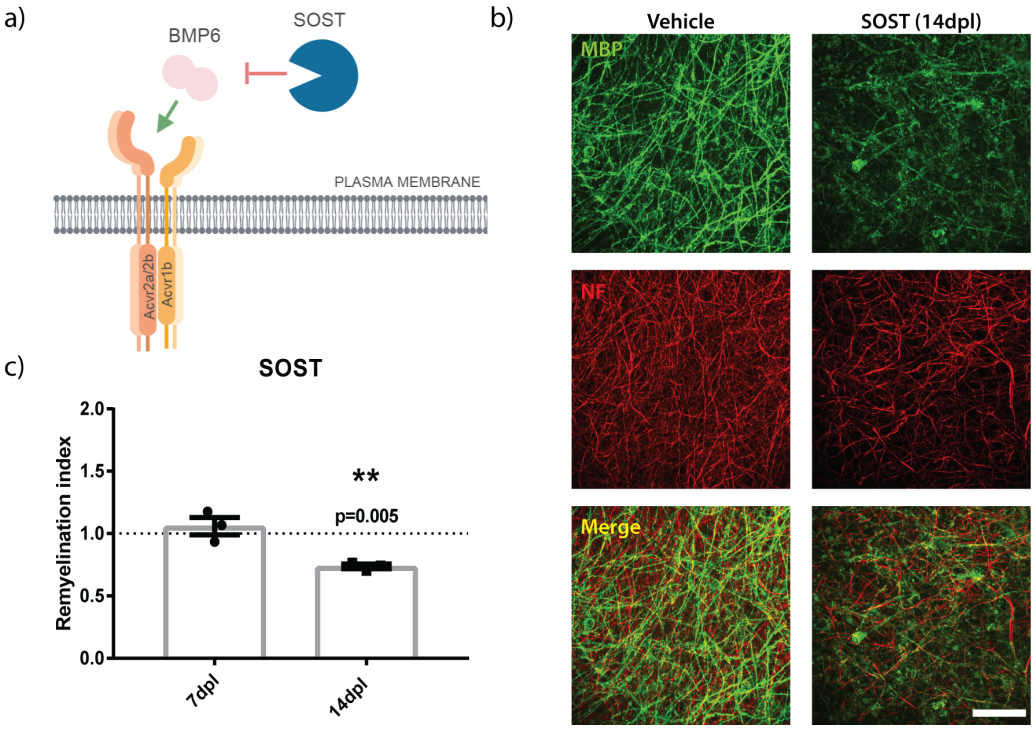

Figure 20. BMP6 inhibition blocks late remyelination. a) BMP6 is blocked by Sclerostin (SOST) which works as a ligand trap and prevents BMP6 from binding its receptors. b) Representative images of slice cultures at 14dpl treated with vehicle control or SOST during remyelination, immunostained against myelin basic protein (MBP, green) and axonal neurofilament-H (NF, red). Scale bar, 50 μm. c) Mean remyelination index ±s.e.m. in SOST treated *ex vivo* slices at 7 and 14 days post lysolecithin (dpl) normalized to vehicle control from the respective time point. n=3 animals, one-sample t-test compared to a theoretical mean of 1 (control), **P=0.005 at 14dpl.

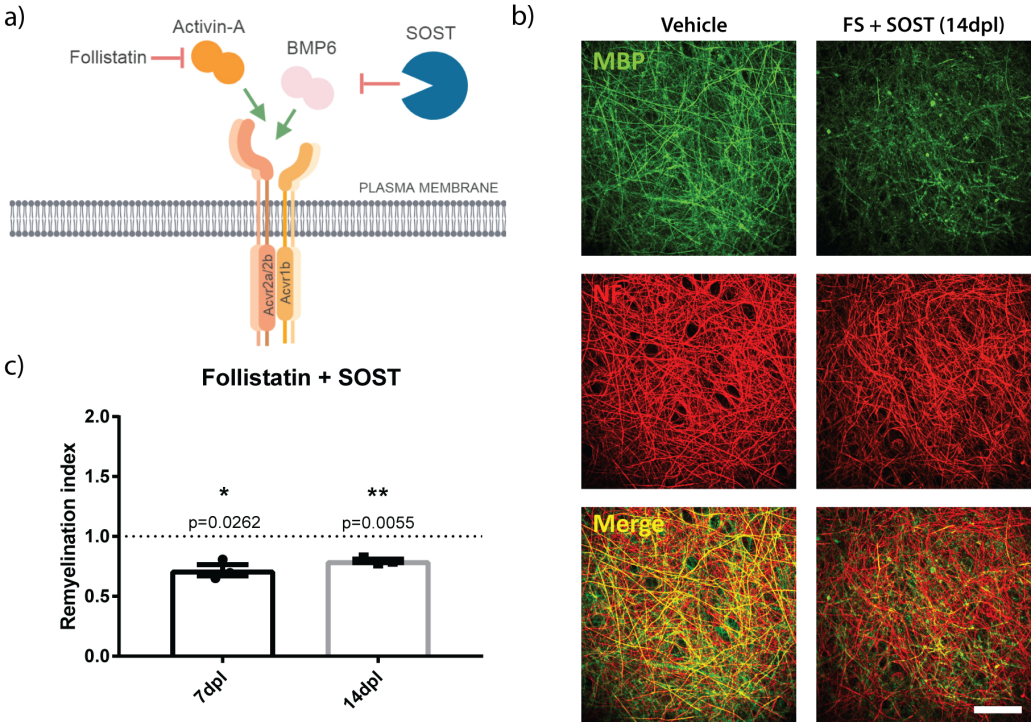

Figure 21. Blocking BMP6 and activin-A together inhibits early and late remyelination. a) BMP6 and activin-A are inhibited by SOST and Follistatin. b) Representative images of slice cultures at 14dpl treated with vehicle control or Follistatin (FS) + SOST during remyelination, immunostained against myelin basic protein (MBP, green) and axonal neurofilament-H (NF, red). Scale bar, 50 μm. c) Mean remyelination index ±s.e.m. in Follistatin + SOST treated *ex vivo* slices at 7 and 14 days post lysolecithin (dpl) normalized to vehicle control from the respective time point. n=3 animals, one-sample t-test compared to a theoretical mean of 1 (control), *P=0.0262 and **P=0.0055 at 7dpl and 14dpl, respectively.

4.2.7 Inhibition of BMP6 *in vivo* does not affect remyelination

To determine whether blocking BMP6 *in vivo* reflected the observed effects in the *ex vivo* model, implantable osmotic mini-pumps with attached brain cannula were used to supplement SOST or vehicle control directly to lysolecithin-induced focal lesions in the corpus callosum of mice. Lesion areas were processed at 14dpl based on the above *ex vivo* results. Electron microscopy was then carried out to determine effects on myelin thickness and density of myelinated axons. There were no significant differences between SOST treated and controls in terms of overall or average g ratio (Figure 22a, b). Additionally, when g ratio was plotted by axon diameter, the slopes were not different between treatment and control (Figure 22c), suggesting myelin thickness by axon calibre is not affected by BMP6 inhibition. In terms of number of myelinated axons, there were no overall or axon calibre-dependent differences in SOST treated animals compared to controls; however, there was a small trend in the number of myelinated small-calibre axons ($<0.4\mu$m), with slightly higher numbers in SOST treated animals (Figure 22d, e). These results show that although remyelination was significantly reduced upon blocking BMP6 *ex vivo*, this was not reflected in the *in vivo* model.

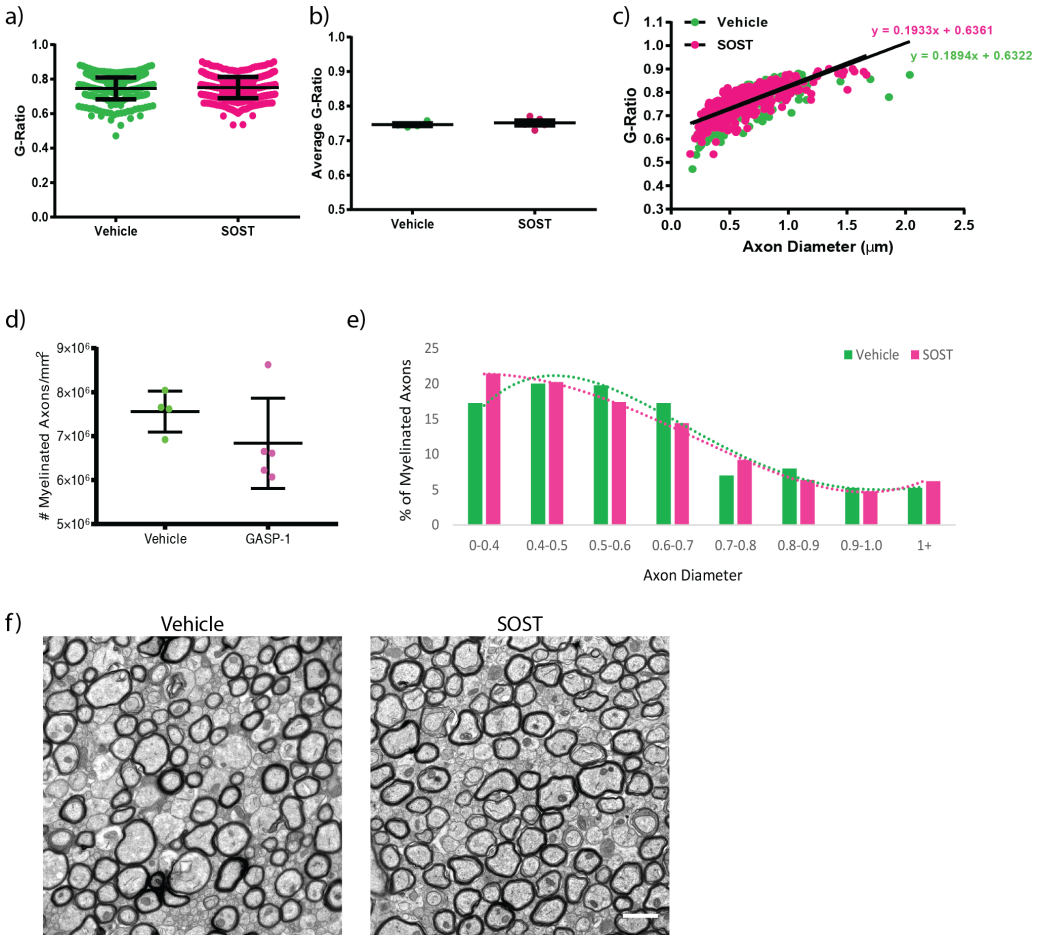

Figure 22. Blocking BMP6 in focal lesions *in vivo* does not affect remyelination. a) Overall g ratio ±s.d. of SOST-treated animals compared to control, n=100 per animal, 4-5 animals per condition. Mann-Whitney test, non-significant. b) Mean of g ratio ±s.e.m. of SOST-treated animals compared to control. Mann-Whitney test, non-significant. c) G ratio versus axon diameter in SOST treated (magenta) and vehicle controls (green). Extra sum of squares F-test between slopes, non-significant. d) Mean of total number of myelinated axons ±s.e.m. in SOST treated animals and vehicle controls. Mann-Whitney test, non-significant. e) Proportion of myelinated axons by axon diameter in SOST treated mice (magenta) and vehicle control (green), overlaid with polynomial best-fit regression curves (Kolmogorov-Smirnov test, non-significant). n=4-5 animals per condition, 100 axons measured per animal. 2-way ANOVA with Bonferroni's multiple comparisons test, non-significant. f) Representative images of SOST and vehicle treated corpus callosum. Scale bar, 1μm.

4.2.8 Supplementing activin receptor ligands other than activin-A does not affect remyelination *ex vivo*

To investigate whether activin receptor activity can be modulated during remyelination by ligands other than activin-A, GDF1, GDF11, and BMP6 recombinant proteins were supplemented to *ex vivo* cerebellar slice cultures during remyelination (Figure 23a). Here, there were no significant differences in remyelination at 7dpl, compared to the significant (>2 fold) increase in remyelination upon treatment with activin-A (Figure 23b, c). These results demonstrate that while the presence of some of these ligands is important for remyelination *ex vivo*, none are sufficient to accelerate remyelination.

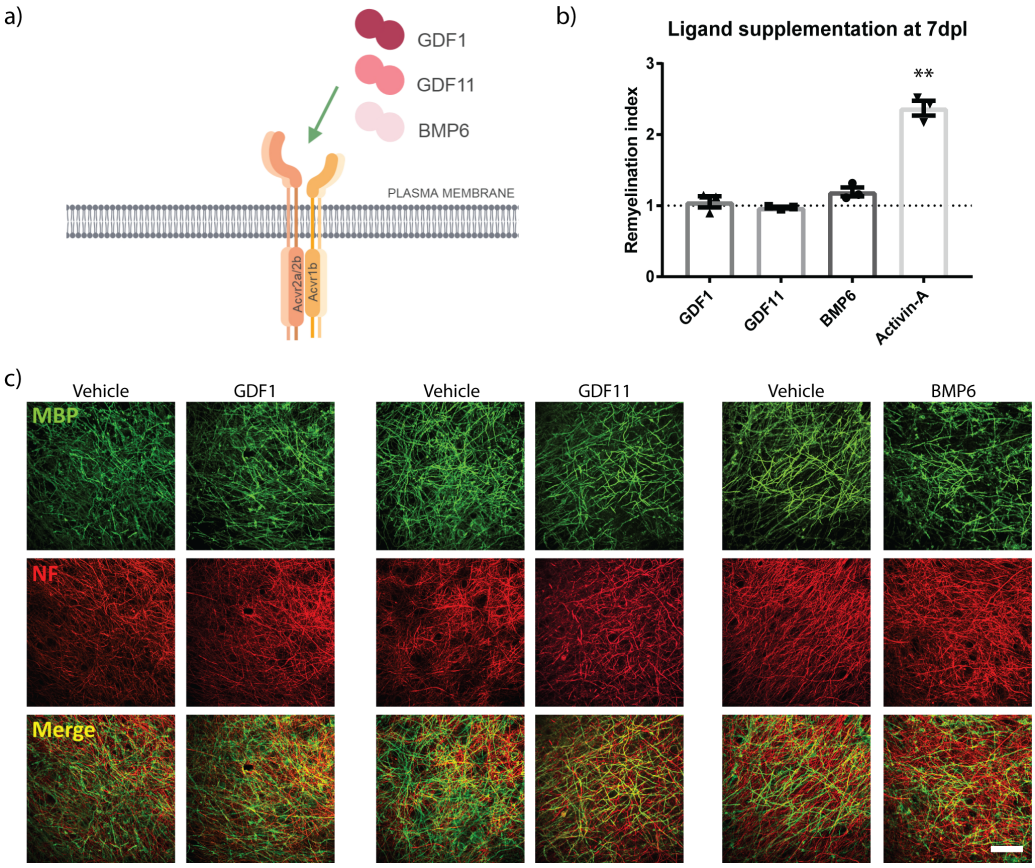

Figure 23. Supplementing GDF1, GDF11, and BMP6 to slice cultures did not improve remyelination. a) GDF1, GDF11, and BMP6 were added to *ex vivo* slice cultures individually during remyelination. b) Mean remyelination index ±s.e.m. in GDF1, GDF11, and BMP6 treated *ex vivo* slices at 7 days post lysolecithin (dpl) normalized to vehicle control from the respective time point. n=3 animals, one-sample t-test compared to a theoretical mean of 1 (control). Activin-A treated condition shown as comparison of highly significant effect (**P=0.0057). Activin-A treated condition data taken from Figure 6 in Chapter 3. c) Representative images of slice cultures at 7dpl treated with ligands (GDF1, GDF11, BMP6) and their vehicle controls during remyelination, immunostained against myelin basic protein (MBP, green) and axonal neurofilament-H (NF, red). Scale bar, 50 μm.

4.3 Discussion

Activin receptor ligands are dynamically expressed during remyelination

In this chapter, I identified three novel proteins within the TGF-β superfamily with roles in remyelination. Data from a panel of 11 activin receptor ligands revealed dynamic mRNA expression during remyelination in both *ex vivo* and *in vivo* models. From the 11 initial proteins, the top three hits were chosen for further investigation. Their expression was confirmed at the protein level by Western blot and immmunohistochemistry. It was encouraging that across both *ex vivo* and *in vivo* lesioning models, the same three proteins came up as top hits during remyelination. This suggests that despite many differences between these models (such as age and brain region), the expression of proteins relevant in myelin regeneration is conserved.

Interestingly, the dynamic mRNA-level expression was not reflected at the protein level in the *ex vivo* model. This could be due to the tight regulatory systems controlling TGF-β protein activity, or general regulatory mechanisms controlling post-transcriptional, translational, and protein degradation processes. Indeed, a poor correlation between mRNA and protein-level expression has been widely reported [346–348]. In this superfamily of proteins, where activity is strictly controlled by several mechanisms (such as precursor cleavage into mature peptides and ligand-binding proteins [306, 307]), it is perhaps not surprising that protein expression is more stable than the relative mRNA transcript levels may suggest.

The low expression of activin-A mRNA during remyelination in *ex vivo* and *in*

vivo models was unexpected. As mentioned above, mRNA transcript expression may not reflect protein levels; therefore, it would have been interesting to confirm protein-level expression for activin-A during remyelination in the slices. Given previous research, I would hypothesize that activin-A is expressed at the protein level after a demyelinating injury. Indeed, activin-A protein has been detected by immunohistochemistry at 10dpl in an *in vivo* remyelination model [142]. Further, activin-A is expressed in human perinatal white matter injury areas and in acute active lesions of MS patients [327], pointing to its role in inflammation and repair in human disease. Therefore, the dynamic expression of activin-A mRNA *ex vivo* and its lack of expression *in vivo* may not reflect protein-level expression and activity.

Importantly, all three of the proteins identified in qPCR screens were expressed at the protein level in both *ex vivo* and *in vivo* models during remyelination. To confirm their relevance for remyelination, I then tested whether modulating each protein's activity had any effects on this regenerative process.

GDF1, GDF11, and BMP6 can modulate remyelination

Each of the three novel candidates tested for potential effects on remyelination revealed unique effects. Each ligand was inhibited (both alone and with activin-A inhibitor) and supplemented to the *ex vivo* model. To determine whether *ex vivo* results are similar across models, each ligand was also blocked *in vivo*. The observed effects of each ligand will be discussed in turn (see Figure 24 for summary of *ex vivo* effects). A general limitation that applies to the blocking strategy used in

this chapter is that the pharmacokinetics and pharmacodynamics of these blocking agents were not established within the models used. It may have been interesting to determine whether blocking agents were indeed binding to their targets using fluorescent tagging or immunohistochemistry.

GDF1

GDF1 is a recently characterized member of the TGF-β superfamily found mainly in the central nervous system, with important functions during forebrain development [290, 349], and no previously reported associations with remyelination. When Lefty-1, a GDF1 inhibitor, was administered to organotypic slice cultures alone, there was a non-significant increase in remyelination at 7dpl followed by a decrease at 14dpl. When slices were treated with Lefty-1 combined with Follistatin (an activin-A inhibitor), the slight increase at 7dpl with Lefty-1 alone returned to baseline, and the decrease in remyelination at 14dpl became significant. When *in vivo* focal demyelinating lesions were treated with Lefty-1, there was an overall increase in the number of myelinated axons at 14dpl, notably in axons $<0.4\mu$m and between 0.7-0.8μm in diameter. However, the proportion of myelinated axons between Lefty-1 and controls were not significantly different within axon diameter bins. Further, while there were no overall differences in g ratio, the slopes between treatments were significantly different when plotted against axon diameter, suggesting that myelin thickness across axon diameter is affected by Lefty-1 treatment.

This is in line with previous work on interactions between EGF-CFC co-receptors,

activin-A, GDF1, and Lefty-1. There is substantial evidence for the requirement of EGF-CFC co-receptors (such as Cripto) for complex formation of GDF1 with activin receptors 2a and 2b [344, 345, 350]. Cripto is able to bind Acvr1b and facilitate signalling of GDF1 via Acvr2a/2b. Activin-A, however, does not require EGF-CFC co-receptors to bind Acvr2a/2b. Researchers found that differences in a 14 amino acid sequence between activin-A and GDF1 determines EGF-CFC dependence [345]. In fact, not only is activin-A able to signal independently of Cripto, the presence of this co-receptor can actually inhibit activin signalling. There is evidence indicating that an activin-A-Cripto-Acvr2a/2b complex is mutually exclusive with an activin-A-Acvr2a/2b-Acvr1b complex. Additionally, when cells are transfected with Cripto, activin-A mediated signalling is inhibited [344]. An additional layer of complexity is added when we consider inhibitors of EGF-CFC co-receptors, such as Lefty-1. Lefty proteins are monomers that have been shown to inhibit EGF-CFC co-receptors, and therefore GDF1 activity, in xenopus and zebrafish studies [345]. Taken together, the evidence points towards an inhibitory role for EGF-CFC in activin-A-mediated signalling, which is disinhibited by Lefty-1.

The complex functions of Lefty-1 are consistent with the varied results from Lefty-1 treatment on remyelination both *ex vivo* and *in vivo*. Specifically, remyelination is increased then decreased with Lefty-1 treatment alone in slice cultures, suggesting that an early disinhibition of activin-A is beneficial, while a late inhibition of GDF1 is detrimental. Indeed, when activin-A was blocked together with GDF1, the early beneficial effects of Lefty-1 treatment disappeared, and the late detrimental effects

were more severe. Interestingly, *in vivo* Lefty-1 administration resulted in a higher number of myelinated axons. This could reflect an early disinhibitory function of Lefty-1 on activin-A mediated signalling, rather than the inhibitory effect of GDF1. To test this, an immunohistochemistry-based technique (proximity ligation assay, PLA) may have been used to detect whether there is more activin-A bound to activin receptors with Lefty-1 treatment at 14dpl compared to controls. Further, analysis of number of myelinated axons at later times (21dpl, roughly parallel to 14dpl *ex vivo*) may have revealed results more reflective of GDF1 inhibition. Finally, it would have been interesting to characterize the expression of EGF-CFC co-receptors in both models, as differences in frequency of these proteins may affect Lefty-1 efficiency.

GDF11

GDF11 is expressed in astrocytes, neurons, and oligodendrocytes during development and has many roles within the CNS, including spinal cord patterning, neurogenesis, and cerebral vascular remodeling [294–296]. GASP-1 (GDF-Associated Serum Protein-1) is a strong inhibitor of GDF11, and works by preventing GDF11 from binding to activin receptors. Specifically, there is both *in vitro* and *in vivo* evidence for GASP-1 inhibiting the activity of GDF11 and the closely related protein myostatin/GDF8 [351, 352]. Despite the high similarity between GDF11 and myostatin, they are not functionally equivalent: GDF11 can promote Smad2/3 signalling via Acvr1b more effectively than myostatin [352]. Importantly, I found that myostatin/GDF8 is not highly expressed during remyelination (Figures 12, 13).

GDF11 has not been previously associated with remyelination. Here, when GDF11 was inhibited via GASP-1 administration in slice cultures, a strong and significant reduction in remyelination at both 7dpl and 14dpl was observed. When GDF11 was blocked in conjunction with activin-A, this strong reduction in remyelination persisted across both time points. Inhibition of GDF11 *in vivo* had no overall or calibre-dependent effects on g ratio, suggesting myelin thickness is not regulated by GDF11. While there was only a non-significant trend to a lower number of overall myelinated axons with GASP-1 treatment, the distribution of myelinated axons across diameters was different between treatments. Specifically, GASP-1 treatment resulted in a (non-significant) reduction in numbers of myelinated axons between 0.5-1 μm in diameter, and a significant increase in number of myelinated axons with diameters smaller than 0.4μm. This suggests that GDF11 mediated activin receptor signalling could regulate calibre-dependent myelination.

The strong effects observed in *ex vivo* blocking experiments may reflect the lack of circulation in this model. Given GDF11 is abundant in the blood [353], a possible reason for such strong effects in the *ex vivo* model is the lack of available protein source. The much more subtle *in vivo* effects could therefore be due to input from the circulation providing additional GDF11 to the lesion area as a response to GASP-1 treatment. This hypothesis could have been tested either by co-immunoprecipitation or by PLA to determine differences in the amount of GDF11 bound to activin receptors in GASP-1 treated animals compared to controls. As GASP-1 prevents GDF11 from binding to its receptors, I would expect to find less GDF11 bound to recep-

tors in the GASP-1 treated animals; however, if additional GDF11 is coming in, the amount of GDF11 bound to activin receptors may be stable across conditions.

BMP6

BMP6 is expressed by neurons and oligodendrocytes in the developing CNS. Conflicting roles have been reported for this ligand, such as improvement of ischemic brain injury and defective neurogenesis [298, 299]. Importantly, members of the BMP subfamily generally have been shown to be involved in negative regulation of oligodendrocyte maturation, and inducing astrogliogenesis instead [323, 325]. BMP6 has been specifically shown to be upregulated in demyelinating lesions in EAE mice; however, this was only shown for the mRNA level and was not followed up on, as other BMPs (BMP4 in particular) showed a much higher expression in this study [326]. As stated previously, it is important to investigate specific ligand-receptor-pathway interactions within each context, as the effects of TGF-β ligands vary based on environment. While BMP6 can bind Activin receptors 2a/2b as well as BMP receptor 2 (BMPRII), BMP4 can only bind BMPRII [308]. It is therefore not advisable to generalize findings across members of the BMP subfamily.

BMP6 activity can be blocked by Sclerostin (SOST), a recently identified BMP inhibitor. It has been reported to strongly inhibit BMP6, and weakly inhibit BMP2, BMP4, and BMP7 [308, 354, 355]. While its mechanism of action remains to be fully elucidated, studies have shown that SOST may work via inhibition of BMP-induced Smad phosphorylation [356, 357]. Treatment of *ex vivo* slice cultures with SOST

resulted in impaired late remyelination (14dpl). When SOST was combined with Follistatin (an activin-A inhibitor), remyelination was impaired both early (7dpl) and late (14dpl), pointing to a synergistic effect of BMP6 and activin-A during early remyelination. Indeed, synergism between TGF-β family members and their downstream signalling pathways has been observed in several contexts, including regulatory T cell development and photoreceptor activity in the retina [358–360]. *In vivo*, BMP6 inhibition had no significant effects on remyelination (both in terms of number of myelinated axons and myelin thickness), but a slight increase in number of myelinated axons below 0.4μm in diameter was observed.

The *ex vivo* and *in vivo* systems may have distinct levels of activin receptors vs other ligand-binding receptors, which may influence the differences observed in BMP6 inhibition between models. For example, if BMP receptors are more abundant *in vivo* than *ex vivo*, then BMP6 may be binding BMPRII more than Acvr2a/2b *in vivo*. If this is the case, then blocking BMP6 using SOST *in vivo* may reflect inhibition of BMPRII-mediated signalling more so than Acvr2a/2b-mediated signalling. This could have been tested by techniques which determine ligand-receptor binding (such as PLA or co-immunoprecipitation experiments discussed above), as well as determining expression of BMPRII in each model.

While blocking GDF1, GDF11, and BMP6 all yielded interesting inhibitory effects, supplementing these proteins to *ex vivo* slices did not accelerate or improve remyelination. Since activin-A has a high affinity for activin receptors, this apparent

lack of effect may be due to activin-A outcompeting these other three ligands for receptor binding. Additionally, a lack of effect may be due to endogenous ligands being plentiful and receptors being saturated. Further, it is possible that the concentration at which the proteins were administered to slices was not sufficient to induce activin receptor signalling. To account for this, higher concentrations of these ligands could have been tested to determine the optimal dosage. While GDF1 and GDF11 are only able to bind activin receptors, BMP6 may also bind BMPRII. Therefore, supplementing BMP6 may not have directly affected activin receptor signalling, as it may have activated distinct receptors. As mentioned above, it would be useful to carry out PLA or co-immunoprecipitation experiments to know which receptor BMP6 is more frequently bound to, as well as immunohistochemistry to determine whether BMPRII is widely expressed during remyelination.

It is surprising that blocking the highest affinity activin receptor ligand (activin-A) in *ex vivo* slice cultures yielded no differences in remyelination, but blocking lower affinity ligands (GDF1, GDF11, BMP6) hindered remyelination. This could be due to efficacy of inhibitors: though Follistatin has a very high binding affinity for activin-A, it was not explicitly shown to sequester activin-A in these experiments. However, an additional experiment using anti-activin-A antibody also resulted in no effect on remyelination, bolstering the original Follistatin results. Nevertheless, to irrefutably confirm Follistatin's function in blocking activin-A, either a co-immunoprecipitation experiment or a proximity ligation assay could have been carried out. Another potential reason for this surprising result could be the delicate balance of TGF-β

ligand and receptor interactions. It is possible that there are more abundant stores of activin-A ligand post-injury than that of GDF1, GDF11, or BMP6. Therefore, reducing available activin-A would have a less pronounced effect than depleting all the available GDF1, GDF11, and BMP6. Alternatively, it is also possible that activin-A levels are endogenously very low in slices, and therefore blocking its action does not affect remyelination. Quantitative comparisons of ligand expression by Western blot or immunohistochemistry in the *ex vivo* model may have shed light on this hypothesis. Finally, to corroborate results from ligand-specific antagonists, a genetic approach to induce global deletion of ligand genes (driven by a ROSA26 promoter) after a demyelinating insult may have been useful. As this superfamily is important during development, many TGF-β null experimental animals die prematurely, so it would be important to control the timing of deletion.

Discrepancies between ex vivo and in vivo results

While each ligand inhibitor had strong effects on remyelination *ex vivo*, effects were much more subtle in the *in vivo* model. This is not surprising: given that blocking the activin receptor *in vivo* (Chapter 3) did not strongly affect remyelination potential, it follows that inhibiting any of the activin receptor ligands would have similarly subtle effects. However, these discrepancies could also be due to major differences between models as discussed in Chapter 3. Further, there may be additional differences between models in the regulation of TGF-β superfamily signalling. For example, it is possible that *in vivo*, activin-A is better able to compensate for the loss of GDF1, GDF11, and BMP6, resulting in no major differences between

ligand inhibitors and controls. To account for this possibility, it would have been interesting to first compare relative protein levels of activin-A in the slice and *in vivo*. To further test this theory, Follistatin (activin-A inhibitor) may have been administered to *in vivo* lesions in conjunction with each ligand inhibitor, as well as all 4 ligand inhibitors together. Results from this experiment would inform whether activin-A is responsible for compensatory effects in the absence of each ligand, and whether all 4 ligands work together to support remyelination.

Interestingly, there is a similarity between ligand inhibitor and activin-A treated animals in terms of calibre-specific *in vivo* results. In axons smaller than 0.4μm in diameter, there were slightly higher numbers of myelinated axons when each ligand was blocked compared to their vehicle controls, similarly to when activin-A was administered in Chapter 3. A potential cause for this similarity may be that blocking these ligands is actually 'freeing up' the receptors for activin-A to bind. To test this hypothesis, a co-immunoprecipitation experiment may be carried out to determine whether more activin-A-Acvr2a/2b complexes are observed in conditions where alternative ligands are blocked. Further, the experiment described above, where Follistatin is used in conjunction with ligand antagonists, would be helpful in determining whether this proposed mechanism is driving the axon calibre-dependent increase in number of myelinated axons.

Ligand-specific effects on oligodendrocyte lineage cells

In addition to the quantified differences between ligand blocking treatments and controls discussed above, there were also clear qualitative differences between

conditions in the *ex vivo* model. When investigating differences in morphology of myelin immunostains between control remyelinated slices and poor remyelination in ligand blocking treatment, it is evident that each ligand inhibitor has a distinct effect. Blocking GDF1 appeared to have an effect on overall amount of myelin membrane being made, GDF11 inhibition appeared to affect oligodendrocyte maturation, and BMP6 inhibition may have had an effect on myelin membrane compaction/ensheathment (see Figure 24 for summary). Based on these qualitative observations, a good follow-up experiment would be to test whether blocking each of these ligands in cell cultures (oligodendrocyte progenitor cell cultures, oligodendrocyte-neuronal co-cultures, or oligodendrocyte-microfibre cultures) results in similar effects.

Further, although few effects were observed in the *in vivo* model at the ultrastructural level, it would have been interesting to immunostain brain sections for oligodendrocyte lineage cell markers to determine whether inhibiting GDF1, GDF11, and BMP6 had any direct effects on oligodendrocyte maturation.

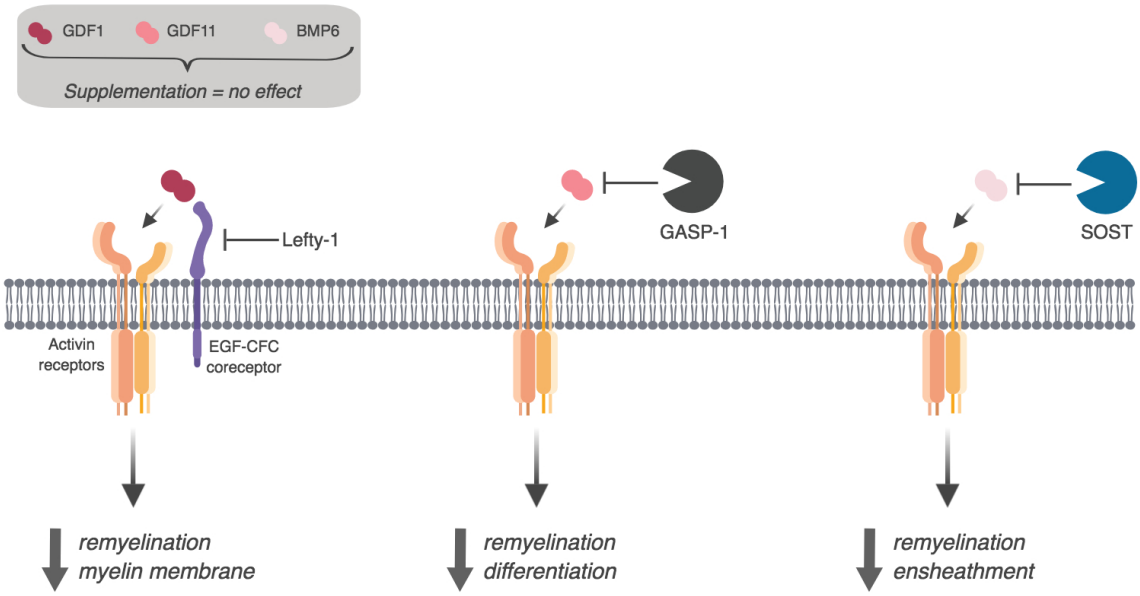

Figure 24. Inhibition of GDF1, GDF11, and BMP6 have distinct effects on remyelination *ex vivo*.

Overall, results from this chapter yield a number of additional questions regarding the role of TGF-β superfamily members during remyelination. Clearly, there is a complex role for these secreted proteins in driving remyelination via activin receptors. However, it is not known which cell types are expressing these ligands during remyelination, or which cells are mediating activin receptor signalling. Further, it is not clear whether these ligands are relevant in human disease. These important outstanding questions will be investigated in the following chapter.

5 Chapter 5: Microglia/macrophages and oligodendrocytes mediate activin receptor signalling during remyelination

5.1 Introduction

To consider activin receptors as a potential target for clinical intervention in Multiple Sclerosis, we must first elucidate their mechanism of action. Given the many functions of activin receptor ligands, especially during development and injury [270], it is important to understand the cell types expressing these ligands, as well as the cells and downstream pathways through which they are actively signalling, in a context-specific manner.

This information is crucial for a) developing therapies targeted to specific cell types, b) understanding whether observed changes in remyelination are due to direct or indirect effects on oligodendrocytes, and c) providing clues as to what the cellular source of ligands is within lesion areas. Previously, activin receptor expression has been reported on axons during development and following excitotoxic injury in rodents [274, 276]. Further, work by Miron and colleagues showed that during remyelination *in vivo*, $NG2^+$ oligodendrocyte progenitor cells and microglia/macrophages expressed both ligand-binding receptors (Acvr2a/2b) and the signal-transducing receptor Acvr1b. Importantly, microglia/macrophages also expressed activin-A, the primary ligand for these receptors [142]. Developmental data for alternative activin

receptor binding ligands identified in Chapter 4 revealed expression on neurons, astrocytes, and oligodendrocytes [302].

Given the significant contribution of cellular and microenvironmental context to ultimate signalling outcome in this superfamily of ligands and receptors, several unexplored questions remain regarding the mechanism of action of activin receptors during remyelination. In this chapter, I determined whether GDF1, GDF11, and BMP6 are relevant in human disease, and what cell types express these proteins within MS lesions. Results from human tissue were then confirmed in remyelinating mouse tissue. Additionally, reporter mice (described in detail below) were used to identify cell types actively signalling through activin receptors. Finally, cell-specific activin receptor expression in human tissue was elucidated, uncovering a potential receptor subtype specific effect.

5.2 Results

5.2.1 Ligands are expressed on microglia in active MS lesions

To determine whether the activin receptor binding proteins identified in Chapter 4 were relevant in human disease, immunohistochemistry was carried out on post-mortem MS tissue to investigate a) whether GDF1, GDF11, and BMP6 are expressed in lesions, and b) which cell types express these proteins. Post-mortem tissue is characterized using Luxol Fast Blue (LFB) staining to delineate white matter (WM, dark blue) from grey matter (GM, light blue). White matter lesions are then pathologically characterized according to the International Classification of Neurological Diseases, again using LFB to stain intact myelin and Oil Red O (ORO) to identify myelin debris (Figure 25a-b). Remyelinated lesions are characterized by intermediate LFB staining (often called a 'shadow plaque'), and little myelin debris. Acute active lesions exhibit a diffuse LFB border, demyelination, and ample amounts of myelin debris. Chronic active lesions show a lack of LFB staining and some myelin debris. Chronic inactive lesions show significant loss of LFB and no myelin debris. Lesion types have different likelihoods of repairing: chronic inactive are least likely to remyelinate, chronic active is moderately likely to repair, and acute active have a good remyelination potential (see Figure 25c for schematic).

Post-mortem tissue was co-stained for each ligand (GDF1, GDF11, and BMP6) and CD68, an activated microglia/macrophage marker (Figure 25d-e). Figure 25d shows the proportion of total ligand$^+$ cells which are also CD68$^+$. In acute active le-

sions, between 70-100% of all ligand expressing cells are $CD68^+$ microglia/macrophages, a significant difference compared to control sections (Dunn's multiple comparisons test, $^*P=0.0404$, $^{**}P=0.0011$, $^*P=0.0266$ for GDF1, GDF11, and BMP6, respectively). Interestingly, microglia/macrophages make up only about 50% of ligand-expressing cells in chronic active, chronic inactive, and remyelinated lesions, suggesting that this is likely an acute post-injury response. Figure 25e shows representative images of $GDF1^+$, $GDF11^+$, and $BMP6^+$ cells co-stained with CD68. Taken together, this data suggests that microglia/macrophages are the major activin receptor ligand expressing cells within active MS lesions. This co-expression data could either indicate that microliga/macrophages are upregulating and producing these ligands, or that the ligands are binding to receptors on microglia and activating downstream signalling. Tissue stains and cell counts in Figure 25 were carried out by an ERASMUS student, Dawid Kargul. Panels a) and b) were published in our recent paper [327].

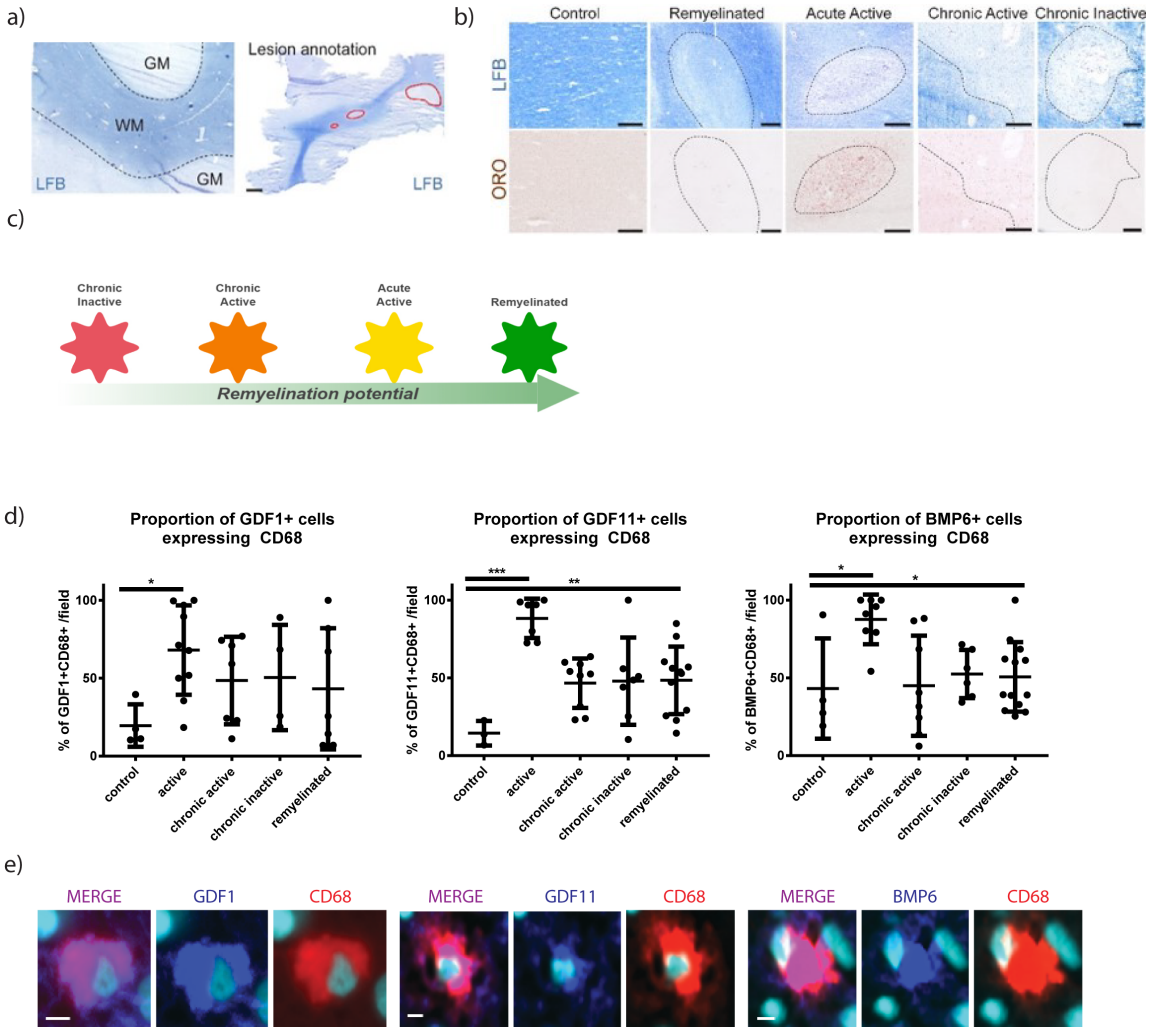

Figure 25. GDF1, GDF11, and BMP6 are highly expressed on microglia/macrophages in active MS lesions. a) Luxol Fast Blue (LFB, blue) staining was used to clearly distinguish white matter (WM) from grey matter (GM). MS lesions were digitally annotated (red circles) in Zen software to ensure that the same area was quantified for various readouts. Scale bar, 2000 μm. b) MS lesions were pathologically characterized according to the International Classification of Neurological Diseases, using LFB to stain intact myelin (blue) and Oil Red O (ORO) to stain myelin debris (brown). Healthy control tissue shows intact myelin and no myelin debris. Fully remyelinated lesions show intermediate intensity of LFB ('shadow plaque') with little to no myelin debris. Acute active lesions show a diffuse LFB border with demyelination and an abundance of myelin debris throughout the lesion. Chronic Active lesions show loss of LFB and some myelin debris. Chronic Inactive lesions show significant demyelination and no myelin debris. Scale bar, 500 μm. c) Schematic of remyelination potential by lesion type. From low to high: chronic inactive (red), chronic active (orange), acute active (yellow), and remyelinated (green). d) Proportion of GDF1$^+$, GDF11$^+$, and BMP6$^+$ cells ($\pm$s.d.) expressing CD68 in MS lesions and controls. Kruskal-Wallis test with Dunn's multiple comparisons: GDF1 (*P=0.0404), GDF11 (**P=0.0011, ***P=0.0003), BMP6 (*P=0.0124, *P=0.0266). e) CD68$^+$ (red) and GDF1$^+$, GDF11$^+$, and BMP6$^+$ (blue) double positive cells in MS lesions. DAPI shown in light blue. Scale bar, 5 μm.

5.2.2 Ligands are expressed on microglia in remyelinating mouse tissue

To determine whether microglia/macrophage specific ligand expression observed in MS tissue was paralleled in the *in vivo* remyelinating mouse model, 14 days post lesion (dpl) tissue was immunostained for GDF1, GDF11, BMP6, and microglial markers (either CD68 or PU.1). Within the lesion area (delineated by dotted lines, Figure 26b), microglia/macrophage-specific ligand expression was observed. CD68 was used as a microglia/macrophage cytoplasmic marker for GDF1 and BMP6 co-stains, as these ligands were expressed mostly in the cytoplasm. However, GDF11 expression looked to be nuclear; therefore, PU.1 (a nuclear microglia/macrophage marker) was used for this co-stain. Notably, GDF11 was also expressed on $NeuN^+$ neuronal cell bodies outside of the lesion area. Within the lesion area, however, all three ligands were clearly co-localized with microliga/macrophages, suggesting that findings from the active MS lesions in Figure 25 are reflected in the *in vivo* focal lesioning model.

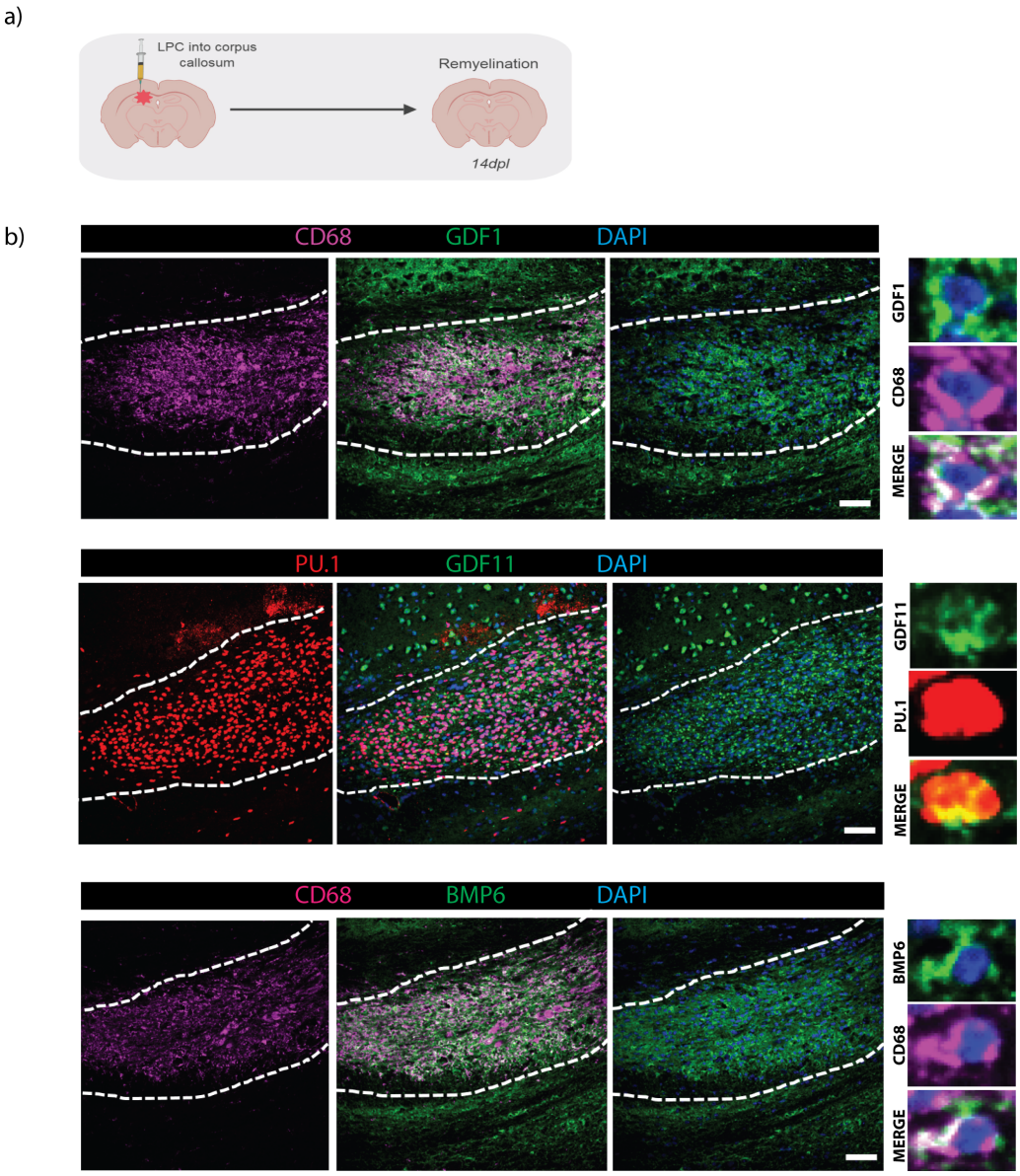

Figure 26. GDF1, GDF11, and BMP6 are expressed on microglia in remyelinating lesions *in vivo*. a) Diagram of *in vivo* focal demyelinating lesion model. b) Images of focal lesions at 14 days post lesion (dpl), dotted lines delineate corpus callosum lesion. $CD68^+$ (magenta) or $PU.1^+$ (red) microglia/macrophages expressing GDF1, GDF11, or BMP6 (green), counterstained with DAPI. Close-up images of individual cells shown on right. Scale bar, 50 μm.

5.2.3 Canonical activin receptor signalling occurs through microglia and oligodendrocytes during remyelination

Given that activin receptor ligands are important during remyelination and their expression within acute lesions is abundant on microglia/macrophages, and as our previous work identified activin receptors on oligodendrocytes [142, 327], I next wanted to determine whether these same cells were also mediating activin receptor signalling. To do this, I used an AR8-mCherry reporter mouse line, where mCherry expression is under the control of an activin response element (AR8) and is expressed in cells that receive Smad2/3 mediated signalling (for schematic, see Figure 27a). Remyelinating organotypic cerebellar slices from AR8-mCherry mice were collected at 0dpl, 2dpl and 7dpl for Flow cytometry analysis (Figure 27b-d). Cells from slice lysates were either stained with CD11b (microglia) or with oligodendrocyte lineage markers PDGFRα (progenitors), O4 (immature oligodendrocytes), and MAG (mature oligodendrocytes). Cells were first gated for mCherry$^+$ DAPI$^-$ live cells, then for single cells. Finally, mCherry was plotted against either CD11b (Figure 27b), and side scatter was plotted against each of the oligodendrocyte lineage markers (Figure 27c) to determine the percentage of total mCherry$^+$ population that was also positive for each cellular marker (Figure 27d).

Surprisingly, the majority of mCherry$^+$ cells do not express CD11b or oligodendrocyte lineage cell markers at any time. At 0dpl (before demyelination), 18.33% ($\pm$1.097) of mCherry$^+$ cells are CD11b$^+$. However, shortly after demyelination

(2dpl), there are only 2.925% (±1.64) mCherry$^+$CD11b$^+$ cells, subsequently rising slightly to 7.125% (±2.572) by 7dpl. Interestingly, when inhibin was administered to remyelinating slice cultures and mCherry expression subsequently analyzed by Flow, the percentage of mCherry$^+$CD11b$^+$ cells remained unchanged (6.475% ±1.729). At all time points analyzed (0, 2, 7dpl), percentage of mCherry$^+$ cells expressing any oligodendrocyte lineage cell marker remained below 5%. Taken together, this data suggests that only a small proportion of Smad2/3-mediated activin receptor signalling occurs through microglia and oligodendrocyte lineage cells in the slice culture model, but does confirm that these cells do signal through activin receptors.

To determine whether Flow cytometry results in Figure 27 are also observed using other techniques, AR8-mCherry slices were fixed at 7dpl and stained with CD68, a microglial marker (Figure 28b). Here, abundant co-localization between mCherry and CD68 can be observed, suggesting a much higher proportion of mCherry$^+$ cells are microglia than the Flow experiment may have indicated. To check whether cells expressing both mCherry and microglial markers could be detected in live tissue, AR8-mCherry mice were bred to MacGreen mice (macrophage/microglia reporter mice described in Chapter 2) and live imaging snapshots of organotypic slices were taken at 7dpl. Figure 28c shows images of a live mCherry$^+$MacGreen$^+$ cell, confirming that microglia do actively signal through Smad2/3 during remyelination. Finally, to determine whether the functional activin receptor (Acvr1b) was also expressed on microglia, and whether its expression could be observed on other cell types, wild-type cerebellar slices were stained at 7dpl for Acvr1b, and co-stained

with either β-tubulinIII (neurons) and CD68 (microglia, Figure 28a, top row); or GFAP (reactive astrocytes) and Olig2 (oligodendrocytes, Figure 28a, bottom row). Here, Acvr1b expression was observed only on $CD68^+$ microglia and $Olig2^+$ cells (indicated by white arrows in Figure 28a). Interestingly, some $Acvr1b^+$ cells were not positive for either microglia or oligodendrocyte lineage cell markers, suggesting that other cell types (such as neural progenitor cells, endothelial cells, or pericytes) may also signal through Acvr1b during remyelination.

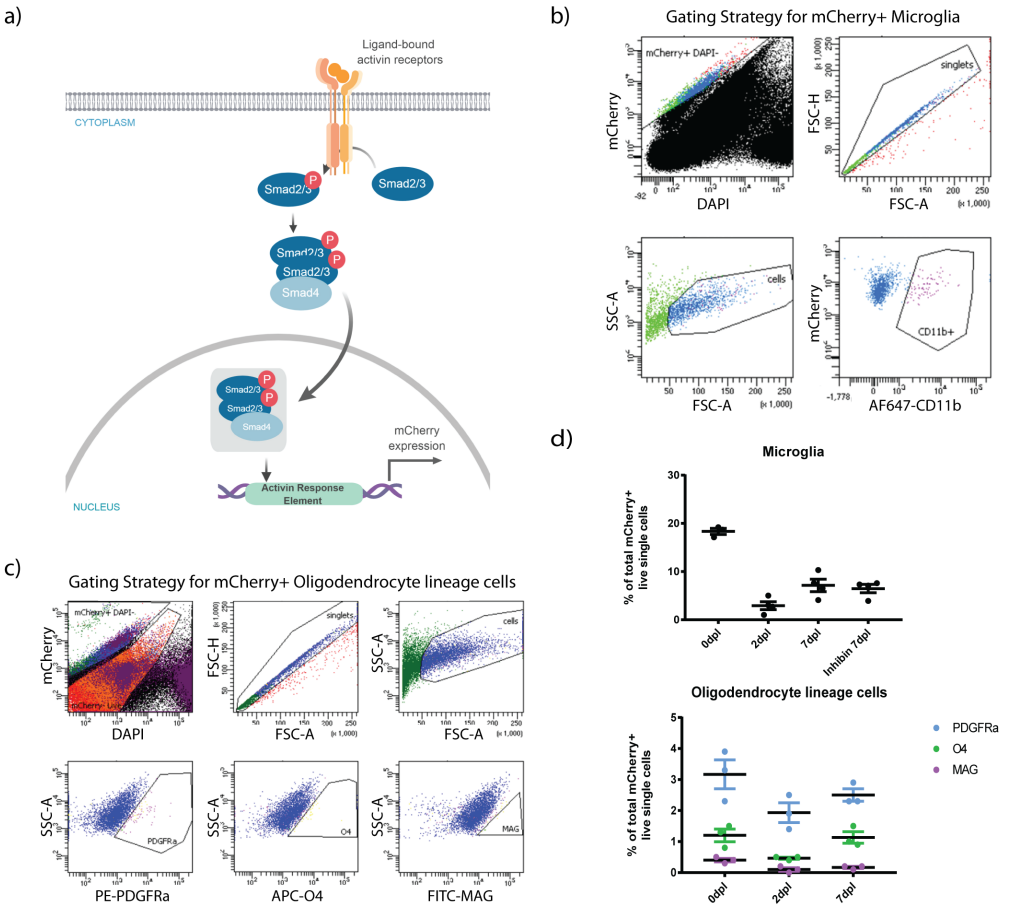

Figure 27. Activin receptors signal partly through microglia during remyelination. a) Schematic of activin response element-driven mCherry expression in AR8-mCherry mice. Once ligand is bound, Smad2/3 is phosphorylated and binds to Smad4. This complex is translocated to the nucleus and binds activin response element which drives mCherry expression. b) Gating strategy for analysing mCherry$^+$CD11b$^+$ cells. Live mCherry$^+$ DAPI$^-$ cells were gated first, followed by singlet cells, and finally forward scatter (FSC-A) and side scatter (SSC-A) to eliminate cell debris and clusters. AF647-CD11b (x axis) was plotted against mCherry (y axis) to determine CD11b$^+$ and CD11b$^-$ mCherry cell populations. c) Gating strategy for analysing mCherry$^+$ and PDGFRa$^+$, O4$^+$, or MAG$^+$ cells. Live mCherry$^+$ DAPI$^-$ cells were gated first, followed by singlet cells, and finally forward and side scatter to eliminate cell debris and clusters. Single stained samples were used to set PDGFRa, O4, and MAG gates (bottom row of plots). d) Proportion of mCherry$^+$ cells expressing CD11b and Oligodendrocyte lineage cell markers (±s.e.m.), n=3-4 experiments per time point.

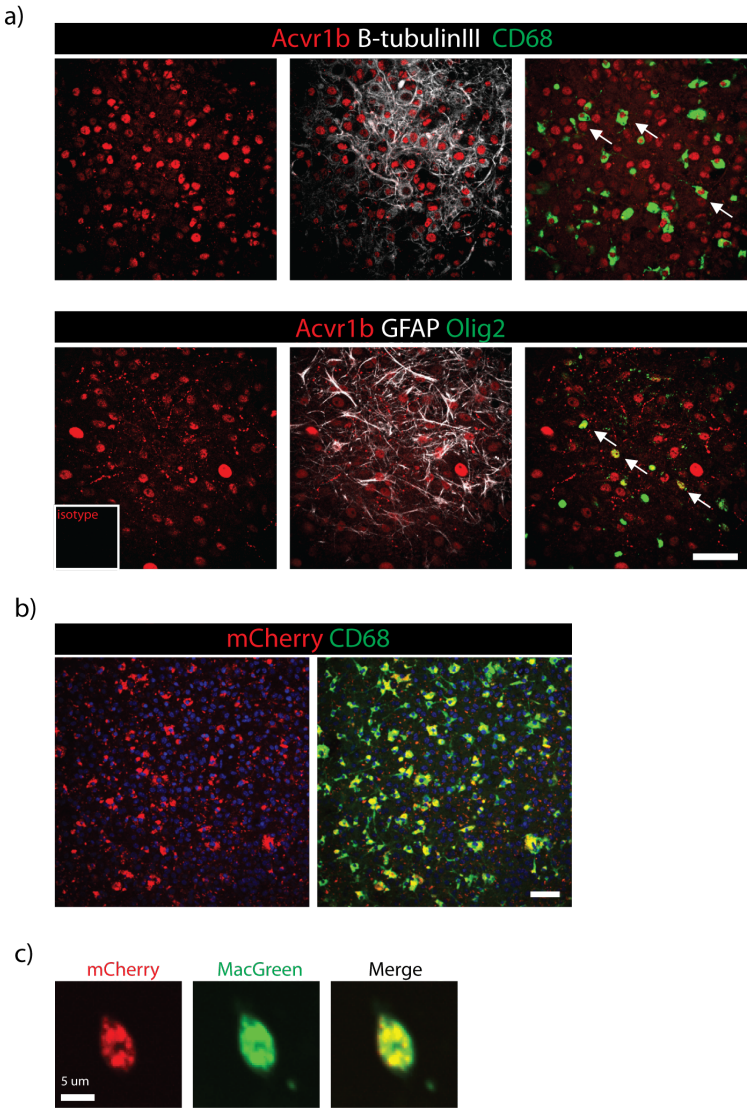

Figure 28. Functional activin receptor Acvr1b and downstream Activin Response Element-driven mCherry expression on microglia and oligodendrocytes. a) Images of remyelinating *ex vivo* mouse tissue at 7dpl showing Acvr1b$^+$ (red, both rows), β-TubulinIII$^+$ (white, top row), CD68$^+$ (green, top row), GFAP$^+$ (white, bottom row), and Olig2$^+$ (green, bottom row) cells. Acvr1b$^+$ CD68$^+$ double positive cells (top row) and Acvr1b$^+$ Olig2$^+$ double positive cells (bottom row) indicated by white arrows. Scale bar, 50 μm. b) Images of fixed remyelinating *ex vivo* AR8-mCherry mouse tissue at 7dpl. mCherry$^+$ (red) CD68$^+$ (green) double positive cells were observed. Scale bar, 50 μm. c) Live imaging snapshot of AR8-mCherry/MacGreen mouse explants, showing mCherry$^+$ MacGreen$^+$ double positive cell. Scale bar, 5 μm.

5.2.4 Activin receptors 2a/2b are expressed on oligodendrocytes and microglia in MS tissue

Given activin receptor ligands are expressed on microglia/macrophages (GDF1, GDF11, BMP6) and oligodendrocyte lineage cells (activin-A, [327]) in MS lesions, I next determined cell-specific ligand-binding activin receptor expression in human tissue. Tissue was characterised as above (Figure 25a), and stained for activin receptors 2a/2b and either CD68 (microglia) or Olig2 (oligodendrocytes). Activin receptors 2a and 2b were observed on both oligodendrocytes and microglia/macrophages (Figure 29c-d). When percentage of total oligodendrocytes expressing either Acvr2a or Acvr2b was quantified, an interesting difference between receptor subtype expression within lesion types emerged. Specifically, in lesions with good remyelinating potential (acute active and chronic active, Figure 29a), there was a higher proportion of $Acvr2a^{+}Olig2^{+}$ cells compared to $Acvr2b^{+}Olig2^{+}$ cells (Figure 29b). However, in chronic inactive lesions, which have a very low remyelinating potential (Figure 29a), the proportion of $Acvr2b^{+}Olig2^{+}$ cells is increased. Taken together, this increase in Acvr2b expression within oligodendrocyte lineage cells combined with its relatively higher affinity for activin-A [304] may suggest that this receptor subtype sequesters the ligand and restricts Acvr2a-mediated signalling in oligodendrocytes. The activin receptor/oligodendrocyte co-expression data was published in our recent paper [327].

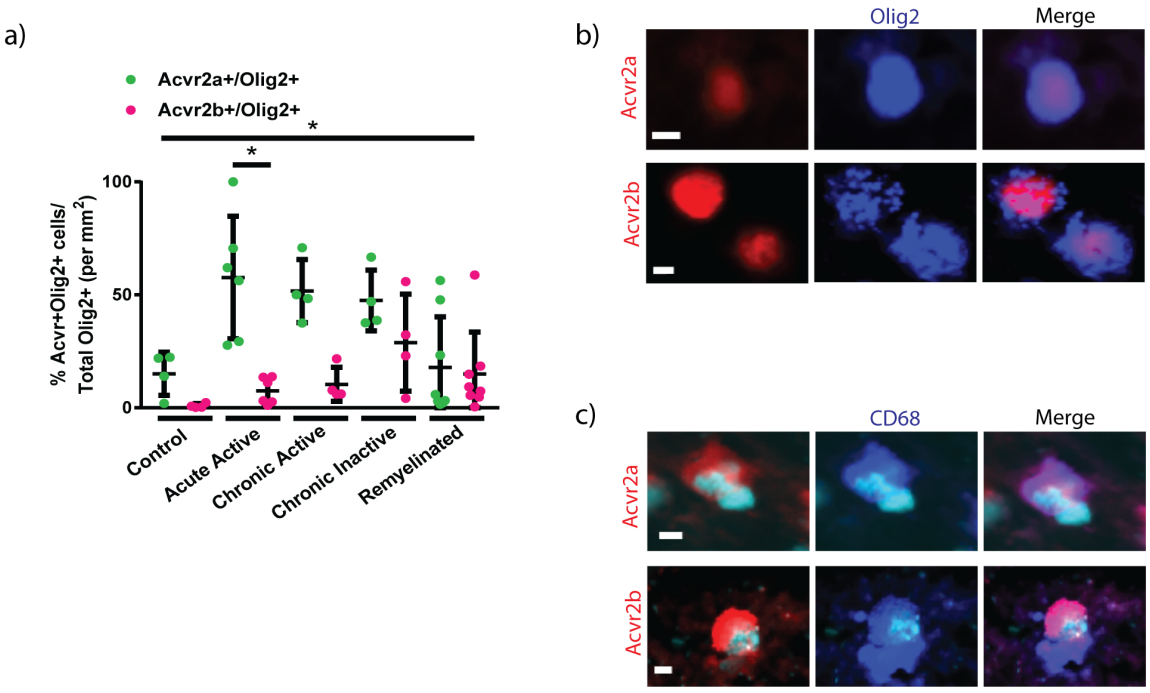

Figure 29. Activin receptors 2a/2b are expressed on oligodendrocytes and microglia/macrophages in MS tissue. a) Proportion of Acvr2a$^+$Olig2$^+$ or Acvr2b$^+$Olig2$^+$ from total Olig2$^+$ cells ($\pm$s.d.) in healthy control tissue or MS lesions (remyelinated, acute active, chronic active, chronic inactive). N for each lesion type indicated in Chapter 2. Kruskal-Wallis test and Dunn's multiple comparison test, *P$<$0.05. b) Acvr2a$^+$ (top row, red) or Acvr2b$^+$ (bottom row, red) and Olig2$^+$ (blue) double positive cells in MS lesions. Scale bar, 5 μm. c) Acvr2a$^+$ (top row, red) or Acvr2b$^+$ (bottom row, red) and CD68$^+$ (blue) double positive cells in MS lesions. Scale bar, 5 μm.

5.3 Discussion

Activin receptor ligands are expressed on microglia/macrophages

In this chapter, I established that activin receptor ligands important during remyelination (GDF1, GDF11, and BMP6) are expressed on microglia/macrophages both in MS tissue and in a remyelinating mouse model. This is consistent with previous work which identified activin-A (the primary ligand for activin receptors) as a factor released by microglia/macrophages during remyelination [142]. In our recent paper, we also showed that activin-A expression was upregulated in active MS lesions compared to non-injured controls [327]. Here, I found that expression of alternative ligands in microglia/macrophages was dynamic between lesions. Almost 100% of ligand-expressing cells in active MS lesions were microglia/macrophages, while in other lesions and controls, this number dropped to 50% or less. This may suggest a microglia/macrophage-specific upregulation of GDF1, GDF11, and BMP6 in acute active lesions, hinting at the involvement of these ligands in post-injury inflammation. Alternatively, other lesion types may contain higher numbers of cells other than microglia expressing these ligands, which would influence the proportion of total ligand$^+$ cells which are microglia/macrophages. An important caveat to this expression data is that it does not elucidate whether these ligands are being upregulated and produced by microglia/macrophages themselves, or if the ligands are simply found on microglia/macrophages because they are binding to receptors on those cells. To address this, conditioned media from microglial cell cultures induced

to either pro-inflammatory or anti-inflammatory phenotypes could be analysed by ELISA to determine whether each ligand is present in the media. If GDF1, GDF11, or BMP6 were detected, it would suggest that the microglia of a certain phenotype may produce these proteins. Further, *in situ* hybridization may be used to determine whether microglia/macrophages express ligand mRNA, which would also show that these cells are producing the proteins.

In remyelinating *in vivo* mouse tissue, activin receptor binding ligands were also observed to be expressed on microglia/macrophages. Additionally, GDF11 was expressed on neuronal cell bodies adjacent to the corpus callosum lesion area. Therefore, while GDF1 and BMP6 seem to be exclusively expressed on microglia during remyelination, GDF11 can also be expressed on neurons, suggesting that it may have neuronal-specific effects. Importantly, differences between cell-specific developmental expression (outlined in Table 4) and adult post-injury expression (determined here) support the notion that TGF-β ligand function/expression may change depending on contextual factors such as age and healthy or diseased microenvironment.

Activin receptors signal through microglia and oligodendrocytes during remyelination

Results from this chapter suggest that activin receptors signal, at least in part, through microglia and oligodendrocytes. Evidence from both Flow cytometry and immunohistochemical experiments using AR8-mCherry reporter mice show that activin receptor-driven Smad2/3 signalling is present in CD11b$^+$, CD68$^+$, and MacGreen$^+$

microglia. As these experiments used organotypic slice cultures, there is no contribution from the periphery, and therefore cells detected by microglia/macrophage markers can be assumed to be only microglia. Surprisingly, there were some discrepancies between staining and Flow experiments regarding the proportion of cells signalling through microglial activin receptors during remyelination. While Flow results suggest that only a small percentage (7.125% $\pm$2.572) of total mCherry$^+$ cells are CD11b$^+$ at 7dpl, images from immunohistochemistry experiments appear to have abundant mCherry$^+$ CD68$^+$ cells. There may be a number of reasons for this observed inconsistency. First, the sensitivity of Flow has been reported to be much higher than that of immunohistochemistry [361, 362]; suggesting that Flow data may be more reflective of the true amount of microglia-mediated Smad2/3 signalling in the slices. Conversely, tissue processing for Flow could result in transfer of cell debris from one cell to another; this transfer could cause the low signal in CD11b$^+$mCherry$^+$ double positive cells. Other differences between experiments, such as the fact that Flow uses cells from a whole slice, while stained images were taken from a section of the slice; or that the two microglial markers CD11b and CD68 reflect different subpopulations of microglia (all microglia vs activated microglia, respectively), may also account for some of this variance.

Importantly, however, Acvr1b, the functional activin receptor, was detected on both Olig2$^+$ oligodendrocytes and CD68$^+$ microglia. This confirms that the signal-transducing receptor is present on both microglia and oligodendrocytes during remyelination. While Flow results suggested only a very low number of mCherry$^+$

cells signal through oligodendrocyte lineage cells, given the presence of Acvr1b on these cells, it is likely that oligodendrocyte-specific activin receptor signalling is important for remyelination. In fact, when Acvr1b was deleted from oligodendrocyte progenitors, mice had myelin abnormalities and died prematurely at 3 weeks, phenotypes consistent with other transgenic mice exhibiting developmental myelination problems [327]. This finding, however, does not preclude receptor activity on other cell types being important for myelination or remyelination. Indeed, here, there were some Acvr1b$^+$ cells that were neither CD68$^+$ nor Olig2$^+$, suggesting that there are other cell types that may signal through activin receptors during remyelination.

To confirm these results and perhaps shed some light on the apparent discrepancies between techniques, several experiments could have been conducted. First, it would have been interesting to sort cells from slices using FACS and/or MACS, and subsequently use Western blotting to check for both mCherry and phosphorylated Smad2/3 (p-Smad2/3) expression on microglia and oligodendrocytes. P-Smad2/3 is a marker of activated Smad signalling [306], and may be used to confirm whether AR8-mCherry expression reflects all Smad2/3 mediated signalling. The AR8-mCherry reporter mouse was preferable to using p-Smad2/3: once induced, mCherry expression is stable, and p-Smads may only be detected transiently. Still, using p-Smad2/3 as a secondary measure of Smad2/3 signalling could be important for confirming the AR8-mCherry reporter, and co-staining slices from AR8-mCherry mice with p-Smad2/3 would have been a good control. Finally, a co-immunoprecipitation technique may be used to pull down receptors and determine

which cell types express Acvr2a/2b/1b during remyelination. This technique may also have been useful in determining which ligands were bound to Acvr2a/2b, further clarifying the role of activin receptor ligands during remyelination.

Surprisingly, when inhibin treatment was administered to slices, the proportion of mCherry$^+$ CD11b$^+$ cells remained unchanged (mean rank difference of 0.75, non-significant). This may reflect the stable expression of mCherry discussed above. There is a clear decrease in mCherry$^+$CD11b$^+$ cells from 0dpl (pre-demyelination) to 2dpl. This reduction in mCherry expression on microglia could be due to cell death. Indeed, unpublished work (currently under review) from our lab established that within the first two days following demyelination, a switch in microglial phenotypes (from pro-inflammatory to anti-inflammatory) may occur through a controlled necrosis (termed necroptosis). Following this, there is an increase in mCherry$^+$CD11b$^+$ expression from 2dpl to 7dpl. As inhibin treatment was administered from 3-4dpl, it is possible that mCherry expression on microglia has already ramped up by then and remains constant. If inhibin treatment does not induce microglial cell death, then mCherry expression can be expected to be detected at a similar level, even if Smad2/3 signalling is inhibited after inhibin treatment induction. If this hypothesis is correct, I would expect levels of mCherry$^+$CD11b$^+$ cells to be similar between 4 and 7dpl; therefore, to confirm this, an additional Flow cytometry experiment run at 3-4dpl (pre-inhibin treatment) would have been useful. Additionally, slice cultures treated with inhibin could be stained for microglial markers to determine whether there are any effects on the phenotype/survival of these cells with inhibin treatment.

Activin receptors are expressed on oligodendrocytes and microglia in MS tissue

Finally, this chapter identified ligand-binding activin receptor (Acvr2a/2b) expression on both oligodendrocytes and microglia/macrophages in MS tissue. Interestingly, the two receptor subtypes showed differential expression by lesion type on oligodendrocyte lineage cells. Actively remyelinating lesions (active and chronic active) had relatively higher densities of oligodendrocyte lineage cells expressing Acvr2a compared to Acvr2b. In lesions that were failing to remyelinate (chronic inactive), the density of Acvr2b$^+$ oligodendrocytes increased. This data was published in our recent paper, alongside additional experiments showing that Acvr2b overexpression blocks the positive effects of activin-A on oligodendrocyte lineage cells (specifically differentiation and membrane actin depolymerization required for compaction, [327]). As Acvr2b has been shown to have a relatively higher affinity for activin-A ligand compared to Acvr2a [304], our working hypothesis is that Acvr2b downregulation after injury allows Acvr2a to bind ligands more efficiently and drive oligodendrocyte lineage cell responses required for repair. If this downregulation fails, as it may occur in chronic inactive MS lesions, Acvr2b sequesters ligands and impairs any Acvr2a-mediated effects. An interesting future experiment could quantify activin receptor density on microglia/macrophages in MS tissue, as this may reveal whether immune cell receptors share this lesion-specific expression pattern with oligodendrocyte activin receptors.

Taken together, this data shows that while alternative activin receptor ligands are mostly expressed on microglia, activin receptors signal through both microglia and oligodendrocytes during remyelination. A hypothetical model (summarized in Figure 30) is that microglia/macrophages secrete TGF-β ligands important for remyelination, and these ligands subsequently act in an autocrine or paracrine fashion, binding to activin receptors on microglia/macrophages and oligodendrocytes, driving downstream pathways, and activating genes required for efficient remyelination. Important caveats to this model, such as axon calibre and ligand-binding receptor subtype, as well as implications for future therapies, will be discussed in the next chapter.

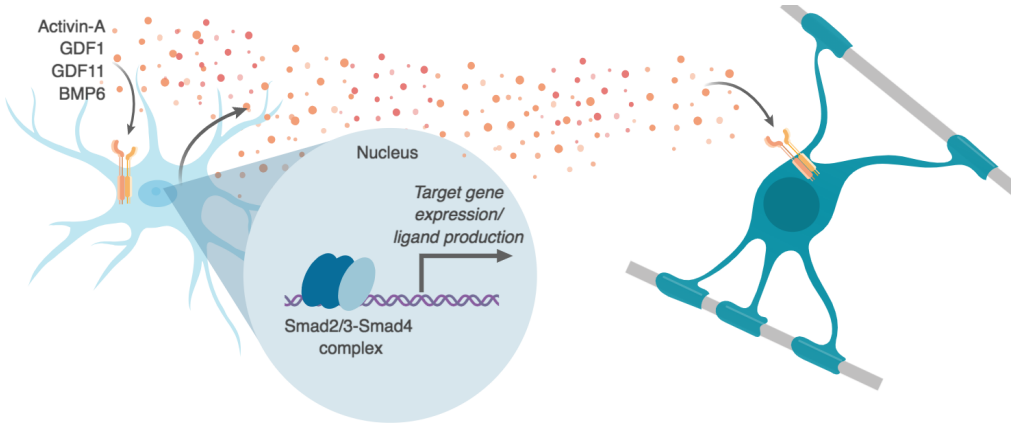

Figure 30. Hypothetical model of how microglia-derived ligands act on activin receptors and drive remyelination. Activin receptor ligands may be secreted by microglia and act in a paracrine or autocrine fashion, binding to receptors on oligodendrocytes and/or microglia and driving downstream pathways important for remyelination.

6 Chapter 6: Discussion

6.1 Overview of thesis

Stimulation of activin receptors using activin-A in an *ex vivo* model was sufficient to accelerate remyelination, and blocking activin receptors using inhibin severely impaired remyelination. Similar effects were observed *in vivo*; however, they were less pronounced and mostly relevant in small diameter axons. Blocking activin-A ligand *ex vivo* had no effect, suggesting that alternative ligands may bind activin receptors and drive remyelination. To investigate the feasibility of this hypothesis, it was first determined whether alternative ligands were present in toxin-induced focal lesioning models during remyelination. GDF1, GDF11, and BMP6 were identified as activin receptor ligands highly expressed during remyelination. Next, I investigated whether these ligands were required for remyelination by inhibiting the activity of each ligand using blocking proteins. These experiments yielded interesting effects: GDF1 appeared to be important during late remyelination, as blocking its activity had a slight negative effect at 14dpl. GDF11 was found to be important during both early and late remyelination, as blocking its activity severely impaired this process at 7 and 14dpl. Blocking BMP6 resulted in impaired remyelination at 14dpl; when activin-A was also blocked, this impairment was evident earlier at 7dpl (see Figure 31, top and bottom panels). *In vivo* blocking experiments revealed a potential axon calibre-dependent effect of activin receptor activity on remyelination (see Figure 31, middle panel). Interestingly, while activin-A was sufficient to accelerate remyelina-

tion in Chapter 3, supplementing alternative ligands had no effect. While activin receptors are required for remyelination, it is clear that each receptor-binding ligand produces distinct effects, both in terms of timing and myelin morphology. This suggests each factor may be activating distinct downstream pathways. Given the importance of context in dictating cellular response upon activation of any TGF-β superfamily receptor, a logical next step was to clarify which cell types were involved in expressing ligands, receptors, and active signalling markers. GDF1, GDF11, and BMP6 were found to be expressed on microglia/macrophages in active MS lesions and in remyelinating focal lesions in mice. Further, active Smad2/3-mediated activin receptor signalling was observed in microglia and oligodendrocytes during remyelination. Finally, ligand-binding activin receptors were expressed both on microglia and oligodendrocytes in MS lesions. An intriguing difference was uncovered in the expression of activin receptor subtypes on oligodendrocytes, where Acvr2a is high in actively remyelinating lesions, and Acvr2b is upregulated in lesions which fail to remyelinate.

Taken together, data from this thesis supports the following working hypothesis (summarised in Figure 31): activin receptor ligands may be secreted from microglia/macrophages in actively remyelinating lesions. These ligands may act in an autocrine or paracrine fashion, binding to receptors on microglia/macrophages, or on oligodendrocyte lineage cells. These ligand-receptor interactions may drive downstream signalling important for remyelination at many stages. Ligand availability, specific ligand-receptor interactions, density of receptor subtypes, and axon calibre

may dictate ultimate cellular outcomes and determine remyelination efficacy.

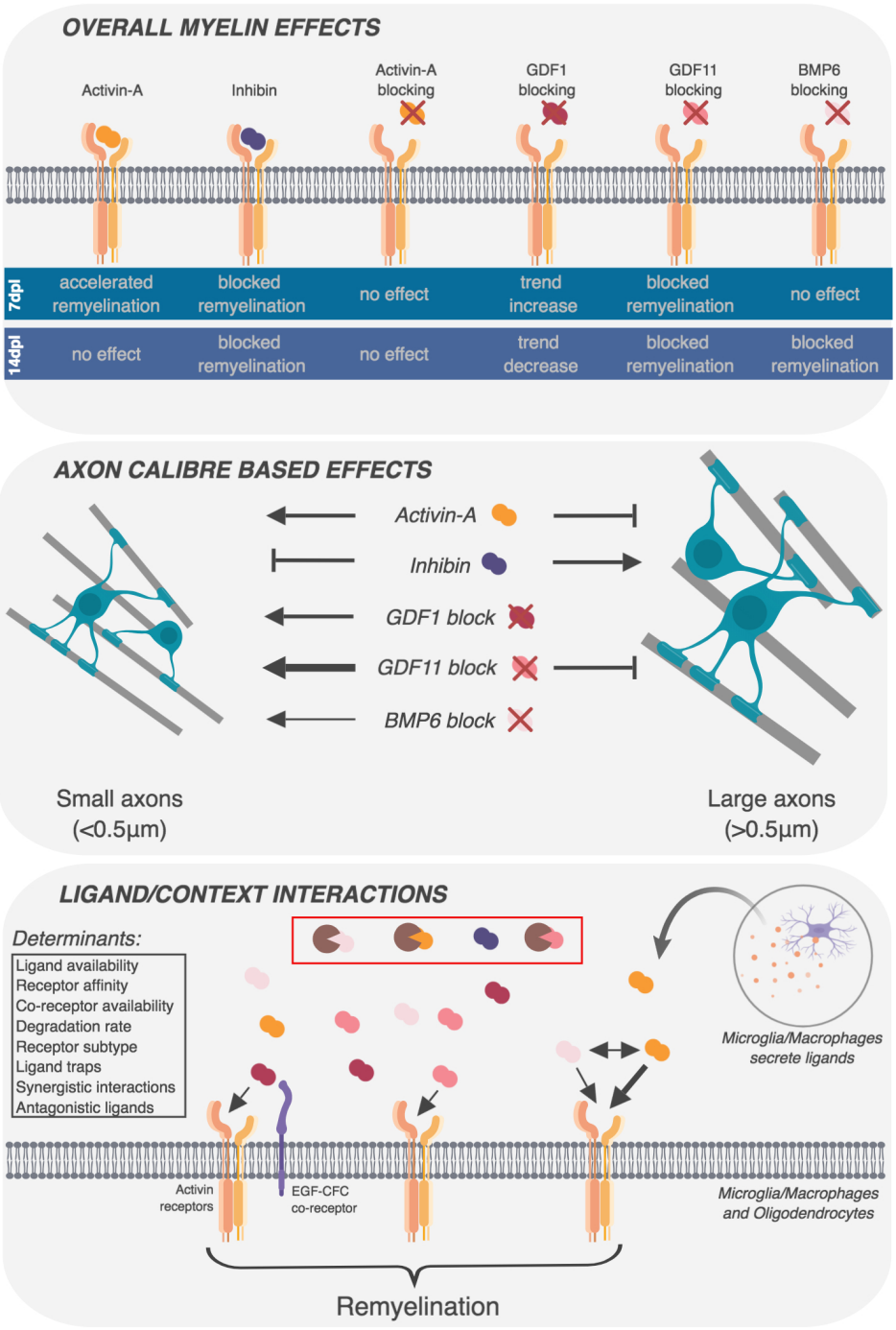

Figure 31. Summary and Working Hypothesis. In the top panel, overall myelin effects from modulating activity of each ligand are summarized at 7 days post lesion (dpl) and 14dpl. In the middle panel, axon calibre based effects are summarized for each ligand. Arrow thickness represents the strength of effect. No arrow indicates no clear effects. In the bottom panel, contextual determinants of activin receptor signalling during remyelination are shown. The red box indicates signalling inhibitors (ligand traps, inhibitory ligands). Arrow thickness represents affinity for activin receptors. Double arrows represent synergistic interactions between ligands.

6.2 Future Directions

6.2.1 Microglia/macrophage derived factors during remyelination

Here, I determined that activin receptor ligands GDF1, GDF11, and BMP6 are expressed on microglia/macrophages during remyelination in both human and experimental mouse tissue. Given previous studies have identified several microglia-derived factors which play a role in remyelination (reviewed in [363]), a likely hypothesis for this co-expression is that microglia/macrophages are producing these proteins. To test this, conditioned media from microglial cell cultures could be analysed to determine whether ligand is present in the media at the protein level using ELISA. Detection of GDF1, GDF11, or BMP6 would point towards microglial production of these proteins. Additionally, inducing microglia to either a pro-inflammatory or an anti-inflammatory phenotype first, then running the above experiment, may reveal whether microglia of a specific phenotype secrete these proteins. To further confirm ligand production by microglia in a remyelinating context, *in situ* hybridization may be used in both *in vivo* and *ex vivo* tissue to determine ligand mRNA expression within these cells.

Importantly, there is evidence suggesting that macrophages and microglia may have distinct roles during remyelination. Specifically, one study stratified microglia from macrophage cell populations from EAE mice by FACS and analysed their transcriptomes using RNA sequencing. Throughout the course of EAE, microglia vs macrophage transcriptomes were distinct, suggesting differential functions between

these two immune cell types [364]. These findings were confirmed in two other studies [365, 366], one of which found that expression of the same gene in either microglia or macrophages can have distinct effects on EAE disease course [366]. Therefore, it may be important to distinguish between these two cell types in our *in vivo* models and in human tissue. As previously mentioned, in the *ex vivo* model, there is no input from the periphery, and therefore no infiltrating macrophages. Until recently, there were no good markers to distinguish microglia from macrophages in immunohistochemical studies. A potential new marker that may be specific to a subset of microglia is TMEM119 [367]. Future studies may use this marker to characterize microglial-specific expression of activin receptors or their ligands in human tissue.

6.2.2 Cell-specific activin receptor effects

The working hypothesis diagram (Figure 31) stipulates that activin receptors influencing remyelination could be present on both microglia/macrophages and oligodendrocytes. To tease apart the contributions of each of these cell-specific receptors, genetic approaches may be used. Specifically, our lab currently has access to a conditional knockout mouse where Acvr1b (the functional signalling receptor) is deleted from PDGFRα oligodendrocyte progenitor cells. However, as these mice die prematurely at P21, it is not possible to study the effects of activin receptor signalling knockout during remyelination. To address this, an inducible knockout could be developed, where an additional breeding step with a Cre-ERT2 mouse results in a tamoxifen-inducible OPC-specific Acvr1b knockout animal.

Additionally, we could create a new mouse line where *Acvr1b* is excised specifically from microglia/macrophages. It would be interesting to compare myelination in this conditional knockout mouse to the OPC-specific knockout effects during development, such as hypomyelination and enlarged inner tongues [327]. If these mice also die prematurely, it would be important to create an inducible conditional knockout as outlined above. Generating mouse lines is expensive and time-consuming; however, studying differences between microglia/macrophage-specific and OPC-specific Acvr1b knockouts during remyelination would shed light on the requirement of cell-specific activin receptors during myelin regeneration, and have important implications for developing drug therapies.

6.2.3 Ligand contributions during remyelination

In this thesis, I conducted experiments where ligands of interest were inhibited using blocking proteins, administered directly to *ex vivo* cultures via media and to *in vivo* lesions through osmotic mini-pumps. To further confirm the role of these proteins during remyelination, it would be important to use a different technique. An inducible genetic deletion of each ligand in an *in vivo* focal demyelination model may be more effective and reliable in eliminating target ligands, and may therefore reveal more robust effects. Floxed alleles for GDF1, GDF11, and BMP6 exist and are commercially available. Importantly, mice with mutations in genes for each of these ligands results in severe developmental defects, and early death (24-48 hours) in GDF1 and GDF11 null mice [368–370]. Therefore, it would be crucial to create

inducible knockout animals in order to determine the effects of a lack of each ligand after adult demyelinating injury. Additionally, these mouse lines could be used to test effects of an inducible knockout in *ex vivo* slices. Knockout mice for each ligand may be interbred to develop double or triple knockouts, perhaps elucidating the compensatory or synergistic effects of ligand combinations.

Further, it would have been interesting to determine if GDF1, GDF11, and BMP6 directly affect oligodendrocyte lineage cells (as observed with activin-A [142]). Primary oligodendrocyte progenitor cell cultures may have been used to test whether each ligand may influence remyelination via direct effects on oligodendrocyte proliferation, differentiation, or survival. Additionally, as we have identified activin receptor activity to be important for compaction via actin depolymerization [327], oligodendrocyte cultures treated with ligands or ligand blocking agents could also be analyzed for Phalloidin signal, a marker of non-polymerized filamentous actin.

6.2.4 Ligand-receptor combinations and their downstream pathways

To understand how blocking each ligand may elicit a distinct effect on remyelination, it would be important to determine which downstream pathways are activated by specific ligand-receptor combinations. To do this, a forward phase phospho-antibody microarray may be used (as previously described [327]). Specifically, a microarray containing antibodies against both phosphorylated and unphosphorylated residues in proteins associated with 5 TGF-β signalling pathways (summarised in Figure 3) would be useful in determining which canonical or non-canonical down-

stream events are active in each condition. As we have found activin receptors to be expressed in both oligodendrocytes and microglia, it would be interesting to treat either OPC or microglial cell cultures with each ligand and then process these samples for forward phase phospho-antibody analysis. Additionally, protein lysates from slice cultures may be used, as these samples would contain both oligodendrocyte and microglial activin receptors. However, the former cell culture experiment would be more specific in terms of pathways upregulated within specific cell types.

Further, given that we found ligand-binding activin receptor subtypes may elicit distinct effects, it would be important to characterize which receptor subtype these ligands are endogenously binding to. To do this, a proximity ligation assay (PLA) may be used. PLA is an immunoassay-based technique which identifies interactions between proteins in close proximity. Using antibodies for Acvr2a or Acvr2b, together with GDF1, GDF11, or BMP6 antibodies, interactions between each ligand and receptor subtype may be characterized. Additionally, to test our hypothesis that Acvr2b-mediated signalling may be detrimental for remyelination by preventing ligands binding to Acvr2a, Acvr2b could be overexpressed in slice cultures using a lentivirus (as previously reported in [327]). If remyelination is negatively affected by this overexpression, it would support the notion that activin receptor subtypes have distinct roles in remyelination.

6.2.5 Axon calibre-dependent effects of activin receptor signalling during remyelination

Given the axon diameter-dependent effects observed during remyelination *in vivo* (summarized in Figure 31, middle panel), as well as during myelination [327], it would be important to follow up on how axon calibre may affect activin receptor-mediated myelination and remyelination. Since I observed stronger effects *ex vivo* compared to *in vivo*, and *in vivo* effects were mainly observed on small calibre axons, an attractive explanation would be that 4-5 week old *ex vivo* cerebellar fibres are smaller in diameter than 6-8 week old *in vivo* corpus callosum axons. However, the evidence is against this theory: previous work where EM was carried out on cerebellar slice cultures shows that most axon diameters were between approximately 0.3-1.5μm [45]. Despite previous reports that axon diameters may vary up to 100 fold across brain regions [371], our *in vivo* corpus callosum axon diameters are very similar to the *ex vivo* diameters reported in the *ex vivo* cerebellar slice study, suggesting that differences in axon calibre between these particular brain regions is not a major contributor to the remyelination differences across models. It is possible, however, that other differences between models (discussed throughout this thesis) contribute to a nuanced calibre-dependent effect only observable in the *in vivo* context.

To fully establish whether axon calibre influences activin receptor-mediated effects on myelin, several experiments may be carried out. First, experiments using microfibre/oligodendrocyte cultures may be used to test whether administering or

blocking activin receptor activity affects the cell's ability to myelinate fibres of specific sizes. There is evidence that certain properties of myelin sheaths, such as length, are intrinsic properties of oligodendrocytes, and are not regulated by axonal signals [372]. Specifically, one study used microfibres to test whether oligodendrocytes require external signals to myelinate. Remarkably, results showed that oligodendrocytes generate sheaths of different lengths based on microfibre diameter, suggesting that there are oligodendrocyte-intrinsic signals regulating myelin sheath length [372]. Modulating activin receptor signalling in microfibre/oligodendrocyte cultures as suggested above may reveal a potential signalling pathway regulating myelin sheath length. Additionally, it would be interesting to coat fibres with activin receptor ligands to see whether myelination could be induced in fibre sizes which are not normally myelinated.

The myelinating cells of the peripheral nervous system (Schwann cells) are triggered to myelinate axons larger than 1 μm, and axonal Neuregulin-1 type III helps the Schwann cell determine how much myelin to make based on axon diameter [373]. In the CNS, however, it is not known how oligodendrocytes recognize axon calibre in order to make the appropriate amount of myelin. The experiments described above may point towards a potential contribution of activin receptors and their ligands in calibre-dependent myelination.

6.2.6 Determining the feasibility of activin receptor-driven therapeutics

Overall, results from this thesis suggest that activin receptors may prove an interesting (albeit difficult) therapeutic target. We know that activin receptor activity is important during remyelination, and different activin receptor ligands may modulate remyelination in distinct ways. Given the contribution of contextual factors, such as the cell type expressing receptors, the subtype of these receptors, and the availability of the many activin receptor ligands and their extracellular inhibitors, there are a few challenges that must be considered. First, there is a need to understand how we can target a specific activin receptor subtype. If Acvr2a and Acvr2b truly have opposing effects as we have seen in our experimental models, then this would be a crucial aspect of drug development. Second, it may be important to target the correct cell type. Cell-targeted drug delivery may be accomplished using targeted nanoparticles: a previous study has shown that nanoparticle delivery of a pro-myelination factor directly to OPCs was effective in promoting myelin repair [374]. Before we know which cell type to target however, we need to understand more about the downstream pathways that are activated by specific combinations of ligand-receptor-cell. Experiments suggested above may help shed light on the outcomes of these interactions. Finally, it may be important to fully characterize extracellular factors regulating activin receptor activity in human lesions, as these may act against any therapeutic strategy targeting these receptors.

Another important consideration is whether targeting specific subsets of oligo-

dendrocyte lineage cells or microglia/macrophages matters to the ultimate outcome. Recent advances in single-cell transcriptomics have revealed distinct sub-populations of microglia and oligodendrocytes, introducing heterogeneity to cell populations previously thought of as a homogeneous entities [375, 376]. As we learn more about these subtypes of microglia/oligodendrocytes, and whether their transcriptomic differences reflect distinct cellular states or separate cell types, we may uncover an important caveat to developing therapeutic strategies for MS. If, for example, activin receptor signalling is only relevant for efficient remyelination on a subset of glial cells, it may be crucial to target this sub-population in order to avoid any confounding effects.

A final point to consider in activin receptor therapeutics is potential axon calibre-dependent effects. The experiments outlined in the above section would help determine whether the calibre-dependent effects observed in my *in vivo* experiments reflect a robust difference in activin receptor-mediated myelination/remyelination outcomes based on axon diameter. If calibre becomes an important consideration, it would further complicate therapeutic potential, as it may require targeting axons of specific sizes.

6.3 Concluding remarks

Taken together, results from this thesis provide evidence for the role of activin receptors in driving remyelination. I found that activin receptors are required for remyelination, and their stimulation results in accelerated remyelination. Further, I identified 3 additional activin receptor ligands expressed on microglia with distinct roles in remyelination. Finally, I established active signalling of receptors to occur through microglia/macrophages and oligodendrocytes during remyelination. These findings suggest that activin receptors mediate the process of myelin regeneration via several ligands and two cell types. This work contains important implications for Activin receptors as a potential therapeutic target for demyelinating diseases such as multiple sclerosis.

7 Abbreviations Used

Acvr1b: Activin Receptor 1b

Acvr2a: Activin Receptor 2a

Acvr2b: Activin Receptor 2b

Akt: Protein Kinase B

aOPCs: Adult Oligodendrocyte Progenitor Cells

APP: Amyloid Precursor Protein

AR8: Activin Response Element 8

BMP: Bone Morphogenic Protein

BMPRII: BMP Receptor 2

BrdU: Bromodeoxyuridine

Chrm1: Cholinergic Receptor Muscarinic 1

CNPase: 2'-3'-Cyclic Nucleotide 3'-Phosphodiesterase

CNS: Central Nervous System

DMT: Disease-Modifying Therapy

EAE: Experimental Autoimmune Encephalomyelitis

EGF-CFC: Embryonic Growth Factor-Cripto/FRL-1/Cryptic

EGFP: Enhanced Green Fluorescent Protein

ERK1/2: Extracellular Regulated Kinase 1/2

fMRI: Functional Magnetic Resonance Imaging

GASP-1: GDF-Associated Serum Protein -1

GDF: Growth And Differentiation Factor

GFAP: Glial Fibrillary Acidic Protein

GM: Grey Matter

HDAC: Histone Deacetylases

IGF-1: Insulin-Like Growth Factor 1

LFB: Luxol Fast Blue

LINGO-1: Leucine Rich Repeat And Immunoglobulin-Like Domain Containing Protein 1

LPC: lysophosphatidyl choline/lysolecithin

MAG: Myelin-Associated Glycoprotein

MAPK: Mitogen-Activated Protein Kinase

MBP: Myelin Basic Protein

MHC: Major Histocompatibility Complex

MOG: Myelin/Oligodendrocyte Glycoprotein

MS: Multiple Sclerosis

MTC1: Monocarboxylate Transporter 1

mTOR: Mechanistic Target Of Rapamycin

MTR: Magnetisation Transfer Ratio

NAA: N-Acetyl Aspartic Acid

NF: Neurofilament

NG2: Neural/Glial Antigen 2

OMgp: Oligodendrocyte/Myelin Glycoprotein

OPC: Oligodendrocyte Progenitor Cell

ORO: Oil Red O

PBS: Phosphate-buffered saline

PDGFRα: Platelet-Derived Growth Factor Receptor α

PET: Positron Emission Tomography

PFA: Paraformaldehyde

PI3K: Phosphoinositide 3-kinase

PLA: Proximity Ligation Assay

PLP: Proteolipid Protein

PPMS: Primary Progressive Multiple Sclerosis

PSA-NCAM: Polysialated-Neural Cell Adhesion Molecule

PTEN: Phopsohotase and Tensin Homolog

RRMS: Relapse Remitting Multiple Sclerosis

RXR: Retinoid X Receptor

SOST: Sclerostin

SPMS: Secondary Progressive Multiple Sclerosis

TGF-β: Transforming Growth Factor β

TGF-βRII: TGF-β receptor 2

TMEV: Theilers Murine Encephalomyelitis Virus

VEP: Visually Evoked Potentials

WM: White Matter

8 Appendix

This section includes a peer-reviewed publication on which I am shared first author. This publication is open access, and therefore permission is granted to include it in this Appendix. Data from this publication included in this thesis was clearly identified within the data chapters.

Acta Neuropathologica (2018) 135:887–906
https://doi.org/10.1007/s00401-018-1813-3

ORIGINAL PAPER

Activin receptors regulate the oligodendrocyte lineage in health and disease

Alessandra Dillenburg[1] · Graeme Ireland[1] · Rebecca K. Holloway[1] · Claire L. Davies[1] · Frances L. Evans[1] · Matthew Swire[2] · Marie E. Bechler[2] · Daniel Soong[1] · Tracy J. Yuen[3,7] · Gloria H. Su[4] · Julie-Clare Becher[5] · Colin Smith[6] · Anna Williams[2] · Veronique E. Miron[1]

Received: 4 October 2017 / Revised: 16 January 2018 / Accepted: 29 January 2018 / Published online: 3 February 2018

Abstract

The most prevalent neurological disorders of myelin include perinatal brain injury leading to cerebral palsy in infants and multiple sclerosis in adults. Although these disorders have distinct etiologies, they share a common neuropathological feature of failed progenitor differentiation into myelin-producing oligodendrocytes and lack of myelin, for which there is an unmet clinical need. Here, we reveal that a molecular pathology common to both disorders is dysregulation of activin receptors and that activin receptor signaling is required for the majority of myelin generation in development and following injury. Using a constitutive conditional knockout of all activin receptor signaling in oligodendrocyte lineage cells, we discovered this signaling to be required for myelination via regulation of oligodendrocyte differentiation and myelin compaction. These processes were found to be dependent on the activin receptor subtype Acvr2a, which is expressed during oligodendrocyte differentiation and axonal ensheathment in development and following myelin injury. During efficient myelin regeneration, Acvr2a upregulation was seen to coincide with downregulation of Acvr2b, a receptor subtype with relatively higher ligand affinity; Acvr2b was shown to be dispensable for activin receptor-driven oligodendrocyte differentiation and its overexpression was sufficient to impair the abovementioned ligand-driven responses. In actively myelinating or remyelinating areas of human perinatal brain injury and multiple sclerosis tissue, respectively, oligodendrocyte lineage cells expressing Acvr2a outnumbered those expressing Acvr2b, whereas in non-repairing lesions Acvr2b+ cells were increased. Thus, we propose that following human white matter injury, this increase in Acvr2b expression would sequester ligand and consequently impair Acvr2a-driven oligodendrocyte differentiation and myelin formation. Our results demonstrate dysregulated activin receptor signaling in common myelin disorders and reveal Acvr2a as a novel therapeutic target for myelin generation following injury across the lifespan.

Keywords Myelin · Remyelination · Oligodendrocyte · Multiple sclerosis · Perinatal brain injury · Activin receptor

Introduction

Myelin ensures axon health and function in the CNS via trophic/metabolic support and insulation for electrical impulse conduction [14, 16, 26, 32, 37, 46]. The lack of myelin is, therefore, associated with axon dysfunction and/or loss, causing deficits in movement, sensation, and cognition, as observed in prevalent myelin disorders of development (perinatal brain injury leading to cerebral palsy/cognitive deficits) and adulthood [multiple sclerosis (MS)]. Although these have distinct etiologies, a shared neuropathological feature involves failed differentiation of oligodendrocyte precursor cells (OPCs) into myelin-producing oligodendrocytes following injury, resulting in impaired myelin

Alessandra Dillenburg and Graeme Ireland contributed equally to this work.

Electronic supplementary material The online version of this article (https://doi.org/10.1007/s00401-018-1813-3) contains supplementary material, which is available to authorized users.

✉ Veronique E. Miron
vmiron@ed.ac.uk

Extended author information available on the last page of the article

formation (myelination) [8, 10, 33, 36, 57] or regeneration (remyelination) [38], respectively. However, the mechanisms underpinning this pathology are not fully understood, as evidenced by the lack of approved therapies aimed at promoting oligodendrocyte differentiation and myelin generation.

Our previous work identified activin-A, a member of the transforming growth factor beta (TGF-β) superfamily, as being a promising pro-differentiation therapeutic target [45]. We found that at the onset of remyelination of focally demyelinated white matter lesions, microglia/macrophages express activin-A, and oligodendrocyte lineage cells express the ligand-binding activin receptors (Acvr2a, Acvr2b) and the signal-transducing co-receptor (Acvr1b) [45]; depletion of these microglia/macrophages caused impairment of remyelination [45]. In addition, healthy developmental myelination has recently been shown to be regulated by other TGF-β family members, TGF-β1 and activin-B [19, 49], albeit primarily via signaling through distinct receptors (TGFβR1) or co-receptors (Acvr1c), respectively. However, how activin receptor signaling regulates oligodendroglial lineage cell behavior, and whether this is required for myelination and remyelination, remains to be fully elucidated.

Here, we reveal the requirement for activin receptor signaling in regulating oligodendrocyte lineage cell responses during healthy white matter development and following injury. Furthermore, we demonstrate how dysregulation of activin receptor expression underpins myelin pathology in human perinatal brain injury and multiple sclerosis, revealing potentially targetable receptors for clinical intervention in myelin disorders across the lifespan.

Materials and methods

Animals

All experiments were performed under UK Home Office project licenses issued under the Animals (Scientific Procedures) Act. Animals were housed at 6 animals per cage in a 12 h light/dark cycle with unrestricted access to food and water. For animal experiments, power was calculated by two-sided 95% confidence interval via the normal approximation method using OpenEpi software, and reached > 80% power (84–100%) for all experiments. *ARRIVE* guidelines were followed in providing details of experiments, quantifications, and reporting.

Organotypic cerebellar slice cultures

Postnatal day 0–2 (P0-P2) CD1 pup cerebellum and attached hindbrains were sagittally sectioned at 300 µm on a McIlwain tissue chopper and plated onto Millipore-Millicel-CM mesh inserts (Fisher Scientific) in 6-well culture plates at six slices per insert. Media was composed of 50% minimal essential media, 25% heat-inactivated horse serum, 25% Earle's balanced salt solution (all from GIBCO), 6.5 mg ml^{-1} glucose (Sigma), 1% penicillin–streptomycin, and 1% glutamax. At 21 days in vitro when myelination is complete and compact, demyelination was induced by incubation in 0.5 mg ml^{-1} lysolecithin (Sigma) for 18-20 h. Slices were then washed in media for 10 min and treated at 2 days post lysolecithin (dpl) until 7, 10, or 14 dpl with activin-A (100 ng ml^{-1}, R&D Systems), inhibin-A (100 ng ml^{-1}, R&D Systems) or vehicle controls. Slices were fixed in 4% paraformaldehyde (PFA, wt/vol) for 10 min and blocked in 5% normal horse serum (GIBCO) and 0.3% Triton-X-100 (Fisher Scientific) for 1 h. Primary antibodies rat anti-MBP (1:250, AbD Serotec; MCA409S) and chicken anti-neurofilament-H (1:10,000, EnCor Biotech; CPCA-NF-H) were applied for 48 h at 4 °C. Slices were washed twice in 0.1% Triton-X-100 and fluorescently conjugated antibodies applied for 2 h at 20–25 °C (Life Technologies-Molecular Probes). Following counterstaining with Hoechst, slices were washed thrice and mounted onto glass slides using Fluoromount-G. Z-stacks were captured using an Olympus 3i Spinning Disk microscope (60× silicone objective) and SlideBook software. Stacks were cropped to 14 slices (0.59 µm/slice) in SlideBook (3i), and images blinded and imported into Volocity (Perkin Elmer) as an image sequence. Remyelination index was calculated by normalizing voxel counts of values of co-localization of myelin (MBP) and axon (NF) to NF voxel counts, and this value for treated slices was further normalized to vehicle controls. Both males and females were assessed.

Breeding strategy for conditional knockout generation

Sperm from *Acvr1b* LoxP mice was generously provided by Dr. Gloria H. Su (Columbia University) where exons 2–3 are flanked with Cre-LoxP sites, which upon Cre recombination causes deletion of a 3.3-kb sequence, frameshift mutation, and abolishment of Acvr1b protein expression [53]. Sperms were injected into pseudopregnant C57Bl/6J females. The offspring were intercrossed to generate mice homozygous for the LoxP allele and subsequently crossed to PDGFRa-Cre mice (Jax laboratories, 013148). Mice identified as being positive for PDGFRa-Cre and heterozygous for the LoxP allele were then crossed back to homozygous *Acvr1b* LoxP mice to generate homozygous conditional knockout (cKO) mice. Mice were confirmed as a cKO by performing PCR on the genomic DNA for detection of the Cre recombinase gene and homozygosity of the *Acvr1b* LoxP allele. Further analysis of the recombination by PCR and Cre recombinase immunohistochemistry in the corpus callosum confirmed the conditional status of these mice (Online Resource

Supplemental Fig. 1). This was confirmed by DNA extraction from cortical OPCs of transgenic mice using the Wizard SV genomic purification system (Promega) and PCR using Q5 High Fidelity DNA Polymerase (New England Biolabs) using amplification with primers P4 and P5 (sequence in genotyping section below) (Online Resource Supplemental Fig. 1). Both males and females were assessed.

Genotyping

Genomic DNA was extracted from ear tissue using the Wizard SV genomic purification system (Promega) according to the manufacturer's instructions. *Acvr1b* floxed mice were genotyped using PCR strategies as previously described [53]. Briefly, *Acvr1b* floxed mice were genotyped using primers P1 (ATGAAAAGTGCTTGCGTGTG) and P2 (CAGGGAAGGGCAGATATCAA). PDGFRa-Cre mice were genotyped using primers 1084 (GCGGTCTGGCAG TAAAAACTATC), 1085 (GTGAAACAGCATTGCTGT CACTT), 7338 (CTAGGCCACAGAATTGAAAGATCT) and 7339 (GTAGGTGGAAATTCTAGCATCATCC). Cre-mediated recombination was detected using P4 (CCAGCA CCTACATCACATGG) and P5 (CTCTATGGAGAGCAC CCTCTTTG) (Online Resource Supplemental Fig. 1).

Immunohistochemistry of rodent cryosections

Animals were intracardially perfused with 4% PFA (wt/vol; Sigma), brains post-fixed overnight and cryoprotected in sucrose prior to embedding in OCT (Tissue-Tech) and storage at − 80 °C. 8–10 µm cryosections were air-dried, permeabilized and blocked for 1 h with 5% normal horse serum (GIBCO) and 0.3% Triton-X-100 (Fisher Scientific). For Caspr staining, blocking solution and antibody diluent was composed of 10% normal horse serum and 0.1% Triton-X-100. For myelin protein staining, sections were permeabilized in methanol at − 20 °C for 10 min. For Olig1 and Olig2 staining, sections were permeabilized in Vector Unmasking Solution (Vector) by microwaving for 5 min followed by a 30-min incubation at 60 °C. Primary antibodies were applied overnight at 4 °C in a humid chamber and include rat anti-MBP (AbD Serotec, 1:250; MCA409S), mouse anti-MAG (Millipore, 1:100; MAB1567), mouse anti-Olig2 (Millipore, 1:100; MABN50), rabbit anti-Olig2 (1:100, Millipore; AB960), mouse anti-Olig1 (Millipore, 1:100; MAB5540), mouse anti-NG2 (1:200, Millipore; MAB5384), mouse anti-CC1 (1:100, Abcam; ab16794), rabbit anti-Caspr (1:500, Abcam; ab34151), rabbit anti-cleaved caspase-3 (1:500, BD Pharmingen; 559565), rabbit anti-Acvr2a (1:100, Abcam; ab135634), goat anti-Acvr2a (1:40, RnD Biosystems; AF340), rabbit anti-Acvr2b (1:100, Abgent; AP7105a). Fluorescently conjugated secondary antibodies were applied for 2 h at 20–25 °C in a humid chamber (1:500, Life Technologies-Molecular Probes). Following counterstaining with Hoechst, slides were coverslipped with Fluoromount-G (Southern Biotech). Antibody isotype controls added to sections at the same final concentration as the respective primary antibodies showed little or no nonspecific staining. Terminal deoxynucleotidyl transferase dUTP nick end labeling (TUNEL; Promega) assay for apoptosis was carried out according to the manufacturer's instructions; DNase I (10 units ml^{-1}) was applied as a positive control for double stranded breaks. Sections were imaged on a Leica SPE confocal microscope (40× objective) or an Olympus 3i Spinning Disk microscope (30×, 60×, or 100× oil immersion objectives). Intensity of MAG or MBP staining in selected white matter areas was determined using the Histogram function in Adobe Photoshop and normalized to background levels in a non-white matter area from the respective sample. Percentage area of NF co-localizing with Caspr was calculated using Volocity software.

Western blotting

CNS samples were lysed with RIPA buffer (Thermo Scientific) supplemented with 1% protease inhibitor cocktail set III ethylenediaminetetraaceticacid (EDTA)-free (Calbiochem). Protein concentrations were determined using the Pierce BCA Protein Assay Kit (according to the manufacturer's instructions). Samples were diluted in Laemmli buffer (Bio-Rad) and 5% β-mercaptoethanol (Sigma)], heated at 95 °C for 2 min, and 10 µg of protein was loaded onto an acrylamide gel (4–20%; Thermo Scientific). Gel electrophoresis was performed in tris-hydroxyethyl piperazineethanesulfonic acid (HEPES)-sodium dodecyl sulfate (SDS) running buffer (Thermo Scientific) at 100 V and proteins transferred onto polyvinylidene difluoride (PVDF) membranes (Millipore) for 2 h at 10 V in 10% transfer buffer [3% Tris–HCl (Sigma-Aldrich), 15% glycine (Sigma-Aldrich), pH 8.3] and 20% methanol (Fisher Chemical) diluted in water. Membranes were blocked with 4% bovine serum albumin in Tris-buffered saline (TBST) [4% sodium chloride (NaCl), 0.1% potassium chloride (KCl), 1.5% Tris–HCl, 0.1% Tween-20 (all from Sigma-Aldrich), pH 7.4] for 1 h at room temperature on an orbital shaker, then incubated overnight at 4 °C with rabbit anti-MBP (1:1000, AB980; Merck Millipore) or mouse anti-CNPase (1:1000, AMAb91068; Atlas Antibodies). Membranes were washed thrice in TBST for 5 min and incubated with horseradish peroxidase (HRP)-IgG secondary antibody conjugates (1:2000; Calbiochem) for 1 h at room temperature. Chemiluminescent substrate detection reagent RapidStep ECL Reagent (Calbiochem) was used to visualize bands. For loading control purposes, all membranes were re-blotted with anti-mouse or anti-rabbit beta-Actin.

Resin embedding, semi-thin sections, and electron microscopy

Mice were intracardially perfused with 4% PFA (wt/vol) and 2% glutaraldehyde (vol/vol; TAAB Laboratories) in 0.1 M phosphate buffer. Tissue was post-fixed overnight at 4 °C and transferred to 1% glutaraldehyde (vol/vol) until embedding. 1 mm tissue sections were processed into araldite resin blocks. 1 µm microtome-cut sections were stained with a 1% toluidine blue/2% sodium borate solution prior to bright field imaging at 100× magnification using a Zeiss Axio microscope. Number of myelinated axons was blindly quantified in 50 µm × 50 µm images of corpus callosum, with 2–4 sections counted per mouse and then values averaged. Ultrathin sections (60 nm) were cut from corpus callosum, stained in uranyl acetate and lead citrate, and grids imaged on a JEOL Transmission Electron Microscope. Axon diameter, myelin thickness, and inner tongue thickness were calculated from measured area based on assumption of circularity using Fiji/ImageJ (Fiji.sc) (diameter $= 2 \times \sqrt{[\text{area}/\pi]}$), with a minimum of 100 axons per animal analyzed. Enlarged inner tongues in conditional knockout mice precluded standard *g*-ratio analysis of myelin thickness, which was instead calculated by subtracting the diameter to the innermost compact myelin layer from the diameter to the outermost compact myelin layer (see Online Resource Supplemental Fig. 5 for outline of quantification methods). Inner tongue thickness was calculated by subtracting the axonal diameter from the diameter to the innermost compact layer (Online Resource Supplemental Fig. 5). 'Proportion of myelinated axons' per axon diameter was determined by plotting the proportion of total myelinated axons (across all axons diameters) from each animal that were of a specific diameter, which was fitted with a best-fit polynomial regression.

Oligodendrocyte lineage cell cultures

Cortical mixed glial cultures generated from both male and female Sprague–Dawley rat P0–P2 pups were expanded for 10–14 days in vitro, and microglia depleted by de-adhesion following 1 h on a rotary shaker at 37 °C at 250 rpm. OPCs were subsequently isolated from collection of the floating fraction following 16 h on the rotary shaker, followed by depletion of contaminating astrocytes by differential adhesion. OPCs were plated in DMEM containing 4.5 g l^{-1} glucose, L-glutamine, pyruvate, SATO [16 µg ml^{-1} putrescine, 400 ng ml^{-1} l-thyroxine, 400 ng ml^{-1} tri-iodothyroxine, 60 ng ml^{-1} progesterone, 5 ng ml^{-1} sodium selenite, 100 µg ml^{-1} bovine serum albumin fraction V, 10 µg ml^{-1} insulin, 5.5 µg ml^{-1} halo-transferrin (all from Sigma-Aldrich)], 0.5% fetal calf serum (GIBCO), 1% penicillin/streptomycin, 10 ng ml^{-1} platelet-derived growth factor, and 10 ng ml^{-1} fibroblast growth factor-2, at 2×10^4 cells per well in 8-well PDL-coated permanox chamberslides (Lab-TEK). OPCs were treated with activin-A (10 ng ml^{-1}, R&D Systems) or vehicle control (0.0002% BSA) for 3 days. In a subset of experiments, OPCs were co-treated with activin-A and neutralizing antibodies against Acvr2a or Acvr2b (30 µg ml^{-1}, R&D Systems; AF340, AF339) or goat IgG isotype control (30 µg ml^{-1}, Santa Cruz Biotechnology). Cells were matured to oligodendrocytes by withdrawal of growth factors from the media and treated with activin-A or vehicle control, with or without neutralizing antibodies for 5 days as above. An average of 120 cells were counted per image, with 2 images assessed per condition per biological replicate (a total of > 700 cells quantified per condition); values were averaged per biological sample. For quantification of mature oligodendrocyte membrane area, images were imported into Columbus software (Perkin Elmer), individual cells identified (by the software) by Hoechst, oligodendrocytes identified by MBP staining, and size of cytoplasm measured in square pixels (px^2) with a threshold of 2000 px^2 set to exclude background/false positives. For Phalloidin intensity measurements, Columbus was used to first identify cells (Hoechst+ nuclei) then mature oligodendrocytes (MBP+), and Phalloidin signal intensity was measured in each MBP+ cell.

Immunocytochemistry

Cells were fixed with 4% PFA (wt/vol) for 10–15 min and blocked for 30 min in 10% goat serum (Sigma), 2% horse serum (GIBCO), and 0.3% Triton-X-100 at 20–25 °C. Primary antibodies were diluted in blocking solution and applied for 1 h at 20–25 °C, and included mouse anti-MAG (1:100, Millipore; MAB1567), rat anti-MBP (1:250; AbD Serotec; MCA409S), and chicken anti-GFP (1:100; Abcam; ab13970). Cells were incubated with fluorescently conjugated secondary antibodies diluted in blocking solution (1:1000, Life Technologies-Molecular Probes), and in a subset of experiments with Phalloidin-Alexa-568 (1:40; ThermoFisher), for 1 h at 20–25 °C. Slides were counterstained with Hoechst (5 µg ml^{-1}) and coverslipped with Fluoromount-G. Cells were imaged on a Leica SPE confocal microscope (40× objective) or an Olympus 3i Spinning Disk microscope (30× or 60× objectives).

Lentiviral-based overexpression

Lentivirus particles generated using 3rd generation lentivirus packaging were purchased from Insight Bio/Origene (stock 10^7 TU ml^{-1}), inducing expression of GFP only for control transfection (PS100071V), or inducing overexpression of mouse Acvr2b and GFP (MR212153L2V). Particles were added to cultures of OPCs or differentiating oligodendrocytes at a multiplicity of infection (MOI) of 2.5 for 3

or 5 days, respectively. Cells were then fixed and immunostained or lysed for protein as above.

Microfiber myelination assays

OPCs were plated onto PDL-coated parallel-aligned 2 µm electrospun poly-L-lactide acid (PLLA) fibers in 12-well plate inserts (The Electrospinning Company) at 35,000 cells per insert, as done previously [7]. Media was composed of 50:50 Neurobasal media and DMEM with high glucose supplemented with SATO [16 µg ml^{-1} putrescine, 400 ng ml^{-1} l-thyroxine, 400 ng ml^{-1} tri-iodothyroxine, 60 ng ml^{-1} progesterone, 5 ng ml^{-1} sodium selenite, 100 µg ml^{-1} bovine serum albumin fraction V, 10 µg ml^{-1} insulin, 5.5 µg ml^{-1} halo-transferrin), 5 µg ml^{-1} *N*-acetyl cysteine, 10 ng ml^{-1} D-Biotin (all from Sigma-Aldrich)], ITS supplement (Sigma), B27 (Invitrogen), and 1% penicillin/streptomycin. Cultures were treated with activin-A (1–100 ng ml^{-1}, R&D Systems) or vehicle control for 14 days, fixed with 4% paraformaldehyde (wt/vol, Sigma), permeabilized with 0.1% Triton-X-100 (Fisher Scientific) and incubated overnight at 4 °C with rat anti-MBP antibody (1:250, AbD Serotec; MCA409S). Following three washes in PBS, inserts were incubated with secondary antibody (1:1000, Life Technologies-Molecular Probes) for 1 h at 20–25 °C, counterstained with Hoechst and mounted onto glass coverslips with Fluoromount G. Inserts were imaged as Z-stacks on an Olympus 3i Spinning Disk microscope (60×). Myelin sheath number per oligodendrocyte and lengths from 20 oligodendrocytes per biological preparation were analyzed in a blinded manner using the segmented line tool in Fiji/ImageJ (Fiji.sc) on maximum intensity images, using Z stacks to confirm complete wrapping around fibers.

Forward phase phospho-antibody microarray

OPCs were plated at 1×10^6 cells per well in a 6-well PDL-coated plate and treated with activin-A (10 ng ml^{-1}) or vehicle control (0.0002% BSA). Cultures were washed with cold phosphate buffered saline on ice, scraped, and centrifuged thrice at 10,000 rpm at 4 °C and supernatant discarded. Protein extraction, lysate purification, and protein biotinylation were performed using the Antibody Array Assay Kit (Full Moon Biosystems) according to the manufacturer's instructions. Samples were applied to TGF-β phospho-antibody microarray slides (Full Moon Biosystems) which have 176 immobilized antibodies against phosphorylated and unphosphorylated specific residues in proteins associated with the 5 TGFβ signaling pathways, with 6 technical replicates per antibody. All antibodies are against activating phosphorylation states, to the exception of Abl Thr754/735, GEF2 Ser885, Cofilin Ser3, Myc Ser373/Ser62/Thr358/Thr58. Following incubation with streptavidin-Cy3 (1:1000), signal was detected on an Axon4200 microarray scanner (Edinburgh Genomics, The University of Edinburgh). Subsequent to background signal subtraction, values from phosphorylated signal were normalized to total protein signal for each protein site, then normalized to vehicle control. Data were then Log2 transformed and plotted as heat maps using GraphPad Prism 7 (San Diego, USA).

In vivo focal demyelinated lesions

Demyelinating lesions were induced in the caudal cerebellar peduncles of 12-week-old female Sprague–Dawley rats by stereotaxic injection of 4 µl of 0.01% ethidium bromide (vol/vol) using a Hamilton syringe. Rats were intracardially perfused with 4% PFA, cryoprotected, cryosectioned, and stained as above. Non-lesioned CCP served as a control.

Post-mortem brain tissue

Formalin-fixed paraffin-embedded post-mortem perinatal brain injury tissue was obtained with full ethical approval from the Medical Research Council Edinburgh Brain and Tissue Bank (EBTB) (REC/1-/S1402/69). Tissue with evidence of white matter injury was selected with neuropathological support from Dr. Julie-Clare Becher (Royal Infirmary of Edinburgh) and Dr. Colin Smith (University of Edinburgh) (Table S1, Online Resource Supplemental Fig. 9a–c). Sections were de-paraffinized twice at 20–25 °C in Histoclear for 10 min then rehydrated through an ethanol gradient (100% (twice), 95, 70, and 50%, 5 min each). Following washes in 0.1% Tween20 (vol/vol) in Tris-buffered Saline (TBS), sections were microwaved in Vector Unmasking Solution for 10 min, washed once, and endogenous phosphatase and peroxidase activity blocked for 5 min (Bloxall, Vector). Primary antibody was prepared in 2.5% Normal Horse Serum (Vector) and applied overnight in a humid chamber at 4 °C. Antibodies used included mouse CD68 (1:100, DAKO; M0814), rat anti-MBP (AbD Serotec, 1:250; MCA409S), rabbit anti-INHBA (activin-A subunit; 1:100, Sigma-Aldrich; HPA020031), rabbit anti-Acvr2a (1:100, Abcam; ab135634), rabbit anti-Acvr2b (1:100, Abgent; AP7105a), rabbit anti-PCNA (1:400, Abcam; ab18197), and mouse anti-Olig2 (1:100, EMD Millipore; MABN50). Following washes, alkaline phosphatase-conjugated anti-mouse or anti-rabbit secondary antibody was applied for 30 min at 20–25 °C in a humid chamber. Sections were washed in TBS and stains visualized by Vector Blue substrate kit according to the manufacturer's instructions (maximum 15 min). For co-staining, sections were washed thrice and re-blocked to quench any remaining phosphatase activity (Bloxall, Vector) prior to application of primary antibody, then developed using Vector Red substrate kit according to the manufacturer's instructions (maximum 15 min). Following washes

in water, the sections were counterstained with Hoechst and mounted with Fluoromount-G. Entire tissue sections were imaged using a Zeiss AxioScan SlideScanner. Due to non-neurological age-matched controls not being available, areas of injury (high CD68 densities; average 122 ± 30 cells/mm^2) were compared to areas of non-injury (low CD68 densities; average 10 ± 10 cells/mm^2) within the same section (pathology assessment shown in Online Resource Supplemental Fig. 9a–c). Lesion maps were defined for analysis in Zeiss Zen2 software; fields of 360 µm × 360 µm were counted per sample (injured or non-injured) and counts were multiplied to determine density of immunopositive cells per mm^2. Post-mortem tissue from MS patients and controls who died of non-neurological causes were obtained via a UK prospective donor scheme with full ethical approval from the UK Multiple Sclerosis Tissue Bank (MREC/02/2/39). MS diagnosis was confirmed by neuropathological means by F. Roncaroli (Imperial College London) and clinical history was provided by R. Nicholas (Imperial College London). Snap frozen unfixed tissues blocks (2 × 2 × 1 cm) were cut at 10 µm and stored at − 80 °C. MS lesions were classified according to the International Classification of Neurological Disease using Luxol Fast Blue staining and Oil Red O immunoreactivity using standard methods (pathological assessment shown in Online Resource Supplemental Fig. 9d–f). We analyzed 4 control blocks and 10 tissue blocks from 8 MS patients (Table S2). Sections were fixed in 4% PFA for 1 h at 20–25 °C, washed in TBS and permeabilized in methanol for 10 min at − 20 °C. Sections were subsequently stained, imaged and quantified as above.

Statistics

All manual cell counts were performed in a blinded manner. Data are represented as mean ± s.e.m. Power calculations for sample size were performed (using OpenEpi), and showed power between 84 and 100% for all experiments. Statistical tests include one-sample *t* test for data where values were normalized to control, two-tailed Student's *t* test or Mann–Whitney test, and non-parametric one-way ANOVA (Kruskal–Wallis) with Dunn's multiple comparison post hoc test when > 3 comparisons were made. A paired Student's *t* test was used when variation between experiments was high, to normalize to baseline levels within each biological preparation. Slopes of myelin thickness versus axon diameter were compared using the Extra Sum of Squares F test. Curve distributions of proportion of myelinated axons per axon diameter were compared using the Kolmogorov–Smirnov test. Proportions of CC1+ or CC1− negative cells within the Olig2+ population were compared using Multiple *t* tests and two stage step up linear procedure of Benjamini, Krieger, and Yekutieli with a false discovery rate of 1%. $P < 0.05$ was considered to be statistically significant. Data handling and statistical processing were performed using Microsoft Excel and GraphPad Prism Software.

Results

Activin receptor signaling is required for developmental myelination

To determine whether activin receptor signaling is required for developmental myelination, we sought to constitutively eliminate all activin receptor signaling in oligodendrocyte lineage cells. We achieved this by targeting *Acvr1b*, the activin co-receptor that is required for all intracellular signal transduction downstream of activin-A binding to either activin receptor Acvr2a or Acvr2b [6] (Fig. 1a). We thus created a constitutive conditional knockout in which oligodendroglial lineage cells cannot respond to any activin receptor ligation due to *Acvr1b* excision in OPCs (PDGFRa-Cre; Acvr1b$^{fl/fl}$) [6, 53] (Fig. 1a; Online Resource Supplemental Fig. 1a–c). By immunofluorescence, Cre expression was confirmed to be in Olig2+ oligodendrocyte lineage cells (Online Resource Supplemental Fig. 1d). At postnatal day 16 (P16) when myelination is normally underway, PDGFRa-Cre; Acvr1b$^{fl/fl}$ mice displayed a tremor, hunched posture, and a stiff tail (Online Resource Supplemental Video 1), all behaviors associated with myelin abnormalities [17, 44] or damage (e.g. in experimental autoimmune encephalomyelitis) [12, 58].

To determine whether this reflected myelin pathology, we assessed myelin-associated protein expression in the brains of Acvr1b$^{fl/fl}$ control and PDGFRa-Cre; Acvr1b$^{fl/fl}$ mice by Western blot and observed a decrease in 2′,3′-cyclic nucleotide 3′-phosphodiesterase (CNP) and myelin basic protein (MBP) in the conditional knockout mice (Fig. 1b). We further analyzed expression of myelin protein by immunofluorescence in multiple white matter tracts (corpus callosum, cerebellum, spinal cord) in PDGFRa-Cre; Acvr1b$^{fl/fl}$ mice and observed a severe reduction in myelin-associated glycoprotein (MAG) intensity compared to Acvr1b$^{fl/fl}$ control and heterozygous (PDGFRa-Cre; Acvr1b$^{fl/+}$) littermates (Fig. 1c, d; Online Resource Supplemental Fig. 2a, b). Hypomyelination in PDGFRa-Cre; Acvr1b$^{fl/fl}$ mice was further verified by histological analysis of semi-thin resin sections, which showed a significantly reduced density of myelinated axons by 60% (Fig. 1e, f). Peripheral nervous system myelin on dorsal root ganglia was unaffected in conditional knockout mice (Online Resource Supplemental Fig. 2c, d), as expected given the absence of PDGFRα expression in that compartment. Ultrastructural assessment of the sparse myelin that was produced by P16 in PDGFRa-Cre; Acvr1b$^{fl/fl}$ mice revealed that of all the myelinated axons, the largest

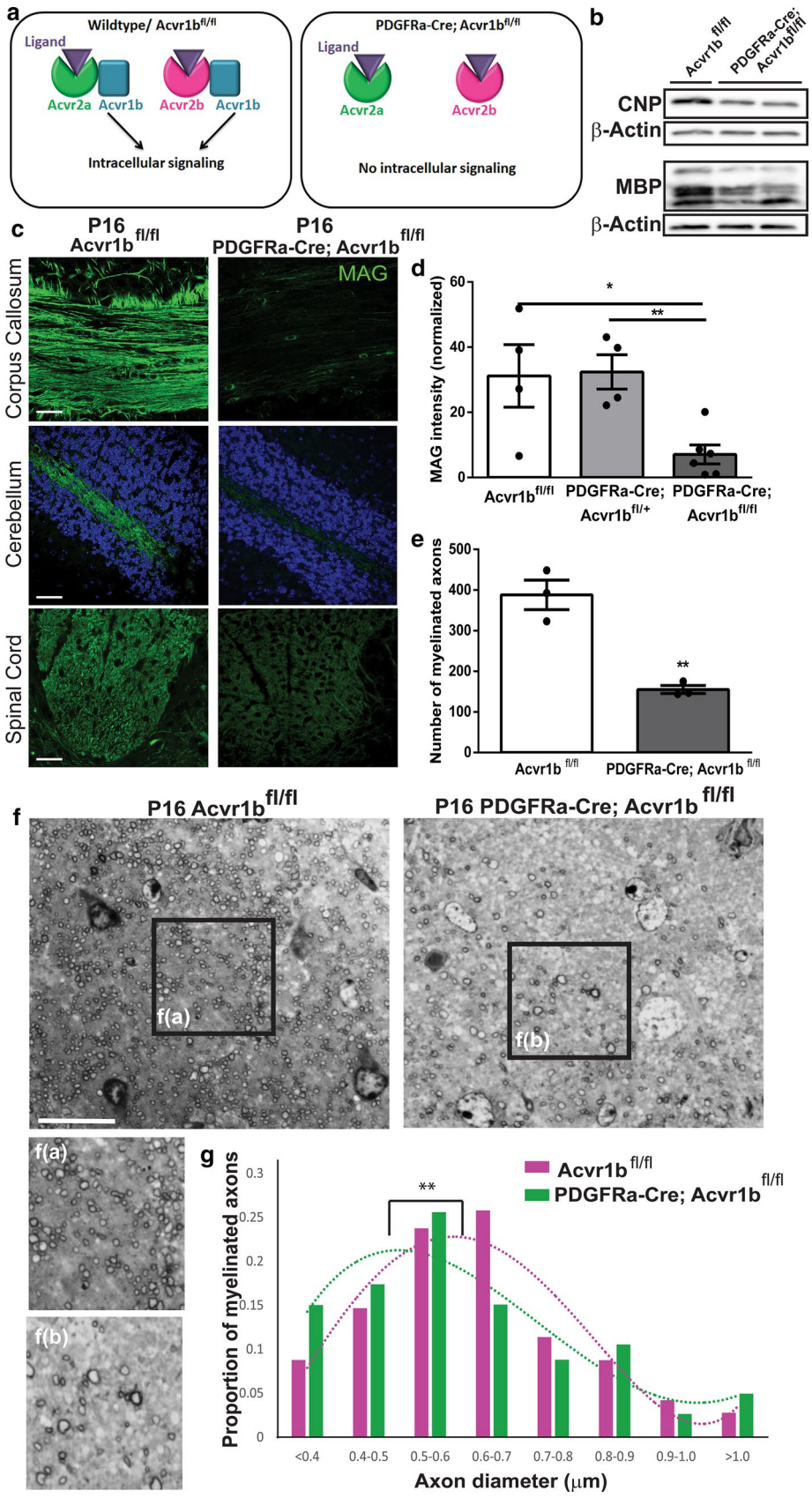

Fig. 1 Activin receptor signaling is required for developmental myelination. **a** Diagram of activin receptor signaling: Acvr2a and Acvr2b are ligand-binding receptors that require Acvr1b to induce intracellular signallng. In PDGFRa-Cre; Acvr1b$^{fl/fl}$ mice, the knock-out of Acvr1b eliminates all activin receptor signaling from both ligand binding receptors. **b** Western blots of brain lysates from P16 Acvr1b$^{fl/fl}$ and PDGFRa-Cre; Acvr1b$^{fl/fl}$ mice (cerebellum) labeled for CNP (46 kDa) or MBP (14–21 kDa) with β-Actin as a loading control. **c** Images of corpus callosum, cerebellum [counterstained with Hoechst (blue)] and dorsal spinal cord in P16 Acvr1b$^{fl/fl}$ and PDGFRa-Cre; Acvr1b$^{fl/fl}$ mice immunostained for myelin protein MAG (green). Scale bar 25 μm. **d** Mean MAG intensity normalized to background ± s.e.m. in the corpus callosum of P16 Acvr1b$^{fl/fl}$ ($n = 4$ mice), PDGFRa-Cre; Acvr1b$^{fl/+}$ ($n = 4$ mice) and PDGFRa-Cre; Acvr1b$^{fl/fl}$ mice ($n = 6$ mice). Two-tailed Student's t test, $^{*}P = 0.0211$, $^{**}0.0018$. **e** Mean number of myelinated fibers ± s.e.m. per field of toluidine-blue stained semi-thin resin sections of corpus callosum at P16 in Acvr1b$^{fl/fl}$ and PDGFRa-Cre; Acvr1b$^{fl/fl}$ mice ($n = 3$ mice per group). Two-tailed Student's t test, $^{**}P = 0.0034$. **f** Toluidine-blue stained semi-thin resin sections of corpus callosum in Acvr1b$^{fl/fl}$ (left) and PDGFRa-Cre; Acvr1b$^{fl/fl}$ mice (right), with expanded field of view (**f**(a) and **f**(b), respectively). Scale bar 20 μm. **g** Analysis of distribution of myelinated axons in relation to axon diameter, represented as proportion of myelinated axons only (from all diameters), in Acvr1b$^{fl/fl}$ (magenta) and PDGFRa-Cre; Acvr1b$^{fl/fl}$ mice (green) mice ($n = 3$ mice per genotype) overlaid with polynomial best-fit regression curves ($R^2 = 0.8897$, 0.8344, respectively). Kolmogorov–Smirnov test, $^{**}P = 0.002$

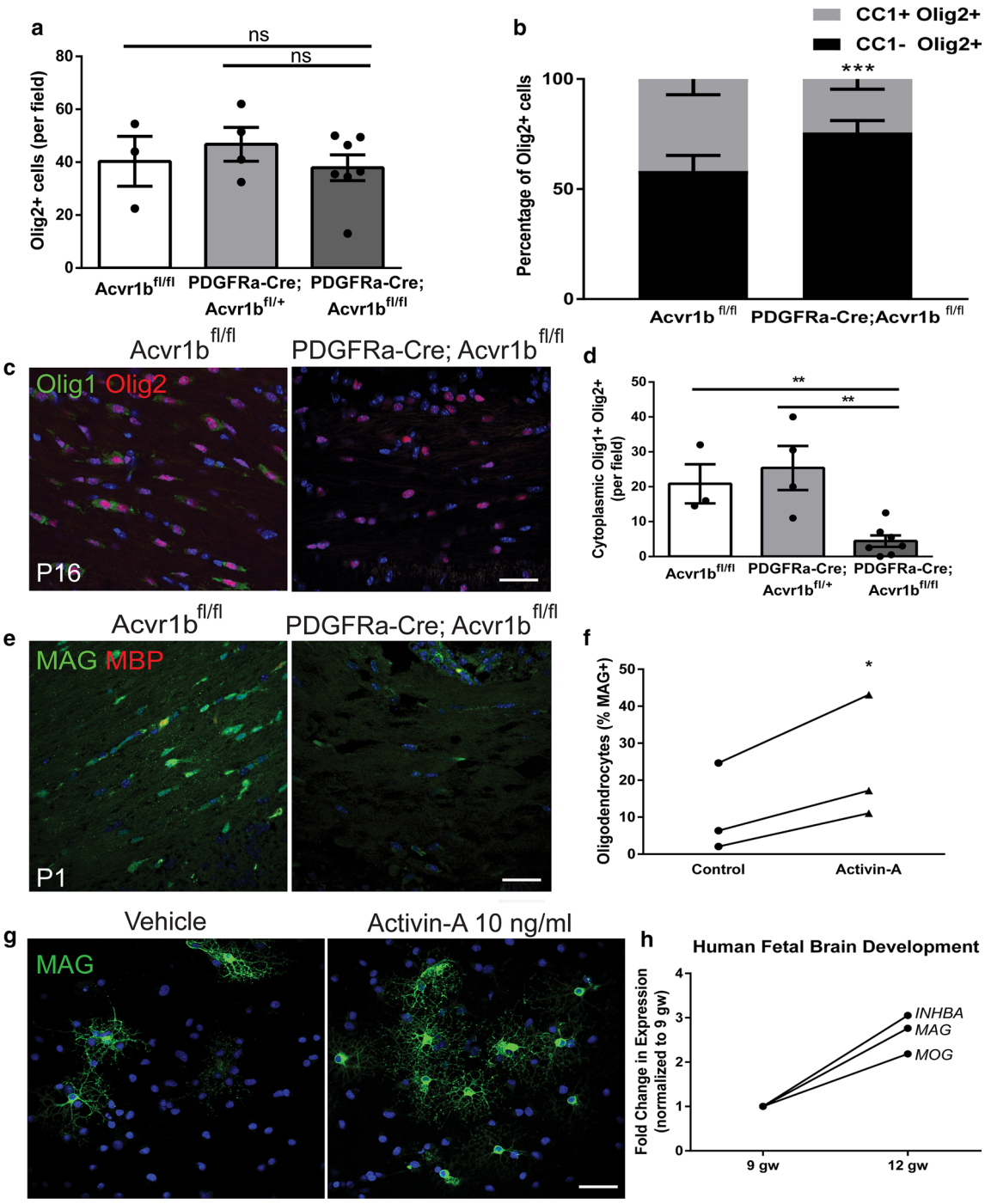

proportion was of a diameter of 0.5–0.6 µm, in comparison to that being 0.6–0.7 µm in floxed controls (Fig. 1g). A polynomial best-fit regression of the proportion of myelinated axons per axon diameter confirmed a statistically significant shift towards myelination of smaller diameter axons in activin receptor conditional knockouts (Fig. 1g). All PDGFRa-Cre; Acvr1b$^{fl/fl}$ mice died by P21 precluding longitudinal analysis of myelination; juvenile death is also a feature of some other hypomyelinating mutants [9, 15, 18, 34, 54, 64]. Nonetheless, analysis of mice at P21 showed some myelination, although hypomyelination was still prevalent in the corpus callosum and cerebellum (Online Resource Supplemental Fig. 2e). Overall, these data show the requirement for activin receptor signaling in timely myelination of a significant proportion of CNS axons in development.

Fig. 2 Activin receptor signaling regulates oligodendrocyte differentiation. **a** Mean number of oligodendrocyte lineage cells (Olig2+) per field ± s.e.m. in corpus callosum of P16 Acvr1b$^{fl/fl}$ (n = 3 mice), PDGFRa-Cre; Acvr1b$^{fl/+}$ (n = 4 mice) and PDGFRa-Cre; Acvr1b$^{fl/fl}$ mice (n = 7 mice). **b** Mean proportion of oligodendrocyte lineage cells (Olig2+) which are mature oligodendrocytes (CC1+) versus immature cells (CC1−), per field ± s.e.m. in corpus callosum of P16 Acvr1b$^{fl/fl}$ (n = 4 mice) and PDGFRa-Cre; Acvr1b$^{fl/fl}$ mice (n = 7 mice). Multiple t tests with false discovery rate of 1%, ***P = 0.000026. **c** Images of differentiating oligodendrocytes (cytoplasmic Olig1+ and nuclear Olig2+) in corpus callosum of P16 Acvr1b$^{fl/fl}$ and PDGFRa-Cre; Acvr1b$^{fl/fl}$ mice. Scale bar 25 µm. **d** Mean number of cytoplasmic Olig1 and Olig2 double positive cells per field ± s.e.m. in corpus callosum of P16 Acvr1b$^{fl/fl}$ (n = 3 mice), PDGFRa-Cre; Acvr1b$^{fl/+}$ (n = 4 mice) and PDGFRa-Cre; Acvr1b$^{fl/fl}$ mice (n = 7 mice). Two-tailed Student's t test, **P = 0.0047, 0.0026, respectively. **e** Images of maturing oligodendrocytes (MAG+ MBP−) at P1 in corpus callosum of Acvr1b$^{fl/fl}$ and PDGFRa-Cre; Acvr1b$^{fl/fl}$ mice. Scale bar 25 µm. **f** Mean number of MAG+ cultured oligodendrocytes per field in vehicle control-treated or activin-A-treated conditions (10 ng ml^{-1}) in vitro. n = 3 biological replicates. Two-tailed paired Student's t test, *P = 0.0484. **g** Images of cultured OPCs treated with vehicle or 10 ng ml^{-1} activin-A and immunostained for MAG (green), counterstained with Hoechst (blue). Scale bar 25 µm. **h** Data-mining of microarray of human fetal brain at 9 and 12 gestational weeks (gw) represented as fold change in expression (normalized to 9 gw), showing paralleled expression changes between activin-A (*INHBA*) and oligodendrocyte differentiation-associated genes (*MAG*, *MOG*) in development

Activin receptor signaling drives oligodendrocyte differentiation

We next sought to determine the cellular mechanisms underpinning the hypomyelination in PDGFRa-Cre; Acvr1b$^{fl/fl}$ mice, by assessing oligodendroglial responses. Between genotypes at P16, there were no differences in total oligodendroglial lineage cell number (Olig2+) (Fig. 2a); we did not observe cell death in the lineage at either P16 or earlier (cleaved caspase-3 negative and TUNEL negative) in any genotype (Online Resource Supplemental Fig. 3), consistent with oligodendrocyte death normally occurring later in development [24]. However, whereas in floxed control mice, the proportion of Olig2+ cells that were mature oligodendrocytes (CC1+) was not significantly different from that which were immature cells (CC1−), PDGFRa-Cre; Acvr1b$^{fl/fl}$ mice had significantly less CC1+ Olig2+ cells versus CC1− Olig2+ cells (Fig. 2b), suggesting impaired differentiation into mature oligodendrocytes. To specifically address this, we quantified differentiating oligodendrocytes (cytoplasmic Olig1+ Olig2+ cells) and found that these were significantly decreased in PDGFRa-Cre; Acvr1b$^{fl/fl}$ mice compared to controls (Fig. 2c, d). The oligodendrocyte maturation defect in activin receptor conditional knockout mice was observed as early as P1, when few immature oligodendrocytes (MAG+ MBP−) cells were observed (Fig. 2e). These data support that activin receptor signaling is required for differentiation of a significant proportion of oligodendrocyte lineage cells.

To assess the sufficiency of activin receptor signaling in driving oligodendrocyte differentiation, primary cultures of wildtype OPCs were treated with the most potent activating ligand, activin-A. Even in the presence of proliferation-inducing growth factors (platelet-derived growth factor and fibroblast growth factor) which normally preclude differentiation, activin-A significantly enhanced OPC differentiation into mature oligodendrocytes (MAG+) (Fig. 2f, g). Consistent with this finding, data-mining of the human fetal brain transcriptome [39] revealed that as development proceeds, increased gene expression of activin-A (*INHBA*) parallels that of oligodendrocyte maturation-associated genes *MAG* and *MOG* (Fig. 2h). The activin-A subunit (Inhba) was also found to be expressed in developing mouse brain during myelination (Online Resource Supplemental Fig. 4).

Activin receptor signaling drives oligodendrocyte membrane compaction

Although we demonstrated impaired oligodendrocyte differentiation in the activin receptor conditional mutant mouse, there were still some oligodendrocytes that were generated resulting in limited myelination taking place. We next analyzed whether this myelin was normally formed, to determine whether activin receptor signaling is required for proper myelination. In PDGFRa-Cre; Acvr1b$^{fl/fl}$ mice at P16, we observed increased myelin inner tongue thickness in PDGFRa-Cre; Acvr1b$^{fl/fl}$ mice compared to floxed controls (Fig. 3a–c), most prominently in association with small-diameter axons (Fig. 3b, c; measurement protocol outlined in Online Supplemental Resource Fig. 5). Enlarged myelin inner tongues are normally seen in early myelination during the active growth phase, resulting from accumulation of new myelin membrane prior to actin disassembly mediated compaction and fusion with myelin sheaths [48, 60, 66]. Persistent enlargement of inner tongues may thus result either from (i) increased membrane growth rate, or (ii) impaired actin disassembly and myelin membrane compaction [48, 61, 66]. Given that the former postulate would result in a thicker myelin sheath, we measured thickness of compacted layers (as done previously [66]; measurement protocol outlined in Online Supplemental Resource Fig. 5), yet documented significantly thinner myelin at all axon diameters in PDGFRa-Cre; Acvr1b$^{fl/fl}$ mice (Fig. 3d) thereby ruling out increased membrane growth. The thinner myelin in conditional knockout mice was confirmed to be compact (Fig. 3e). To address the latter postulate, we assessed expression of myelin basic protein (MBP), which is required for actin disassembly and myelin membrane compaction [60, 66]. PDGFRa-Cre; Acvr1b$^{fl/fl}$ mice

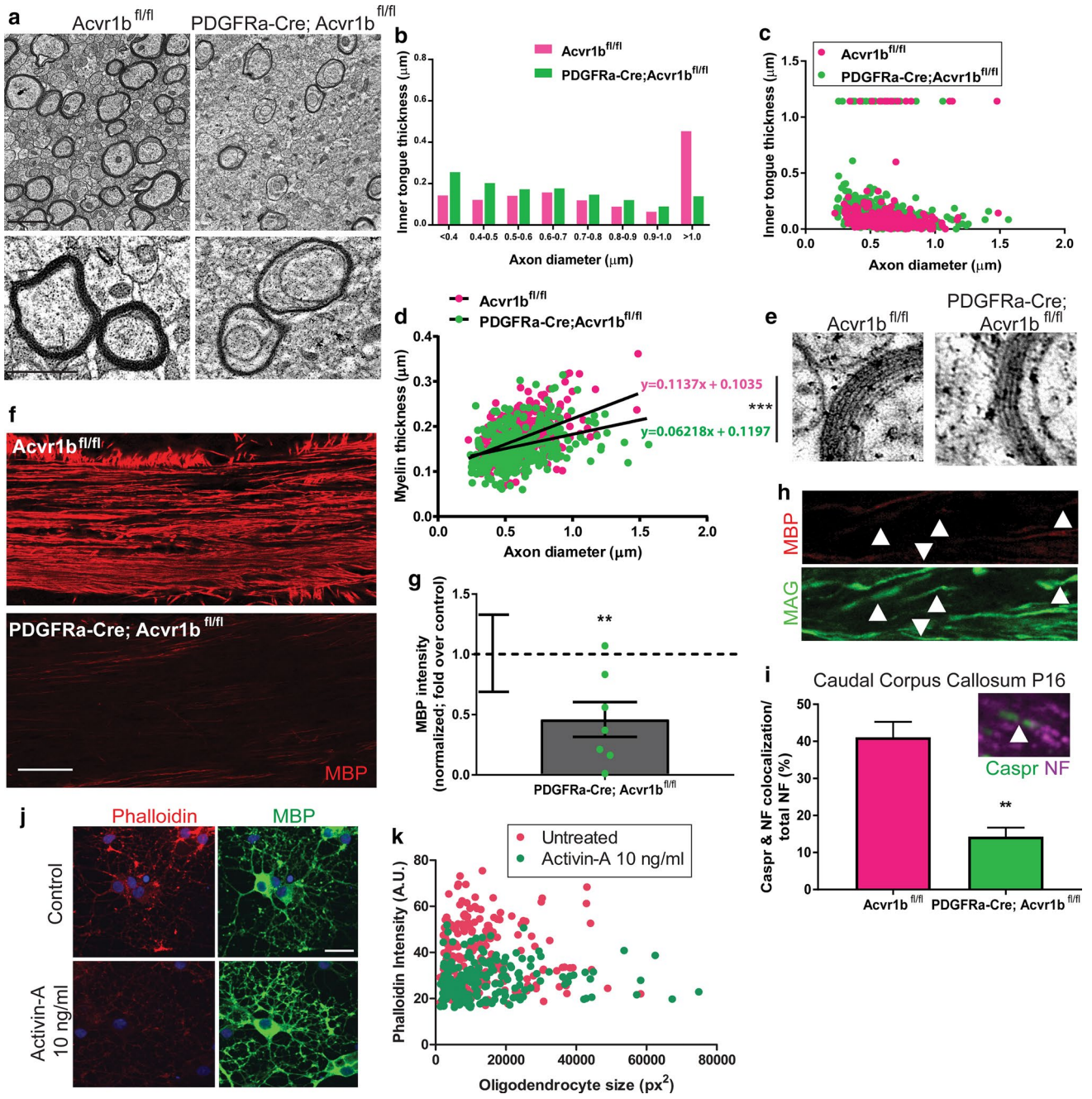

Fig. 3 Activin receptor signaling regulates myelin membrane compaction/maturation. **a** Electron micrographs of myelinated axons in P16 Acvr1b$^{fl/fl}$ and PDGFRa-Cre; Acvr1b$^{fl/fl}$ mice. Scale bars 1 µm. **b** Average inner tongue thickness per axon diameter per animal in Acvr1b$^{fl/fl}$ (magenta) and PDGFRa-Cre; Acvr1b$^{fl/fl}$ mice (green). $n = 3$ mice per genotype. **c** Dot plot of inner tongue thickness per axon diameter for all myelinated axons for all animals, in Acvr1b$^{fl/fl}$ (magenta) and PDGFRa-Cre; Acvr1b$^{fl/fl}$ mice (green). **d** Myelin thickness versus axon diameter in Acvr1b$^{fl/fl}$ (magenta) and PDGFRa-Cre; Acvr1b$^{fl/fl}$ mice (green). Extra sum of squares F test between slopes, $***P = 0.0014$. **e** Electron micrographs of compact myelin layers in P16 Acvr1b$^{fl/fl}$ and PDGFRa-Cre; Acvr1b$^{fl/fl}$ mice. **f** Images of myelin basic protein (MBP) in corpus callosum of Acvr1b$^{fl/fl}$ and PDGFRa-Cre; Acvr1b$^{fl/fl}$ mice at P16. Scale bar 25 µm. **g** MBP intensity in PDGFRa-Cre; Acvr1b$^{fl/fl}$ mice normalized to background and to levels in Acvr1b$^{fl/fl}$ mice. s.e.m. for variance in Acvr1b$^{fl/fl}$ samples indicated. One sample *t* test against theoretical mean of 1, $**P = 0.0097$. **h** Image of PDGFRa-Cre; Acvr1b$^{fl/fl}$ corpus callosum showing MAG+ (green), MBP negative (red) myelin sheaths (arrows). **i** Percentage of total axonal area (neurofilament (NF)+) co-localizing with compaction marker Caspr in caudal corpus callosum at P16 in Acvr1b$^{fl/fl}$ and PDGFRa-Cre; Acvr1b$^{fl/fl}$ mice. Two-tailed Student's *t* test, $**P = 0.0038$, $n = 2$–4 mice per group. Inset example of Caspr clusters (green) at paranodes along axon (NF+; purple) (arrow). **j** Images of cultured mature oligodendrocytes treated with vehicle control or activin-A (10 ng ml^{-1}) stained with Phalloidin-Alexa-568 (red) and MBP (green). Scale bar 20 µm. **k** Phalloidin intensity (arbitrary units; A.U.) in MBP+ sheets of mature oligodendrocytes plotted against oligodendrocyte size (pixels squared; px^2) in control (magenta) or activin-A (10 ng ml^{-1}) treated (green) conditions

showed significantly decreased MBP intensity relative to floxed controls (Fig. 3f, g); MAG+ myelin sheaths devoid of MBP were also observed in these mice (Fig. 3h), indicative of non-compact myelin as MAG is normally excluded from compact myelin sheaths by MBP [2, 3]. These data suggest that activin receptor signaling in oligodendroglial lineage cells is required for normal MBP expression and myelin membrane compaction.

We next asked whether this impairment in compaction would be maintained as myelination proceeds in the conditional knockout mice. Due to these mice dying by P21, we addressed this by examining the caudal region of the corpus callosum in P16 mice, where myelination is more advanced relative to rostral regions. As clustering of the axonal adhesion molecule Caspr along axons only occurs when myelin is compacted at the internode [63], we used the percentage of axonal area co-localizing with Caspr clusters as a readout of compaction. In comparison to Acvr1b$^{fl/fl}$ mice, the percentage of total axonal area (NF+) occupied by Caspr clusters was significantly lower in caudal corpus callosum of PDGFRa-Cre; Acvr1b$^{fl/fl}$ mice, indicative of a maintained deficiency in myelin compaction (Fig. 3i).

Given that myelin compaction requires actin disassembly [48, 66], the sufficiency of activin receptor signaling in accelerating actin depolymerization in oligodendrocyte membranes was assessed. Maturing wildtype oligodendrocytes were treated with activin-A, and non-depolymerized filamentous actin was detected using fluorescently conjugated Phalloidin, a method established in recent studies of actin dynamic-driven oligodendrocyte membrane compaction [48, 66]. Oligodendrocyte membranes in control conditions had high Phalloidin signal throughout MBP+ membranes at 5 days of in vitro maturation, indicative of non-depolymerized actin (average intensity/cell 38.3 ± 0.9 A.U.; Fig. 3j, k). Conversely, activin-A-treated oligodendrocyte membranes showed a reduced Phalloidin intensity, demonstrating increased actin depolymerization consequent to activin receptor signaling (average intensity/cell of 28.0 ± 0.5 A.U.; Fig. 3j, k).

To next test whether activin signaling regulates the total amount of myelin membrane made by oligodendrocytes, we first measured the average size of oligodendrocyte membranes in activin-A-treated cultures, yet found no difference to vehicle-treated cultures (Fig. 3k and Online Resource Supplemental Fig. 6a, b). We assessed the number and length of myelin sheaths formed by oligodendrocytes on poly-L-lactic acid microfibers, and also found no significant effect of activin-A treatment (Online Resource Supplemental Fig. 6c, d). Overall these results demonstrate that although activin receptor signaling does not increase the amount of membrane produced once an oligodendrocyte has differentiated, it has an important role in efficient oligodendrocyte membrane actin disassembly and myelin compaction.

Activin receptor subtype Acvr2a regulates oligodendrocyte differentiation and membrane actin disassembly

Having shown that signal transduction via the co-receptor Acvr1b is required for oligodendrocyte differentiation and membrane compaction, we next asked which ligand-binding activin receptor drives this effect. Activin-A can bind to two activin receptor subtypes, Acvr2a and Acvr2b; whether these have differential function or protein expression patterns in the CNS is unknown. We assessed Acvr2a and Acvr2b expression in the oligodendrocyte lineage during developmental myelination. Acvr2a expression in the cell bodies of Olig2+ cells was found to progressively increase over time while oligodendrocyte differentiation is underway (P1–P8), and was later also associated with myelin at the peak of myelination (P14) (Fig. 4a). We detected Acvr2a expression in both NG2+ immature cells and CC1+ mature oligodendrocytes (Fig. 4b). Data-mining of oligodendrocyte lineage single-cell transcriptomes in later development (P21–30; [41]; linnarssonlab.org/oligodendrocytes) confirmed sustained *Acvr2a* expression throughout the lineage, including in subsets of precursors and myelinating oligodendrocytes (Fig. 4c). Conversely, Acvr2b protein was not detectable at any time point in development (Fig. 4a), in contrast to the robust signal observed in positive control placental tissue (Online Resource Supplemental Fig. 7a) [56], and consistent with undetectable *Acvr2b* mRNA in the developing brain at the onset of myelination (Online Resource Supplemental Fig. 7b).

Given that Acvr2a is the receptor subtype expressed at the onset of differentiation and myelination, we next tested whether this receptor drives these responses by co-treating oligodendrocyte lineage cells with activin-A and an Acvr2a-specific neutralizing antibody, or an isotype IgG control. Protein blasting the epitope sequences for the Acvr2a antibody showed 100% specificity and selectivity for this receptor subtype. Blocking Acvr2a reversed the effects of activin-A on differentiation of OPCs into mature oligodendrocytes (MBP+) (Fig. 4d, e), and prevented activin-A-driven actin disassembly in oligodendrocytes (causing increased Phalloidin intensity in MBP+ membranes; Fig. 4f, g). Conversely, blocking Acvr2b had no significant effect on oligodendrocyte differentiation (Online Resource Supplemental Fig. 8a), although it did reduce activin-A-driven actin disassembly (Online Resource Supplemental Fig. 8b). Nevertheless, this data revealed that Acvr2a is the activin receptor subtype expressed by the oligodendrocyte lineage during developmental myelination and can drive activin-A-mediated oligodendrocyte differentiation and membrane actin disassembly.

To next determine which signaling pathways mediate Acvr2a-driven oligodendrocyte differentiation and membrane actin depolymerization, we assessed activation of

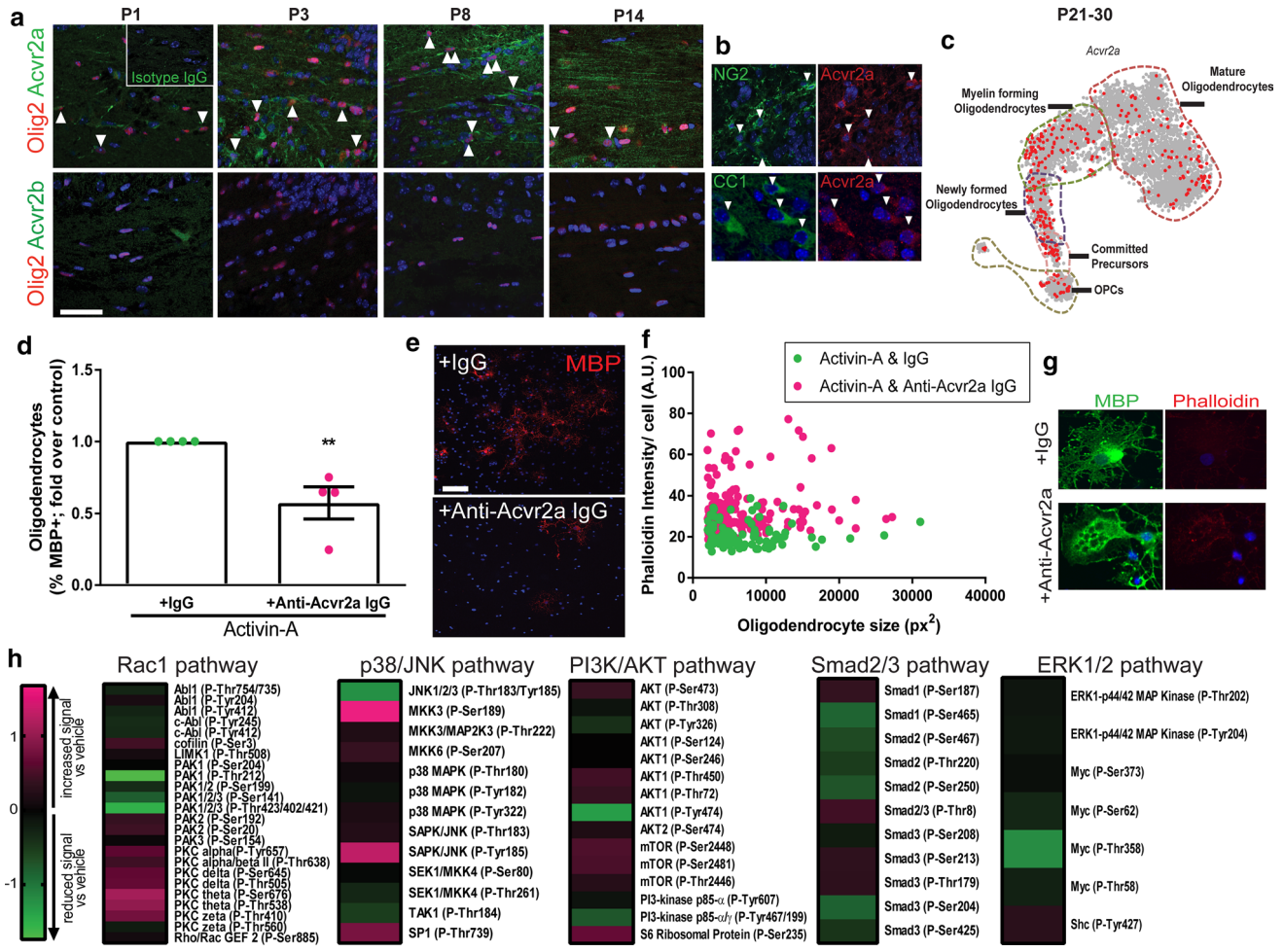

Fig. 4 Activin receptor Acvr2a regulates oligodendrocyte lineage cell behavior. **a** Acvr2a (top row; green) and Acvr2b (bottom row; green) expression by oligodendrocyte lineage (Olig2+; red) throughout development (P1–P14; double positive cells indicated by arrows), counterstained with Hoechst (blue). Inset; isotype control for Acvrs. Scale bar 50 µm. **b** Expression of Acvr2a (red) by NG2+ cells (green) (top row), and by CC1+ cells (green) (bottom row). **c** Data-mining of oligodendrocyte lineage cell transcriptomes from P21–30 for *Acvr2a* expression, represented as *t* distributed stochastic neighbor embedding projection. **d** OPCs co-treated with activin-A and neutralizing antibodies for Acvr2a or isotype IgG. Mean percentage of oligodendrocytes (MBP+) normalized to isotype control ± s.e.m. $n = 3$ biological replicates, two-tailed Student's *t* test, $P = 0.0087$. **e** Images of MBP+ cells (red) in cultures treated with activin-A (10 ng ml^{-1}) and isotype IgG or Acvr2a-neutralizing IgG. Scale bar 75 µm. **f** Phalloidin intensity signal (arbitrary units; AU) per oligodendrocyte plotted against oligodendrocyte size (px^2) in cultures co-treated with activin-A (10 ng ml^{-1}) and IgG control or neutralizing antibody against Acvr2a. $n = 3$ biological replicates. **g** Images of MBP+ oligodendrocytes (green) and filamentous actin (Phalloidin+; red) in cultures treated with activin-A and IgG or Acvr2a neutralizing antibody. **h** Log2-transformed phosphorylation signal of TGFβ superfamily pathways following treatment with activin-A, normalized to respective total protein signal then to vehicle control. Heat map: compared to vehicle, magenta indicates increased signal, black no change, and green reduced signal

the 5 TGFβ signaling pathways induced downstream of activin receptors (Rac1 GTPase, p38 MAPK/JNK, PI3K/AKT, Smad2/3, ERK1/2,) which are also associated with regulation of oligodendroglial lineage responses and myelination [4, 27, 29, 47, 61]. Activation of all pathways in activin-A-stimulated oligodendroglial lineage cells was simultaneously assessed by measuring phosphorylation levels of signaling proteins using a forward-phase antibody microarray; phosphorylation signal was normalized to respective total protein signal, and values then normalized to vehicle control. We found that activin-A increased phosphorylation signal in all pathways, with the highest increase in signal observed in the Rac1 GTPase and p38/MAPK pathways (Fig. 4h). Taken together with our findings, these results are consistent with known roles for the Rac1 GTPase and p38 MAPK pathways in regulating oligodendrocyte differentiation, myelination, and myelin compaction [11, 13, 19, 25, 29, 61].

Activin receptor signaling regulates remyelination

Having shown the role of activin receptor signaling in developmental myelination, we next asked whether it is also relevant to regeneration of myelin following injury. Our previous work showed that at the onset of remyelination, activin-A levels increase and activin receptors are expressed by OPCs [45]. To examine whether this expression has functional significance for remyelination, we used activin-A to stimulate activin receptors during remyelination of ex vivo organotypic cerebellar brain explants which were demyelinated with lysolecithin. Activin-A significantly increased remyelination at 7 days post lysolecithin (dpl) compared to vehicle control, as measured by remyelination index (co-localization of myelin basic protein (MBP) and axonal neurofilament, normalized to area of neurofilament) [63, 65] (Fig. 5a, b). Due to remyelination subsequently occurring efficiently in controls, no significant differences between vehicle and activin-A-treated explants were observed at later time points (10, 14 dpl) (Fig. 5b). These data demonstrate that activin receptor stimulation is sufficient to accelerate remyelination. To determine whether activin receptor signaling is required for remyelination, demyelinated cerebellar explants were treated with an inhibitor of activin receptors, inhibin-A, which competitively binds these receptors to prevent endogenous ligand binding [42]. Remyelination was significantly repressed by inhibin-A treatment at 7, 10 and 14 dpl compared to vehicle control (Fig. 5c, d), demonstrating for the first time that activin receptor signaling is required for remyelination.

To assess activin receptor subtype expression during efficient remyelination, we took advantage of the temporally discrete OPC responses occurring following focal demyelinated lesion induction of the caudal cerebellar peduncles. At the time of initiation of oligodendrocyte differentiation and remyelination (10 dpl), Acvr2b levels decreased and Acvr2a levels concomitantly increased (Fig. 5e, g); these changes in expression were confirmed to occur in oligodendroglial lineage cells (NG2+, Olig2+; Fig. 5f). Non-lesioned CCP had no Acvr2b signal, confirming the absence of its expression in healthy adult white matter (Fig. 5h). Thus, in contrast to the absence of Acvr2b expression during development or homeostasis, its transient induction after demyelination is an early response to injury, which is followed by a transition to Acvr2a expression during efficient remyelination.

Activin receptor expression is dysregulated in non-repairing lesions in human myelin disorders

In light of our results showing that activin receptor signaling regulates developmental myelination and remyelination, and that activin receptor subtype expression by oligodendroglial lineage cells is strictly controlled following injury, we predicted that dysregulation of activin receptor expression may underpin chronic failure of oligodendrocyte differentiation and myelin formation in human disorders [10, 38]. We first investigated brain tissue from perinatal brain injury cases (Online Resource Supplemental Table 1) and compared areas of normally developing white matter (low microglia density: average 10 ± 10 cells/mm^2) to areas of injury (high microglia density: average 122 ± 30 cells/mm^2) (Online Resource Supplemental Fig. 9a–c). We observed increased densities of cells positive for the activin-A subunit INHBA in the brain parenchyma in injured vs. non-injured areas (Fig. 6a, b), consistent with previously reported elevated INHBA in the cerebrospinal fluid following perinatal brain injury [23]. However, injured areas had lower densities of oligodendroglial cells (Olig2+) expressing Acvr2a, and higher densities of those expressing Acvr2b (Fig. 6d), compared to non-injured areas. This was not associated with a normal regenerative response to injury, as proliferating oligodendroglial lineage cells (PCNA+ Olig2+) were not increased relative to in non-injured regions (Fig. 6e).

We next examined adult progressive MS brain lesions with four types of pathology displaying a range of remyelination potential: lesions with completed remyelination ('remyelinated'), ongoing damage and active remyelination ('acute active', rim of 'chronic active'), and little to no remyelination ('chronic inactive') (Online Resource Supplemental Table 2, Online Resource Supplemental Fig. 9d–f). Activin-A (INHBA)+ cells were present in lesions regardless of pathology, yet densities were significantly increased in acute active lesions (Fig. 6f, g) consistent with increased INHBA detected in cerebrospinal fluid following recent adult brain injury [52]. Within actively remyelinating lesions (acute active and chronic active lesions), the proportion of Olig2+ cells that were Acvr2a+ was higher than the proportion that were Acvr2b+ (Fig. 6h). However, the proportion of Acvr2b+ Olig2+ cells was significantly increased in chronic inactive lesions (Fig. 6h), the lesions with the lowest remyelination potential. Thus, a common feature of lesions with limited oligodendrocyte differentiation and myelin generation in both developmental and adult disorders was an increase in Acvr2b+ oligodendroglial lineage cells. Both the increase in Acvr2b expression and its relatively higher affinity for activin-A [5] would be predicted to sequester the ligand thereby restricting Acvr2a-mediated signaling in oligodendrocyte lineage cells.

To test this hypothesis, Acvr2b was overexpressed in oligodendrocyte lineage cells via lentiviral delivery of a construct driving expression of Acvr2b along with a membrane-tagged green fluorescent protein (GFP) (Acvr2b-LV), and using a lentivirus driving GFP expression only as a control (control-LV). Successful transfection of OPCs at 3 days of exposure was confirmed by detection of GFP expression in 99% of cells (Fig. 6k). Compared to control-LV conditions,

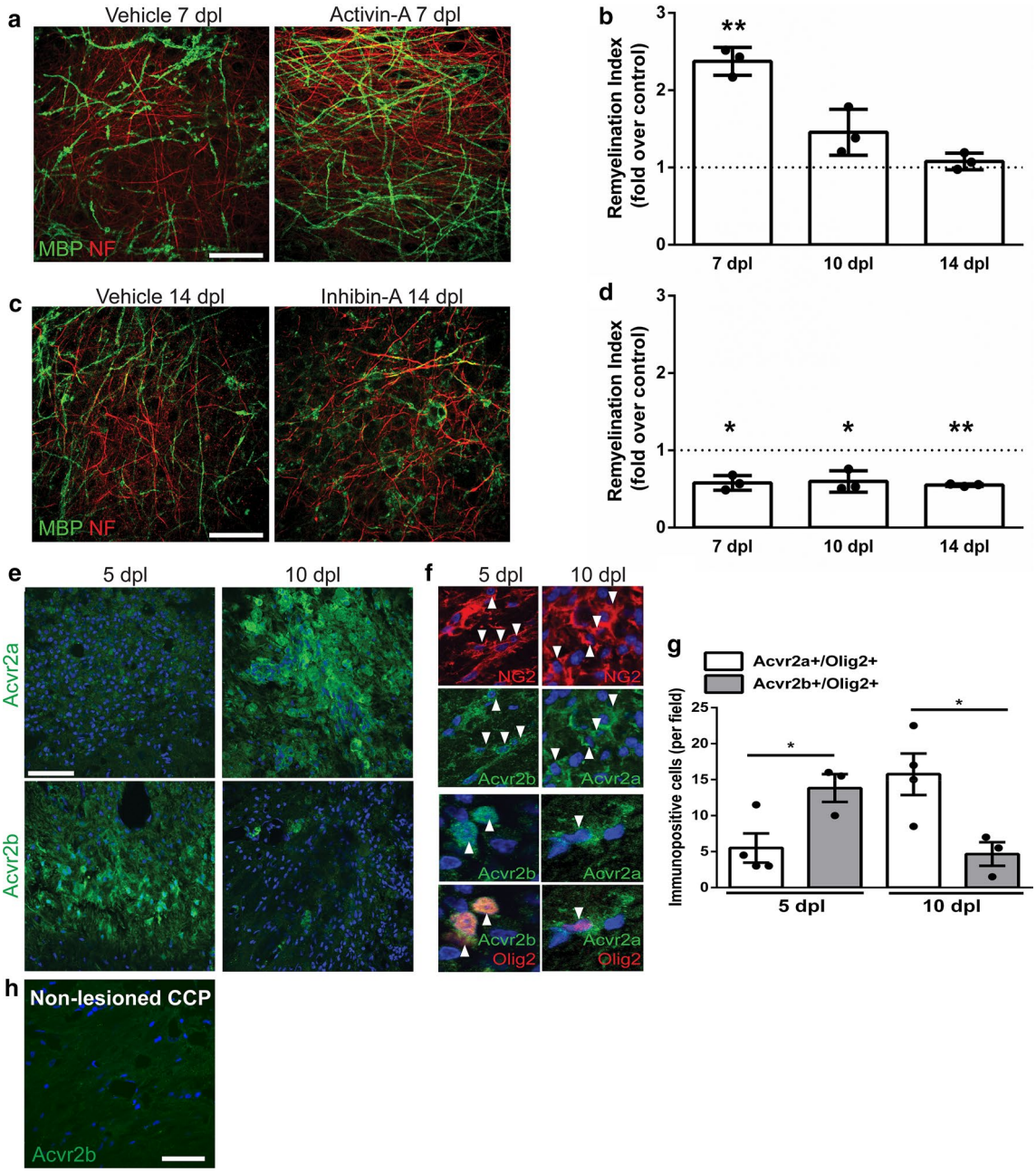

Fig. 5 Activin receptor signaling regulates remyelination. **a** Representative images of organotypic cerebellar slice cultures at 7 days post lysolecithin-induced demyelination, treated with vehicle control or activin receptor agonist activin-A during remyelination, immunostained against myelin basic protein (MBP; green), and axonal neurofilament-H (NF; red). Scale bar 50 µm. **b** Mean remyelination index ± s.e.m. in activin-A-treated explants at 7, 10, and 14 days post lysolecithin (dpl) normalized to vehicle control from the respective time point. $n = 3$ animals, one-sample t test compared to theoretical mean of 1 (control), $^{**}P = 0.0057$. **c** Representative images of slice cultures at 14 dpl treated with vehicle control or an inhibitor of activin receptor signaling inhibin-A during remyelination, immunostained against myelin basic protein (MBP; green) and axonal neurofilament-H (NF; red). Scale bar 50 µm. **d** Mean remyelination index ± s.e.m. in inhibin-A-treated explants at 7, 10, and 14 dpl normalized to vehicle control from the respective time point. $n = 3$ animals, one-sample t test compared to theoretical mean of 1 (control), $^{*}P = 0.0165$, *0.0374, **0.0004, respectively. **e** Acvr2a and Acvr2b expression (green) in demyelinated caudal cerebellar peduncles (CCP) at 5 days post-lesion (dpl; prior to remyelination) and 10 dpl (onset of remyelination), counterstained with Hoechst (blue). Scale bar 25 µm. **f** Colocalization of Acvr2b or Acvr2a (green) with NG2 (top 2 rows; red; arrowheads) or Olig2 (bottom 2 rows; red; arrowheads) at 5 and 10 dpl in CCP, counterstained with Hoechst (blue). **g** Mean number of cells double positive for Olig2 and Acvr2a or Acvr2b per field ± s.e.m. at 5 and 10 dpl. $n = 3 = 4$ animals per group. Two-tailed Student's t test, $P = 0.0345$ (5 dpl), 0.0298 (10 dpl). **h** Non-lesioned CCP shows no staining of Acvr2b (green). Scale bar 10 µm

overexpression of Acvr2b significantly impaired both activin-A-driven OPC differentiation into mature MBP+ oligodendrocytes (Fig. 6j, k) and actin depolymerization in maturing oligodendrocyte membranes (causing an increase in Phalloidin intensity per cell; Fig. 6l, m). These experiments confirm that increased expression of Acvr2b by oligodendroglial lineage cells impairs ligand-driven oligodendrocyte differentiation and actin dynamics involved in myelin compaction.

Discussion

In this study, we reveal the role of activin receptor signaling in CNS myelin generation during healthy development and following injury. Using a conditional knockout approach, in vitro manipulation of oligodendrocyte lineage cells, ex vivo/in vivo modeling of remyelination, and human post-mortem brain tissue analysis, we uncover the requirement for activin receptor signaling in driving timely oligodendrocyte differentiation and myelin compaction, and its dysregulation in disease (summarized in Fig. 6n). These findings go beyond previous studies showing that activin receptor stimulation is protective for neurons [22, 30, 55], by demonstrating a direct and disease-relevant role in oligodendrocyte lineage cells. Our results also extend the functions of the TGFβ superfamily beyond supporting oligodendrocyte differentiation [19, 49] to now include regulation of myelin compaction and an appropriate response to white matter injury in human disease.

We eliminated all activin receptor responses in the oligodendroglial lineage by conditionally knocking out the co-receptor *Acvr1b* at the OPC stage, which would prevent all downstream signaling subsequent to ligand binding to activin receptors Acvr2a or Acvr2b. By postnatal day 16, this caused a 60% reduction in the number of myelinated axons, particularly those of intermediate caliber. This finding reveals that there are activin receptor-dependent and -independent mechanisms driving axonal ensheathment with myelin membrane. This may be regulated by differential expression of activin receptor ligands across axon calibers, as experimental augmentation of axon caliber to support myelination is associated with increased expression of the activin-A subunit [28]. Myelination may also be regulated by heterogeneity of activin receptor expression in oligodendroglial lineage cells, as our data-mining of a single-cell RNA sequencing dataset [41] showed that only a subset of cells express Acvr2a at each stage of oligodendrocyte maturation.

The hypomyelination in activin receptor conditional knockout mice was associated with reduced numbers of maturing oligodendrocytes, showing the requirement for activin receptor signaling in the differentiation of a significant subset of oligodendroglial lineage cells. Importantly, activin receptor stimulation of wildtype OPCs (with activin-A) was sufficient to enhance oligodendrocyte differentiation, even in the presence of proliferation-stimulating growth factors. Although in the knockout some myelinating oligodendrocytes were still generated, these cells demonstrated impaired myelin membrane compaction, as evidenced by a persistent enlargement of the inner tongue, thinner layers of compact myelin, and myelin sheaths devoid of the compaction-inducing protein MBP. In addition, stimulation of activin receptors on wildtype maturing oligodendrocytes enhanced depolymerization of actin in membranes, a process required for myelin membrane compaction [48, 66]. Thus, we established that activin receptor signaling regulates myelination by driving oligodendrocyte differentiation and myelin membrane compaction, which to our knowledge is the first time a receptor axis has been directly linked to both processes.

These effects were found to be mediated by the ligand-binding activin receptor subtype Acvr2a, as its neutralization in wildtype cells eliminated activin-A-driven oligodendrocyte differentiation and membrane actin depolymerization. Accordingly, we showed that Acvr2a expression on oligodendroglial lineage cells in vivo coincides with oligodendrocyte differentiation and myelin generation during development and following injury. At the onset of successful remyelination, there was a concomitant downregulation of Acvr2b. Acvr2b has relatively higher affinity for activin-A compared to Acvr2a [5], and importantly its overexpression was found to impair activin-A-induced oligodendrocyte differentiation and membrane actin depolymerization. Thus, the downregulation of Acvr2b after injury may allow Acvr2a to bind ligand more readily to drive oligodendroglial lineage responses and initiate repair.

Following CNS injury, the rapid increase in expression of activin-A [1, 23, 43, 62] likely represents an attempt at repair, supported by our previous observation of increased activin-A subunit expression in focal demyelinated lesions at the onset of remyelination [45]. However, activin-A (INHBA)+ cells were found to be present in both repairing and non-repairing regions of damaged human white matter, indicating that following injury oligodendrocyte lineage cell responses are likely not regulated by activin-A, but rather by activin receptors. Indeed, regions that were actively myelinating (in perinatal tissue) or remyelinating (in multiple sclerosis lesions) demonstrated relatively higher densities of oligodendroglial lineage cells expressing Acvr2a compared to those expressing Acvr2b. However, an increase in Acvr2b+ oligodendroglial lineage cells was observed in non-repairing white matter (injured regions following perinatal brain injury, and chronic inactive multiple sclerosis lesions), which would be predicted to sequester ligand and consequently impair Acvr2a-regulated oligodendrocyte differentiation and myelin formation. Consistent with this

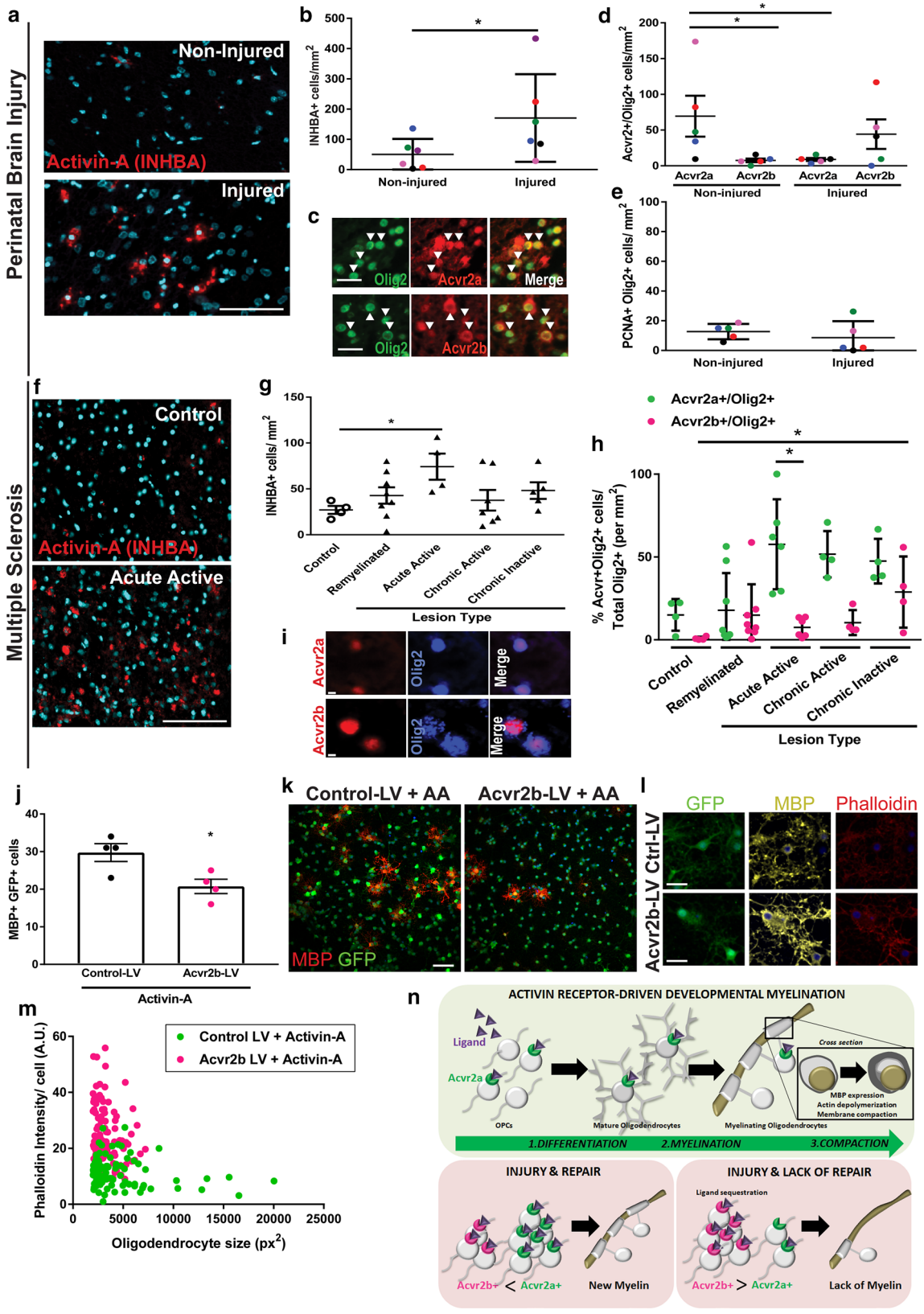
a
Perinatal Brain Injury
Non-Injured
Activin-A (INHBA)
Injured
b
INHBA+ cells/mm2
Non-injured
Injured
c
Olig2
Acvr2a
Merge
Olig2
Acvr2b
d
Acvr2+/Olig2+ cells/mm2
Acvr2a
Acvr2b
Acvr2a
Acvr2b
Non-injured
Injured
e
PCNA+ Olig2+ cells/ mm2
Non-injured
Injured
f
Multiple Sclerosis
Control
Activin-A (INHBA)
Acute Active
g
INHBA+ cells/ mm2
Control
Remyelinated
Acute Active
Chronic Active
Chronic Inactive
Lesion Type
h
Acvr2a+/Olig2+
Acvr2b+/Olig2+
% Acvr+Olig2+ cells/ Total Olig2+ (per mm2)
Control
Remyelinated
Acute Active
Chronic Active
Chronic Inactive
Lesion Type
i
Acvr2a
Acvr2b
Olig2
Merge
j
MBP+ GFP+ cells
Control-LV
Acvr2b-LV
Activin-A
k
Control-LV + AA
Acvr2b-LV + AA
MBP GFP
l
GFP
MBP
Phalloidin
Acvr2b-LV
Ctrl-LV
m
Control LV + Activin-A
Acvr2b LV + Activin-A
Phalloidin Intensity/ cell (A.U.)
Oligodendrocyte size (px2)
n
ACTIVIN RECEPTOR-DRIVEN DEVELOPMENTAL MYELINATION
Ligand
Acvr2a
Cross section
MBP expression
Actin depolymerization
Membrane compaction
OPCs
Mature Oligodendrocytes
Myelinating Oligodendrocytes
1.DIFFERENTIATION
2.MYELINATION
3.COMPACTION
INJURY & REPAIR
Acvr2b+ < Acvr2a+
New Myelin
INJURY & LACK OF REPAIR
Ligand sequestration
Acvr2b+ > Acvr2a+
Lack of Myelin

Fig. 6 Activin receptor expression dysregulation in developmental and adult human myelin disorders. **a** Images of activin-A subunit (INHBA; red) immunostaining in non-injured and injured developing white matter in a case of perinatal brain injury, counterstained with Hoechst (turquoise). Scale bar 25 µm. **b** Mean densities of INHBA+ cells ± s.e.m. per mm^2 in non-injured and injured developing white matter in perinatal brain injury. $n = 5$ cases (Table S1); each patient block is represented by different color. Mann–Whitney test, $^*P = 0.0411$. **c** Images of oligodendrocyte lineage cells (Olig2+; green) expressing Acvr2a or Acvr2b (red) in developing white matter, indicated by arrowheads. Scale bar 25 µm. **d** Densities of Acvr2a+ Olig2+ and Acvr2b+ Olig2+ cells per mm^2 in non-injured versus injured areas of developing white matter. $n = 5$ cases; each patient block is represented by different color. Mann–Whitney test, $^*P = 0.0238$ (non-injured Acvr2a+ Olig2+ vs Acvr2b+ Olig2+), $^*P = 0.0317$ (non-injured Acvr2a+ Olig2+ vs injured Acvr2a+ Olig2+). **e** Densities of PCNA+ Olig2+ proliferating oligodendrocyte lineage cells per mm^2 in non-injured vs injured areas of developing white matter. $n = 5$ cases; each patient block represented by different color. **f** Images of INHBA+ cells (red) in control and acute active multiple sclerosis (MS) lesion tissue, counterstained with Hoechst (turquoise). Scale bar 100 µm. **g** Mean densities of INHBA+ cells per mm^2 in post-mortem brain tissue from healthy control, or MS lesions (remyelinated, acute active, chronic active (rim), chronic inactive). *n* for each lesion type indicated in Table S2. Mann–Whitney test, $^*P = 0.0286$. **h** Proportion of Acvr2a+ Olig2+ or Acvr2b+ Olig2+ from total Olig2+ cells in healthy control tissue or MS lesions (remyelinated, acute active, chronic active (rim), chronic inactive). *n* for each lesion type indicated in Table S2. Kruskal–Wallis test and Dunn's multiple comparison test, $^*p < 0.05$. **i** Acvr2a+ (top row; red) or Acvr2b+ (bottom row; red) and Olig2+ (blue) double positive cells in MS lesions. Scale bar 5 µm. **j** Quantification of differentiation of OPCs into mature oligodendrocytes (MBP+; per field) following transfection with lentivirus (GFP+), either control (control-LV) or Acvr2b-expressing (Acvr2b-LV), and treated with activin-A (10 ng ml^{-1}) for 3 days. $^*P = 0.0247$, two-tailed Student's *t* test. **k** Representative images of OPC cultures treated with activin-A and Control-LV or Acvr2b-LV for 3 days immunostained for MBP (red) and GFP (green). Scale bar 50 µm. **l** Representative images of maturing oligodendrocytes transfected with Control-LV or Acv2b-LV for 3 days and treated with activin-A (10 ng ml^{-1}) for 5 days, stained for GFP (green), MBP (false colored yellow), and Phalloidin (red). Scale bar 20 µm. **m** Phalloidin intensity signal (arbitrary units; AU) per MBP+ transfected (GFP+) oligodendrocyte plotted against oligodendrocyte size (px^2) in cultures co-treated with activin-A (10 ng ml^{-1}) and Control-LV or Acvr2b-LV. **n** Model for role of activin receptor signaling in oligodendrocyte lineage cells. Acvr2a is expressed during developmental myelination, inducing oligodendrocyte differentiation, myelination, and myelin membrane compaction. Following injury, successful repair involves a transition in expression from Acvr2b to Acvr2a to support new myelin formation. In myelin disorders, failed repair is associated with an upregulation of Acvr2b, impairing Acvr2a-driven responses, leading to lack of myein

postulate, increased levels of *Acvr2b* mRNA in umbilical cord blood at birth is associated with more severe clinical outcome in infants following hypoxic-ischemic perinatal brain injury [40].

Oligodendrocyte differentiation, myelination, and remyelination have also been associated with activation of other receptors, such as endothelin receptor B [63], RXRγ [31], and CXCR4 [50]. As we observed both activin receptor-dependent and -independent oligodendrocyte differentiation in vivo, this suggests that complementary pathways likely coordinate oligodendroglial lineage responses in parallel. This may involve distinct subsets of oligodendroglial lineage cells preferentially expressing specific receptors; indeed data-mining of a single-cell RNAseq database confirms distinct expression patterns of the abovementioned receptors within the oligodendrocyte lineage [41] (data not shown). An alternate mechanism may involve context-dependent availability of ligand; for example, we have previously demonstrated dynamic changes in activin-A protein levels during the course of remyelination [45]. Here, we provide the first evidence for a receptor axis that is dysregulated in both myelin disorders of development (perinatal brain injury) and adulthood (MS), despite having distinct etiologies. These disorders also share dysregulation of an intracellular signaling cascade, the Wnt/β-catenin pathway [20, 21], which may further antagonize Acvr2a signaling via upregulation of an inhibitor of activin-A (follistatin) [35] and a pseudoreceptor acting as a dominant negative Acvr1b (BAMBI) [59]. Whereas other members of the TGFβ superfamily (e.g. bone morphogenic proteins) have recently been shown to impair remyelination via signaling through distinct receptors (BMPR1, Acvr1a) and pathways (Smad1/5/8) [51], our data demonstrate the pro-myelination/remyelination properties of the TGFβ superfamily via activin receptor signaling. Thus, we propose that therapies specifically restoring Acvr2a-mediated signaling in oligodendroglial lineage cells could represent a novel strategy to enhance differentiation and myelin generation following CNS injury across the lifespan.

Acknowledgements We thank the United Kingdom Multiple Sclerosis Society Tissue Bank for providing MS tissue, the Medical Research Council Edinburgh Brain and Tissue Bank for providing perinatal brain injury tissue, Dr. F. Roncaroli (Imperial College London) for neuropathological diagnosis of MS lesions, and Dr. R. Nicholas (Imperial College London) for providing clinical history of MS patients. Placental control tissue was kindly provided by Prof. Simon Riley (The University of Edinburgh). Antibody microarray scanning service was provided by Edinburgh Genomics (The University of Edinburgh). We also thank Amanda Boyd, Lida Zoupi, Corrie Watkins, and Becky Price for technical assistance. We thank Charles ffrench-Constant, Robin J.M. Franklin, and David A. Lyons for helpful discussions. The authors have no conflict of interest to declare.

Author contributions VEM conceived the project; AD, GI, CD, RKH, FE, MS, MEB, and VEM designed and performed experiments, acquired and analyzed data; TJY performed focal in vivo lesioning; DS assisted in image analysis protocols; GS generated the Acvr1b floxed mice; CS and J-CB performed neuropathological selection of perinatal brain tissue; CS assisted in neuropathological interpretation of human tissue; AW characterized MS tissue; AD, GI, and VEM made the figures; AD, GI, MEB, TY, AW edited the manuscript; VEM wrote the manuscript.

Funding This work was funded by a Medical Research Council and United Kingdom Multiple Sclerosis Society Career Development Award (V.E.M.; MR/M020827/1), a grant from Action Medical Research (V.E.M.; GN2318), a PhD studentship from the

Commonwealth Scholarship Commission in the United Kingdom (A.D.), and funds from the Medical Research Council Center for Reproductive Health (MR/N02256/1).

Compliance with ethical standards

Conflict of interest The authors have nothing to declare.

Animal studies All applicable international, national, and/or institutional guidelines for the care and use of animals were followed. All experiments were carried out in accordance with ethical standards of the institution or practice at which the studies were conducted.

Human tissue All tissue used in the study was obtained from tissue banks where informed consent by the patient and/or their families was given.

References

1. Abdipranoto-Cowley A, Park JS, Croucher D, Daniel J, Henshall S, Galbraith S, Mervin K, Vissel B (2009) Activin A is essential for neurogenesis following neurodegeneration. Stem cells 27:1330–1346. https://doi.org/10.1002/stem.80
2. Aggarwal S, Snaidero N, Pahler G, Frey S, Sanchez P, Zweckstetter M, Janshoff A, Schneider A, Weil MT, Schaap IA et al (2013) Myelin membrane assembly is driven by a phase transition of myelin basic proteins into a cohesive protein meshwork. PLoS Biol 11:e1001577. https://doi.org/10.1371/journal.pbio.1001577
3. Aggarwal S, Yurlova L, Snaidero N, Reetz C, Frey S, Zimmermann J, Pahler G, Janshoff A, Friedrichs J, Muller DJ et al (2011) A size barrier limits protein diffusion at the cell surface to generate lipid-rich myelin-membrane sheets. Dev Cell 21:445–456. https://doi.org/10.1016/j.devcel.2011.08.001
4. Atanasoski S, Notterpek L, Lee HY, Castagner F, Young P, Ehrengruber MU, Meijer D, Sommer L, Stavnezer E, Colmenares C et al (2004) The protooncogene Ski controls Schwann cell proliferation and myelination. Neuron 43:499–511. https://doi.org/10.1016/j.neuron.2004.08.001
5. Attisano L, Wrana JL, Cheifetz S, Massague J (1992) Novel activin receptors: distinct genes and alternative mRNA splicing generate a repertoire of serine/threonine kinase receptors. Cell 68:97–108
6. Attisano L, Wrana JL, Montalvo E, Massague J (1996) Activation of signalling by the activin receptor complex. Mol Cell Biol 16:1066–1073
7. Bechler ME, Byrne L, Ffrench-Constant C (2015) CNS myelin sheath lengths are an intrinsic property of oligodendrocytes. Curr Biol 25:2411–2416. https://doi.org/10.1016/j.cub.2015.07.056
8. Billiards SS, Haynes RL, Folkerth RD, Borenstein NS, Trachtenberg FL, Rowitch DH, Ligon KL, Volpe JJ, Kinney HC (2008) Myelin abnormalities without oligodendrocyte loss in periventricular leukomalacia. Brain Pathol 18:153–163. https://doi.org/10.1111/j.1750-3639.2007.00107.x
9. Billings-Gagliardi S, Nunnari JN, Nadon NL, Wolf MK (1999) Evidence that CNS hypomyelination does not cause death of jimpy-msd mutant mice. Dev Neurosci 21:473–482 **(17414)**
10. Buser JR, Maire J, Riddle A, Gong X, Nguyen T, Nelson K, Luo NL, Ren J, Struve J, Sherman LS et al (2012) Arrested preoligodendrocyte maturation contributes to myelination failure in premature infants. Ann Neurol 71:93–109. https://doi.org/10.1002/ana.22627
11. Chew LJ, Coley W, Cheng Y, Gallo V (2010) Mechanisms of regulation of oligodendrocyte development by p38 mitogen-activated protein kinase. J Neurosci 30:11011–11027. https://doi.org/10.1523/JNEUROSCI.2546-10.2010
12. Chiba K, Kataoka H, Seki N, Shimano K, Koyama M, Fukunari A, Sugahara K, Sugita T (2011) Fingolimod (FTY720), sphingosine 1-phosphate receptor modulator, shows superior efficacy as compared with interferon-beta in mouse experimental autoimmune encephalomyelitis. Int Immunopharmacol 11:366–372. https://doi.org/10.1016/j.intimp.2010.10.005
13. Chung SH, Biswas S, Selvaraj V, Liu XB, Sohn J, Jiang P, Chen C, Chmilewsky F, Marzban H, Horiuchi M et al (2015) The p38alpha mitogen-activated protein kinase is a key regulator of myelination and remyelination in the CNS. Cell Death Dis 6:e1748. https://doi.org/10.1038/cddis.2015.119
14. Craner MJ, Lo AC, Black JA, Waxman SG (2003) Abnormal sodium channel distribution in optic nerve axons in a model of inflammatory demyelination. Brain 126:1552–1561. https://doi.org/10.1093/brain/awg153
15. Csiza CK, de Lahunta A (1979) Myelin deficiency (md): a neurologic mutant in the Wistar rat. Am J Pathol 95:215–224
16. Duncan ID, Brower A, Kondo Y, Curlee JF Jr, Schultz RD (2009) Extensive remyelination of the CNS leads to functional recovery. Proc Natl Acad Sci USA 106:6832–6836. https://doi.org/10.1073/pnas.0812500106
17. Duncan ID, Kondo Y, Zhang SC (2011) The myelin mutants as models to study myelin repair in the leukodystrophies. Neurotherapeutics 8:607–624. https://doi.org/10.1007/s13311-011-0080-y
18. Duncan ID, Nadon NL, Hoffman RL, Lunn KF, Csiza C, Wells MR (1995) Oligodendrocyte survival and function in the long-lived strain of the myelin deficient rat. J Neurocytol 24:745–762
19. Dutta DJ, Zameer A, Mariani JN, Zhang J, Asp L, Huynh J, Mahase S, Laitman BM, Argaw AT, Mitiku N et al (2014) Combinatorial actions of Tgfbeta and Activin ligands promote oligodendrocyte development and CNS myelination. Development 141:2414–2428. https://doi.org/10.1242/dev.106492
20. Fancy SP, Baranzini SE, Zhao C, Yuk DI, Irvine KA, Kaing S, Sanai N, Franklin RJ, Rowitch DH (2009) Dysregulation of the Wnt pathway inhibits timely myelination and remyelination in the mammalian CNS. Genes Dev 23:1571–1585. https://doi.org/10.1101/gad.1806309
21. Fancy SP, Harrington EP, Yuen TJ, Silbereis JC, Zhao C, Baranzini SE, Bruce CC, Otero JJ, Huang EJ, Nusse R et al (2011) Axin2 as regulatory and therapeutic target in newborn brain injury and remyelination. Nat Neurosci 14:1009–1016. https://doi.org/10.1038/nn.2855
22. Fang L, Wang YN, Cui XL, Fang SY, Ge JY, Sun Y, Liu ZH (2012) The role and mechanism of action of activin A in neurite outgrowth of chicken embryonic dorsal root ganglia. J Cell Sci 125:1500–1507. https://doi.org/10.1242/jcs.094151
23. Florio P, Luisi S, Bruschettini M, Grutzfeld D, Dobrzanska A, Bruschettini P, Petraglia F, Gazzolo D (2004) Cerebrospinal fluid activin a measurement in asphyxiated full-term newborns predicts hypoxic ischemic encephalopathy. Clin Chem 50:2386–2389. https://doi.org/10.1373/clinchem.2004.035774

24. Foran DR, Peterson AC (1992) Myelin acquisition in the central nervous system of the mouse revealed by an MBP-Lac Z transgene. J Neurosci 12:4890–4897
25. Fragoso G, Haines JD, Roberston J, Pedraza L, Mushynski WE, Almazan G (2007) p38 mitogen-activated protein kinase is required for central nervous system myelination. Glia 55:1531–1541. https://doi.org/10.1002/glia.20567
26. Funfschilling U, Supplie LM, Mahad D, Boretius S, Saab AS, Edgar J, Brinkmann BG, Kassmann CM, Tzvetanova ID, Mobius W et al (2012) Glycolytic oligodendrocytes maintain myelin and long-term axonal integrity. Nature 485:517–521. https://doi.org/10.1038/nature11007
27. Fyffe-Maricich SL, Karlo JC, Landreth GE, Miller RH (2011) The ERK2 mitogen-activated protein kinase regulates the timing of oligodendrocyte differentiation. J Neurosci 31:843–850. https://doi.org/10.1523/JNEUROSCI.3239-10.2011
28. Goebbels S, Wieser GL, Pieper A, Spitzer S, Weege B, Yan K, Edgar JM, Yagensky O, Wichert SP, Agarwal A et al (2017) A neuronal PI(3,4,5)P3-dependent program of oligodendrocyte precursor recruitment and myelination. Nat Neurosci 20:10–15. https://doi.org/10.1038/nn.4425
29. Haines JD, Fragoso G, Hossain S, Mushynski WE, Almazan G (2008) p38 Mitogen-activated protein kinase regulates myelination. J Mol Neurosci 35:23–33. https://doi.org/10.1007/s12031-007-9011-0
30. He JT, Mang J, Mei CL, Yang L, Wang JQ, Xing Y, Yang H, Xu ZX (2012) Neuroprotective effects of exogenous activin A on oxygen-glucose deprivation in PC12 cells. Molecules 17:315–327. https://doi.org/10.3390/molecules17010315
31. Huang JK, Jarjour AA, Nait Oumesmar B, Kerninon C, Williams A, Krezel W, Kagechika H, Bauer J, Zhao C, Baron-Van Evercooren A et al (2011) Retinoid X receptor gamma signaling accelerates CNS remyelination. Nat Neurosci 14:45–53. https://doi.org/10.1038/nn.2702
32. Irvine KA, Blakemore WF (2008) Remyelination protects axons from demyelination-associated axon degeneration. Brain 131:1464–1477. https://doi.org/10.1093/brain/awn080
33. Jablonska B, Scafidi J, Aguirre A, Vaccarino F, Nguyen V, Borok E, Horvath TL, Rowitch DH, Gallo V (2012) Oligodendrocyte regeneration after neonatal hypoxia requires FoxO1-mediated p27Kip1 expression. J Neurosci 32:14775–14793. https://doi.org/10.1523/JNEUROSCI.2060-12.2012
34. Jackson KF, Duncan ID (1988) Cell kinetics and cell death in the optic nerve of the myelin deficient rat. J Neurocytol 17:657–670
35. Jones AE, Price FD, Le Grand F, Soleimani VD, Dick SA, Megeney LA, Rudnicki MA (2015) Wnt/beta-catenin controls follistatin signalling to regulate satellite cell myogenic potential. Skelet Muscle 5:14. https://doi.org/10.1186/s13395-015-0038-6
36. Khwaja O, Volpe JJ (2008) Pathogenesis of cerebral white matter injury of prematurity. Arch Dis Child Fetal Neonatal Ed 93:F153–F161. https://doi.org/10.1136/adc.2006.108837
37. Kornek B, Storch MK, Weissert R, Wallstroem E, Stefferl A, Olsson T, Linington C, Schmidbauer M, Lassmann H (2000) Multiple sclerosis and chronic autoimmune encephalomyelitis: a comparative quantitative study of axonal injury in active, inactive, and remyelinated lesions. Am J Pathol 157:267–276. https://doi.org/10.1016/S0002-9440(10)64537-3
38. Kuhlmann T, Miron V, Cui Q, Wegner C, Antel J, Bruck W (2008) Differentiation block of oligodendroglial progenitor cells as a cause for remyelination failure in chronic multiple sclerosis. Brain 131:1749–1758. https://doi.org/10.1093/brain/awn096
39. Lindsay SJ, Xu Y, Lisgo SN, Harkin LF, Copp AJ, Gerrelli D, Clowry GJ, Talbot A, Keogh MJ, Coxhead J et al (2016) HDBR expression: a unique resource for global and individual gene expression studies during early human brain development. Front Neuroanat 10:86. https://doi.org/10.3389/fnana.2016.00086
40. Looney AM, Ahearne CE, Hallberg B, Boylan GB, Murray DM (2016) Downstream mRNA target analysis in neonatal hypoxic-ischaemic encephalopathy identifies novel marker of severe injury: a proof of concept paper. Mol Neurobiol. https://doi.org/10.1007/s12035-016-0330-4
41. Marques S, Zeisel A, Codeluppi S, van Bruggen D, Mendanha Falcao A, Xiao L, Li H, Haring M, Hochgerner H, Romanov RA et al (2016) Oligodendrocyte heterogeneity in the mouse juvenile and adult central nervous system. Science 352:1326–1329. https://doi.org/10.1126/science.aaf6463
42. Martens JW, de Winter JP, Timmerman MA, McLuskey A, van Schaik RH, Themmen AP, de Jong FH (1997) Inhibin interferes with activin signaling at the level of the activin receptor complex in Chinese hamster ovary cells. Endocrinology 138:2928–2936. https://doi.org/10.1210/endo.138.7.5250
43. Martinez G, Carnazza ML, Di Giacomo C, Sorrenti V, Vanella A (2001) Expression of bone morphogenetic protein-6 and transforming growth factor-beta1 in the rat brain after a mild and reversible ischemic damage. Brain Res 894:1–11
44. Meikle L, Talos DM, Onda H, Pollizzi K, Rotenberg A, Sahin M, Jensen FE, Kwiatkowski DJ (2007) A mouse model of tuberous sclerosis: neuronal loss of Tsc1 causes dysplastic and ectopic neurons, reduced myelination, seizure activity, and limited survival. J Neurosci 27:5546–5558. https://doi.org/10.1523/JNEUROSCI.5540-06.2007
45. Miron VE, Boyd A, Zhao JW, Yuen TJ, Ruckh JM, Shadrach JL, van Wijngaarden P, Wagers AJ, Williams A, Franklin RJ et al (2013) M2 microglia and macrophages drive oligodendrocyte differentiation during CNS remyelination. Nat Neurosci 16:1211–1218. https://doi.org/10.1038/nn.3469
46. Murray PD, McGavern DB, Sathornsumetee S, Rodriguez M (2001) Spontaneous remyelination following extensive demyelination is associated with improved neurological function in a viral model of multiple sclerosis. Brain 124:1403–1416
47. Narayanan SP, Flores AI, Wang F, Macklin WB (2009) Akt signals through the mammalian target of rapamycin pathway to regulate CNS myelination. J Neurosci 29:6860–6870. https://doi.org/10.1523/JNEUROSCI.0232-09.2009
48. Nawaz S, Sanchez P, Schmitt S, Snaidero N, Mitkovski M, Velte C, Bruckner BR, Alexopoulos I, Czopka T, Jung SY et al (2015) Actin filament turnover drives leading edge growth during myelin sheath formation in the central nervous system. Dev Cell 34:139–151. https://doi.org/10.1016/j.devcel.2015.05.013
49. Palazuelos J, Klingener M, Aguirre A (2014) TGFbeta signaling regulates the timing of CNS myelination by modulating oligodendrocyte progenitor cell cycle exit through SMAD3/4/FoxO1/Sp1. J Neurosci 34:7917–7930. https://doi.org/10.1523/JNEUROSCI.0363-14.2014
50. Patel JR, McCandless EE, Dorsey D, Klein RS (2010) CXCR4 promotes differentiation of oligodendrocyte progenitors and remyelination. Proc Natl Acad Sci USA 107:11062–11067. https://doi.org/10.1073/pnas.1006301107
51. Petersen MA, Ryu JK, Chang KJ, Etxeberria A, Bardehle S, Mendiola AS, Kamau-Devers W, Fancy SPJ, Thor A, Bushong EA et al (2017) Fibrinogen activates BMP signaling in oligodendrocyte progenitor cells and inhibits remyelination after vascular damage. Neuron 96(1003–1012):e1007. https://doi.org/10.1016/j.neuron.2017.10.008
52. Phillips DJ, Nguyen P, Adamides AA, Bye N, Rosenfeld JV, Kossmann T, Vallance S, Murray L, Morganti-Kossmann MC (2006) Activin a release into cerebrospinal fluid in a subset of patients with severe traumatic brain injury. J Neurotrauma 23:1283–1294. https://doi.org/10.1089/neu.2006.23.1283
53. Qiu W, Li X, Tang H, Huang AS, Panteleyev AA, Owens DM, Su GH (2011) Conditional activin receptor type 1B (Acvr1b)

knockout mice reveal hair loss abnormality. J Invest Dermatol 131:1067–1076. https://doi.org/10.1038/jid.2010.400
54. Sakai N, Inui K, Tatsumi N, Fukushima H, Nishigaki T, Taniike M, Nishimoto J, Tsukamoto H, Yanagihara I, Ozono K et al (1996) Molecular cloning and expression of cDNA for murine galactocerebrosidase and mutation analysis of the twitcher mouse, a model of Krabbe's disease. J Neurochem 66:1118–1124
55. Sakai T, Xu Y (2012) Stem cells decreased neuronal cell death after hypoxic stress in primary fetal rat neurons in vitro. Cell Transplant 21:355–364. https://doi.org/10.3727/096368911X580545
56. Schneider-Kolsky ME, Manuelpillai U, Waldron K, Dole A, Wallace EM (2002) The distribution of activin and activin receptors in gestational tissues across human pregnancy and during labour. Placenta 23:294–302. https://doi.org/10.1053/plac.2002.0787
57. Segovia KN, McClure M, Moravec M, Luo NL, Wan Y, Gong X, Riddle A, Craig A, Struve J, Sherman LS et al (2008) Arrested oligodendrocyte lineage maturation in chronic perinatal white matter injury. Ann Neurol 63:520–530. https://doi.org/10.1002/ana.21359
58. Seki Y, Kato TA, Monji A, Mizoguchi Y, Horikawa H, Sato-Kasai M, Yoshiga D, Kanba S (2013) Pretreatment of aripiprazole and minocycline, but not haloperidol, suppresses oligodendrocyte damage from interferon-gamma-stimulated microglia in co-culture model. Schizophr Res 151:20–28. https://doi.org/10.1016/j.schres.2013.09.011
59. Sekiya T, Adachi S, Kohu K, Yamada T, Higuchi O, Furukawa Y, Nakamura Y, Nakamura T, Tashiro K, Kuhara S et al (2004) Identification of BMP and activin membrane-bound inhibitor (BAMBI), an inhibitor of transforming growth factor-beta signaling, as a target of the beta-catenin pathway in colorectal tumor cells. J Biol Chem 279:6840–6846. https://doi.org/10.1074/jbc.M310876200
60. Snaidero N, Mobius W, Czopka T, Hekking LH, Mathisen C, Verkleij D, Goebbels S, Edgar J, Merkler D, Lyons DA et al (2014) Myelin membrane wrapping of CNS axons by PI(3,4,5)P3-dependent polarized growth at the inner tongue. Cell 156:277–290. https://doi.org/10.1016/j.cell.2013.11.044
61. Thurnherr T, Benninger Y, Wu X, Chrostek A, Krause SM, Nave KA, Franklin RJ, Brakebusch C, Suter U, Relvas JB (2006) Cdc42 and Rac1 signaling are both required for and act synergistically in the correct formation of myelin sheaths in the CNS. J Neurosci 26:10110–10119. https://doi.org/10.1523/JNEUROSCI.2158-06.2006
62. Werner S, Alzheimer C (2006) Roles of activin in tissue repair, fibrosis, and inflammatory disease. Cytokine Growth Factor Rev 17:157–171. https://doi.org/10.1016/j.cytogfr.2006.01.001
63. Yuen TJ, Johnson KR, Miron VE, Zhao C, Quandt J, Harrisingh MC, Swire M, Williams A, McFarland HF, Franklin RJ et al (2013) Identification of endothelin 2 as an inflammatory factor that promotes central nervous system remyelination. Brain 136:1035–1047. https://doi.org/10.1093/brain/awt024
64. Yuen TJ, Silbereis JC, Griveau A, Chang SM, Daneman R, Fancy SP, Zahed H, Maltepe E, Rowitch DH (2014) Oligodendrocyte-encoded HIF function couples postnatal myelination and white matter angiogenesis. Cell 158:383–396. https://doi.org/10.1016/j.cell.2014.04.052
65. Zhang H, Jarjour AA, Boyd A, Williams A (2011) Central nervous system remyelination in culture–a tool for multiple sclerosis research. Exp Neurol 230:138–148. https://doi.org/10.1016/j.expneurol.2011.04.009
66. Zuchero JB, Fu MM, Sloan SA, Ibrahim A, Olson A, Zaremba A, Dugas JC, Wienbar S, Caprariello AV, Kantor C et al (2015) CNS myelin wrapping is driven by actin disassembly. Dev Cell 34:152–167. https://doi.org/10.1016/j.devcel.2015.06.011

Affiliations

Alessandra Dillenburg[1] · Graeme Ireland[1] · Rebecca K. Holloway[1] · Claire L. Davies[1] · Frances L. Evans[1] · Matthew Swire[2] · Marie E. Bechler[2] · Daniel Soong[1] · Tracy J. Yuen[3,7] · Gloria H. Su[4] · Julie-Clare Becher[5] · Colin Smith[6] · Anna Williams[2] · Veronique E. Miron[1]

1 Medical Research Council Centre for Reproductive Health, The Queen's Medical Research Institute, The University of Edinburgh, 47 Little France Crescent, Edinburgh EH16 4TJ, UK

2 Medical Research Council Centre for Regenerative Medicine, The University of Edinburgh, 5 Little France Drive, Edinburgh EH16 5UU, UK

3 Department of Veterinary Medicine, Wellcome Trust MRC Cambridge Stem Cell Institute, University of Cambridge, Cambridge CB3 0E5, UK

4 Department of Pathology and Cell Biology, Herbert Irving Comprehensive Cancer Center, Columbia University Medical Centre, New York 10032, USA

5 Simpson's Centre for Reproductive Health, Royal Infirmary of Edinburgh, Edinburgh EH16 4SA, UK

6 Centre for Clinical Brain Sciences, Centre for Comparative Pathology, The University of Edinburgh, Chancellor's Building, Edinburgh EH16 4TJ, UK

7 Present Address: Department of Neuroscience, Genentech Inc., South San Francisco, CA 94080, USA

References

1. Bercury, K. K. & Macklin, W. B. Dynamics and mechanisms of CNS myelination. *Developmental Cell* **32,** 447–458. ISSN: 18781551 (2015).
2. Nave, K.-A. & Werner, H. B. Myelination of the Nervous System: Mechanisms and Functions. *Annual Review of Cell and Developmental Biology* **30,** 503–533. ISSN: 1081-0706 (2014).
3. Morell, P & Quarles, R. in *Basic Neurochemistry: Molecular, Cellular and Medical Aspects* (ed et al. Siegel GJ, Agranoff BW, Albers RW) 6th (Lippincott-Raven, Philadelphia, 1999).
4. Coetzee, T. *et al.* Myelination in the absence of galactocerebroside and sulfatide: Normal structure with abnormal function and regional instability. *Cell* **86,** 209–219. ISSN: 00928674 (1996).
5. Schwab, M. E. & Schnell, L. Region-specific appearance of myelin constituents in the developing rat spinal cord. *Journal of Neurocytology* **18,** 161–169. ISSN: 03004864 (1989).
6. Tosic, M., Rakic, S., Matthieu, J. M. & Zecevic, N. Identification of Golli and myelin basic proteins in human brain during early development. *Glia* **37,** 219–228. ISSN: 08941491 (2002).
7. Young, K. M. *et al.* Oligodendrocyte dynamics in the healthy adult CNS: Evidence for myelin remodeling. *Neuron* **77,** 873–885. ISSN: 10974199 (2013).
8. Yeung, M. S. Y. *et al.* Dynamics of oligodendrocyte generation and myelination in the human brain. *Cell* **159,** 766–774. ISSN: 10974172 (2014).
9. Bengtsson, S. L. *et al.* Extensive piano practicing has regionally specific effects on white matter development. *Nature Neuroscience* **8,** 1148–1150. ISSN: 1097-6256 (2005).
10. Scholz, J., Klein, M. C., Behrens, T. E. J. & Johansen-Berg, H. Training induces changes in white-matter architecture. *Nature Neuroscience* **12,** 1370–1371. ISSN: 1097-6256 (2009).
11. Schlegel, A. A., Rudelson, J. J. & Tse, P. U. White Matter Structure Changes as Adults Learn a Second Language. *Journal of Cognitive Neuroscience* **24,** 1664–1670 (2012).
12. Miller, R. H. Regulation of oligodendrocyte development in the vertebrate CNS. *Progress in Neurobiology* **67,** 451–467. ISSN: 03010082 (2002).
13. Sobottka, B., Ziegler, U., Kaech, A., Becher, B. & Goebels, N. CNS live imaging reveals a new mechanism of myelination: The liquid croissant model. *Glia* **59,** 1841–1849. ISSN: 08941491 (2011).
14. Snaidero, N. *et al.* Myelin membrane wrapping of CNS axons by PI(3,4,5)P3-dependent polarized growth at the inner tongue. *Cell* **156,** 277–290. ISSN: 00928674 (2014).
15. Almeida, R. G., Czopka, T., Ffrench-Constant, C. & Lyons, D. A. Individual axons regulate the myelinating potential of single oligodendrocytes in vivo. *Development* **138,** 4443–4450. ISSN: 0950-1991 (2011).
16. Tasaki, I. The Electro-saltatory transmission of the nerve impulse and the effect of narcosis upon the nerve fiber. *The American journal of physiology* **129,** 1–13 (1939).

17. Sherman, D. L. & Brophy, P. J. Mechanisms of axon ensheathment and myelin growth. *Nature reviews. Neuroscience* **6,** 683–690. ISSN: 1471-003X (2005).

18. Edgar, J. M. *et al.* Oligodendroglial modulation of fast axonal transport in a mouse model of hereditary spastic paraplegia. *Journal of Cell Biology* **166,** 121–131. ISSN: 00219525 (2004).

19. Griffiths, I *et al.* Axonal swellings and degeneration in mice lacking the major proteolipid of myelin. *Science (New York, N.Y.)* **280,** 1610–1613. ISSN: 00368075 (1998).

20. Lee, Y. *et al.* Oligodendroglia metabolically support axons and contribute to neurodegeneration. *Nature* **487,** 443–448. ISSN: 0028-0836 (2012).

21. Funfschilling, U. *et al.* Glycolytic oligodendrocytes maintain myelin and long-term axonal integrity. *Nature,* 0–5. ISSN: 0028-0836 (2012).

22. Nave, K.-A. Myelination and support of axonal integrity by glia. *Nature* **468,** 244–252. ISSN: 0028-0836 (2010).

23. Mehndiratta, M. M. & Gulati, N. S. Central and peripheral demyelination. *Journal of Neurosciences in Rural Practice* **5,** 84–86. ISSN: 0976-3147 (2014).

24. Dimou, L. & Götz, M. Glial Cells as Progenitors and Stem Cells: New Roles in the Healthy and Diseased Brain. *Physiological reviews* **94,** 709–737. ISSN: 1522-1210 (2014).

25. Robinson, A. P., Rodgers, J. M., Goings, G. E. & Miller, S. D. Characterization of Oligodendroglial Populations in Mouse Demyelinating Disease Using Flow Cytometry: Clues for MS Pathogenesis. *PLoS ONE* **9,** e107649. ISSN: 1932-6203 (2014).

26. Franklin, R. J. M. & Ffrench-Constant, C. Regenerating CNS myelin from mechanisms to experimental medicines. *Nature Reviews Neuroscience* **18,** 753–769. ISSN: 1471-003X (2017).

27. Dawson, M. R., Polito, A., Levine, J. M. & Reynolds, R. NG2-expressing glial progenitor cells: An abundant and widespread population of cycling cells in the adult rat CNS. *Molecular and Cellular Neuroscience* **24,** 476–488. ISSN: 10447431 (2003).

28. Ffrench-Constant, C. & Raff, M. C. Proliferating bipotential glial progenitor cells in adult rat optic nerve. *Nature* **319,** 499–502. ISSN: 00280836 (1986).

29. Zawadzka, M. *et al.* CNS-Resident Glial Progenitor/Stem Cells Produce Schwann Cells as well as Oligodendrocytes during Repair of CNS Demyelination. *Cell Stem Cell* **6,** 578–590. ISSN: 19345909 (2010).

30. Tripathi, R. B., Rivers, L. E., Young, K. M., Jamen, F. & Richardson, W. D. PDGFRA / NG2 glia generate new oligodendrocytes but few astrocytes in a murine EAE model of demyelinating disease. *Journal of Neuroscience* **30,** 16383–16390 (2010).

31. Hesp, Z. C., Goldstein, E. A., Miranda, C. J., Kaspar, B. K. & McTigue, D. M. Chronic Oligodendrogenesis and Remyelination after Spinal Cord Injury in Mice and Rats. *Journal of Neuroscience* **35,** 1274–1290. ISSN: 0270-6474 (2015).

32. Crawford, A. H., Tripathi, R. B., Richardson, W. D. & Franklin, R. J. M. Developmental Origin of Oligodendrocyte Lineage Cells Determines Response to Demyelination and Susceptibility to Age-Associated Functional Decline. *Cell Reports* **15,** 761–773. ISSN: 22111247 (2016).

33. Xing, Y. L. *et al.* Adult Neural Precursor Cells from the Subventricular Zone Contribute Significantly to Oligodendrocyte Regeneration and Remyelination. *Journal of Neuroscience* **34,** 14128–14146. ISSN: 0270-6474 (2014).

34. Samanta, J. *et al.* Inhibition of Gli1 mobilizes endogenous neural stem cells for remyelination. *Nature* **526,** 448–452. ISSN: 14764687 (2015).

35. Kazanis, I. *et al.* Subependymal Zone-Derived Oligodendroblasts Respond to Focal Demyelination but Fail to Generate Myelin in Young and Aged Mice. *Stem Cell Reports* **8,** 685–700. ISSN: 22136711 (2017).

36. Moyon, S. *et al.* Demyelination Causes Adult CNS Progenitors to Revert to an Immature State and Express Immune Cues That Support Their Migration. *Journal of Neuroscience* **35,** 4–20. ISSN: 0270-6474 (2015).

37. Boyd, A., Zhang, H. & Williams, A. Insufficient OPC migration into demyelinated lesions is a cause of poor remyelination in MS and mouse models. *Acta Neuropathologica* **125,** 841–859. ISSN: 00016322 (2013).

38. Wegener, A. *et al.* Gain of Olig2 function in oligodendrocyte progenitors promotes remyelination. *Brain* **138,** 120–135. ISSN: 14602156 (2015).

39. Hammond, T. R. *et al.* Astrocyte-Derived Endothelin-1 Inhibits Remyelination through Notch Activation. *Neuron* **81,** 588–602. ISSN: 08966273 (2014).

40. Arai, K. & Lo, E. H. An Oligovascular Niche: Cerebral Endothelial Cells Promote the Survival and Proliferation of Oligodendrocyte Precursor Cells. *Journal of Neuroscience* **29,** 4351–4355. ISSN: 0270-6474 (2009).

41. Casaccia-Bonnefil, P. *et al.* Oligodendrocyte precursor differentiation is perturbed in the absence of the cyclin-dependent kinase inhibitor p27(Kip1). *Genes and Development* **11,** 2335–2346. ISSN: 08909369 (1997).

42. Hughes, E. G., Kang, S. H., Fukaya, M. & Bergles, D. E. Oligodendrocyte progenitors balance growth with self-repulsion to achieve homeostasis in the adult brain. *Nature Neuroscience* **16,** 668–676. ISSN: 10976256 (2013).

43. Rosenberg, S. S., Kelland, E. E., Tokar, E., De la Torre, A. R. & Chan, J. R. The geometric and spatial constraints of the microenvironment induce oligodendrocyte differentiation. *Proceedings of the National Academy of Sciences of the United States of America* **105,** 14662–14667. ISSN: 0027-8424 (2008).

44. Dietz, K. C., Polanco, J. J., Pol, S. U. & Sim, F. J. Targeting human oligodendrocyte progenitors for myelin repair. *Experimental Neurology* **283,** 489–500. ISSN: 10902430 (2016).

45. Zhang, H., Jarjour, A. A., Boyd, A. & Williams, A. Central nervous system remyelination in culture A tool for multiple sclerosis research. *Experimental Neurology* **230,** 138–148. ISSN: 0014-4886 (2011).

46. Williams, A. Remyelination in multiple sclerosis: what do we know and where are we going? *Neurodegenerative Disease Management* **5,** 49–59 (2015).

47. Franklin, R. J. M. & Hinks, G. L. Understanding CNS remyelination: Clues from developmental and regeneration biology. *Journal of Neuroscience Research* **58,** 207–213. ISSN: 03604012 (1999).

48. Smith, R. S. & Koles, Z. Myelinated thickness nerve fibers : computed velocity effect of myelin on conduction. *American Journal of Physiology* **219,** 5–7. ISSN: 0002-9513 (1970).

49. Dennis, J. *et al.* Phosphodiesterase-Iα/autotaxin's MORFO domain regulates oligodendroglial process network formation and focal adhesion organization. *Molecular and Cellular Neuroscience* **37,** 412–424. ISSN: 10447431 (2008).

50. Dennis, J., Morgan, M. K., Graf, M. R. & Fuss, B. P2Y12receptor expression is a critical determinant of functional responsiveness to ATX's MORFO domain. *Purinergic Signalling* **8,** 181–190. ISSN: 15739538 (2012).

51. Fox, M. A., Colello, R. J., Macklin, W. B. & Fuss, B. Phosphodiesterase-Iα/autotaxin: A counteradhesive protein expressed by oligodendrocytes during onset of myelination. *Molecular and Cellular Neuroscience* **23,** 507–519. ISSN: 10447431 (2003).

52. Wheeler, N. A., Lister, J. A. & Fuss, B. The Autotaxin-Lysophosphatidic Acid Axis Modulates Histone Acetylation and Gene Expression during Oligodendrocyte Differentiation. *Journal of Neuroscience* **35,** 11399–11414. ISSN: 0270-6474 (2015).

53. Yuelling, L. M. & Fuss, B. Autotaxin (ATX): A multi-functional and multi-modular protein possessing enzymatic lysoPLD activity and matricellular properties. *Biochimica et Biophysica Acta - Molecular and Cell Biology of Lipids* **1781,** 525–530. ISSN: 13881981 (2008).

54. Wheeler, N. A. & Fuss, B. Extracellular cues influencing oligodendrocyte differentiation and (re)myelination. *Experimental Neurology* **283,** 512–530. ISSN: 10902430 (2016).

55. Omari, K. M., John, G. R., Sealfon, S. C. & Raine, C. S. CXC chemokine receptors on human oligodendrocytes : implications for multiple sclerosis. *Brain* **128,** 1003–1015 (2005).

56. Omari, K. M., John, G., Lango, R. & Raine, C. S. Role for CXCR2 and CXCL1 on glia in multiple sclerosis. *Glia* **53,** 24–31. ISSN: 08941491 (2006).

57. Omari, K. M., Lutz, S. E., Santambrogio, L., Lira, S. A. & Raine, C. S. Neuroprotection and remyelination after autoimmune demyelination in mice that inducibly overexpress CXCL1. *American Journal of Pathology* **174,** 164–176. ISSN: 15252191 (2009).

58. Patel, J. R., McCandless, E. E., Dorsey, D. & Klein, R. S. CXCR4 promotes differentiation of oligodendrocyte progenitors and remyelination. *Proceedings of the National Academy of Sciences* **107,** 11062–11067. ISSN: 0027-8424 (2010).

59. Münzel, E. J. & Williams, A. Promoting remyelination in multiple sclerosis-recent advances. *Drugs* **73,** 2017–2029. ISSN: 00126667 (2013).

60. Gadea, A., Aguirre, A., Haydar, T. F. & Gallo, V. Endothelin-1 Regulates Oligodendrocyte Development. *Journal of Neuroscience* **29,** 10047–10062. ISSN: 0270-6474 (2009).

61. Yuen, T. J. *et al.* Identification of endothelin 2 as an inflammatory factor that promotes central nervous system remyelination. *Brain* **136,** 1035–1047. ISSN: 00068950 (2013).

62. McMorris, F. A. & Dubois-Dalcq, M. Insulin-Like Growth Factor I Promotes Cell Proliferation and Oligodendroglial Commitment in Rat Glial Progenitor Cells Developing In Vitro. *Journal of Neuroscience Research* **21,** 199–209 (1988).

63. McMorris, F. A., Smith, T. M., DeSalvo, S & Furlanetto, R. W. Insulin-like growth factor I/somatomedin C: a potent inducer of oligodendrocyte development. *Proceedings of the National Academy of Sciences of the United States of America* **83,** 822–6. ISSN: 0027-8424 (1986).

64. Ye, P, Carson, J & D'Ercole, A. J. In vivo actions of insulin-like growth factor-I (IGF-I) on brain myelination: studies of IGF-I and IGF binding protein-1 (IGFBP-1) transgenic mice. *The Journal of neuroscience : the official journal of the Society for Neuroscience* **15,** 7344–56. ISSN: 0270-6474 (1995).

65. Mason, J. L., Ye, P, Suzuki, K, D'Ercole, a. J. & Matsushima, G. K. Insulin-like growth factor-1 inhibits mature oligodendrocyte apoptosis during primary demyelination. *The Journal of neuroscience : the official journal of the Society for Neuroscience* **20,** 5703–8. ISSN: 0270-6474 (2000).

66. Bibollet-Bahena, O. & Almazan, G. IGF-1-stimulated protein synthesis in oligodendrocyte progenitors requires PI3K/mTOR/Akt and MEK/ERK pathways. *Journal of Neurochemistry* **109,** 1440–1451. ISSN: 00223042 (2009).

67. Cui, Q. L. & Almazan, G. IGF-I-induced oligodendrocyte progenitor proliferation requires PI3K/Akt, MEK/ERK, and Src-like tyrosine kinases. *Journal of Neurochemistry* **100,** 1480–1493. ISSN: 00223042 (2007).

68. Beck, K. D., Powell-Braxtont, L., Widmer, H. R., Valverde, J. & Hefti, F. Igf1 gene disruption results in reduced brain size, CNS hypomyelination, and loss of hippocampal granule and striatal parvalbumin-containing neurons. *Neuron* **14,** 717–730. ISSN: 08966273 (1995).

69. Chesik, D., De Keyser, J. & Wilczak, N. Insulin-like growth factor system regulates oligodendroglial cell behavior: Therapeutic potential in CNS. *Journal of Molecular Neuroscience* **35,** 81–90. ISSN: 08958696 (2008).

70. Buttery, P. C. & Ffrench-Constant, C. Laminin-2/integrin interactions enhance myelin membrane formation by oligodendrocytes. *Molecular and Cellular Neurosciences* **14,** 199–212. ISSN: 10447431 (1999).

71. Chun, S. J., Rasband, M. N., Sidman, R. L., Habib, A. A. & Vartanian, T. Integrin-linked kinase is required for laminin-2-induced oligodendrocyte cell spreading and CNS myelination. *Journal of Cell Biology* **163,** 397–408. ISSN: 00219525 (2003).

72. Baron, W., Colognato, H. & Ffrench-Constant, C. Integrin-growth factor interactions as regulators of oligodendroglial development and function. *Glia* **49,** 467–479. ISSN: 08941491 (2005).

73. Colognato, H. *et al.* CNS integrins switch growth factor signalling to promote target-dependent survival. *Nature Cell Biology* **4,** 1–9. ISSN: 14657392 (2002).

74. Frost, E. E., Buttery, P. C., Milner, R & Ffrench-Constant, C. Integrins mediate a neuronal survival signal for oligodendrocytes. *Current biology : CB* **9,** 1251–4. ISSN: 0960-9822 (1999).

75. Laursen, L. S., Chan, C. W. & Ffrench-Constant, C. An Integrin-Contactin Complex Regulates CNS Myelination by Differential Fyn Phosphorylation. *Journal of Neuroscience* **29,** 9174–9185. ISSN: 0270-6474 (2009).

76. Leiton, C. V. *et al.* Laminin promotes metalloproteinase-mediated dystroglycan processing to regulate oligodendrocyte progenitor cell proliferation. *Journal of Neurochemistry* **135,** 522–538. ISSN: 14714159 (2015).

77. Zhao, C., Fancy, S. P., Franklin, R. J. & Ffrench-Constant, C. Up-regulation of oligodendrocyte precursor cell αV integrin and its extracellular ligands during central nervous system remyelination. *Journal of Neuroscience Research* **87,** 3447–3455. ISSN: 03604012 (2009).

78. Noble, M., Murray, K., Stroobant, P., Waterfield, M. D. & Riddle, P. Platelet-derived growth factor promotes division and motility and inhibits premature differentiation of the oligodendrocyte/type-2 astrocyte progenitor ceil. *Nature* **333,** 560–562. ISSN: 00280836 (1988).

79. Redwine, J. M. & Armstrong, R. C. In vivo proliferation of oligodendrocyte progenitors expressing PDGF??R during early remyelination. *Journal of Neurobiology* **37,** 413–428. ISSN: 00223034 (1998).

80. Woodruff, R. H., Fruttiger, M., Richardson, W. D. & Franklin, R. J. Platelet-derived growth factor regulates oligodendrocyte progenitor numbers in adult CNS and their response following CNS demyelination. *Molecular and Cellular Neuroscience* **25,** 252–262. ISSN: 10447431 (2004).

81. Huang, J. K. *et al.* Retinoid X receptor gamma signaling accelerates CNS remyelination. *Nature neuroscience* **14,** 45–53. ISSN: 1097-6256 (2011).

82. Spassky, N. *et al.* Directional guidance of oligodendroglial migration by class 3 semaphorins and netrin-1. *The Journal of neuroscience : the official journal of the Society for Neuroscience* **22,** 5992–6004. ISSN: 1529-2401 (2002).

83. Piaton, G. *et al.* Class 3 semaphorins influence oligodendrocyte precursor recruitment and remyelination in adult central nervous system. *Brain* **134,** 1156–1167. ISSN: 00068950 (2011).

84. Williams, A. *et al.* Semaphorin 3A and 3F: Key players in myelin repair in multiple sclerosis? *Brain* **130,** 2554–2565. ISSN: 00068950 (2007).

85. Sloane, J. a. *et al.* Hyaluronan blocks oligodendrocyte progenitor maturation and remyelination through TLR2. *Proceedings of the National Academy of Sciences of the United States of America* **107,** 11555–11560. ISSN: 0027-8424 (2010).

86. Back, S. a. *et al.* Hyaluronan accumulates in demyelinated lesions and inhibits oligodendrocyte progenitor maturation. *Nature medicine* **11,** 966–972. ISSN: 1078-8956 (2005).

87. Struve, J. *et al.* Disruption of the hyaluronan-based extracellular matrix in spinal cord promotes astrocyte proliferation. *Glia* **52,** 16–24. ISSN: 08941491 (2005).

88. Mi, S. *et al.* LINGO-1 antagonist promotes spinal cord remyelination and axonal integrity in MOG-induced experimental autoimmune encephalomyelitis. *Nature medicine* **13,** 1228–1233. ISSN: 1078-8956 (2007).

89. Mi, S. *et al.* Promotion of central nervous system remyelination by induced differentiation of oligodendrocyte precursor cells. *Annals of Neurology* **65,** 304–315. ISSN: 03645134 (2009).

90. Pepinsky, R. B. *et al.* Production of a PEGylated Fab of the anti-LINGO-1 Li33 Antibody and Assessment of Its Biochemical and Functional Properties in Vitro and in a Rat Model of Remyelination. *Bioconjugate Chemistry* **22,** 200–210. ISSN: 1043-1802 (2011).

91. Wang, S. *et al.* Notch Receptor Activation Inhibits Oligodendrocyte Differentiation. *Neuron* **21,** 63–75. ISSN: 0896-6273 (1998).

92. John, G. R. *et al.* Multiple sclerosis: Re-expression of a developmental pathway that restricts oligodendrocyte maturation. *Nature Medicine* **8,** 1115 (2002).

93. Givogri, M. *et al.* Central nervous system myelination in mice with deficient expression of Notch1 receptor. *Journal of Neuroscience Research* **67,** 309–320. ISSN: 0360-4012 (2002).

94. Hibbits, N., Yoshino, J., Le, T. Q. & Armstrong, R. C. Astrogliosis During Acute and Chronic Cuprizone Demyelination and Implications for Remyelination. *ASN Neuro* **4,** AN20120062. ISSN: 1759-0914 (2012).

95. Satoh, J. I., Tabunoki, H. & Yamamura, T. Molecular network of the comprehensive multiple sclerosis brain-lesion proteome. *Multiple Sclerosis* **15,** 531–541. ISSN: 13524585 (2009).

96. Stoffels, J. M. *et al.* Fibronectin aggregation in multiple sclerosis lesions impairs remyelination. *Brain* **136,** 116–131. ISSN: 14602156 (2013).

97. Milner, R, Edwards, G, Streuli, C & Ffrench-Constant, C. A role in migration for the alpha V beta 1 integrin expressed on oligodendrocyte precursors. *The Journal of neuroscience : the official journal of the Society for Neuroscience* **16,** 7240–7252. ISSN: 0270-6474 (1996).

98. Gard, A. L. & Pfeiffer, S. Glial cell mitogens bFGF and PDGF differentially regulate development of O4+GalC- oligodendrocyte progenitors. *Developmental Biology* **159,** 618–630 (1993).

99. McKinnon, R. D., Smith, C., Behar, T., Smith, T. & DuboisDalcq, M. Distinct effects of bFGF and PDGF on oligodendrocyte progenitor cells. *Glia* **7,** 245–254. ISSN: 10981136 (1993).

100. Bribián, A., Barallobre, M. J., Soussi-Yanicostas, N. & de Castro, F. Anosmin-1 modulates the FGF-2-dependent migration of oligodendrocyte precursors in the developing optic nerve. *Molecular and Cellular Neuroscience* **33,** 2–14. ISSN: 10447431 (2006).

101. Milner, R. *et al.* Contrasting Effects of Mitogenic Growth Factors on Oligodendrocyte Precursor Cell Migration. *Glia* **90,** 85–90 (1997).

102. Lindner, M. *et al.* Fibroblast growth factor signalling in multiple sclerosis: Inhibition of myelination and induction of pro-inflammatory environment by FGF9. *Brain* **138,** 1875–1893. ISSN: 14602156 (2015).

103. Chen, Y. *et al.* The oligodendrocyte-specific G protein-coupled receptor GPR17 is a cell-intrinsic timer of myelination. *Nature Neuroscience* **12,** 1398–1406. ISSN: 10976256 (2009).

104. Fumagalli, M. *et al.* Phenotypic changes, signaling pathway, and functional correlates of GPR17-expressing neural precursor cells during oligodendrocyte differentiation. *Journal of Biological Chemistry* **286,** 10593–10604. ISSN: 00219258 (2011).

105. Lecca, D. *et al.* The Recently Identified P2Y-Like Receptor GPR17 Is a Sensor of Brain Damage and a New Target for Brain Repair. *PLOS ONE* **3,** e3579 (2008).

106. Coppi, E. *et al.* UDP-glucose enhances outward K+ currents necessary for cell differentiation and stimulates cell migration by activating the GPR17 receptor in oligodendrocyte precursors. *Glia* **61,** 1155–1171. ISSN: 08941491 (2013).

107. Ceruti, S. *et al.* Expression of the new P2Y-like receptor GPR17 during oligodendrocyte precursor cell maturation regulates sensitivity to ATP-induced death. *Glia* **59,** 363–378. ISSN: 08941491 (2011).

108. Fumagalli, M. *et al.* The ubiquitin ligase Mdm2 controls oligodendrocyte maturation by intertwining mTOR with G protein-coupled receptor kinase 2 in the regulation of GPR17 receptor desensitization. *Glia* **63,** 2327–2339. ISSN: 10981136 (2015).

109. Sugimoto, Y. *et al.* Guidance of glial procursor cell migration by selected cues in the developing optic nerve. *Development* **128,** 3321–3330 (2001).

110. Jarjour, A. a. *et al.* Netrin-1 Is a Chemorepellent for Oligodendrocyte Precursor Cells in the Embryonic Spinal Cord. *J Neurosci* **23,** 3735–3744. ISSN: 1529-2401 (2003).

111. Tsai, H.-H., Tessier-Lavigne, M. & Miller, R. H. Netrin 1 mediates spinal cord oligodendrocyte precursor dispersal. *Development* **130,** 2095–2105. ISSN: 09501991 (2003).

112. Tsai, H.-H., Macklin, W. B. & Miller, R. H. Netrin-1 Is Required for the Normal Development of Spinal Cord Oligodendrocytes. *Journal of Neuroscience* **26,** 1913–1922. ISSN: 0270-6474 (2006).

113. Rajasekharan, S. *et al.* Netrin 1 and Dcc regulate oligodendrocyte process branching and membrane extension via Fyn and RhoA. *Development* **136,** 415–426. ISSN: 0950-1991 (2009).

114. Tepavčevic, V. *et al.* Early netrin-1 expression impairs central nervous system remyelination. *Annals of Neurology* **76,** 252–268. ISSN: 15318249 (2014).

115. Bin, J. M. *et al.* Full-length and fragmented netrin-1 in multiple sclerosis plaques are inhibitors of oligodendrocyte precursor cell migration. *American Journal of Pathology* **183,** 673–680. ISSN: 00029440 (2013).

116. Bartsch, U, Kirchhoff, F & Schachner, M. Highly sialylated N-CAM is expressed in adult mouse optic nerve and retina. *Journal of Neurocytology* **19,** 550–565. ISSN: 1573-7381 (1990).

117. Charles, P *et al.* Negative regulation of central nervous system myelination by polysialylated-neural cell adhesion molecule. *Proceedings of the National Academy of Sciences of the United States of America* **97,** 7585–7590. ISSN: 00278424 (2000).

118. Trotter, J, Bitter-Suermann, D & Schachner, M. Differentiation-Regulated Loss of the Polysialylated Embryonic Form and Expression of the Different Polypeptides of the Neural Cell Adhesion Molecule by Cultured Oligodendrocytes and Myelin. *Journal of Neuroscience Research* **22,** 369–383 (1989).

119. Jakovcevski, I., Mo, Z. & Zecevic, N. Down-regulation of the axonal polysialic acid-neural cell adhesion molecule expression coincides with the onset of myelination in the human fetal forebrain. *Neuroscience* **149,** 328–337. ISSN: 03064522 (2007).

120. Fewou, S. N., Ramakrishnan, H., Büssow, H., Gieselmann, V. & Eckhardt, M. Down-regulation of polysialic acid is required for efficient myelin formation. *Journal of Biological Chemistry* **282,** 16700–16711. ISSN: 00219258 (2007).

121. Decker, L., Avellana-Adalid, V., Nait-Oumesmar, B., Durbec, P. & Baron-Van Evercooren, A. Oligodendrocyte precursor migration and differentiation: Combined effects of PSA residues, growth factors, and substrates. *Molecular and Cellular Neurosciences* **16,** 422–439. ISSN: 10447431 (2000).

122. Zhang, H., Vutskits, L, Calaora, V, Durbec, P & Kiss, J. A role for the polysialic acid - neural cell adhesion molecule in PDGF-induced chemotaxis of oligodendrocyte precursor cells. *Journal of Cell Science* **117,** 93–103. ISSN: 0021-9533 (2004).

123. Hu, Y. *et al.* Sphingosine 1-phosphate receptor modulator fingolimod (FTY720) does not promote remyelination in vivo. *Molecular and Cellular Neuroscience* **48,** 72–81. ISSN: 10447431 (2011).

124. Kim, H. J. *et al.* Neurobiological effects of sphingosine 1-phosphate receptor modulation in the cuprizone model. *The FASEB Journal* **25,** 1509–1518. ISSN: 0892-6638 (2011).

125. Coelho, R. P., Payne, S. G., Bittman, R., Spiegel, S. & Sato-Bigbee, C. The immunomodulator FTY720 has a direct cytoprotective effect in oligodendrocyte progenitors. *The Journal of pharmacology and experimental therapeutics* **323,** 626–635. ISSN: 0022-3565 (2007).

126. Cui, Q. L., Fang, J., Kennedy, T. E., Almazan, G. & Antel, J. P. Role of p38MAPK in S1P receptor-mediated differentiation of human oligodendrocyte progenitors. *Glia* **62,** 1361–1375. ISSN: 10981136 (2014).

127. Jung, C. *et al.* Functional Consequences of S1P Receptor Modulation in Rat Oligodendroglial Lineage Cells. *Glia* **55,** 1416–1425. ISSN: 08941491 (2007).

128. Miron, V. E. *et al.* FTY720 modulates human oligodendrocyte progenitor process extension and survival. *Annals of Neurology* **63,** 61–71. ISSN: 03645134 (2008).

129. Miron, V. E. *et al.* Fingolimod (FTY720) enhances remyelination following demyelination of organotypic cerebellar slices. *American Journal of Pathology* **176,** 2682–2694. ISSN: 15252191 (2010).

130. Feigenson, K., Reid, M., See, J., Crenshaw, E. B. & Grinspan, J. B. Wnt signaling is sufficient to perturb oligodendrocyte maturation. *Molecular and Cellular Neuroscience* **42,** 255–265. ISSN: 10447431 (2009).

131. Guo, F. *et al.* Canonical Wnt signaling in the oligodendroglial lineage-puzzles remain. *Glia* **63,** 1671–1693. ISSN: 10981136 (2015).

132. Ye, F. *et al.* HDAC1 and HDAC2 regulate oligodendrocyte differentiation by disrupting the -catenin-TCF interaction. *Nature Neuroscience* **12,** 829–838. ISSN: 10976256 (2009).

133. Fancy, S. P. J. *et al.* Dysregulation of the Wnt pathway inhibits timely myelination and remyelination in the mammalian CNS. *Genes and Development* **23,** 1571–1585. ISSN: 08909369 (2009).

134. Fancy, S. P. J. *et al.* Parallel states of pathological Wnt signaling in neonatal brain injury and colon cancer. *Nature Neuroscience* **17,** 506–512. ISSN: 15461726 (2014).

135. Miller, R. H., Fyffe-Maricich, S. & Caprariello, A. V. *Animal Models for the Study of Multiple Sclerosis* 1037–1057. ISBN: 9780124158948. doi:10.1016/B978-0-12-415894-8.00042-7 (Elsevier, 2013).

136. Blakemore, W. F., Eames, R. A., Smith, K. J. & Mcdonald, W. I. Remyelination in the spinal cord of the cat following intraspinal injections of lysolecithin. *Journal of the Neurological Sciences* **33,** 31–43. ISSN: 0022510X (1977).

137. Magalon, K., Cantarella, C., Monti, G., Cayre, M. & Durbec, P. Enriched environment promotes adult neural progenitor cell mobilization in mouse demyelination models. *European Journal of Neuroscience* **25,** 761–771. ISSN: 0953816X (2007).

138. Riet-Correa, G, Fernandes, C., Pereira, L. & Graça, D. Ethidium bromide-induced demyelination in the sciatic nerve of adult Wistar rats. *Brazilian Jounral of Medical and Biological Research* **35,** 99–104. ISSN: 0004282X (2002).

139. Waxman, S., Kocsis, J. & Nitta, K. Lysophosphatidyl choline-induced focal demyelination in the rabbit corpus callosum: light-microscopic observations. *Journal of Neurological Sciences* **44,** 45–53 (1979).

140. Griffin, J. W., Stocks, E. A., Fahnestock, K., Van Praagh, A. & Trapp, B. D. Schwann cell proliferation following lysolecithin-induced demyelination. *Journal of Neurocytology* **19,** 367–384. ISSN: 03004864 (1990).

141. Dousset, V. *et al.* Lysolecithin-induced demyelination in primates: Preliminary in vivo study with MR and magnetization transfer. *American Journal of Neuroradiology* **16,** 225–231. ISSN: 01956108 (1995).

142. Miron, V. E. *et al.* M2 microglia and macrophages drive oligodendrocyte differentiation during CNS remyelination. *Nature neuroscience* **16,** 1211–8. ISSN: 1546-1726 (2013).

143. Cho, S., Wood, A. & Bowlby, M. R. Brain slices as models for neurodegenerative disease and screening platforms to identify novel therapeutics. *Current neuropharmacology* **5,** 19–33. ISSN: 1570-159X (2007).

144. Pasquini, L. A. *et al.* The neurotoxic effect of cuprizone on oligodendrocytes depends on the presence of pro-inflammatory cytokines secreted by microglia. *Neurochemical Research* **32,** 279–292. ISSN: 03643190 (2007).

145. Torkildsen, Brunborg, L. A., Myhr, K. M. & Bø, L. The cuprizone model for demyelination. *Acta Neurologica Scandinavica* **117,** 72–76. ISSN: 00016314 (2008).

146. Irvine, K. A. & Blakemore, W. F. Age increases axon loss associated with primary demyelination in cuprizone-induced demyelination in C57BL/6 mice. *Journal of Neuroimmunology* **175,** 69–76. ISSN: 01655728 (2006).

147. Mancardi, G *et al.* Demyelination and axonal damage in a non-human primate model of multiple sclerosis. *Journal of the neurological sciences* **184,** 41–49. ISSN: 0022-510X (2001).

148. Ransohoff, R. M. Animal models of multiple sclerosis: The good, the bad and the bottom line. *Nature Neuroscience* **15,** 1074–1077. ISSN: 10976256 (2012).

149. Arnett, H. A. & Viney, J. L. Considerations for the sensible use of rodent models of inflammatory disease in predicting efficacy of new biological therapeutics in the clinic. *Advanced Drug Delivery Reviews* **59,** 1084–1092. ISSN: 0169409X (2007).

150. Ulrich, R., Seeliger, F., Kreutzer, M., Germann, P. G. & Baumgärtner, W. Limited remyelination in Theiler's murine encephalomyelitis due to insufficient oligodendroglial differentiation of nerve/glial antigen 2 (NG2)-positive putative oligodendroglial progenitor cells. *Neuropathology and Applied Neurobiology* **34,** 603–620. ISSN: 03051846 (2008).

151. Noseworthy, J. H., Lucchinetti, C., Rodriguez, M. & Weinshenker, B. G. Multiple Sclerosis. *The New England Journal of Medicine* **343,** 938–952 (2000).

152. Trapp, B. D. *et al.* Axonal Transection in the Lesions of Multiple Sclerosis. *New England Journal of Medicine* **338,** 278–285. ISSN: 0028-4793 (1998).

153. Lassmann, H., van Horssen, J. & Mahad, D. Progressive multiple sclerosis: pathology and pathogenesis. *Nature Reviews Neurology* **8,** 647–656. ISSN: 1759-4758 (2012).

154. Weinshenker, B. G. *et al.* the Natural History of Multiple Sclerosis : a Geographically Based Study I. Clinical Course and Disability. *Brain* **112,** 133–146 (1989).

155. Cottrell, D. A. *et al.* The natural history of multiple sclerosis: a geographically based study. 6. Applications to planning and interpretation of clinical therapeutic trials in primary progressive multiple sclerosis. *Brain : a journal of neurology* **122 (Pt 4,** 641–7. ISSN: 0006-8950 (1999).

156. Weinshenker, B. G. *et al.* The natural history of multiple sclerosis: a geographically based study. 4. Applications to planning and interpretation of clinical therapeutic trials. *Brain : a journal of neurology* **112,** 1057–1067. ISSN: 0006-8950 (1991).

157. Ebers, G. C. Environmental factors and multiple sclerosis. *The Lancet Neurology* **7,** 268–277. ISSN: 14744422 (2008).

158. Gourraud, P.-A., Harbo, H. F., Hauser, S. L. & Baranzini, S. E. The genetics of multiple sclerosis: an up-to-date review. *Immunological Reviews* **248,** 87–103 (2012).

159. Kurtzke, J. F. & Heltberg, A. Multiple sclerosis in the Faroe Islands: An epitome. *Journal of Clinical Epidemiology* **54,** 1–22. ISSN: 08954356 (2001).

160. Beck, C. a., Metz, L. M., Svenson, L. W. & Patten, S. B. Regional variation of multiple sclerosis prevalence in Canada. *Multiple Sclerosis* **11,** 516–9. ISSN: 1352-4585 (2005).

161. Dean, G. Annual incidence, prevalence, and mortality of multiple sclerosis in white South-African-born and in white immigrants to South Africa. *British Journal of Medicine* **2,** 724–730. ISSN: 0959-8138 (1967).

162. Alter, M., Leibowitz, U. & Speer, J. Risk of Multiple Sclerosis Related to Age at Immigration to Israel. *Arch Neurol* **15** (1966).

163. Cantorna, M. T. Vitamin D and multiple sclerosis: An update. *Nutrition Reviews* **66,** 135–138. ISSN: 1973798X (2008).

164. Lucchinetti, C. *et al.* Heterogeneity of multiple sclerosis lesions: Implications for the pathogenesis of demyelination. *Annals of Neurology* **47,** 707–717. ISSN: 03645134 (2000).

165. Stys, P. K., Zamponi, G. W., Van Minnen, J. & Geurts, J. J. G. Will the real multiple sclerosis please stand up? *Nature Reviews Neuroscience* **13,** 507–514. ISSN: 1471003X (2012).

166. Trapp, B. D. & Nave, K.-A. Multiple sclerosis: an immune or neurodegenerative disorder? *Annual review of neuroscience* **31,** 247–269. ISSN: 0147-006X (2008).

167. Haines, J. *et al.* A complete genomic screen for multiple sclerosis underscores a role for the major histocompatability complex. *Nature Genetics* **13,** 469–471. ISSN: 1061-4036 (1996).

168. Ota, K. *et al.* T-cell recognition of an immuno-dominant myelin basic protein epitope in multiple sclerosis. *Nature* **346,** 183–187. ISSN: 00219797 (1990).

169. Zhang, J. & Raus, J. Myelin basic protein-reactive T cells in multiple sclerosis: Pathologic relevance and therapeutic targeting. *Cytotechnology* **16,** 181–187. ISSN: 09209069 (1994).

170. Huseby, E. S. *et al.* A pathogenic role for myelin-specific CD8(+) T cells in a model for multiple sclerosis. *The Journal of experimental medicine* **194,** 669–676. ISSN: 0022-1007 (2001).

171. Sun, D *et al.* Role of chemokines, neuronal projections, and the blood-brain barrier in the enhancement of cerebral EAE following focal brain damage. *Journal of neuropathology and experimental neurology* **59,** 1031–1043. ISSN: 0022-3069 (2000).

172. Bauer, J *et al.* The role of macrophages, perivascular cells, and microglial cells in the pathogenesis of experimental autoimmune encephalomyelitis. *Glia* **15,** 437–46. ISSN: 0894-1491 (1995).

173. Ajami, B., Bennett, J. L., Krieger, C., McNagny, K. M. & Rossi, F. M. V. Infiltrating monocytes trigger EAE progression, but do not contribute to the resident microglia pool. *Nature Neuroscience* **14,** 1142–1150. ISSN: 10976256 (2011).

174. Mildner, A. *et al.* CCR2+Ly-6Chimonocytes are crucial for the effector phase of autoimmunity in the central nervous system. *Brain* **132,** 2487–2500. ISSN: 00068950 (2009).

175. Saederup, N. *et al.* Selective chemokine receptor usage by central nervous system myeloid cells in CCR2-red fluorescent protein knock-in mice. *PLoS ONE* **5.** ISSN: 19326203. doi:10.1371/journal.pone.0013693 (2010).

176. Tran, E., Hoekstra, K., van Rooijen, N., Dijkstra, C. & Owens, T. Immune Invasion of the Central Nervous System Parenchyma and Experimental Allergic Encephalomyelitis, But Not Leukocyte Extravasation from Blood, Are Prevented in Macrophage-Depleted Mice. *The Journal of Immunology* **161,** 3767–3775 (1998).

177. Barnett, M. H. & Prineas, J. W. Relapsing and Remitting Multiple Sclerosis: Pathology of the Newly Forming Lesion. *Annals of Neurology* **55,** 458–468. ISSN: 03645134 (2004).

178. Henderson, A. P. D., Barnett, M. H., Parratt, J. D. E. & Prineas, J. W. Multiple sclerosis: Distribution of inflammatory cells in newly forming lesions. *Annals of Neurology* **66,** 739–753. ISSN: 03645134 (2009).

179. Locatelli, G. *et al.* Primary oligodendrocyte death does not elicit anti-CNS immunity. *Nature Neuroscience* **15,** 543–550. ISSN: 1097-6256 (2012).

180. Traka, M., Podojil, J. R., Mccarthy, D. P., Miller, S. D. & Popko, B. Oligodendrocyte death results in immune-mediated CNS demyelination. *Nature Neuroscience* **19,** 65–74. ISSN: 15461726 (2015).

181. Stadelmann, C., Wegner, C. & Brück, W. Inflammation, demyelination, and degeneration - Recent insights from MS pathology. *Biochimica et Biophysica Acta - Molecular Basis of Disease* **1812,** 275–282. ISSN: 09254439 (2011).

182. Bjartmar, C., Kidd, G., Mörk, S., Rudick, R. & Trapp, B. D. Neurological disability correlates with spinal cord axonal loss and reduced N-acetyl aspartate in chronic multiple sclerosis patients. *Annals of Neurology* **48,** 893–901. ISSN: 03645134 (2000).

183. Ferguson, B, Matyszak, M. K., Esiri, M. M. & Perry, V. H. Axonal damage in acute multiple sclerosis lesions. *Brain : a journal of neurology* **120 (Pt 3,** 393–399. ISSN: 0006-8950 (1997).

184. Pitt, D, Werner, P & Raine, C. S. Glutamate excitotoxicity in a model of multiple sclerosis. *Nat Med* **6,** 67–70. ISSN: 1078-8956 (2000).

185. Groom, A. J., Smith, T. & Turski, L. Multiple sclerosis and glutamate. *Annals of the New York Academy of Sciences* **993,** 229–75; discussion 287–8. ISSN: 0077-8923 (2003).

186. Srinivasan, R., Sailasuta, N., Hurd, R., Nelson, S. & Pelletier, D. Evidence of elevated glutamate in multiple sclerosis using magnetic resonance spectroscopy at 3 T. *Brain* **128,** 1016–1025. ISSN: 00068950 (2005).

187. Witte, M. E., Mahad, D. J., Lassmann, H. & van Horssen, J. Mitochondrial dysfunction contributes to neurodegeneration in multiple sclerosis. *Trends in Molecular Medicine* **20,** 179–187. ISSN: 14714914 (2014).

188. Dutta, R. *et al.* Mitochondrial dysfunction as a cause of axonal degeneration in multiple sclerosis patients. *Annals of Neurology* **59,** 478–489. ISSN: 03645134 (2006).

189. Franklin, R. J. M., Ffrench-Constant, C., Edgar, J. M. & Smith, K. J. Neuroprotection and repair in multiple sclerosis. *Nature Reviews Neurology* **8,** 624–634. ISSN: 17594758 (2012).

190. Reddy, H *et al.* Evidence for adaptive functional changes in the cerebral cortex with axonal injury from multiple sclerosis. *Brain* **123,** 2314–20. ISSN: 0006-8950 (2000).

191. Pantano, P. *et al.* Cortical motor reorganization after a single clinical attack of multiple sclerosis. *Brain* **125,** 1607–1615. ISSN: 0006-8950 (2002).

192. Parry, A. M. M., Scott, R. B., Palace, J., Smith, S. & Matthews, P. M. Potentially adaptive functional changes in cognitive processing for patients with multiple sclerosis and their acute modulation by rivastigmine. *Brain* **126,** 2750–2760. ISSN: 00068950 (2003).

193. Morgen, K. *et al.* Distinct mechanisms of altered brain activation in patients with multiple sclerosis. *NeuroImage* **37,** 937–946. ISSN: 10538119 (2007).

194. Trapp, B. D., Ransohoff, R. M., Fisher, E. & Rudick, R. a. Neurodegeneration in Multiple Sclerosis: Relationship to Neurological Disability. *The Neuroscientist* **5,** 48–57. ISSN: 1073-8584 (1999).

195. Franklin, R. J. M. & Goldman, S. A. Glia Disease and Repair Remyelination. *Cold Spring Harbor Perspectives in Biology.* doi:10.1101/cshperspect.a020594 (2015).

196. Blakemore, W. F. & Franklin, R. J. M. Remyelination in experimental models of toxin-induced demyelination. *Current Topics in Microbiology and Immunology* **318,** 193–212. ISSN: 0070217X (2008).

197. Prineas, J. W., Kwon, E. E., Cho, E. S. & Sharer, L. R. Continual breakdown and regeneration of myelin in progressive multiple sclerosis plaques. *Annals of the New York Academy of Sciences* **436,** 11–32. ISSN: 0077-8923 (1984).

198. Patrikios, P. *et al.* Remyelination is extensive in a subset of multiple sclerosis patients. *Brain* **129,** 3165–3172. ISSN: 14602156 (2006).

199. Patani, R., Balaratnam, M., Vora, A. & Reynolds, R. Remyelination can be extensive in multiple sclerosis despite a long disease course. *Neuropathology and Applied Neurobiology* **33,** 277–287. ISSN: 03051846 (2007).

200. Bramow, S. *et al.* Demyelination versus remyelination in progressive multiple sclerosis. *Brain* **133,** 2983–2998. ISSN: 14602156 (2010).

201. Dutta, R. & Trapp, B. D. Mechanisms of neuronal dysfunction and degeneration in multiple sclerosis. *Progress in Neurobiology* **93,** 1–12. ISSN: 03010082 (2011).

202. Kornek, B. *et al.* Multiple sclerosis and chronic autoimmune encephalomyelitis: A comparative quantitative study of axonal injury in active, inactive, and remyelinated lesions. *American Journal of Pathology* **157,** 267–276. ISSN: 00029440 (2000).

203. Irvine, K. A. & Blakemore, W. F. Remyelination protects axons from demyelination-associated axon degeneration. *Brain,* 1464–1477 (2008).

204. Pohl, H. B. F. *et al.* Genetically Induced Adult Oligodendrocyte Cell Death Is Associated with Poor Myelin Clearance, Reduced Remyelination, and Axonal Damage. *Journal of Neuroscience* **31,** 1069–1080. ISSN: 0270-6474 (2011).

205. Mei, F. *et al.* Accelerated remyelination during inflammatory demyelination prevents axonal loss and improves functional recovery. *eLife* **5,** 1–21. ISSN: 2050084X (2016).

206. Smith, K. J., Blakemore, W. F. & Mcdonald, W. I. Central remyelination restores secure conduction. *Nature* **280,** 395–396. ISSN: 00068950 (1979).

207. Duncan, I., Brower, A, Kondo, Y, Curlee, J. & Schultz, R. Extensive remyelination of the CNS leads to functional recovery. *PNAS* **106,** 12207–12208. ISSN: 0027-8424 (2009).

208. Kuhlmann, T. *et al.* Differentiation block of oligodendroglial progenitor cells as a cause for remyelination failure in chronic multiple sclerosis. *Brain* **131,** 1749–1758. ISSN: 00068950 (2008).

209. Howe, C. L. & Mobley, W. C. Signaling Endosome Hypothesis: A Cellular Mechanism for Long Distance Communication. *Journal of Neurobiology* **58,** 207–216. ISSN: 00223034 (2004).

210. Howe, C. L., Howe, C. L., Mobley, W. C. & Mobley, W. C. Long-distance retrograde neurotrophic signaling. *Current Opinion in Neurobiology* **15,** 40–48. ISSN: 09594388 (2005).

211. Beattie, E. C. *et al.* A signaling endosome hypothesis to explain NGF actions: Potential implications for neurodegeneration. *Cold Spring Harbor Symposia on Quantitative Biology* **61,** 389–406. ISSN: 00917451 (1996).

212. Bitsch, a, Schuchardt, J, Bunkowski, S, Kuhlmann, T & Brück, W. Acute axonal injury in multiple sclerosis. Correlation with demyelination and inflammation. *Brain : a journal of neurology* **123 (Pt 6,** 1174–1183. ISSN: 0006-8950 (2000).

213. Craner, M. J., Hains, B. C., Lo, A. C., Black, J. a. & Waxman, S. G. Co-localization of sodium channel Nav1.6 and the sodium-calcium exchanger at sites of axonal injury in the spinal cord in EAE. *Brain* **127,** 294–303. ISSN: 00068950 (2004).

214. Confavreux, C. & Vukusic, S. Age at disability milestones in multiple sclerosis. *Brain* **129,** 595–605. ISSN: 00068950 (2006).

215. Absinta, M. *et al.* Persistent 7-tesla phase rim predicts poor outcome in new multiple sclerosis patient lesions. *Journal of Clinical Investigation* **126,** 2597–2609. ISSN: 15588238 (2016).

216. Goldschmidt, T., Antel, J., König, F. B., Brück, W. & Kuhlmann, T. Remyelination capacity of the MS brain decreases with disease chronicity. *Neurology* **72,** 1914–1921. ISSN: 00283878 (2009).

217. Sim, F. J., Zhao, C., Penderis, J. & Franklin, R. J. M. The age-related decrease in CNS remyelination efficiency is attributable to an impairment of both oligodendrocyte progenitor recruitment and differentiation. *The Journal of neuroscience : the official journal of the Society for Neuroscience* **22,** 2451–2459. ISSN: 1070-8022 (2002).

218. Franklin, R. J. M. & Ffrench-Constant, C. Remyelination in the CNS: from biology to therapy. *Nature reviews. Neuroscience* **9,** 839–855. ISSN: 1471-003X (2008).

219. Wolswijk, G. Chronic stage multiple sclerosis lesions contain a relatively quiescent population of oligodendrocyte precursor cells. *The Journal of neuroscience : the official journal of the Society for Neuroscience* **18,** 601–609. ISSN: 0270-6474 (1998).

220. Chang, a, Nishiyama, a, Peterson, J, Prineas, J & Trapp, B. D. NG2-positive oligodendrocyte progenitor cells in adult human brain and multiple sclerosis lesions. *The Journal of neuroscience : the official journal of the Society for Neuroscience* **20,** 6404–6412. ISSN: 0270-6474 (2000).

221. Doucette, J. R., Jiao, R. & Nazarali, A. J. Age-related and cuprizone-induced changes in myelin and transcription factor gene expression and in oligodendrocyte cell densities in the rostral corpus callosum of mice. *Cellular and Molecular Neurobiology* **30,** 607–629. ISSN: 02724340 (2010).

222. Lucchinetti, C. *et al.* A quantitative analysis of oligodendrocytes in multiple sclerosis lesions. A study of 113 cases. *Brain* **122,** 2279–2295. ISSN: 00068950 (1999).

223. Shields, S. A., Gilson, J. M., Blakemore, W. F. & Franklin, R. J. M. Remyelination occurs as extensively but more slowly in old rats compared to young rats following gliotoxin-induced CNS demyelination. *Glia* **28,** 77–83. ISSN: 08941491 (1999).

224. Hampton, D. W. *et al.* Focal immune-mediated white matter demyelination reveals an age-associated increase in axonal vulnerability and decreased remyelination efficiency. *American Journal of Pathology* **180,** 1897–1905. ISSN: 00029440 (2012).

225. Pfeifenbring, S., Nessler, S., Wegner, C., Stadelmann, C. & Brück, W. Remyelination After Cuprizone-Induced Demyelination Is Accelerated in Juvenile Mice. *Journal of neuropathology and experimental neurology* **74,** 756–66. ISSN: 1554-6578 (2015).

226. Shen, S. *et al.* Age-dependent epigenetic control of differentiation inhibitors is critical for remyelination efficiency. *Nature Neuroscience* **11,** 1024–1034. ISSN: 10976256 (2008).

227. Charles, P. *et al.* Re-expression of PSA-NCAM by demyelinated axons: an inhibitor of remyelination in multiple sclerosis? *Brain : a journal of neurology* **125,** 1972–1979. ISSN: 0006-8950 (2002).

228. Chang, A, Tourtellotte, W. W., Rudick, R & Trapp, B. D. Premyelinating oligodenrocytes in chronic lesions of multiple sclerosis. *N Engl J Med* **346,** 165–173 (2002).

229. Banati, R. B., Gehrmann, J, Schubert, P & Kreutzberg, G. W. Cytotoxicity of microglia. *Glia* **7,** 111–118. ISSN: 01655728 (1993).

230. Fernandes, A., Miller-Fleming, L. & Pais, T. F. Microglia and inflammation: conspiracy, controversy or control? *Cellular and Molecular Life Sciences,* 3969–3985. ISSN: 1420682X (2014).

231. Kotter, M. R., Setzu, A., Sim, F. J., Van Rooijen, N. & Franklin, R. J. M. Macrophage depletion impairs oligodendrocyte remyelination following lysolecithin-induced demyelination. *Glia* **35,** 204–212. ISSN: 08941491 (2001).

232. Robinson, S. & Miller, R. H. Contact with central nervous system myelin inhibits oligodendrocyte progenitor maturation. *Developmental biology* **216,** 359–368. ISSN: 00121606 (1999).

233. Trapp, B. D., Nishiyama, A., Cheng, D. & Macklin, W. Differentiation and death of premyelinating oligodendrocytes in developing rodent brain. *Journal of Cell Biology* **137,** 459–468. ISSN: 00219525 (1997).

234. Plemel, J. R., Manesh, S. B., Sparling, J. S. & Tetzlaff, W. Myelin inhibits oligodendroglial maturation and regulates oligodendrocytic transcription factor expression. *Glia* **61,** 1471–1487. ISSN: 08941491 (2013).

235. Kotter, M. R., Li, W.-W., Zhao, C. & Franklin, R. J. M. Myelin impairs CNS remyelination by inhibiting oligodendrocyte precursor cell differentiation. *The Journal of neuroscience : the official journal of the Society for Neuroscience* **26,** 328–332. ISSN: 0270-6474 (2006).

236. Vogel, D. Y. *et al.* Macrophages in inflammatory multiple sclerosis lesions have an intermediate activation status. *Journal of Neuroinflammation* **10,** 1. ISSN: 17422094 (2013).

237. Mikita, J. *et al.* Altered M1/M2 activation patterns of monocytes in severe relapsing experimental rat model of multiple sclerosis. Amelioration of clinical status by M2 activated monocyte administration. *Multiple Sclerosis Journal* **17,** 2–15. ISSN: 13524585 (2011).

238. Wingerchuk, D. M. & Carter, J. L. Multiple sclerosis: Current and emerging disease-modifying therapies and treatment strategies. *Mayo Clinic Proceedings* **89,** 225–240. ISSN: 19425546 (2014).

239. Dhib-Jalbut, S. Mechanisms of action of interferons and glatiramer acetate in multiple sclerosis. *Neurology* **58,** S3–9. ISSN: 0028-3878 (2002).

240. Vidal-Jordana, A. New Advances in Disease-Modifying Therapies for Relapsing and Progressive Forms of Multiple Sclerosis. *Neurologic Clinics* **36,** 173–183. ISSN: 07338619 (2018).

241. Hauser, S. L. *et al.* Ocrelizumab versus Interferon Beta-1a in Relapsing Multiple Sclerosis. *New England Journal of Medicine* **376,** 221–234. ISSN: 0028-4793 (2017).

242. Montalban, X. *et al.* Ocrelizumab versus Placebo in Primary Progressive Multiple Sclerosis. *New England Journal of Medicine* **376,** 209–220. ISSN: 0028-4793 (2017).

243. Mei, F. *et al.* Micropillar arrays as a high-throughput screening platform for therapeutics in multiple sclerosis. *Nature medicine* **20,** 954–60. ISSN: 1546-170X (2014).

244. Cadavid, D. *et al.* Safety and efficacy of opicinumab in acute optic neuritis (RENEW): a randomised, placebo-controlled, phase 2 trial. *The Lancet Neurology* **16,** 189–199. ISSN: 14744465 (2017).

245. Mullard, A. Remyelination researchers regroup after proof-of-concept setback in multiple sclerosis. *Nature Reviews Drug Discovery* **15,** 519–521. ISSN: 14741784 (2016).

246. Deshmukh, V. A. *et al.* A regenerative approach to the treatment of multiple sclerosis. *Nature* **502,** 327–332. ISSN: 00280836 (2013).

247. Green, A. J. *et al.* Clemastine fumarate as a remyelinating therapy for multiple sclerosis (ReBUILD): A randomised, controlled, double-blind, crossover trial. *The Lancet* **6736.** ISSN: 1474547X. doi:10.1016/S0140-6736(17)32346-2 (2017).

248. Schwartzbach, C. J. *et al.* Lesion remyelinating activity of GSK239512 versus placebo in patients with relapsing-remitting multiple sclerosis: a randomised, single-blind, phase II study. *Journal of Neurology* **264,** 304–315. ISSN: 14321459 (2017).

249. Sedel, F. *et al.* High doses of biotin in chronic progressive multiple sclerosis: A pilot study. *Multiple Sclerosis and Related Disorders* **4,** 159–169. ISSN: 22110356 (2015).

250. Sedel, F., Bernard, D., Mock, D. M. & Tourbah, A. Targeting demyelination and virtual hypoxia with high-dose biotin as a treatment for progressive multiple sclerosis. *Neuropharmacology* **110,** 644–653. ISSN: 18737064 (2016).

251. Tourbah, A. *et al.* MD1003 (high-dose biotin) for the treatment of progressive multiple sclerosis: A randomised, double-blind, placebo-controlled study. *Multiple Sclerosis Journal* **22,** 1719–1731. ISSN: 1352-4585 (2016).

252. Plemel, J. R., Liu, W.-q. & Yong, V. W. Remyelination therapies : multiple sclerosis. *Nat Rev Drug Discov.* doi:10.1038/nrdnrd.2017.115 (2017).

253. Halliday, A. M., McDonald, W. I. & Mushin, J. Visual evoked response in diagnosis of multiple sclerosis. *British Medical Journal* **4,** 661–664. ISSN: 00071447 (1973).

254. Green, A. J. in *Aminoff's electrodiagnosis in clinical neurology* (ed Aminoff, M.) 6th, 477–503 (Elsevier Saunders, Philadelphia, PA, 2012).

255. Toussaint, D, Périer, O, Verstappen, a & Bervoets, S. Clinicopathological study of the visual pathways, eyes, and cerebral hemispheres in 32 cases of disseminated sclerosis. *Journal of clinical neuro-ophthalmology* **3,** 211–20. ISSN: 0272-846X (1983).

256. Van den Elskamp, I. *et al.* Lesional magnetization transfer ratio: a feasible outcome for remyelinating treatment trials in multiple sclerosis. *Multiple Sclerosis Journal* **16,** 660–669. ISSN: 1352-4585 (2010).

257. Turati, L. *et al.* In vivo quantitative magnetization transfer imaging correlates with histology during de- and remyelination in cuprizone-treated mice. *NMR in Biomedicine* **28,** 327–337. ISSN: 10991492 (2015).

258. Brown, R. A., Narayanan, S. & Arnold, D. L. Segmentation of magnetization transfer ratio lesions for longitudinal analysis of demyelination and remyelination in multiple sclerosis. *NeuroImage* **66,** 103–109. ISSN: 10538119 (2013).

259. Bodini, B. *et al.* Dynamic Imaging of Individual Remyelination Profiles in Multiple Sclerosis. *Annals of Neurology* **79,** 726–738. ISSN: 15318249 (2016).

260. Stankoff, B. *et al.* Imaging central nervous system myelin by positron emission tomography in multiple sclerosis using [methyl-11C]-2-(4-methylaminophenyl)- 6-hydroxybenzothiazole. *Annals of Neurology* **69,** 673–680. ISSN: 03645134 (2011).

261. Kotter, M. R., Zhao, C., Van Rooijen, N. & Franklin, R. J. M. Macrophage-depletion induced impairment of experimental CNS remyelination is associated with a reduced oligodendrocyte progenitor cell response and altered growth factor expression. *Neurobiology of Disease* **18,** 166–175. ISSN: 09699961 (2005).

262. Napoli, I. & Neumann, H. Protective effects of microglia in multiple sclerosis. *Experimental Neurology* **225,** 24–28. ISSN: 00144886 (2010).

263. Ireland, G. *et al. A novel role for Activin-A in Remyelination* in *Poster Presented at Edinburgh Neuroscience Day Conference* (Edinburgh, Scotland, 2014), 3.

264. Ebert, S. *et al.* Activin A concentrations in human cerebrospinal fluid are age-dependent and elevated in meningitis. *Journal of the Neurological Sciences* **250,** 50–57. ISSN: 0022510X (2006).

265. Luisi, S, Florio, P, Reis, F. M. & Petraglia, F. Expression and secretion of activin A: possible physiological and clinical implications. *European journal of endocrinology / European Federation of Endocrine Societies* **145,** 225–236. ISSN: 0804-4643 (2001).

266. Phillips, D. J., de Kretser, D. M. & Hedger, M. P. Activin and related proteins in inflammation: Not just interested bystanders. *Cytokine and Growth Factor Reviews* **20,** 153–164. ISSN: 13596101 (2009).

267. Robertson, D. M., Foulds, L. M., Prisk, M & Hedger, M. P. Inhibin/activin beta-subunit monomer: isolation and characterization. *Endocrinology* **130,** 1680–1687. ISSN: 0013-7227 (1992).

268. Brown, C. W., Houston-Hawkins, D. E., Woodruff, T. K. & Matzuk, M. M. Insertion of Inhbb into the Inhba locus rescues the Inhba-null phenotype and reveals new activin functions. *Nature Genetics* **25,** 453–457. ISSN: 10614036 (2000).

269. Wharton, K. & Derynck, R. TGFbeta family signaling: novel insights in development and disease. *Development (Cambridge, England)* **136,** 3691–3697. ISSN: 0950-1991 (2009).

270. Tsuchida, K. *et al.* Activin signaling as an emerging target for therapeutic interventions. *Cell communication and signaling : CCS* **7,** 15. ISSN: 1478-811X (2009).

271. Palazuelos, J., Klingener, M. & Aguirre, A. TGFβ Signaling Regulates the Timing of CNS Myelination by Modulating Oligodendrocyte Progenitor Cell Cycle Exit through SMAD3/4/FoxO1/Sp1. *The Journal of neuroscience : the official journal of the Society for Neuroscience* **34,** 7917–30. ISSN: 1529-2401 (2014).

272. Dutta, D. J. *et al.* Combinatorial actions of Tgfβ and Activin ligands promote oligodendrocyte development and CNS myelination. *Development (Cambridge, England)* **141,** 2414–28. ISSN: 1477-9129 (2014).

273. He, J.-T. *et al.* Neuroprotective Effects of Exogenous Activin A on Oxygen-Glucose Deprivation in PC12 Cells. *Molecules* **17,** 315–327 (2011).

274. Abdipranoto-Cowley, A. *et al.* Activin A is essential for neurogenesis following neurodegeneration. *Stem Cells* **27,** 1330–1346. ISSN: 10665099 (2009).

275. Satoh, M., Sugino, H. & Yoshida, T. Activin promotes astrocytic differentiation of a multipotent neural stem cell line and an astrocyte progenitor cell line from murine central nervous system. *Neuroscience Letters* **284,** 143–146. ISSN: 03043940 (2000).

276. Rodríguez-Martínez, G., Molina-Hernández, A. & Velasco, I. Activin a promotes neuronal differentiation of cerebrocortical neural progenitor cells. *PLoS ONE* **7.** ISSN: 19326203. doi:10.1371/journal.pone.0043797 (2012).

277. Krieglstein, K., Zheng, F., Unsicker, K. & Alzheimer, C. More than being protective: Functional roles for TGF-??/activin signaling pathways at central synapses. *Trends in Neurosciences* **34,** 421–429. ISSN: 01662236 (2011).

278. Link, A. S., Zheng, F. & Alzheimer, C. Activin Signaling in the Pathogenesis and Therapy of Neuropsychiatric Diseases. *Frontiers in Molecular Neuroscience* **9,** 1–7. ISSN: 1662-5099 (2016).

279. Hughes, P. E., Alexi, T., Williams, C. E., Clark, R. G. & Gluckman, P. D. Administration of recombinant human activin-A has powerful neurotrophic effects on select striatal phenotypes in the quinolinic acid lesion model of Huntington's disease. *Neuroscience* **92,** 197–209. ISSN: 03064522 (1999).

280. Stayte, S., Rentsch, P., Li, K. M. & Vissel, B. Activin a protects midbrain neurons in the 6-hydroxydopamine mouse model of Parkinson's disease. *PLoS ONE* **10,** 1–15. ISSN: 19326203 (2015).

281. Lau, D., Bengtson, C. P., Buchthal, B. & Bading, H. BDNF Reduces Toxic Extrasynaptic NMDA Receptor Signaling via Synaptic NMDA Receptors and Nuclear-Calcium-Induced Transcription of inhba/Activin A. *Cell Reports* **12,** 1353–1366. ISSN: 22111247 (2015).

282. Liang, X., Draghi, N. a. & Resh, M. D. Signaling from integrins to Fyn to Rho family GTPases regulates morphologic differentiation of oligodendrocytes. *The Journal of neuroscience : the official journal of the Society for Neuroscience* **24,** 7140–7149. ISSN: 0270-6474 (2004).

283. Thurnherr, T. *et al.* Cdc42 and Rac1 signaling are both required for and act synergistically in the correct formation of myelin sheaths in the CNS. *The Journal of neuroscience : the official journal of the Society for Neuroscience* **26,** 10110–10119. ISSN: 0270-6474 (2006).

284. Flores, A. I. *et al.* Constitutively active Akt induces enhanced myelination in the CNS. *The Journal of neuroscience : the official journal of the Society for Neuroscience* **28,** 7174–7183. ISSN: 0270-6474 (2008).

285. Guardiola-Diaz, H. M., Ishii, A. & Bansal, R. Erk1/2 MAPK and mTOR signaling sequentially regulates progression through distinct stages of oligodendrocyte differentiation. *Glia* **60,** 476–486. ISSN: 08941491 (2012).

286. Derynck, R. & Zhang, Y. E. Smad-dependent and Smad-independent pathways in TGF-. *Nature* **4,** 577–84. ISSN: 0028-0836 (2003).

287. Thompson, T. B., Lerch, T. F., Cook, R. W., Woodruff, T. K. & Jardetzky, T. S. The structure of the follistatin: Activin complex reveals antagonism of both type I and type II receptor binding. *Developmental Cell* **9,** 535–543. ISSN: 15345807 (2005).

288. Welt, C., Sidis, Y., Keutmann, H. & Schneyer, A. Activins, Inhibins, and Follistatins: From Endocrinology to Signaling. A Paradigm for the New Millenium. *Experimental Biology and Medicine* **227,** 724–752 (2002).

289. Shen, M. M. Nodal signaling: developmental roles and regulation. *Development* **134,** 1023–1034. ISSN: 0950-1991 (2007).

290. Lee, S.-J. Identification of a Novel Member (GDF-1) of the Transforming Growth Factor-β Superfamily. *Molecular Endocrinology* **4,** 1034–1040. ISSN: 0888-8809 (1990).

291. Hanson, L. R. *et al.* Intranasal delivery of growth differentiation factor 5 to the central nervous system. *Drug Delivery* **19,** 149–154. ISSN: 1071-7544 (2012).

292. O'Keeffe, G. W., Hanke, M., Pohl, J. & Sullivan, A. M. Expression of growth differentiation factor-5 in the developing and adult rat brain. *Brain research. Developmental brain research* **151,** 199–202. ISSN: 0165-3806 (Print) (2004).

293. Iwasaki, S. *et al.* Expression of myostatin in neural cells of the olfactory system. *Molecular Neurobiology* **47,** 1–8. ISSN: 08937648 (2013).

294. Katsimpardi, L. *et al.* Vascular and neurogenic rejuvenation of the aging mouse brain by young systemic factors. *Science (New York, N.Y.)* **344,** 630–4. ISSN: 1095-9203 (2014).

295. Wu, H. H. *et al.* Autoregulation of neurogenesis by GDF11. *Neuron* **37,** 197–207. ISSN: 08966273 (2003).

296. Liu, J.-P. The function of growth/differentiation factor 11 (Gdf11) in rostrocaudal patterning of the developing spinal cord. *Development (Cambridge, England)* **133,** 2865–2874. ISSN: 0950-1991 (2006).

297. Mabie, P. C., Mehler, M. F. & Kessler, J. a. Multiple roles of bone morphogenetic protein signaling in the regulation of cortical cell number and phenotype. *The Journal of neuroscience : the official journal of the Society for Neuroscience* **19,** 7077–7088. ISSN: 1529-2401 (1999).

298. Wang, Y *et al.* Bone morphogenetic protein-6 reduces ischemia-induced brain damage in rats. *Stroke; a journal of cerebral circulation* **32,** 2170–2178. ISSN: 0039-2499 (2001).

299. Crews, L. *et al.* Increased BMP6 levels in the brains of Alzheimer's disease patients and APP transgenic mice are accompanied by impaired neurogenesis. *The Journal of neuroscience : the official journal of the Society for Neuroscience* **30,** 12252–12262. ISSN: 0270-6474 (2010).

300. Chou, J. *et al.* Neuroregenerative effects of BMP7 after stroke in rats. *Journal of the Neurological Sciences* **240,** 21–29. ISSN: 0022510X (2006).

301. Wyatt, A. W., Osborne, R. J., Stewart, H. & Ragge, N. K. Bone Morphogenetic Protein 7 (BMP7) mutations are associated with variable ocular, brain, ear, palate, and skeletal anomalies. *Human Mutation* **31,** 781–787. ISSN: 10597794 (2010).

302. Zhang, Y *et al.* An RNA-sequencing transcriptome and splicing database of glia, neurons, and vascular cells of the cerebral cortex. *Journal of Neuroscience* **34,** 11929–11947. ISSN: 1529-2401 (2014).

303. Söderström, S. & Ebendal, T. Localized expression of BMP and GDF mRNA in the rodent brain. *Journal of Neuroscience Research* **56,** 482–492. ISSN: 03604012 (1999).

304. Attisano, L, Wrana, J. L., Cheifetz, S & Massagué, J. Novel activin receptors: distinct genes and alternative mRNA splicing generate a repertoire of serine/threonine kinase receptors. *Cell* **68,** 97–108. ISSN: 00928674 (1992).

305. Sako, D. *et al.* Characterization of the ligand binding functionality of the extracellular domain of activin receptor type IIB. *Journal of Biological Chemistry* **285,** 21037–21048. ISSN: 00219258 (2010).

306. Massagué, J. How cells read TGF-beta signals. *Nature reviews. Molecular cell biology* **1,** 169–178. ISSN: 1471-0072 (2000).

307. Massagué, J. TGFβ signalling in context. *Nature Reviews Molecular Cell Biology* **13,** 616–630. ISSN: 14710072 (2012).

308. Gordon, K. J. & Blobe, G. C. Role of transforming growth factor-β superfamily signaling pathways in human disease. *Biochimica et Biophysica Acta - Molecular Basis of Disease* **1782,** 197–228. ISSN: 09254439 (2008).

309. Lewis, K. A. *et al.* Betaglycan binds inhibin and can mediate functional antagonism of activin signalling. *Nature* **404,** 411–414. ISSN: 00280836 (2000).

310. Villapol, S., Wang, Y., Adams, M. & Symes, A. J. Smad3 deficiency increases cortical and hippocampal neuronal loss following traumatic brain injury. *Experimental Neurology* **250,** 353–365. ISSN: 00144886 (2013).

311. Chen, W. & Ten Dijke, P. Immunoregulation by members of the TGFβ superfamily. *Nature Reviews Immunology* **16,** 723–740. ISSN: 14741741 (2016).

312. McKinnon, R. D., Piras, G, Ida, J. a. & Dubois-Dalcq, M. A role for TGF-beta in oligodendrocyte differentiation. *The Journal of cell biology* **121,** 1397–1407. ISSN: 0021-9525 (1993).

313. Lalive, P. H. *et al.* TGF-β-treated microglia induce oligodendrocyte precursor cell chemotaxis through the HGF-c-Met pathway. *European Journal of Immunology* **35,** 727–737. ISSN: 00142980 (2005).

314. Schulz, R., Vogel, T., Dressel, R. & Krieglstein, K. TGF-β superfamily members, ActivinA and TGF-β1, induce apoptosis in oligodendrocytes by different pathways. *Cell and Tissue Research* **334,** 327–338. ISSN: 0302766X (2008).

315. Schuster, N. *et al.* TGF-β induces cell death in the oligodendroglial cell line OLI-neu. *Glia* **40,** 95–108. ISSN: 08941491 (2002).

316. Siegel, P. M. & Massagué, J. Cytostatic and apoptotic actions of TGF-β in homeostasis and cancer. *Nature Reviews Cancer* **3,** 807 (2003).

317. Li, M. O. & Flavell, R. A. TGF-β: A Master of All T Cell Trades. *Cell* **134,** 392–404. ISSN: 0092-8674 (2008).

318. Vergelli, M *et al.* Transforming growth factorβ1 inhibits the proliferation of rat astrocytes induced by serum and growth factors. *Journal of Neuroscience Research* **40,** 127–133. ISSN: 0360-4012 (1995).

319. García-Campmany, L. & Martí, E. The TGFβ intracellular effector Smad3 regulates neuronal differentiation and cell fate specification in the developing spinal cord. *Development* **134,** 65 LP –75 (2007).

320. Misumi, S. *et al.* Enhanced neurogenesis from neural progenitor cells with G1/S-phase cell cycle arrest is mediated by transforming growth factor β1. *European Journal of Neuroscience* **28,** 1049–1059. ISSN: 0953816X (2008).

321. Sabo, J. K., Aumann, T. D., Merlo, D., Kilpatrick, T. J. & Cate, H. S. Remyelination is altered by bone morphogenic protein signaling in demyelinated lesions. *The Journal of neuroscience : the official journal of the Society for Neuroscience* **31,** 4504–4510. ISSN: 0270-6474 (2011).

322. Petersen, M. A. *et al.* Fibrinogen Activates BMP Signaling in Oligodendrocyte Progenitor Cells and Inhibits Remyelination after Vascular Damage. *Neuron,* 1–10. ISSN: 08966273 (2017).

323. Grinspan, J. B. in *Vitamins & Hormones* 195–222 (Academic Press, 2015). ISBN: 9780128024423. doi:10.1016/BS.VH.2015.05.005.

324. Fuller, M. L. *et al.* Bone morphogenetic proteins promote gliosis in demyelinating spinal cord lesions. *Annals of Neurology* **62,** 288–300. ISSN: 03645134 (2007).

325. See, J. *et al.* Oligodendrocyte maturation is inhibited by bone morphogenetic protein. *Molecular and Cellular Neuroscience* **26,** 481–492. ISSN: 10447431 (2004).

326. Ara, J. *et al.* Bone Morphogenetic Proteins 4, 6, and 7 Are Up-Regulated in Mouse Spinal Cord during Experimental Autoimmune Encephalomyelitis. *Journal of neuroscience research* **86,** 368–377. ISSN: 03604012 (2008).

327. Dillenburg, A. *et al.* Activin receptors regulate the oligodendrocyte lineage in health and disease. *Acta Neuropathologica.* ISSN: 0001-6322. doi:10.1007/s00401-018-1813-3 (2018).

328. Tan, G. A. *et al.* Organotypic Cultures from the Adult CNS: A Novel Model to Study Demyelination and Remyelination Ex Vivo. *Cellular and molecular neurobiology* **38,** 317–328. ISSN: 1573-6830 (2017).

329. Arsenault, J. & O'Brien, J. A. Optimized heterologous transfection of viable adult organotypic brain slices using an enhanced gene gun. *BMC Research Notes* **6.** ISSN: 17560500. doi:10.1186/1756-0500-6-544 (2013).

330. Li, Q., Han, X. & Wang, J. Organotypic Hippocampal Slices as Models for Stroke and Traumatic Brain Injury. *Molecular Neurobiology* **53,** 4226–4237. ISSN: 15591182 (2016).

331. Hinks, G. L. & Franklin, R. J. Delayed changes in growth factor gene expression during slow remyelination in the CNS of aged rats. *Molecular and Cellular Neuroscience* **16,** 542–556. ISSN: 10447431 (2000).

332. Grabert, K. *et al.* Microglial brain regionâ 'dependent diversity and selective regional sensitivities to aging. *Nature Neuroscience* **19,** 504–516. ISSN: 15461726 (2016).

333. Zhao, C., Li, W.-W. & Franklin, R. J. M. Differences in the early inflammatory responses to toxin-induced demyelination are associated with the age-related decline in CNS remyelination. *Neurobiology of Aging* **27,** 1298–1307. ISSN: 0197-4580 (2006).

334. Beckmann, N. *et al.* Brain region-specific enhancement of remyelination and prevention of demyelination by the CSF1R kinase inhibitor BLZ945. *Acta Neuropathologica Communications* **6,** 9. ISSN: 2051-5960 (2018).

335. Ornelas, I. M. *et al.* Heterogeneity in oligodendroglia: Is it relevant to mouse models and human disease? *Journal of Neuroscience Research* **94,** 1421–1433. ISSN: 10974547 (2016).

336. Bakiri, Y., Káradóttir, R., Cossell, L. & Attwell, D. Morphological and electrical properties of oligodendrocytes in the white matter of the corpus callosum and cerebellum. *Journal of Physiology* **589,** 559–573. ISSN: 00223751 (2011).

337. Goebbels, S. *et al.* A neuronal PI(3,4,5)P 3 -dependent program of oligodendrocyte precursor recruitment and myelination. *Nature Neuroscience* **20,** 10–15. ISSN: 15461726 (2017).

338. Weiss, A. & Attisano, L. The TGFbeta superfamily signaling pathway. *Wiley Interdisciplinary Reviews: Developmental Biology* **2,** 47–63. ISSN: 17597684 (2013).

339. Hooi, H. K. & Hearn, M. T. W. A molecular recognition paradigm: Promiscuity associated with the ligand-receptor interactions of the activin members of the TGF-?? superfamily. *Journal of Molecular Recognition* **18,** 385–403. ISSN: 09523499 (2005).

340. Aykul, S. & Martinez-Hackert, E. Transforming growth factor-β family ligands can function as antagonists by competing for type II receptor binding. *Journal of Biological Chemistry* **291,** 10792–10804. ISSN: 1083351X (2016).

341. Vale, W. *et al.* Activins and inhibins and their signaling. *Annals of the New York Academy of Sciences* **1038,** 142–147. ISSN: 00778923 (2004).

342. Mueller, T. D. & Nickel, J. Promiscuity and specificity in BMP receptor activation. *FEBS Letters* **586,** 1846–1859. ISSN: 00145793 (2012).

343. Goumans, M. J. & Mummery, C. Functional analysis of the TGFbeta receptor/Smad pathway through gene ablation in mice. *The International journal of developmental biology* **44,** 253–65. ISSN: 0214-6282 (2000).

344. Gray, P. C., Harrison, C. A. & Vale, W. Cripto forms a complex with activin and type II activin receptors and can block activin signaling. *Proceedings of the National Academy of Sciences of the United States of America* **100,** 5193–8. ISSN: 0027-8424 (2003).

345. Cheng, S. K., Olale, F., Brivanlou, A. H. & Schier, A. F. Lefty blocks a subset of TGFβ signals by antagonizing EGF-CFC coreceptors. *PLoS Biology* **2.** ISSN: 15449173. doi:10.1371/journal.pbio.0020030 (2004).

346. Maier, T., Güell, M. & Serrano, L. Correlation of mRNA and protein in complex biological samples. *FEBS Letters* **583,** 3966–3973. ISSN: 00145793 (2009).

347. Koussounadis, A., Langdon, S. P., Um, I. H., Harrison, D. J. & Smith, V. A. Relationship between differentially expressed mRNA and mRNA-protein correlations in a xenograft model system. *Scientific Reports* **5,** 1–9. ISSN: 20452322 (2015).

348. De Sousa Abreu, R., Penalva, L. O., Marcotte, E. M. & Vogel, C. Global signatures of protein and mRNA expression levels. *Molecular BioSystems* **5,** 1512–1526. ISSN: 1742206X (2009).

349. Lee, S. J. Expression of growth/differentiation factor 1 in the nervous system: conservation of a bicistronic structure. *Proceedings of the National Academy of Sciences of the United States of America* **88,** 4250–4. ISSN: 0027-8424 (1991).

350. Cheng, S. K., Olale, F., Bennett, J. T., Brivanlou, A. H. & Schier, A. F. EGF-CFC proteins are essential coreceptors for the TGF-β signals VG1 and GDF1. *Genes and Development* **17,** 31–36. ISSN: 08909369 (2003).

351. Lee, Y.-S. & Lee, S.-J. Regulation of GDF-11 and myostatin activity by GASP-1 and GASP-2. *Proceedings of the National Academy of Sciences* **110,** E3713–E3722. ISSN: 0027-8424 (2013).

352. Walker, R. G. *et al.* Structural basis for potency differences between GDF8 and GDF11. *BMC Biology* **15,** 1–22. ISSN: 17417007 (2017).

353. Egerman, M. A. *et al.* GDF11 Increases with Age and Inhibits Skeletal Muscle Regeneration. *Cell Metabolism* **22,** 164–174. ISSN: 19327420 (2015).

354. Yanagita, M. BMP antagonists: Their roles in development and involvement in pathophysiology. *Cytokine and Growth Factor Reviews* **16,** 309–317. ISSN: 13596101 (2005).

355. Walsh, D. W., Godson, C., Brazil, D. P. & Martin, F. Extracellular BMP-antagonist regulation in development and disease: Tied up in knots. *Trends in Cell Biology* **20,** 244–256. ISSN: 09628924 (2010).

356. Winkler, D. G. *et al.* Osteocyte control of bone formation via sclerostin, a novel BMP antagonist. *EMBO Journal* **22,** 6267–6276. ISSN: 02614189 (2003).

357. Kusu, N. *et al.* Sclerostin is a novel secreted osteoclast-derived bone morphogenetic protein antagonist with unique ligand specificity. *Journal of Biological Chemistry* **278,** 24113–24117. ISSN: 00219258 (2003).

358. Guo, X. & Wang, X.-F. Signaling cross-talk between TGF-b/BMP and other pathways. *Cell Research* **19,** 71–88 (2009).

359. Lu, L. *et al.* Synergistic effect of TGF-β superfamily members on the induction of Foxp3+ regulatory T cells. *European Journal of Immunology* **40,** 142–152 (2010).

360. Wells, B. S., Pistillo, D., Barnhart, E. & Desplan, C. Parallel activin and BMP signaling coordinates R7/R8 photoreceptor subtype pairing in the stochastic Drosophila retina. *eLife* **6,** 1–20. ISSN: 2050084X (2017).

361. Diederichsen, A. C. *et al.* A comparison of flow cytometry and immunohistochemistry in human colorectal cancers. *APMIS : acta pathologica, microbiologica, et immunologica Scandinavica* **106,** 562–70. ISSN: 0903-4641 (1998).

362. Jung, K. M. *et al.* Comparison of flow cytometry and immunohistochemistry in non-radioisotopic murine lymph node assay using bromodeoxyuridine. *Toxicology Letters* **192,** 229–237. ISSN: 03784274 (2010).

363. Miron, V. E. Microglia-driven regulation of oligodendrocyte lineage cells, myelination, and remyelination. *Journal of Leukocyte Biology* **101,** 1103–1108. ISSN: 0741-5400 (2017).

364. Lewis, N. D., Hill, J. D., Juchem, K. W., Stefanopoulos, D. E. & Modis, L. K. RNA sequencing of microglia and monocyte-derived macrophages from mice with experimental autoimmune encephalomyelitis illustrates a changing phenotype with disease course. *Journal of Neuroimmunology* **277,** 26–38. ISSN: 18728421 (2014).

365. Yamasaki, R. *et al.* Differential roles of microglia and monocytes in the inflamed central nervous system. *The Journal of Experimental Medicine* **211,** 1533–1549. ISSN: 0022-1007 (2014).

366. Gao, H. *et al.* Opposing Functions of Microglial and Macrophagic TNFR2 in the Pathogenesis of Experimental Autoimmune Encephalomyelitis. *Cell Reports* **18,** 198–212. ISSN: 22111247 (2017).

367. Ichi Satoh, J. *et al.* TMEM119 marks a subset of microglia in the human brain. *Neuropathology* **36,** 39–49. ISSN: 14401789 (2016).

368. Solloway, M. *et al.* Mice Lacking BMP6 function. *Molecular and Cellular Biology* **339,** 321–339 (1998).

369. Mcpherron, A., Lawler, A. & Lee, S. Regulation of anterior / posterior patterning of the axial skeleton by growth / differentiation factor 11. *Nature* **22,** 1–5 (1999).

370. Rankin, C., Bunton, T, Lawler, A. & Lee, S. Regulation of left-right patterning in mice by growth/differentiation factor-1. *Nature Genetics* **24,** 262–265. ISSN: 10614036 (2000).

371. Perge, J. A., Niven, J. E., Mugnaini, E., Balasubramanian, V. & Sterling, P. Why Do Axons Differ in Caliber? *Journal of Neuroscience* **32,** 626–638. ISSN: 0270-6474 (2012).

372. Bechler, M. E., Byrne, L. & Ffrench-Constant, C. CNS Myelin Sheath Lengths Are an Intrinsic Property of Oligodendrocytes. *Current Biology* **25,** 2411–2416. ISSN: 09609822 (2015).

373. Nave, K. A. & Salzer, J. L. Axonal regulation of myelination by neuregulin 1. *Current Opinion in Neurobiology* **16,** 492–500. ISSN: 09594388 (2006).

374. Rittchen, S *et al.* Myelin repair invivo is increased by targeting oligodendrocyte precursor cells with nanoparticles encapsulating leukaemia inhibitory factor (LIF). *Biomaterials* **56,** 78–85. ISSN: 18785905 (2015).

375. Hanisch, U.-K. Functional diversity of microglia how heterogeneous are they to begin with? *Frontiers in Cellular Neuroscience* **7,** 1–18. ISSN: 1662-5102 (2013).

376. Van Bruggen, D, Agirre, E & Castelo-Branco, G. Single-cell transcriptomic analysis of oligodendrocyte lineage cells. *Current Opinion in Neurobiology* **47,** 168–175. ISSN: 18736882 (2017).